U.PORTO

DOUTORAMENTO

BIOTECNOLOGIA MOLECULAR E CELULAR APLICADA ÀS CIÊNCIAS DA SAÚDE

Bioengineering an Immunomodulatory Microenvironment for Bone Healing

Mafalda Bessa Martins Gonçalves

D

2021

U.PORTO

Mafalda Bessa Martins Gonçalves. Bioengineering an Immunomodulatory Microenvironment for Bone Healing

Bioengineering an Immunomodulatory Microenvironment for Bone Healing
Mafalda Bessa Martins Gonçalves

D.ICBAS **2021**

SEDE ADMINISTRATIVA

INSTITUTO DE CIÊNCIAS BIOMÉDICAS ABEL SALAZAR
FACULDADE DE FARMÁCIA

U.PORTO

DOUTORAMENTO

BIOTECNOLOGIA MOLECULAR E CELULAR APLICADA ÀS CIÊNCIAS DA SAÚDE

Bioengineering an Immunomodulatory Microenvironment for Bone Healing

Mafalda Bessa Martins Gonçalves

D

2021



MAFALDA BESSA MARTINS GONÇALVES

BIOENGINEERING AN IMMUNOMODULATORY MICROENVIRONMENT FOR BONE HEALING

Tese de Candidatura ao grau de Doutor em Biotecnologia Molecular e Celular Aplicada às Ciências da Saúde, submetida ao Instituto de Ciências Biomédicas Abel Salazar da Universidade do Porto.

Orientador – Doutora Susana Gomes dos Santos Barber

Categoria – Investigadora Auxiliar e Professora Afiliada

Afiliação – i3S – Instituto de Investigação e Inovação em Saúde e INEB – Instituto de Engenharia Biomédica, Universidade do Porto, ICBAS – Instituto de Ciências Biomédicas Abel Salazar, Universidade do Porto

Coorientador – Professora Doutora Regine Willumeit-Römer

Categoria – Director Institute of Metallic Biomaterials

Afiliação – Institute of Metallic Biomaterials, Helmholtz-Zentrum Hereon


INSTITUTO DE INVESTIGAÇÃO
E INOVAÇÃO EM SAÚDE
UNIVERSIDADE DO PORTO


INEB
30 years
Instituto de Engenharia Biomédica


U.PORTO
ICBAS
INSTITUTO DE CIÊNCIAS BIOMÉDICAS ABEL SALAZAR
SCHOOL OF MEDICINE AND
BIOMEDICAL SCIENCES


U.PORTO
FACULDADE DE FARMÁCIA
UNIVERSIDADE DO PORTO


BiotechHealth
International Doctoral Programme in Molecular
and Cellular Biotechnology Applied to Health Sciences


Helmholtz-Zentrum
hereon
U.PORTO
CEMUP
CENTRO DE MATERIAIS DA UNIVERSIDADE DO PORTO
SÃO JOÃO

“Recomeça...

Se puderes

Sem angústia

E sem pressa.

E os passos que deres,

Nesse caminho duro

Do futuro

Dá-os em liberdade. Enquanto não alcances

Não descanses.

De nenhum fruto queiras só metade.”

Miguel Torga

SUPPORT

- This work used clinical grade fibrinogen kindly donated by Grifols (Barcelona, Spain).

FUNDING

The work included in this thesis was financially supported by:

- FCT PhD Programmes and by Programa Operacional Potencial Humano (POCH), BiotechHealth Programme (Doctoral Programme on Cellular and Molecular Biotechnology Applied to Health Sciences – reference PD/BI/128355/2017), and through the PhD studentship PD/BD/135489/2018

- FEDER - Fundo Europeu de Desenvolvimento Regional funds through the COMPETE 2020 - Operacional Programme for Competitiveness and Internationalization (POCI), Portugal 2020.

- Portuguese funds through NORTE-01-0145-FEDER-000012, supported by Norte Portugal Regional Operational Programme (NORTE 2020), under the PORTUGAL 2020 Partnership Agreement, through the European Regional Development Fund (ERDF).



PUBLICATIONS

Under the terms of nº 2, alínea a) do artigo 31º do Decreto-Lei n.º 230/2009, the work presented in this doctoral thesis, is already published or in preparation for publication:

Article I

Original research article published

Bessa-Gonçalves M, Silva AM, Brás JP, Helmholz H, Luthringer-Feyerabend BJC, Willumeit-Römer R, Barbosa MA, Santos SG. **(2020)** Fibrinogen and magnesium combination biomaterials modulate macrophage phenotype, NF-kB signaling and crosstalk with mesenchymal stem/stromal cells. *Acta Biomaterialia*.

DOI: 10.1016/j.actbio.2020.07.028

URL: https://www.sciencedirect.com/science/article/pii/S1742706120304141

Article II

Original research article submitted

Bessa-Gonçalves M, Ribeiro-Machado C, Costa M, Ribeiro CC, Barbosa JN, Barbosa MA, Santos SG. **(2022)** Fibrinogen scaffolds incorporating magnesium ions modulate macrophages towards a M2 phenotype *in vitro* and *in vivo*.

COMPLEMENTARY PUBLICATIONS IN THE FIELD:

1. Araújo M, Silveira J, Sousa A, **Bessa-Gonçalves M**, Santos SG, Barrias CC. **(2021)** A bioinspired multifunctional hydrogel patch targeting inflammation and regeneration in chronic intestinal wounds. *Biomaterials Science*.

DOI: 10.1039/D1BM00118C

URL: https://pubs.rsc.org/en/content/articlelanding/2021/bm/d1bm00118c

2. Almeida AR*, **Bessa-Gonçalves M***, Vasconcelos D, Barbosa MA, Santos SG. **(2019)** Osteoclasts degrade fibrinogen scaffolds and induce mesenchymal stem/stromal osteogenic differentiation. *Journal of Biomedical Materials Research Part A.*

*equal contribution

DOI: 10.1002/jbm.a.36863

URL: https://onlinelibrary.wiley.com/doi/full/10.1002/jbm.a.36863

3. Teixeira JH, Silva AM, Almeida MI, **Bessa-Gonçalves M**, Cunha C, Barbosa MA, Santos SG. **(2019)** The Systemic Immune Response to Collagen-Induced Arthritis and the Impact of Bone Injury in Inflammatory Conditions. *International Journal of Molecular Sciences.*
DOI: 10.3390/ijms20215436
URL: https://www.ncbi.nlm.nih.gov/pmc/articles/PMC6862543/

4. Silva AJ, Ferreira JR, Cunha C, Corte-Real JV, **Bessa-Gonçalves M**, Barbosa MA, Santos SG, Gonçalves RM. **(2019)** Macrophages Down-Regulate Gene Expression of Intervertebral Disc Degenerative Markers Under a Pro-inflammatory Microenvironment. *Frontiers in Immunology.*
DOI: 10.3389/fimmu.2019.01508
URL: https://www.ncbi.nlm.nih.gov/pmc/articles/PMC6616110/

ACKNOWLEDGEMENTS

Chega ao fim esta etapa. Uma etapa feita de altos e baixos. Uma etapa marcada por partilha de saber, apoio e disponibilidade de muitos bons seres humanos com quem tive oportunidade de me cruzar, de aprender, e também de partilhar saberes. Termino esta etapa com a sensação de que sei ainda menos do que sabia quando me decidi a começar. Termino esta etapa feliz e consciente de que o desconhecido e as dúvidas permitem o avanço. Mas não posso terminar esta etapa sem endereçar os respetivos agradecimentos a muitos dos que me permitiram crescer cientifica e pessoalmente. Sou de parcas palavras mas tentarei fazer jus.

À **Susana Santos,** minha orientadora, muito obrigada por ter aceite embarcar nesta jornada e por ter abraçado este desafio com confiança apesar de não me conhecer. Nem sempre estivemos de acordo sobre o caminho a seguir e ainda bem porque foi essa discórdia saudável que me permitiu crescer. Mas sempre nos respeitamos nestas discórdias. A Susana sempre me incentivou a querer mais, a ser melhor, a tirar o máximo partido dos resultados que ia tendo. Deixou-me errar e escolher o meu caminho e isso é essencial também para podermos crescer. Sempre partilhou o seu conhecimento comigo e guiou-me da melhor maneira que pode por estes trilhos que nem sempre foram muito *smooth*. A Susana incutiu-me ainda mais o espirito de equipa e da importância de estar envolvida não somente no nosso projeto mas também em projetos paralelos. Graças a isso também tive oportunidade de participar em projetos de outros colegas e sem dúvida pude fazer translação de conhecimentos e partilhar dúvidas. Com o passar dos anos, podemos estreitar a nossa relação aluna – orientadora, estabelecer uma relação de confiança e diria também de amizade. Hoje sei que a Susana fez sempre o melhor que pode e me deu sempre o seu apoio e respeito e por isso permitiu e deixou-me crescer não só em termos profissionais mas também em termos pessoais.

Ao **Professor Mário Barbosa,** pelo afável acolhimento. Pela sua conduta assertiva e de liderança que me fez caminhar com firmeza. Pela excelente oportunidade que foi trabalhar, (sempre com um espírito de partilha e cooperação) no seu grupo. O apoio do Professor Mário foi essencial nesta jornada. Os momentos de discussão científica que tivemos, sua visão crítica, a sua perspetiva e a sua opinião foram cruciais neste percurso. Agradeço imenso ter tido a oportunidade de partilhar consigo os meus resultados e pesquisas. Agradeço também todo o apoio que me deu na minha tomada de decisões. Por me ter deixado trilhar o meu caminho nem sempre certo de que fosse resultar. Afinal, é a errar que também aprendemos.

To **Prof. Regine Willumeit-Römer,** my special thanks for accepting to be my co-supervisor, despite not knowing me. For having received and welcomed me so well in your group during my “little journey” at Helmholtz-Zentrum hereon in the Institute of Metallic Biomaterials. For all the help with my work. For the availability to share your knowledge. For investing in me and supporting me throughout the whole PhD.

To **Bérengère Luthringer-Feyerabend** also a special thanks for the kindness, the warm and kind reception and welcoming when I was at the Institute of Metallic Biomaterials. For all the support and scientific discussion.

To **Heike Helmholz** and **Monika Lucszak** a thank you for the expert technical assistance but more importantly for their kindness.

To **Prof. Fergal O’Brien**, **Joanna Sadowska** and **Arlying Vázquez** I thank for accepting to collaborate in this work without knowing anything about me. Unfortunately, due to the pandemic, we were not able to meet in person. However, we did not lower our arms and managed to start part of the work that we set out to. Thank you for always being available to help and to clear all my doubts.

Ao **Professor Manuel Vilanova**, Diretor do Programa Doutoral em Biotecnologia Molecular e Celular Aplicada às Ciências da Saúde do ICBAS/FFUP, o meu agradecimento por todo o apoio prestado não só enquanto diretor mas também enquanto membro da minha PAC.

Ao **BiotecHealth** e à **Fundação para a ciência e Tecnologia** agradeço pelo financiamento deste projeto.

Aos ***Internationals*!**, os meus colegas da **4ª edição do BiotechHealth**, **Ana Rita Pinto**, **Andreia Granja**, **Eunice Ferreira**, **Filipe Marques**, **Joana Ferreira**, **José Mateus** e **João Brás** agradeço todo o companheirismo, a entreajuda, a amizade ao longo destes 4-5 anos. Sem dúvida fomos uma edição muito unida e foi um privilégio poder conhecer a autenticidade de cada um de vós. À **Ana Rita Pinto** e **Andreia Granja**, muito obrigada pelas nossas fantásticas e sempre animadoras conversas, pelos momentos partilhados e pela amizade.

A todos os **MiNT** (atuais e antigos) mas em particular à **Ana João Silva**, **Ana Luísa Castro**, **Andreia Silva**, **Carla Cunha**, **Catarina Milheiro**, **Catarina Pereira (Cati)**, **Cristina Ribeiro, Daniela Vasconcelos (Dani)**, **Filipa Lourenço (Pipa)**, **Flávia Castro**, **Jaime Freitas**, **Joana Caldeira (Xu)**, **Joana Ferreira**, **João Brás**, **Joana Oliveira**, **José Henrique Teixeira (Zé)**, **Judite Barbosa**, **Maria Inês Almeida**, **Morena Fiordalisi**, **Raquel Gonçalves**, **Sara Moura**. Obrigada por tornarem, cada um à sua maneira, os meus dias mais felizes e mais fáceis em vários sentidos. Não obstante, algumas ressalvas têm que ser feitas e enaltecidas. À “minha” querida **Ana João Silva** (para mim eterna Cici)

agradeço esta que será uma eterna amizade. Foste das primeiras pessoas com quem falei quando cheguei ao MiNT. Logo percebeste o quão envergonhada sou e logo me deste uma oportunidade de ter que deixar de o ser. Ajudaste-me imenso a perder um bocadinho desta vergonha, a deixar de ser tão "atada", a perder o medo e ir falar com as pessoas. Partilhaste comigo as tuas amizades já estabelecidas no i3S/INEB. E eu partilhei contigo também amizades que já trazia comigo. Agradeço a tua paciência, assertividade, honestidade. Partilhamos imensos momentos, imensas risadas, choradeira também (mas essa parte foi tua). Discutimos, chateamo-nos, fomos sempre honestas e sinceras uma com a outra. Acima de tudo, crescemos uma com a outra, aprendemos uma com a outra. Aliás, foste a minha mentora no que concerne às experiências com macrófagos. Não importa nada a distância (tu no UK e eu em PT), estaremos sempre juntas. À **Ana Luísa Castro** (Luisinha! ☺) não sei de todo como te agradecer. Não há palavras que possam descrever o que tu aturaste, particularmente nesta reta final (nem vale a pena mencionar). Começamos esta jornada uma em cada ponta do lab mas depois cedo te tornaste minha colega de carteira. E cedo percebemos que há muito coisa a unir-nos e obviamente somos diferentes em muitas outras coisas. Mas acima de tudo sempre fomos muito "pão pão queijo queijo" uma com a outra. Sempre frontais. Foste um grande porto de abrigo para mim. Amparaste-me em vários momentos menos bons. Em momentos profissionais, em momentos pessoais. Partilhamos outros tantos momentos de índole científica e outros não tão científicos. És das pessoas mais altruístas que conheço. Estarei para sempre agradecida por te ter conhecido. Espero poder ter sido ¼ daquilo que foste e és para mim. Tu e Cláudia Machado foram e são grandes pilares. Acima de tudo, grandes amigas que espero manter para muitos anos! À **Cláudia Machado** (apesar de não estares na página do MiNT serás sempre MiNT para mim ☺) também devo um agradecimento muito especial - aturaste-me muito (e mais uma vez não vale a pena mencionar). Gabo-te a paciência e determinação. Admiro a tua frontalidade, sinceridade e honestidade. Foi preciso chegar ao fim para finalmente poder trabalhar na bancada contigo. Desde início fomos colegas de carteira e com o passar do tempo tornamo-nos grandes "colegas". Aprendi e cresci imenso contigo. Não estou tão certa que tenhas aprendido e crescido muito comigo. Mas pelo menos grandes momentos de risadas tivemos. Um sorriso por dia não sabe o bem que lhe fazia! To **Morena Fiordalisi** (or should I say "Mirena"? ☺), a special and thoughtful thanks. We've met during your ERASMUS experience and soon we became friends. Since then we became inseperable. You will always have a special place in my crazy heart and you know that. I know that I can count on you as you know (or at least you should know) that you can always count on me for everything. You helped me a lot both on a personal and a professional level. This is a friendship to keep. Thank you for everything my crazy friend! À **Andreia Silva,** um gigante obrigada. Foste e és um exemplo para mim. Foste também uma

das primeira pessoas a acolher-me no MiNT. Desde cedo te disponibilizaste a ajudar-me e ensinar-me tudo o que precisasse independentemente do que tivesses para fazer. Sempre sorridente. Nunca vi uma Andreia que não tivesse um sorriso para partilhar e uma palavra de apoio para dar. À **Cati** e **Dani** agradeço também o acolhimento, a oportunidade de partilhar momentos de bancada e secretária onde estiveram sempre presentes sorrisos, palavras de apoio, entreajuda e companheirismo. Os cafés no bar sem dúvida foram momentos muito relaxantes! Ao **Zé** deixo também um especial agradecimento. Desde cedo tiveste que lidar comigo. Não tiveste grande opção na verdade. Partilhamos momentos vários. Desde muitos bons a menos bons. Fomos sempre francos em relação a angustias e receios. Sempre tiveste, não uma, mas várias palavras de apoio e nunca me deixaste baixar a cabeça. Ainda hoje assim é. E espero que possa ser por mais tempo. À **Flávia Castro** deixo também um gigante obrigada. Foste muito importante na parte das experiências com macrófagos mas ainda mais importante na partilha e apoio. Cati, Dani, Flávia e Zé, vocês foram, sem dúvida, um grande suporte nesta reta final. Sempre com uma palavra amiga, uma palavra de conforto. Ao meu *bro* **João Brás** também devo muita gratidão. Apesar de trabalharmos em áreas totalmente distintas também me ensinaste muito. Foram muitos os westerns que supervisionaste. Mas não foi só disto que se fez o nosso doutoramento. Ainda fizemos vários cursos e trabalhos juntos. Mais que isso, rimo-nos imenso e tu ainda aturaste muitos "picos de stress". Sempre com muita calma. Essa calma que tanto te carateriza. Muito obrigada por me teres aturado e por seres tão bom amigo e tão bom profissional e por me ensinares a relevar muitas situações. Muitas gracias mesmo! Um muito obrigada ainda à **Joana Ferreira** por ter sempre uma palavra de riso e por ter levado com alguns dos meus "picos de stress". Foi mútuo particularmente nesta reta final. E como dizes e muito bem: O que tem que ser tem muita força!". À **Joana Oliveira** um muito especial obrigada pela ajuda e pelas palavras doces e de conforto. À **Sara Moura** ("Xaninha") grata por sempre conseguires fazer-me rir. Fosse que momento fosse, tinhas sempre alguma palhaçada para me pôr a rir. Obrigada ainda pela ajuda no lab. À **Judite Barbosa**, **Maria Inês Almeida, Carla Cunha** e **Raquel Gonçalves** um imenso obrigada, por estarem sempre disponíveis para ajudar tanto em contexto prático, como em contexto teórico. À **Cristina Ribeiro**, sempre disponível para ajudar, quero deixar igualmente um agradecimento especial. Foi a primeira pessoa com quem falei quando fui à entrevista para concorrer a uma bolsa FCT no grupo. Sempre me fez sentir acolhida (não desfazendo dos demais). Sempre com uma voz doce e acolhedora e com transmissão de tranquilidade. Muito obrigada por tudo!

Aos **INEB**ianos **Ana Luísa Torres**, **Andreia Matos**, **Ângela Costa**, **Beatriz Custódio, Catarina Barbosa**, **Dalila Pedro**, **Estrela Neto**, **Flávia Pereira**, **Inês Gonçalves**, **Juliana**

Alves, **Manuela Brás**, **Marco Araújo**, **Maria José Oliveira**, **Maria Lázaro**, **Patrícia Cardoso**, **Pedro Moreno**, **Professor Fernando Jorge**, **Ricardo Vidal**, **Sívia Bidarra** e a todos aqueles que contribuíram para a conclusão desta etapa um muito obrigada! À **Ana Luísa Torres** e **Sílvia Bidarra** obrigada por serem as melhores vizinhas do lado esquerdo do 105 ☺. Obrigada por me acolherem, por partilharem a vossa experiência, por terem sempre uma palavra amiga, por terem sempre um conselho sábio, por transmitirem tranquilidade, por me incutirem força e transmitirem tranquilidade. Acima de tudo, por terem sempre um sorriso e boa disposição para dar, mesmo que não fossem os vossos melhores dias. Foi e é um privilégio ter tido a sorte de vos ter conhecido. Hoje, sou melhor pessoa por vos ter conhecido. Ao **Marco Araújo**, obrigada por teres acreditado que poderia, de alguma forma, contribuir para o avançar num dos teus trabalhos. Obrigada por me teres dado esse voto de confiança. Mas mais importante, por seres um bom amigo, um excelente ser humano. À **Ângela Costa**, **Patrícia Cardoso**, **Flávia Pereira**, **Andreia Matos** e **Catarina Barbosa** obrigada por serem as melhores vizinhas do lado direito do 105 ☺. Vocês também me acolheram muito bem, partilharam saberes e muitas, mas mesmo muitas risadas. Obrigada pela vossa boa disposição e ajuda. **Estrela Neto** e **Juliana Alves** estou grata pela vossa boa energia e positividade. De igual modo, um agradecimento especial à **Inês Gonçalves** por ter aceite fazer parte da minha PAC, pela partilha de conhecimento e pela sempre presente boa disposição.

À **Madalena Costa**, um obrigada muito especial pela disponibilidade em ajudar-me com o in vivo. Não teria sido de todo possível sem s(t)i. Pela paciência e mestria em ensinar e por estar(es) sempre pronta a ajudar. Pelas conversas durante as cirurgias aos ratinhos, pela companhia e simpatia. Foi uma honra ter tido a oportunidade de aprender cons(t)igo.

À **Joana Magalhães** (para sempre a minha Maga ☺), um grandioso obrigada por teres feito parte desta etapa. Obrigada pelas *pep talks*! Por conseguires sempre levantar-me o astral, quando estava mais em baixo, por me fazeres ver o lado positivo das situações, pela transmissão de tranquilidade, pelo apoio incondicional, pela amizade que fomos construindo e que espero que perdure, pela magnífica companhia. Por seres o fantástico ser humano que és. És um exemplo para mim e sou uma privilegiada por te ter conhecido!

À dupla **Ângela Oliveira** (Formiguinha ☺) e **Liliana Almeida** (Lils ☺) um imenso e gigante obrigada. Esta é já a segunda etapa em que me acompanham. Primeiro foi o mestrado e agora o PhD. A nossa amizade já vem de outras andanças. E independentemente de onde estivermos, por onde andarmos, e quanto tempo passe a nossa amizade permanecerá intacta. Podemos ficar algum tempo sem nos vermos, sem nos falarmos mas quando voltamos a fazê-lo vemos que nada mudou. Vocês foram e são um grande pilar nesta

jornada. Vocês e os nossos chás espetaculares. Uns melhores que outros, mas sempre em companhia fenomenal. A companhia das amigas! Assim se mantenha!

Por fim, os agradecimentos mais importantes e mais difíceis de expressar são para os meus pais, o meu irmão e o meu avô paterno.

Aos **meus pais**, os meus ídolos, por tudo o que fizeram e fazem por mim. Pelo amor e apoio incondicional. Pela coragem e força que me dedicaram e incutiram. Por nunca me deixarem desistir, nem desistirem de mim, mesmo quando se revelava a minha face negra. Por me deixarem escolher o meu caminho mesmo que nem sempre concordassem e por serem sempre o meu porto de abrigo. Por serem a minha rede e ampararem as minhas quedas. Por me ajudarem sempre a reerguer-me. Por serem tal como são, ainda que às vezes, seja complicado. Por serem autênticos!

A ti Tiago, **meu irmão**, por seres um pilar importante, para ultrapassar e vencer os desafios a que me propus e que me propuseram. Pela tua autenticidade e sapiência. Por teres as palavras certas na hora certa. Por me dares força e coragem para seguir em frente. Por seres um irmão carinhoso. Por seres o meu melhor amigo ainda que me tires do sério, diversas vezes. Por mostrares que tens orgulho em mim e não teres receio nem vergonha de o mostrar ou dizer. Eu tenho muito orgulho em ti! Por seres a minha segunda rede de segurança. Muitas vezes foste a primeira.

Ao meu **avô paterno** pela força e alento que me consagrou. Pela constante presença, mesmo estando ausente.

A todos, o meu sincero **MUITO OBRIGADA!**

INDEX OF CONTENTS

Abstract	**I**
Resumo	**III**
List of Abbreviations	**VII**
CHAPTER I – General Introduction	**1**
Abstract	**3**
1. Bone	**5**
1.1. Bone tissue	5
1.1.1. Bone metabolism: modelling and remodelling	8
1.2. Bone healing	8
1.2.1. The role of macrophages in fracture healing	12
2. Bone Regeneration Strategies: Biomaterials as Bone Graft Substitutes	**13**
2.1. Inflammatory response to biomaterials	14
2.1.1. Relevance of macrophages in a biomaterial context	16
3. Immunomodulatory Biomaterials – Emerging Trend in Biomaterial Development	**18**
3.1. The promise of Immunomodulatory Degradable Biomaterials for Bone Repair/Regeneration	20
3.1.1. **POLYMERS**	21
Synthetic Polymers	21
Natural Polymers	22
Collagen	22
Chitosan	23
Alginate	23
Decellularized Matrices	24
Fibrinogen	25
3.1.2. **BIOCERAMICS**	26
Bioactive Ceramics	26
Bioactive Glasses	28
Glass-Ceramics	28
3.1.3. **METALS**	34
Iron	34
Zinc	35
Magnesium	36
3.1.4. **COMPOSITES**	42

4. Aims of the Thesis **48**
References **50**

CHAPTER II – Fibrinogen and magnesium combination biomaterials modulate macrophage phenotype, NF-kB signaling and crosstalk with mesenchymal stem/stromal cells **79**
Abstract **82**
1. Introduction **84**
2. Materials and Methods **81**
3. Results **92**
3.1. Fg scaffolds and their combination with Mg discs: 3D architecture and extract composition 92
3.2. FgMg biomaterial extracts decreased LPS-stimulated TNF-α secretion 93
3.3. FgMg biomaterial extracts impaired macrophage M1 polarization 94
3.4. FgMg biomaterial extracts decreased NF-kB p65 phosphorylation, following M1 stimulation 95
3.5. Fg, Mg and FgMg biomaterials extracts influenced cytokine secretion by M1 stimulated macrophages 98
3.6. Secretome from macrophages preconditioned with FgMg biomaterial extracts increased MSCs ALP activity and calcium deposition 100
4. Discussion **102**
5. Conclusion **106**
References **108**
Supplementary material **115**

CHAPTER III – Magnesium sulphate-incorporated fibrinogen scaffolds modulate macrophages towards a M2 phenotype *in vitro* and *in vivo* **117**
Abstract **120**
1. Introduction **121**
2. Materials and Methods **122**
3. Results **131**
3.1. $MgSO_4$ is incorporated in the structure of Fg, increasing its mechanical properties and zeta potential 131
3.2. 10 mM $FgMgSO_4$ scaffolds promote M2 macrophage polarization without cytotoxicity 134

3.3. 10 mM $FgMgSO_4$ scaffolds reduce NF-kB p65 nuclear translocation and pro-inflammatory cytokine secretion 137
3.4. 10 mM $FgMgSO_4$ scaffolds promote M2 macrophage polarization *in vivo* 140
4. Discussion **144**
5. Conclusion **148**
References **149**
Supplementary material **157**

CHAPTER IV – General Discussion / Future Perspectives **161**
1. General Discussion **163**
2. Future Perspectives **168**
References **171**

SUPPLEMENTARY RESULTS – Biomaterial-based non-viral transfection of primary monocytes **177**
1. Introduction **180**
2. Materials and Methods **181**
3. Results **183**
3.1. Monocytes were efficiently transfected with siGLO and siRNA MMP9 183
3.2. siGLO-activated Fg and 10 mM $FgMgSO_4$ scaffolds are capable of transfecting monocytes/macrophages in 3D 185
4. Discussion **188**
5. Conclusion **190**
References **191**

ABSTRACT

Inflammation is a process that occurs naturally after injury. While acute inflammation is beneficial in the regulation of bone healing, chronic inflammation is detrimental and underlies most musculoskeletal diseases. Tuning inflammation using biomaterials is a strategy increasingly explored to promote tissue repair/regeneration. In particular, the modulation of macrophage phenotype, from pro-inflammatory (M1) to pro-regenerative (M2), has the potential to direct appropriate healing outcomes.

For this doctoral dissertation work, the goal was to use biodegradable biomaterials to bioengineer a microenvironment that could modulate macrophages towards a pro-reparative phenotype to improve bone healing. Particularly, we hypothesized that the combination between fibrinogen (Fg) and magnesium (Mg) would act synergistically in the modulation of macrophage phenotype and their crosstalk with mesenchymal stem/stromal cells (MSCs), under physiological and pro-inflammatory conditions. Fg has been investigated in our group either adsorbed to chitosan or as scaffolds with very encouraging results for bone regeneration. On the other hand, Mg is considered the most promising biodegradable biomaterial to be used in orthopedics due to its mechanical properties similar to human bone and natural presence in bone. However, its degradation rate is fast and hard to control. Thus, the combination of Mg-based materials with polymers has been suggested as an attractive approach for orthopedic implants, to improve biodegradability rate, biocompatibility, angiogenesis and osteogenesis. So, herein, we aimed to: (i) combine Fg with Mg and investigate the synergistic immunomodulatory potential of FgMg biomaterials towards macrophages and MSCs; (ii) develop Mg-incorporated Fg scaffolds and evaluate their capacity to modulate macrophage phenotype and inflammation, *in vitro* and *in vivo*; (iii) determine the potential of non-viral transfection to fine-tune biomaterials ability to modulate macrophage polarization.

To accomplish our aims we started by combining Fg scaffolds with Mg discs (multilayer constructs). Then, we investigated the impact of their extracts on macrophage phenotype and paracrine crosstalk with MSCs. Results showed that extracts from FgMg materials impair LPS-IFN**γ**-driven macrophage M1 polarization, resulting in a lower percentage of CD86 positive cells, and reduced secretion of TNF-α and IL-12. Mechanistically, FgMg extracts impaired the LPS-IFN**γ** stimulation of NF-kB p65 activation. Moreover, the secretome from macrophages exposed to FgMg extracts significantly increased the MSCs ALP activity. These findings are reported in chapter II and published in the scientific article *Bessa-Gonçalves M et al. (2020), Acta Biomaterialia, 114 (2020) 471–484.*

Next, we developed an FgMg combination biomaterial, where increasing concentrations of $MgSO_4$ were incorporated in the structure of Fg 3D scaffolds. Results showed that Fg

scaffolds incorporating 10, 25 and 50 mM of $MgSO_4$ presented decreasing porosity with increasing $MgSO_4$ concentration. $MgSO_4$ incorporation increased surface charge, and gradual Mg^{2+} release could be detected along time. $MgSO_4$ incorporation also increased the loss and storage modulus of Fg, with significant differences for the 10 mM $FgMgSO_4$ scaffolds. When macrophages were cultured on these scaffolds, a significant decrease in cell viability was observed for 25 and 50 mM $FgMgSO_4$ scaffolds, either in M0 or M1 conditions. Notably, macrophages differentiated on 10 mM $FgMgSO_4$ scaffolds showed an increased percentage of $CD163^+$ (M2 marker) and a decreased percentage of $CCR7^+$ (M1 marker), in comparison with those cultured on Fg and 25 and 50 mM $FgMgSO_4$ scaffolds, both in unstimulated (M0) conditions and in response to LPS-IFN**γ**-driven macrophage M1 polarization. In agreement with our previous results, NF-kB p65 nuclear translocation, activated in response to M1 stimulation, was significantly decreased in macrophages cultured in 10 mM $FgMgSO_4$ scaffolds, when compared with Fg scaffolds. A cytokine/chemokine panel showed that M1 cells on 10 mM $FgMgSO_4$ secreted significantly less pro-inflammatory mediators (e.g. IFN**γ**, IL-6, IL-12p40, TNF-α, IP-10) than those on Fg scaffolds. *In vivo*, 10 mM $FgMgSO_4$ scaffolds induced a M2 anti-inflammatory macrophage response (increased $CD11b^+CD163^+$ cells), when compared with Fg. Analysis of a cytokine/chemokine panel showed that both scaffolds decreased the levels of pro-inflammatory cytokines, when compared to sham operated animals, but only 10 mM $FgMgSO_4$ was able to significantly decrease IL-1β, IP-10, MIP-2, MDC and MIP-3α. Additionally, MSCs cultured directly on 10 mM $FgMgSO_4$ scaffolds showed significantly increased calcium deposits, in comparison with those cultured on Fg scaffolds. These results are presented in chapter III and a manuscript is currently in preparation to be submitted for publication.

Lastly, we explored non-viral transfection of monocytes/macrophages as a tool to further improve biomaterials ability to modulate macrophage polarization. nHA particles were synthesized, combined with siGLO or a fluorescently tagged siRNA MMP9 and successfully delivered to monocytes 2D cultures. Then, Fg and 10 mM $FgMgSO_4$ scaffolds were loaded with nHA particles loaded with siGLO and monocytes were seeded on top of the scaffolds. Results showed that siGLO was also successfully transfected in monocytes in 3D. These preliminary results are described as supplementary work.

Taken together, our findings revealed that the combination of Fg and Mg can modulate macrophage activation and the inflammatory response to biomaterials. This work opens avenues for the FgMg combination to be explored in the development of a new class of immunomodulatory biomaterials.

RESUMO

A inflamação é um processo que ocorre naturalmente após uma lesão. Embora uma inflamação aguda seja benéfica na regulação da cicatrização óssea, a inflamação crónica é prejudicial e está subjacente à maioria doenças músculo-esqueléticas. O uso de biomateriais para regular a inflamação é uma estratégia cada vez mais explorada na promoção da reparação/regeneração do tecido. Em particular, a modulação do fenótipo dos macrófagos, de pro-inflamatórios (M1) para pro-regenerativos (M2), tem sido realçada como uma estratégia adequada para promover um processo de cicatrização adequado.

O trabalho apresentado nesta tese teve como objetivo utilizar biomateriais biodegradáveis para desenvolver um microambiente capaz de modular a ativação dos macrófagos, promovendo um fenótipo pro-regenerativo, de forma a melhorar a cicatrização óssea. Em particular, colocou-se a hipótese de que a combinação entre fibrinogénio (Fg) e magnésio (Mg) atuaria sinergicamente na modulação do fenótipo dos macrófagos e na sua comunicação com células mesenquimais (MSCs), tanto em condições fisiológicas como em condições pro-inflamatórias. O Fg tem sido investigado no nosso grupo em diferentes formulações, incluindo após adsorção a quitosano e sob a forma de esponjas 3D, com resultados muito promissores para a regeneração óssea. Por outro lado, o Mg é considerado o biomaterial biodegradável mais promissor para uso ortopédico devido à similaridade das suas propriedades mecânicas com aquelas que são encontradas no osso, assim como a sua presença natural no osso. Contudo, a sua taxa de degradação é rápida e difícil de controlar. Deste modo, a combinação de materiais à base de Mg com polímeros tem sido sugerida como uma abordagem interessante para implantes ortopédicos devido aos seus efeitos sinérgicos na biodegradabilidade, biocompatibilidade, angiogénese e osteogénese. Neste contexto, foram definidos os seguintes objetivos para esta tese: (i) combinar Fg com Mg e investigar o potencial imunomodulatório sinérgico dos biomateriais de FgMg na função de macrófagos e MSCs; (ii) desenvolver esponjas de Fg incorporadas com Mg e avaliar o seu efeito na modulação da inflamação e do fenótipo dos macrófagos, *in vitro* e *in vivo*; (iii) determinar o potencial da transfeção não viral para melhorar a capacidade destes biomateriais na modulação da polarização dos macrófagos.

Para atingir os nossos objetivos, começámos por combinar esponjas de Fg com discos de Mg (produzidas por multicamadas). De seguida, investigamos o impacto dos seus extratos no fenótipo dos macrófagos e na sua comunicação parácrina com MSCs. Os resultados mostraram que os extratos dos materiais FgMg atenuam a polarização M1 dos macrófagos, mediada por LPS-IFNγ, resultando numa menor percentagem de células positivas para CD86 assim como numa redução da secreção de TNF-α e IL-12. Simultaneamente, a ativação da NF-kB p65, induzida pelo estímulo com LPS-IFNγ, foi afetada pela exposição

aos extratos de FgMg. Além disso, o secretoma dos macrófagos que foram expostos aos extratos resultantes da combinação entre Fg e Mg, aumentou significativamente a atividade da ALP das MSCs. Estas evidências estão reportadas no capítulo II e publicados no artigo científico *Bessa-Gonçalves M et al. (2020), Acta Biomaterialia 114 (2020), 471–484.*

De seguida, desenvolvemos um biomaterial de combinação FgMg, onde concentrações crescentes de sulfato de magnésio ($MgSO_4$) (10, 25 e 50 mm) foram incorporadas na estrutura das esponjas 3D de Fg. Os resultados mostraram que as esponjas 3D incorporadas com 10, 25 e 50 mM de $MgSO_4$ apresentaram porosidade decrescente, com o aumento da concentração de $MgSO_4$. A incorporação de $MgSO_4$ aumentou a carga superficial, e a libertação gradual de Mg^{2+} pôde ser detetada ao longo do tempo. Adicionalmente, a incorporação de $MgSO_4$ também aumentou o módulo de perda e de armazenamento do Fg, com diferenças significativas para os materiais de combinação 10 mM $FgMgSO_4$. Quando os macrófagos foram cultivados nestes materiais, foi observado um decréscimo significativo da viabilidade das células cultivadas nos materiais de combinação 25 e 50 mM $FgMgSO_4$, tanto em condições M0 como em condições M1. Notavelmente, os macrófagos diferenciados nos materiais de combinação 10 mM $FgMgSO_4$ exibiram um aumento na percentagem de células positivas para CD163 (marcador M2) e uma diminuição na percentagem de células positivas para CCR7 (marcador M1), em comparação com aqueles que foram cultivados no Fg e nos materiais de combinação 25 e 50 mM $FgMgSO_4$, tanto em condições não estimuladas (M0) como em resposta à estimulação M1 induzida por LPS-IFN**γ**. De acordo com os nossos resultados anteriores, a translocação nuclear da NF-kB p65, ativada em reposta à estimulação M1, foi significativamente reduzida nos macrófagos cultivados nos materiais de combinação 10 mM $FgMgSO_4$, quando comparada os materiais compostos apenas por Fg. A análise de um painel de citoquinas/quimiocinas mostrou que as células M1 que foram cultivadas nos materiais de combinação 10 mM $FgMgSO_4$, secretaram níveis significativamente inferiores de mediadores pró-inflamatórios (como por exemplo, IFN**γ**, IL-6, IL-12p40, TNF-α, IP-10) do que aquelas que foram cultivadas apenas em Fg. *In vivo*, as esponjas de 10 mM $FgMgSO_4$ induziram uma resposta anti-inflamatória M2 por parte dos macrófagos (aumento de células duplamente positivas para CD11b e CD163), em comparação com o Fg sozinho. A análise de um painel de citoquinas/quimiocinas mostrou que ambos os materiais promoveram a diminuição da secreção de mediadores pró-inflamatórios, em comparação com os animais controlo, mas apenas os materiais de combinação 10 mM $FgMgSO_4$ foram capazes de diminuir também, de forma significativa, a secreção de IL-1β, IP-10, MIP-2, MDC e MIP-3α. Adicionalmente, MSCs cultivadas diretamente nos materiais de combinação 10 mM $FgMgSO_4$ mostraram um aumento significativo dos depósitos de cálcio,

em comparação com MSCs cultivadas no Fg. Estes resultados estão descritos no capítulo III e, um manuscrito está atualmente em preparação para ser submetido para publicação.

Por fim, exploramos a transfeção não-viral de monócitos/macrófagos como uma ferramenta para melhorar a capacidade destes biomateriais na modulação da polarização dos macrófagos. Para tal, nanopartículas de hidroxiapatite (nHA) foram sintetizadas, combinadas com siGLO ou siRNA MMP9 (com marcação fluorescente) e entregues com sucesso a culturas 2D de monócitos. De seguida, esponjas de Fg e 10 mM $FgMgSO_4$ foram carregadas com nanopartículas de hidroxiapatite, combinadas com siGLO, e os monócitos foram depositados no topo destes materiais. Os resultados demonstraram que o siGLO foi também transfetado com sucesso em monócitos cultivados em 3D. Estes resultados preliminares são descritos como trabalho suplementar.

Em conjunto, os nossos resultados revelaram que a combinação de Fg com Mg pode modular a ativação dos macrófagos e a resposta inflamatória a biomateriais. Este trabalho abre portas para que a combinação FgMg possa ser explorada para o desenvolvimento de uma nova classe de biomateriais imunomoduladores.

LIST OF ABBREVIATIONS

AAS	Atomic absorption spectroscopy
AKT	Akermanite
Alg	Alginate
ALP	Alkaline phosphatase
ANOVA	Analysis of variance
B	Boron
BC	Buffy coats
BCP	Biphasic calcium phosphate
BGC	Bioactive glass-ceramics
BGs	Bioactive glasses
BLCs	Bone lining cells
BMPs	Bone morphogenetic proteins
BMUs	Basic multicellular units
BSA	Bovine serum albumin
C	Carbon
CaP	Calcium phosphate
CaP-CHI-HA	Calcium phosphate/chitosan/hyaluronic acid
CCL17	C-C Motif Chemokine Ligand 17
CCL22	C-C Motif Chemokine Ligand 22
CDHA	Calcium deficient HA
Ce	Cerium
CGRP	Calcitonin gene-related polypeptide-α
Ch	Chitosan
CNTs	Carbon nanotubes
Col	Collagen
Cr-Co	Chromium-cobalt
CS	Calcium silicate
CS-g-PCL	Chitosan-graft-poly(ε-caprolactone) copolymers
Cu	Cooper
DA	Degree of acetylation
DAMPs	Danger-associated molecular patterns
DCP	Dicalcium phosphate
DCs	Dendritic cells
dECM	Decellularized extracellular matrix
DMA	Dynamic mechanical analysis

DMEM	Dulbecco's modified eagle’s medium
ECM	Extracellular matrix
EDC/EDAC	N-(3-Dimethylaminopropyl)-N′-ethylcarbodiimide hydrochloride
EDS	Energy dispersive spectroscopy
EGCG	Epigallocatechin-3-gallate
EGF	Epidermal growth factor
EKA	Electro kinetic analysis
ELISA	Enzyme-linked immunosorbent assay
ERK	Extracellular Signal-Regulated Kinase
Eu	Europium
FACS	Fluorescence-activated cell sorting
Fb	Fibrin
FBGCs	Foreign body giant cells
FBR	Foreign body reaction
FBS	Fetal bovine serum
Fe	Iron
Fg	Fibrinogen
FGF	Fibroblast growth factor
Flt-3 ligand	FMS-related tyrosine kinase 3 ligand
FTIR	Fourier transform infrared spectroscopy
G-CSF	Granulocyte colony-stimulating factor
GAPDH	Glyceraldehyde-3-phosphate dehydrogenase
GM-CSF	Granulocyte-macrophage colony-stimulating factor
GO	Graphene oxide
GRO-α	Growth-regulated alpha protein
H	Hydrogen
HA	Hydroxyapatite
HE	Hematoxylin and eosin
HLA-DR	Human leucocyte antigen DR
HRP	Horseradish peroxidase
ICP-AES	Inductively coupled plasma – atomic emission spectroscopy
IFNα2	Interferon alpha-2
IFNB1	Interferon beta 1
IFNγ	Interferon gamma
IGF	Insulin-like growth factor
Ig	Immunoglobulin

IL	Interleukin
iNOS	Inducible nitric oxide synthase
IOs	Iron oxide nanoparticles
IP-10	Interferon induced protein 10
JNK	Jun N-Terminal Kinase
KC	Keratinocyte chemoattractant
KLF	Krueppel-like factor
LDH	Lactate dehydrogenase
Li	Litium
LIF	Leukemia inhibitor factor
LIX	Lipopolysaccharide-induced CXC chemokine
LPS	Lipopolysaccharide
LRP1	Lipoprotein receptor-related protein 1
M-CSF	Macrophage colony-stimulating factor
Mac-1	αMβ2 integrin
MaFIA	Macrophage-Fas induced apoptosis
MAPK	Mitogen-Activated Protein Kinase
MBGNs	Mesoporous bioactive glass nanoparticles
MCP	Monocyte chemoattractant protein
MCPC	Magnesium-calcium phosphate cement
MDC	Macrophage-derived chemokine
Mg	Magnesium
Mg-β-TCP	β-TCP coated Magnesium
$MgCl_2$	Magnesium chloride
MGF	Mechano-growth factor
MgG	Magnesium gluconate
MgMPs	Micron-sized Mg particles
MgNPs@GNS/DBM	Mg-enriched Graphene Oxide Nanoscrolls decorated biomimetic scaffolds
$MgSO_4$	Magnesium sulphate
MHC	Major histocompatibility complex
MIG	Monokine induced by interferon gamma
MIP-1α	macrophage inflammatory protein-1 alpha
MIP-1β	Macrophage inflammatory protein-1 beta
miRNA	microRNA
MLaHA/CS	Magnetic lanthanum-doped HA/Chitosan scaffolds

MMPs	Matrix metalloproteinases
MNPs	Mg oxide nanoparticles
MSC(s)	Mesenchymal stem/stromal cells
MSNs	Mesoporous silica nanospheres
MT	Masson's Trichrome
N	Nitrogen
NAGEL	Nagelschmidtite
NCPs	Non-collagenous proteins
NF-kB	Nuclear factor kappa-light-chain-enhancer of activated B cells
NK	Natural killer
NLRP3	NOD-like receptor containing pyrin domain 3
NOAEL	No observable adverse effect level
NT	Untransfected
O	Oxygen
o.n	Overnight
OBs	Osteoblasts
OCs	Osteoclasts
OPG	Osteoprotegerin
Osx	Osterix
P/S	Penicillin/streptomycin
PAF	Platelet-activating factor
PAMPs	Pathogen-associated molecular patterns
PBMC	Peripheral blood mononuclear cells
PBS	Phosphate-buffered saline
PCL	Poly(ε-caprolactone)
Pd	Palladium
PDGF	Platelet derived growth factor
PEG	Polyethylene glycol
PEM	Periosteum extracellular matrix
PFA	Paraformaldehyde
PGA	Polyglycolic acid
PGE2	Prostaglandin E2
PLA	Polylactic acid
PLCL	Poly(l-lactic acid-co-ε-caprolactone)
PLGA	Polylactic-co-glycolic acid
PMNs	Polymorphonuclear leukocytes

PMSF	Phenylmethylsulfonyl fluoride
RANK	Receptor activator of NF-κB
RANKL	receptor activator of NF-κB ligand
RANTES	Regulated upon Activation, Normal T cell Expressed, and Secreted
REE	Rare Earth Elements
RFU	Relative fluorescence units
RGD	Arginine-glycine-aspartic acid
ROIs	Reactive oxygen intermediates
ROS	Reactive oxygen species
rpm	Rotations per minute
RPMI	Roswell park memorial institute
RT	Room temperature
RUNX2	Runt-related transcription factor 2
SBG	Sub-micron bioactive glasses
sCD40L	Soluble CD40 ligand
SCSs	Silicified collagen scaffolds
SD	Standard deviation
SEM	Scanning electron microscopy
siRNA	Small interfering RNA
SLIT3	Slit guidance ligand 3
STAT	Signal transducer and activator of transcription
TA	Tannic acid
TARC	Thymus- and activation-regulated chemokine
TBS	Tris-buffered saline
TCP	Tricalcium phosphate
TGFβ	Transforming growth factorβ
TGFα	Transforming growth factor alpha
Ti	Titanium
TIMP	Tissue inhibitor of metalloproteinase
TiO_2	Titanium dioxide
TLR	Toll-like receptors
TNF	Tumor necrosis factor
VEGF	Vascular endothelial growth factor
Wnt	Wingless-related integration site
Zn	Zinc

ZnO	Zinc oxide
ZS/HA/Col	Zinc silicate/nanoHA/ collagen
ZS/PLGA/CP	Zinc silicate/poly(lactic-co-glycolic acid)/calcium phosphate cement

CHAPTER I

GENERAL INTRODUCTION

ABSTRACT

Bone repair/regeneration, after injury or biomaterial implantation, is a complex process where immune cells, particularly macrophages, play a crucial role that conditions tissue restoration and implant integration. The acute inflammatory response is important for adequate and complete bone healing upon injury, but chronic inflammation impairs bone health, with exacerbated/prolonged inflammation underlying most musculoskeletal diseases.

Herein, we start by a brief characterization of bone tissue and the process of bone modeling and remodeling. Fracture healing is discussed, with particular attention to the role of macrophages. Then, we give an overview of strategies for regeneration when fracture healing is impaired, and focus on biomaterial-based strategies for bone repair. This leads us to the inflammatory response to biomaterials, and the role of macrophages in this process is addressed.

Next, we focused our attention on immunomodulatory biomaterials, particularly those that are biodegradable (polymers, ceramics, metals and composites). We discuss their capacity to modulate macrophage polarization, as well as the impact of this process on MSCs. Particular attention is given to Fg and Mg based biomaterials.

Finally, the main aim and sub-aims behind the work developed in this thesis are presented.

1. BONE

Bone is a dynamic tissue, constantly being remodeled to repair small injuries and maintain homeostasis. Bone fractures are one of the most common injuries in humans, representing a major health problem worldwide and resulting in hospital admissions, morbidity and mortality, with well high economic costs [1]. For instance, in Europe fragility fractures alone are estimated to increase from 2.7 million to 3.3 million, from 2017 to 2030, with fracture related costs expected to increase by 27% on top of the €37.5 billion fracture related costs reported for 2017 [2].

While small bone defects can heal without scar formation, requiring only immobilization of the injury site [1, 3], in situations such as fractures or defects above critical size (e.g. those caused by trauma or tumor removal), infection, metabolic disease and aging, bone is not able to completely heal and leads to non-unions [3, 4]. Fracture non-unions, have an incidence estimated in 5-10% [5], remaining a major clinical orthopedic challenge. Their treatment can be prolonged and they may result in permanent disability, and decreased mobility and quality of life [4]. These data, paired with the reduced availability of autografts, highlights the need to design synthetic substitutes that are able not only to replace damaged tissue but also to stimulate the bone healing process.

The following sections briefly discuss bone tissue composition, as well as the bone remodeling and bone healing processes, conditioning the dynamic environment in which synthetic bone grafts will be placed.

1.1. Bone tissue

Bone is a dynamic tissue with crucial functions in the body, formed by specialized cells and a mineralized collagenous extracellular matrix (ECM). It provides structure and support for the body, allows for mobility, confers protection to soft tissues, serves as a mineral deposit and harbors the bone marrow [6-8]. Morphologically, two types of mature bone can be distinguished: cortical or compact bone (*compacta*) and trabecular or cancellous bone (*spongiosa*). Cortical bone is a dense bone that provides strength, while trabecular bone is a less compact and lighter bone with a porous sponge-like structure [7-9]. Molecularly, bone is constituted by an ECM composed by an organic phase, a mineral phase and water [7, 8]. Bone organic phase is primarily composed of type I collagen fibers [7, 8], combined with other collagens (collagen type II), proteoglycans and several non-collagenous proteins (NCPs) (including osteopontin, bone sialoprotein, osteocalcin and osteonectin [7, 10]). On

the other hand, the mineral phase of bone is formed by calcium phosphate, organized in hydroxyapatite (HA) crystals [7]. Bone's matrix arrangement and composition gives this tissue important mechanical properties such as strength and toughness. In particular, collagen fibril orientation has been shown to influence bone strength and fracture toughness [11]. Also, the normal carbonate substitution in bone apatite increases with age and leads to alterations in length and thickness of the bone mineral crystal. These increased substitutions lead to decreased bone toughness [11]

Bone tissue hosts different cells populations: osteoblasts, bone lining cells, osteocytes, osteoclasts and resident populations of macrophages, designated as osteomacs [12, 13]. Moreover, bone is also an enriched source of cytokines and growth factors produced by the cellular fraction, and acting in autocrine and paracrine ways [10, 14]. Osteoblasts (OBs) are cuboid cells responsible for new bone formation, depositing an uncalcified bone matrix (osteoid) and mineralizing it to become mature bone [15]. These cells derive from mesenchymal stem/stromal cells (MSCs), that commit to the osteogenic lineage through the up-regulation of pro- (bone morphogenetic proteins (BMPs), transforming growth factor-β (TGF-β)) and down-regulation of anti-osteoblastogenic factors (such as interleukin (IL)-1β and tumor necrosis factor-α (TNF-α) [15]. During osteoblastic differentiation MSC up-regulate the synthesis of BMPs, like BMP2, which enhances osteoblastogenesis by increasing the expression of runt-related transcription factor 2 (RUNX2), an essential transcription factor required for the proliferation of osteoblast progenitors [14]. OBs are located along the bone surface, organized in groups ranging from immature to mature cells. OB precursors (pre-osteoblasts), characterized by the expression of alkaline phosphatase (ALP), change from spindle-shaped osteoprogenitors to large cuboidal differentiated osteoblasts on bone matrix surfaces. Active mature osteoblasts are cuboid-shaped cells with large nuclei, prominent Golgi complex and extensive endoplasmic reticulum, that express osterix (Osx), secrete Col type I, together with other matrix proteins such as osteocalcin [15]. Therefore, mature osteoblasts, proceed from osteoprogenitor cells that have been stimulated to differentiate during the process of osteogenesis. The basic role of OBs includes the secretion of components of bone ECM, mainly collagen I, proteoglycans, osteocalcin and bone sialoproteins [13, 15]. Once OBs function is completed, these cells may undergo apoptosis or complete their life cycle by transforming into inactive quiescent bone lining cells or osteocytes [15].

Bone lining cells (BLCs) constitute a pool of flat-like shaped quiescent cells found lining the surface of the bone [16, 17]. They do not resorb nor form bone [17], but are pointed as capable of dedifferentiating back into osteoblasts [18], being reported as the main source

of osteoblasts in adulthood [16]. BLCs functions are related with matrix metalloproteinases (MMPs) production and receptor activator of NF-κB ligand (RANKL) generation, which will contribute to demineralized matrix removal before bone formation [16, 19, 20].

Osteocytes are the most abundant and long-lived (up to 25 years) cells in mature bone. They are enclosed and spaced regularly in the mineralized matrix in small cavities called osteocytic lacunae. These star-shaped cells have multifunctional roles in bone remodeling, regulating both osteoblasts and osteoclasts activity, and translating mechanical stimuli to chemical signals [21, 22]. Also, osteocytes were recently demonstrated has possessing the capacity to dedifferentiate back into mature osteoblasts [23].

Osteoclasts (OCs) are terminally differentiated multinucleated cells responsible for resorption of the mineralized bone matrix. Derived from hematopoietic progenitors, OCs share a common precursor with macrophages. OCs multinuclearity is related to their unique function of resorbing bone [24]. Osteoclastogenesis can occur via canonical and non-canonical pathways [25]. The interaction of receptor activator of NF-κB (RANK), expressed on the cell membrane of osteoclast precursors and mature osteoclasts, with its ligand RANKL, secreted by OBs, is considered the canonical and major pathway by which osteoclastogenesis occurs. The RANK/RANKL pathway is influenced by macrophage colony-stimulating factor (M-CSF), which is required for OCs proliferation. This pathway promotes the expression of RANK by OCs [24], and osteoprotegerin (OPG, a known osteoclastogenesis inhibitory factor) by OBs [24]. The ratio of RANKL and OPG regulates osteoclast activation and resorption [26]. Similarly to the canonical pathway, osteoclast formation through the non-canonical pathway is also regulated by the interaction of several factors mainly humoral (e.g. TNF-α, IL-1, TGF-β) which will substitute RANKL to promote osteoclastogenesis, particularly in diseases associated with pathological bone resorption [25].

OsteoMacs are tissue resident macrophages, integrated in the endosteal and periosteal space, described as immune surveillance cells in the bone microenvironment (detecting and responding to antigens) with fundamental roles in bone biology namely on osteoblast mineralization, bone modelling and remodeling [12, 27, 28]. Despite sharing a common precursor, OsteoMacs differ from osteoclasts in expression of Siglec 1 (or CD169), reported to be restricted to mature resident macrophages [29]. OsteoMacs have been shown to be involved in physiological skeletal remodeling [30], to help in the regulation and maintenance of hematopoietic stem cell niches [31, 32], and to promote intramembranous bone healing after fracture [7, 33].

1.1.1. Bone metabolism: modelling and remodeling

Bone is a metabolically active tissue that undergoes both modeling, to form new bone tissue, grow and change shape in response to physiological/mechanical stimuli; and remodeling, to preserve strength and maintain mineral homeostasis [34]. Contrarily to bone remodeling, in bone modeling the resorption and formation processes do not occur in a coupled anatomically or temporally manner, but in an independent manner [35, 36]. Modeling refers to the formation of bone (called formation modeling and carried out by osteoblasts) or to its resorption (called resorptive modeling and carried out by osteoclasts) [35, 36]. Bone modeling functions include increase and maintenance of bone mass and alterations in the shape of bone, occurring predominantly in childhood [34, 35].

Throughout adulthood, bone is constantly being remodeled to repair small injuries and preserve homeostasis, maintained by bone resorption (destruction) and formation (rebuilding) [34]. Bone remodeling is performed by local teams of bone-resorbing osteoclasts, bone-forming osteoblasts and osteoprogenitor reversal cells arranged in a structure known as “basic multicellular units” (BMUs) [37]. BMUs have different morphologies in trabecular and cortical bone. In trabecular bone, BMUs are localized on the surface and are covered by a “roof”-like structure called the canopy (an envelope made of cells from the OB lineage and rich in blood capillaries), above the remodeling site. In cortical bone BMUs comprises a “cutting zone” led by OCs that proceed resorbing bone and are immediately followed by OBs. As resorption occurs, the space is filled by blood vessels, nerves and connective tissue [37]. Bone remodeling functions include the preservation of bone mechanical strength, bone health (repair of damaged; replacement of old osseous tissue) and mineral homeostasis [34, 38].

1.2. Bone Healing

Upon injury, bone is able to heal without scar formation. However, when the lesion is too large (“critical-sized”) healing is compromised [39, 40]. Bone tissue repair and regeneration is reported to occur along a tightly orchestrated cascade of events divided in three overlapping phases: inflammation, repair and remodeling (Fig. 1).

It has long been considered that the immune system plays important roles in bone fracture healing, with inflammatory cells modulating bone cells and vice-versa [39, 41]. The research field osteoimmunology, coined in 2000 by Arron and Choi, focuses on the tight interaction/interplay between skeletal and immune systems [42]. Bone tissue and immune system share physical space, the bone marrow microenvironment harbors the

hematopoietic stem cell's niche; cells: OCs have hematopoietic origin and share precursors with monocytes/macrophages; and many mediators: several cytokines and growth factors are produced by, and act on, both systems [43].

The critical role of immune cells and their cytokines during bone healing is widely recognized, but the mechanisms involved remain under investigation [44]. Immune cells are fundamental throughout fracture healing; yet most of their activity occurs at early stages of this process [45]. While an initial transient stage of acute inflammation is necessary for a precise fracture healing, prolonged chronic inflammation can be detrimental to healing [46], leading to bone destruction in several pathological scenarios, as reviewed by Tsukasaki and Takayanagi [41].

Upon injury, there is a local disruption of bone tissue, surrounding soft tissue and blood supply, leading to cell death and release of danger signals that trigger an acute inflammatory response, crucial for starting the regenerative process [47]. The acute inflammatory response peaks within the first 24h and is normally resolved after 14 days [48]. The blood coagulation cascade is activated, fibrinogen is converted to fibrin by thrombin, and hematoma is formed. The fracture hematoma microenvironment houses blood-derived inflammatory cells and acts as the future template for callus formation [45]. Platelets, neutrophils, natural killer (NK) cells and monocytes/macrophages are the first intervenients to be recruited to bone injury site, invading the hematoma [45, 49]. Neutrophils together with macrophages remove dead cells and debris and release factors that promote the recruitment of MSCs from the periosteum and bone marrow [45, 49].The most relevant secreted soluble factors include IL-1, IL-6, TNF-α, IL-8, IL-11, M-CSF, RANKL, TGF-β and BMPs [45, 50-52]. Hematoma is then reorganized, being gradually replaced by granulation tissue. Once attracted to the local, MSCs, undergo either osteogenic or chondrogenic differentiation to become bone-forming OBs and cartilage-forming chondrocytes [49]. In the later stages of the inflammatory response T cells (secreting RANKL that recruits, differentiates and activates OCs) and B cells (producing OPG that regulates osteoclastic differentiation and activity and helps to suppress pro-inflammatory signals) are recruited to the local, infiltrating the fracture callus [53].

In osteochondral bone formation and repair, callus formation starts at the end of the inflammatory phase. Growing from the periphery to the center of the fracture, chondrocytes drive cartilage formation (cartilaginous callus formation) [51]. Once the fracture gap is bridged by cartilaginous callus, chondrocytes enter terminal differentiation, resulting in hypertrophy and the production of mineralized cartilaginous matrix [49]. At this stage, fracture site becomes stable and the cartilaginous callus is invaded by endothelial cells that

will form new blood vessels [45, 46]. Upon calcification of the fracture callus (bony callus formation), monocytes and MSCs are recruited from the periosteum, bone marrow, vasculature, and surrounding tissue to differentiate into osteoclasts and osteoblasts, respectively [54]. Soft callus establishment and maturation involves the presence and communication of several growth factors: TGFs – synthesize BMPs and attract MSCs, pre-OBs, OBs and chondrocytes; BMPs - regulate OBs and chondroblasts growth, differentiation and apoptosis and stimulate synthesis and secretion of insulin-like growth factor (IGF) and vascular endothelial growth factor (VEGF); fibroblast growth factor (FGF) - 1 and IGF-II – influence chemotaxis, proliferation and differentiation of progenitor cells into osteoblasts or chondrocytes; M-CSF, RANKL, OPG and TNF-α - to initiate mineralized cartilage resorption and help in the recruitment of bone cells [54].

The last stage in bone healing is the remodeling phase. The original structure and function of the bone (cortical and/or trabecular) is restored by the conversion of the typically irregular newly deposited bone (composed by randomly oriented collagen fibrils) into lamellar bone (composed by collagen fibrils clustered in parallel arrays). This process is driven by the concerted action between OCs and OBs, through bone resorption and formation, respectively. During bone resorption, OCs release factors trapped on site such as TGF-β, while producing other factors as Wnt (Wingless-related integration site) 10b, BMP6 and Slit guidance ligand 3 (SLIT3). This production is an important indicator for the promotion of bone formation [49].

In summary, numerous cell types participate in fracture healing and bone repair [49]. In particular, immune cells, which constitute the initial cellular component of the fracture environment, play a significant role as an immune response is crucial for a proper bone healing [44]. The effects of immune cells extend beyond the early stages of fracture healing (Fig. 1), despite the short duration of the inflammatory response [45] Taking this into account, Loi et al. [39] modified the “Diamond Concept” (a conceptual framework that states factors that are mandatory for successful bone healing) in order to include the immune cells and their mediators as a crucial factor for fracture healing [44].

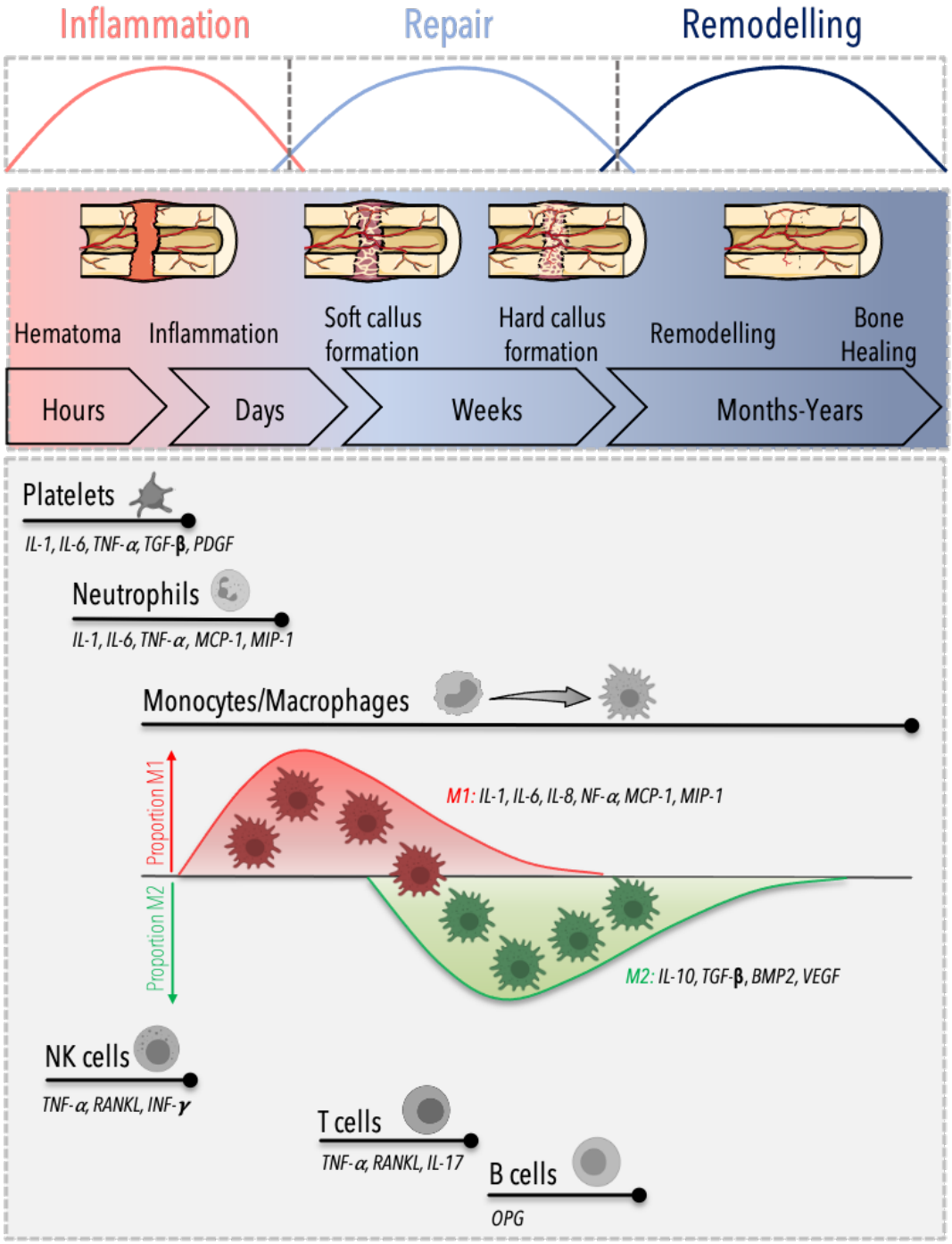


Fig. 1: Illustration of immune cells contribution to fracture repair. This process can be divided into three phases (inflammation, repair and remodeling) where immune cells participate actively particularly occurring during early stages. Adapted from [45, 46, 55]. Graphical content from Biorender and SmartServier.

1.2.1. The role of macrophages in fracture healing

Macrophages are one of the first cell types to arrive to the injury site, assuming an important role in the communication with bone tissue cells as the inflammatory response to bone injury progresses. Bone tissue contains two major distinct populations of macrophages: recruited and resident macrophages, known as OsteoMacs [56, 57]. There are different opinions among the scientific community regarding the origin of tissue resident macrophages [58]. It is believed that tissue-resident macrophages are a very heterogeneous group of cells with diverse origins in mammals including yolk sac, fetal liver and bone marrow [59]. On the other hand, monocyte-derived macrophages are recruited from blood to the bone by inflammatory mediators [60], upon injury and in inflammatory conditions [57, 61]. While monocyte-derived macrophages support the inflammatory and early repair phases [57], OsteoMacs are critical in late repair and remodeling phases [29].

The importance of macrophages in bone healing upon injury is currently under investigation [62]. Using the macrophage-Fas induced apoptosis (MaFIA) transgenic mice, Vi et al. [63] showed that the complete absence of macrophages led to early skeletal growth retardation, reduction on MSCs and their ability to differentiate towards osteoblasts. The same study, also showed, in a tibial fracture model, that the depletion of macrophages resulted in reduced callus formation and bone deposition, and increased fibrotic tissue [63]. Batoon et al. [29] showed that OsteoMacs depletion (using the CD169-DTR knock-in mouse model system) compromised bone repair in two models of bone injury that heal via either intramembranous or endochondral ossification. Besides stressing OsteoMacs importance for osteoblasts maintenance, the authors highlighted the importance of macrophages in the process of bone healing via intramembranous or endochondral ossification [29].

It has been known for several decades that bone repair pace declines with age, slowing after skeletal maturity [64]. More recently, following from parabiosis experiments that showed aged mice rejuvenation when exposed to young circulation [65], Vi et al. [66] demonstrated that macrophages from young animals were implicated in bone repair rejuvenation. This rejuvenation was shown to be associated with the factors produced by these cells. Lipoprotein receptor-related protein 1 (LRP1), produced by young macrophages and with known roles in OBs and OCs function, was found differentially expressed between young and old macrophages. Indeed, the treatment of old mice with LRP1 showed to improve bone repair [66].

Previous work by us and others reported the capacity of immune cells, including dendritic cells (DCs) [67], NK cells [68] and macrophages [63, 69-71] to recruit MSCs via paracrine

factors [67, 68, 72] and to promote their differentiation into osteoblasts [63, 69-71]. For macrophages, while some studies point out the role of the classically activated (M1) macrophages [70, 72] in stimulating MSC differentiation towards the osteogenic lineage, others attribute this function to the alternatively activated (M2) macrophages [69, 71, 73]. As recently reviewed by Pajarinen et al. [74] these differences might be dependent on the design of the study. Another possibility is that all macrophage phenotypes are able to promote osteogenesis, being more or less efficient according to physiological and pathophysiological states.

Additionally, an equilibrated macrophage M1/M2 balance and transition from M1 to M2, which will be further addressed below, is reported to be essential for a successful fracture healing resolution [75]. Macrophage M1 polarization is related to early stages of the inflammatory response (clearing of debris and dead cells) while M2 polarization is associated to inflammation resolution and promotion of tissue regeneration [76-78]. In fact, Löffler et al. [79] showed that an impaired M2 macrophage function, due to aging, compromised bone healing in aged rats, resulting in a diminished revascularization of the bone callus

In summary, macrophages are found throughout all phases of bone healing and thus represent a promising cellular target to improve bone repair/regeneration. However, further research is needed to decipher the underlying cellular and biological mechanisms of macrophage function [62], including their contribution to bone healing, and graft or biomaterial integration.

2. BONE REGENERATION STRATEGIES: BIOMATERIALS AS BONE GRAFT SUBSTITUTES

Current therapeutic approaches to promote bone regeneration involve the implantation of grafting material to support and stimulate the bone healing process [3, 80]. Bone autografts are regarded as the “gold standard” therapeutic approach since they contain viable osteogenic cells and bone matrix proteins which enhance its osteoconductive and osteoinductive properties. However, autografts have limited availability, high morbidity at the donor site and require a second surgical intervention. An alternative solution such as allografts or xenografts carries the risk of immunogenicity and disease transmission [3, 80].

To surpass the drawbacks from both auto and allografts, biomaterials, either non-biodegradable or biodegradable, have been development to support and stimulate bone

healing [3, 80]. Currently, permanent non-degradable materials, such as titanium and its alloys and cobalt-chromium-based alloys (Co-Cr), constitute the vast majority of implants used in the musculoskeletal system. Despite considerable developments in biomaterials, coatings and surgical techniques, to increase their durability, they can have important drawbacks. A second surgery is required for removing such implants in young still growing patients, and permanent prosthesis can suffer wear, releasing debris, which promote chronic inflammation and aseptic loosening, requiring a revision surgery [81]. These procedures decrease patient's quality-of-life and productivity, increasing health care costs.

Despite the intense research on biomaterials for bone repair/regeneration, the optimal biomaterial for bone regeneration is still matter of intense debate [3, 82]. Scaffolds, produced with a wide variety of biomaterials and manufactured using different techniques, act as a template to provide the structural support for tissue repair [80, 83]. Ideally, a scaffold for bone tissue engineering should meet the following requirements: biodegradability, biocompatibility, mechanical stability, porosity, combine good resorptivity with osteoconductivity (ability to promote vascular growth and allow free proliferation of bone cells) and osteoinductivity (ability to promote osteoblastic differentiation and new bone formation) [84]. Albeit several biomaterial-related factors including composition, surface topography, degradability and mechanical properties are crucial, the critical determinant of a biomaterial clinical outcome is the host response to the construct itself [85, 86].

2.1. Inflammatory response to biomaterials

The host response to tissue injury, including that caused during biomaterial implantation, and to the material itself begins immediately upon implantation. Both nondegradable and degradable biomaterials are recognized by the host's immune system as a foreign body triggering an inflammatory response named foreign body reaction (FBR) [87]. Biomaterial-host initial interactions are shared among degradable and nondegradable materials [87] and include protein adsorption, neutrophil recruitment and monocyte/macrophage recruitment. Non-degradable biomaterials typically lead to a FBR that results in the macrophage fusion into foreign body giant cells (FBGCs) and eventually fibrotic encapsulation (Fig. 2). On the other hand, degradable biomaterials are not as susceptible to such encapsulation, being more often integrated in the surrounding tissue [88, 89].

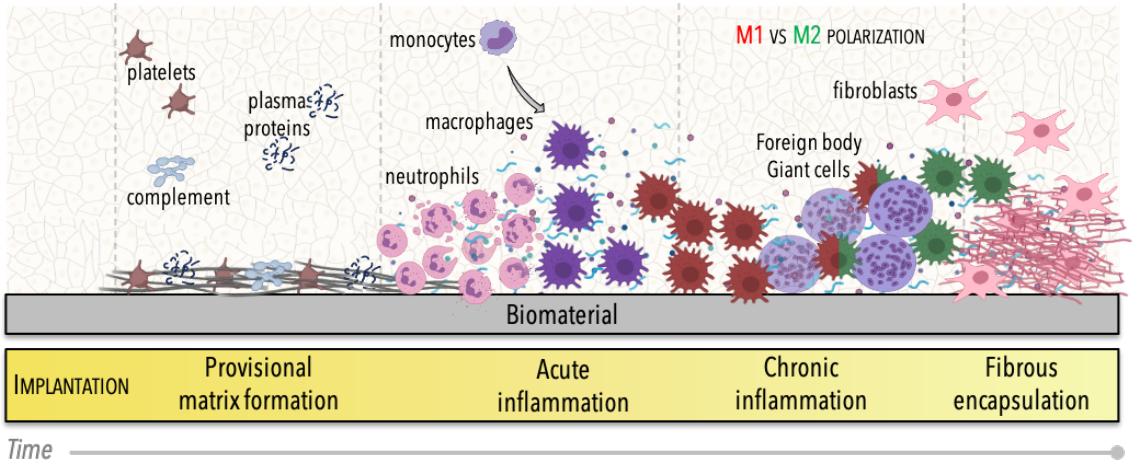


Fig. 2: Time course of the host response after biomaterial implantation. Almost immediately after biomaterial implantation proteins adsorb to biomaterial surface. This layer of adsorbed proteins will define the initiation of the coagulation cascade, complement system, platelets and immune cells leading to the formation of a transitional fibrin matrix at the implant site. Acute inflammation is marked by the presence of neutrophils and some monocyte infiltration and differentiation into macrophages. Chronic inflammation follows acute inflammation, and the macrophage is the central cell type of this phase. Smaller particles are usually phagocytized while larger particles stimulate macrophages to form foreign body giant cells (FBGCs). There is a fibrous encapsulation around the biomaterial due to fibroblast recruiting factors secreted by FBGCs resulting in its activation and collagen deposition. Adapted from [90, 91]

Acute inflammation begins immediately after implantation, the vascular system undergoes changes in the flow, caliber and permeability, leading to exudation of fluid, proteins and blood cells to the injured site and blood clot formation and/or thrombosis [85, 92]. The surface of the biomaterial is then coated with blood and plasma proteins (fibrinogen, fibronectin, vitronectin, among others) in a process known as the Vroman effect [85, 92]. In this layer, proteins are likely to suffer conformational changes upon interaction with the biomaterial surface. This process leads to the activation of the coagulation cascade, complement system, platelets and immune cells [93]. Altogether, these interactions allow the formation of a transient provisional matrix composed of a fibrin network (resultant from fibrinogen cleavage by thrombin) and inflammatory mediators [85, 92]. This provisional matrix will serve as a naturally derived and biodegradable system that bridges and mediates the interaction between the host tissues and the biomaterial [93]. In addition, endogenous danger signals (danger-associated molecular patterns – DAMPs), equivalent of pathogen-associated molecular patterns (PAMPs), are released from injured cells. DAMPs are capable of recruiting and activating different immune cells such as neutrophils, monocytes/macrophages and DCs. DAMPs recognition by these cells occurs primarily through Toll-like receptors (TLR)-2, 4 and 9 [94, 95]. Central to acute inflammation is the recruitment and activation of neutrophils (polymorphonuclear leukocytes, PMNs) [96, 97]. In response to chemotactic factors, neutrophils migrate from the vasculature to the tissues

and constitute the predominant cell type during the first days following injury and exposure to a biomaterial [98]. Neutrophils are short-lived, with a half-life around 8-20h, in circulation, and 1-4 days, after migration into tissues [99]. Different programs of cell death can be triggered by neutrophils (as recently reviewed by Pérez-Figueroa et al. [99]) to give way to a population of macrophages [89]. Neutrophils play important roles in the immune response by initiating a phagocytic response, releasing proteolytic enzymes and reactive oxygen species (ROS) [99]. These cells are able to crosstalk and modulate the recruitment of monocytes, macrophages, immature DCs and lymphocytes, through the release of several cytokines, chemokines and growth factors (as recently reviewed by Tsai et al. [100]).

Acute inflammation is followed by chronic inflammation, which starts 4-7 days after biomaterial implantation, and is characterized by the presence of monocytes, macrophages and lymphocytes, as well as the formation of blood vessels and production of connective tissue [92]. Upon emigration from the vasculature, monocytes differentiate into macrophages. Depending on the type of biomaterial and its properties, monocyte migration and differentiation into macrophages may continue for days or even weeks, particularly for non-degradable biomaterials, ultimately determining variations in the intensity and duration of the inflammatory response [92].

2.1.1. Relevance of macrophages in a biomaterials context

Macrophages are considered the most important cell type in chronic inflammation, being involved in the recognition, degradation and/or phagocytosis of degradable biomaterials, with or without FBGCs involvement. On the other hand, non-degradable biomaterials can lead to continuous infiltration of macrophages, that engulf micro- and nanoparticles, as well as metallic ions generated by the wear and corrosion of the materials, and perpetuate inflammation [101]. Granulation tissue formation, characterized by the proliferation of fibroblasts, synthesis of collagen and proteoglycans and angiogenesis, is also initiated by the action of macrophages [86]. Moreover, macrophages produce a great number of biologically active mediators (cytokines, chemokines, growth factors, reactive oxygen metabolites, coagulation factors, complement components), modulating the inflammatory process and repair [55]. The ability of macrophages to engulf implant-released particles is size dependent. Particles smaller than 10 μm may be phagocyted. When the particle size is larger than 10 μm and smaller than 100 μm, macrophages fuse into multinuclear cells, known as FBGCs, in an attempt to engulf and digest particles [101]. When particles are large enough to prevent phagocytosis, a phenomenon called “frustrated phagocytosis”

occurs leading to the release of mediators of degradation, such as reactive oxygen intermediates (ROIs), enzymes and acid, by macrophages and FBGCs to help the unsuccessful degradation [101]. During this stage, FBGCs secrete fibroblast recruiting factors, resulting in collagen deposition and leading to fibrous encapsulation of the biomaterial and its isolation from the local tissue environment [102]. The role of M1 and M2 macrophages in the fibrous encapsulation of biomaterials has been recently reviewed by Witherel et al. [102].

It has been highlighted that modulating inflammation is a better solution than preventing it, as the initial phase of inflammation is fundamental for healing [103]. The role of macrophages has been vigorously investigated in the context of the response to biomaterials [104]. Whether macrophage participation results in a positive or negative outcome is largely context-dependent, varying with microenvironmental cues that may be biomaterial-dependent [105]. The downstream functional success of implanted biomaterials is dependent on the ability of the host innate immune system to resolve a polarized macrophage response resulting from implantation in a complex microenvironment [105].

Macrophages are highly plastic cells whose phenotype will greatly depend on the surrounding microenvironment, being a continuum ranging from M1 to anti M2 phenotypes [55, 78]. The M1 phenotype (stimulated by TLR agonist, such as lipopolysaccharide (LPS), often accompanied by the Th1 cytokine interferon gamma (IFNγ)) is characterized by the secretion of inflammatory cytokines (e.g. TNF-α, IL-1β, IL-6) and generally identified by increased levels of major histocompatibility complex (MHC)-II, CD86, C-C chemokine receptor type 7 (CCR7), human leucocyte antigen DR (HLA-DR), TLR2, TLR4 at the cell surface [106-109]. On the other hand, the M2 phenotype (stimulated by IL-10 or IL-4) is characterized by the secretion of anti-inflammatory mediators and growth factors like IL-10 and TGF-β, respectively. Importantly, M2 phenotype encompass a range of different subsets (M2a, M2b, M2c, M2d and M2eff) with diverse functions [55]. M2a macrophages are pro-fibrotic, expressing CD206, CD163 and MHC-II in their surface, and secreting IL-10, TGF-β and IL-1Ra [107-111]. M2b are involved in T helper 2 activation, expressing CD86, MHC-II in their surface and secrete TNF-α, IL-1, IL-6 and IL-10 [107, 109, 112]. M2c are pro-healing/tissue remodeling and express CD163, CCR2, TLR1, TLR8 in the surface, secreting IL-10 and TGF-β [107, 109, 113-115]. M2d are tumor associated macrophages that secrete IL-10 and TGF-β (no known cell surface markers) [107, 116]. M2eff exhibit anti-inflammatory functions and secrete TGF-β, prostaglandin E2 (PGE2) and platelet-activating factor (PAF) (no known cell surface markers) [108, 117]. While this nomenclature works well for macrophages induced by defined mediators *in vivo* macrophages are not shaped

by individual cytokines but rather by the combination of the signals/cues present in the surrounding environment [118, 119].

In the context of biomaterial implantation, it has been shown that biomaterials properties directly impact macrophage polarization [103]. Biomaterial surface topography is reported to affect the macrophage adhesion and differentiation. Vassey et al. [120] demonstrated that larger and more disperse micro-pillars driven a M1 phenotype and smaller, dense micro-pillars promoted a M2 phenotype. Another biomaterial feature that influences macrophage polarization is porosity and pore size. Garg et al. [121] tested the effect of fiber and pore size of electrospun scaffolds on macrophage polarization and showed that increased pore sizes were correlated with increased expression of M2 associated markers and decreased expression of M1 markers. Biomaterials chemical properties such as surface charge and hydrophilicity have been also shown to impact macrophage adhesion and polarization. Hotchkiss et al. [122] addressed the effect of hydrophobic and hydrophilic smooth/microrough/nano-and micro-rough titanium on macrophage polarization, showing that hydrophilic rough titanium induced a M2 macrophage polarization. Regarding the effect of biomaterials surface charge on macrophage polarization, Lee et al. [123] showed that the chemical modification of titanium implant surfaces with calcium and strontium divalent cations induced a M2 macrophage phenotype. Besides biomaterials physical and chemical properties, biochemical properties (e.g. synthetic vs natural biomaterials) also play an important role in directing macrophage polarization. Sadtler et al. [124] showed that biologic scaffolds (extracellular matrix, ECM, derived from urinary bladder tissue) increased the expression of M2-associated markers as opposed to synthetic scaffolds (polyethylene, PE and polyethylene glycol, PEG), shown to inhibit CD206 expression.

Overall, the studies discussed above demonstrate that macrophage-biomaterial interactions could provide a basis for macrophage phenotype regulation and thus be considered a strategy to be explored in biomaterial design.

3. IMMUNOMODULATORY BIOMATERIALS - EMERGING TREND IN BIOMATERIAL DEVELOPMENT

The recent appreciation for the roles that innate immune cells, particularly macrophages, play in tissue repair and biomaterial integration contributed to a change in the paradigm of the initially designed biomaterial-based therapies, which were intended to minimize the host inflammatory response [105, 125, 126]. The paradigm shift from “fighting” to “modulating” inflammation is a hot topic in the biomaterials field. The recognition that inflammation and

tissue regeneration are tightly linked and that the interactions between biomaterials and immune system are fundamental for tissue repair, motivated this change and prompted the development of immunomodulatory biomaterials [125, 127-129].

The concept of immunomodulatory biomaterials applies to those able to modulate the naturally occurring inflammatory and immune responses, by interacting with and conditioning the activity of immune cells to promote or facilitate a desired state or phenotype [125, 127-129]. Several strategies have been explored in biomaterial-based immunomodulation, and many of these strategies are focused on the modulation of macrophage polarization. This is because macrophages are highly plastic cells that play a central role in regulating multiple phases of the host response to biomaterials and the tissue repair process [55, 104].

Alterations of biomaterials physicochemical properties has led to some promising outcomes. Chen et al. [130] modified the surface chemistry (amine or acrylic acid) and nano topography (16, 38 and 68 nm) to manipulate macrophage response. Authors showed that the amine chemistry led stronger in modulating macrophage polarization towards a M2 phenotype in comparison with acrylic acid chemistry (increased expression of CD206 and decreased expression of CD11c and CD86). Together with surface chemistry, authors also explored the effect of surface nano topography on the modulation of macrophage polarization and concluded that the addition of nano topographies of 16, 38 or 58 nm inhibited macrophage pro-inflammatory response (decreased expression of CD86, CD11c,TNF-α, IL-6, IL-1β). Lv et al. [131] showed that hydrophilic titanium surfaces downregulated M1 surface markers expression (CCR7, CD11c) and upregulated M2 surface markers (CD163, CD206), in comparison to hydrophobic ones. Zhu et al. [132] evaluated the effect of honeycomb-like titanium surface structures, ranging from nanometer to micrometer scale, on macrophage polarization. Results showed that the smaller scale of titanium honeycomb was corelated with decreased proportion of M1 $CCR7^+$ macrophages and increased proportion of M2 $CD206^+$ macrophages.

Scaffold functionalization, through the inclusion of bioactive molecules including cytokines or RNA-based molecules (gene activating scaffolds) can provide more precise molecular control to immunomodulatory strategies. In tissue regeneration this strategy is being researched to promote macrophage polarization shift from M1 to M2. Yin et al. [133] developed a system of alginate/chitosan multilayer films on IL-4 loaded titania nanotubes to achieve a controlled release of this cytokine. Authors showed that this system had the potential to convert macrophage phenotype from M1 to M2, downregulating the expression of CCR7 and increasing the expression of CD206. Yin et al. [134] designed a biomimetic

anti-inflammatory nano-capsule (membrane coated gold nanocage load with resolvin D1) and showed that it promoted macrophage polarization towards a M2 phenotype (increased expression of IL-10 and TGF-β and decreased expression of IL-6), by the controlled release of resolvin D1. Castaño et al. [135] demonstrated that antagomiR-133a loaded collagen-nHA scaffolds significantly accelerated and enhanced bone repair in a rat calvarial defect. Interestingly, antagomir-133a treatment showed an association with enhanced levels of M2 pro-remodeling $CD206^{+}$ macrophages.

The use of decellularized extracellular matrix (dECM) and/or its components is another way to generate immunomodulatory biomaterials. dECM-based biomaterials were shown to shift macrophage polarization from a M1 to a M2 phenotype [136, 137]. Sadtler et al. [138] showed that dECM scaffolds (obtained from bone- and cardiac muscle-derived tissue) elicited a pro-regenerative response, which was driven by Th2 responses and consequent guided IL-4 dependent macrophage polarization. The different immunoregulatory properties of dECM components have been reviewed by Garcia-Garcia and Martin [139]. Different approaches to engineer ECM to be able to modulate macrophage polarization are also suggested by the authors [139].

Hence, immunomodulatory biomaterials are increasingly seen as a powerful strategy to create a local niche that controls the biomaterial-induced inflammatory response and drives it towards tissue regeneration [125, 140].

3.1. The promise of Immunomodulatory Degradable Biomaterials for Bone Repair/Regeneration

In the context of bone repair/regeneration the ideal biomaterial was defined as providing mechanical support and having osteoinductive and conductive properties. In recent years the capacity to promote an appropriate immune response, that is strong but timely controlled, shifting from pro-inflammatory to anti-inflammatory was added as a desirable property for bone repair/regeneration biomaterials [141]. Numerous studies have been carried out on the osteogenic capacity of biomaterials intended for bone repair/regeneration [142-144]. Yet, a comprehensive and systematic understanding on the impact of material-regulated macrophage responses and the impact of the observed immunomodulation on their crosstalk with MSCs is still lacking.

Degradable biomaterials have aroused great interest in many researchers, because they bring the possibility to fabricate temporary medical implants that avoid the potential long-term effects associated with non-degradable ones, like FBR and fibrous encapsulation

[145]. Thus, designing immunomodulatory pro-regenerative microenvironments, by means of bioactive, biocompatible and degradable biomaterials, is being explored as a strategy, to increase patient's quality-of-life [146]. When designing degradable biomaterials, important requirements must be considered. The material should possess a degradation time that matches with their function, appropriate mechanical properties for its intended use as well as the production of nontoxic degradation products that can be readily resorbed or excreted [146, 147].

The next sections make a brief characterization/overview of each class of biodegradable materials most used for bone repair/regeneration (natural and synthetic polymers, ceramics, bioactive glasses, metals and composites). Then, the current knowledge of their immunomodulatory role/effect on macrophage phenotypic profile will be discussed. The role of material-regulated immune/macrophage responses in material-induced osteogenesis will also be mentioned. Particular attention will be paid to fibrinogen and magnesium as these were the materials studied under the scope of this thesis.

3.1.1. POLYMERS

Polymers are organic carbon (C)-based materials. Essentially, polymers are long chains of C atoms connected to/with other atoms such as hydrogen (H), oxygen (O), and nitrogen (N) [148]. This class of materials can be divided into synthetic or natural polymers [146].

Among biodegradable synthetic polymers, the most extensively studied are Poly(ε-caprolactone) (PCL) and aliphatic polyesters including polylactic acid (PLA), polyglycolic acid (PGA) and polylactic-co-glycolic acid (PLGA) [149]. Synthetic polymers can be produced under controlled conditions, thus being more reproducible when compared to natural ones. The desired mechanical properties, and degradation rates can be achieved by altering chemical composition, molecular weight and distribution of the functional groups of polymers [149]. However, their lack of cellular recognition and adhesion sites, low osteoconductivity and possible adverse reaction of the tissue due to acid degradation products, impose limitations on their use. The most widespread strategy to increase the scaffold bioactivity involves their combination with other materials such as from the family of bioceramics [149]. Various studies reported the capacity of synthetic polymers, including PCL [150, 151], poly(l-lactic acid-co-ε-caprolactone) (PLCL) [152] and PGA [153], to polarize macrophages towards a M2 phenotype. This was achieved by varying biomaterials properties such as topography [151], nanofiber arrangement (aligned versus random) [152] and degradation rate [153].

Natural polymers, including proteins and polysaccharides, have been extensively studied as materials for bone repair/regeneration due to their natural origin, similarity with native ECM, presence of cell recognition and adhesion sites, which helps cell adhesion and function. Increasing evidences highlight the potential for natural polymers, such as collagen, chitosan, alginate, dECM and fibrinogen/fibrin on the modulation of macrophage polarization. However, their use for bone applications is hindered to some extent due to their poor mechanical properties, high water solubility and possible immunogenicity [146, 154]. Thus, to improve the performance of natural materials particularly regarding their mechanical properties and high water solubility, several crosslinking strategies have been developed. The combination of these materials is another possibility being researched [146, 154] . Thus, it is not surprising to often find natural polymers combined with other biomaterial classes, to gain enhanced control towards complete bone healing.

Collagen (Col) is a fibrous protein that accounts as the major organic component of natural bone. One of the major drawbacks of Col is the low mechanical strength, being necessary the use of other biomaterials to tackle collagen limitations. Its combination with bioceramics (Calcium/Phosphate (CaP)-based compounds), generating a composite (further explored below), is one of many strategies used to enhance mechanical properties [146, 154]. Col finds several applications for bone repair and regeneration in the form of carriers for the delivery of bone morphogenetic proteins [155, 156]; as RNA-based scaffolds (topic recently reviewed by Leng et al. [157]; and clinically-used membranes for guided bone regeneration (topic reviewed by Sbricoli et al. [158]). Either alone or in association with other compounds (e.g. chondroitin sulfate and epigallocatechin-3-gallate), Col has been shown to modulate macrophage phenotype [159-161]. Sridharan et al. [161] showed a correlation between macrophage response and collagen scaffold crosslinking method. Specifically, while N-(3-Dimethylaminopropyl)-N′-ethylcarbodiimide hydrochloride (EDAC) crosslinking agent increased pro- and anti-inflammatory response to M1 and M2 factors, respectively, genipin suppressed this response. Larsen et al. [162] disclosed that variations in Col density affects macrophage immunomodulatory profile. High collagen density was shown to induce tumor-associated macrophages towards an immunosuppressive phenotype. By using Col type I scaffold functionalized with chondroitin sulfate, Taraballi et al. [159] were able to modulate macrophage phenotype *in vitro*, decreasing the expression of pro-inflammatory markers and increasing the expression of anti-inflammatory ones. *In vivo*, and in agreement with *in vitro* studies, collagenous scaffolds led a significant downregulation on the expression of pro-inflammatory genes. Similarly, Chu et al. [160] demonstrated that collagen membranes (commercial bio-membrane heal-all®) modified with epigallocatechin-3-gallate (EGCG)

downregulated the secretion of pro-inflammatory mediators, in *vitro* and in *vivo*, and promoted the recruitment of M2 macrophages.

Chitosan (Ch) is a chitin-derived positively charged polysaccharide. This polymer is very versatile and can be used as microspheres, membranes, sponges, fibers and porous scaffolds [163]. Like all natural polymers, Ch also has poor mechanical strength [154], and its combination with other biomaterials is being researched as a strategy to overcome it. Similarly to Col, Ch has also been investigated for bone repair/regeneration, mainly in combination with materials from other classes. Because Ch favors calcium/phosphate ion accumulation its combination with CaP-based compounds reveals to be of high interest to enhance biomineralization, thus promoting bone repair/regeneration. [164]. Another quite interesting characteristic of Ch is the degree of acetylation (DA), i.e. proportion of N-acetyl-D-glucosamine units with respect to the total number of units. DA has showed to influence physicochemical properties such as surface charge [165] and also the biological properties such as alterations in osteoblast morphology and proliferation [166], and more or less severe inflammatory responses depending on Ch DA. Barbosa et al. [167] showed that Ch DA15% induced a more intense inflammatory response (highest leukocytes numbers at the implant site) when compared with Ch DA4%. In the particular case of macrophage response to Ch with different DA, Vasconcelos et al. [168], showed that lower Ch DA (5%) produced a macrophage M2 response, whereas higher DA (15%) had the opposite effect, triggering a macrophage M1 response. Later, Vasconcelos et al. [169] demonstrated that by incorporating pro-resolution lipid mediators (lipoxin A4 and resolvin D1) into Ch scaffolds with DA15%, it was possible to modulate macrophage polarization towards a M2 phenotype. Authors further demonstrated that macrophage NOD-like receptor containing pyrin domain 3 (NLRP3) inflammasome activation was impaired in Ch scaffolds with 4% and 15% DA [170].

Alginate (Alg) is a negatively charged natural occurring polysaccharide with gaining importance in bone tissue engineering due to its gel forming properties, and simple gelation methods. Also, Alg is resistant to acidic conditions, injectable and easy of functionalize [149, 154]. Besides gels, Alg can also be shaped to form fibers, films, multilayers and nanoparticles. The difficulty in sterilization together with poor mechanical properties are its main disadvantages. The last one can try to be improved by crosslink strategies [149, 154]. Unless functionalization is performed (e.g. grafting of arginine-glycine-aspartic acid (RGD) peptides to the polymer backbone [171]) cells are not able to specifically interact with Alg network. Like other natural polymers, Alg is also investigated in the context of bone repair/regeneration, either alone [172] but mostly in combination with other materials [171,

173, 174]. Focusing on Alg own ability to modulate macrophage polarization, Jain et al. [175] demonstrated that targeted alginate nanoparticles loaded with IL-10 plasmid DNA were able to re-polarize macrophages from M1 to M2. Kerschenmeyer et al. [176] showed that sulfated alginate derivatives promoted a M2-like phenotype together with a decreased expression of pro-inflammatory markers in human THP-1 macrophages.

Decellularized Matrices (dECM) are prepared by the removal of tissue cellular component while maintaining the biochemical composition and structure of ECM [177]. The incomplete removal of the cellular components is a major issue when preparing decellularized structures because these can cause an immunogenic response. Nevertheless, ECM-derived materials have been shown to establish a pro-healing microenvironment with interesting results upon-recellularization and *in vivo* implantation [177]. In the context of bone repair/regeneration, Bracey et al. [178] showed that decellularized bone scaffolds from the femur of pigs allowed for spontaneous new bone formation and blood vessel formation, upon being subcutaneously implanted in mice. More recently, Lee et al. [179] demonstrated that the implantation of a decellularized bovine bone ECM, in mouse calvarial defects, improved bone formation and density, when compared with demineralized bone matrix and bone powder. The immunomodulatory effects of dECM biomaterials comprise cells from both adaptive and innate immune system [180]. In the context of macrophage polarization, these materials have been proposed to direct macrophages towards a M2 phenotype. Sicari et al. [181] showed that degradation products from ECM bioscaffolds were able to promote a M2 macrophage phenotype. This was observed by a decreased percentage of iNOS (M1), increased percentage of Fizz1 (M2) as well as increased CD206 expression. In other study, also analyzing macrophage phenotype following exposure to dECM degradation products, Huleihel et al. [182] showed that there was a marked downregulation of genes associated with an pro-inflammatory profile including inducible nitric oxide synthase (iNOS), signal transducer and activator of transcription (STAT)1, STAT2, and krueppel-like factor (KLF)6. Similarly, Slivka et al. [183] demonstrated that dECM modulates macrophage towards a M2 phenotype. In particular, authors assessed the role of structural and soluble ECM components, from a urinary bladder matrix, in the modulation of macrophage behavior. Both structural and soluble components showed low TNF-α and IL-1β secretion levels. Differently, structural components decreased phagocytosis whereas soluble ones increased phagocytosis and IL-1RA secretion levels. Importantly, the effect of ECM in guiding macrophages towards a M2 phenotype appears to be lost when using aged ECM/ECM derived from aged animals [184]. The relationship between dECM immunomodulatory effects towards macrophages and subsequent effect on MSCs

differentiation and/or bone application is under investigation. Wu et al. [185] produced bone ECMs in the form of filler particles and gel bioscaffolds from porcine bone and investigated their influences on both macrophages and MSCs. Macrophages had a greater tendency to polarize towards M1 on the dECM particles (increased Nos2 and Il1b expression), whilst on the dECM gels macrophages were polarized towards M2 (increased CD163 expression). Regarding MSCs, there was an increase on the expression of osteogenic-related genes (Alp, Osx and Ocn) both dECM gels and dECM particles at earlier time points (day 7). At late time-points (day 21) MSCs on dECM particles exhibited higher expression of Osx than in the dECM gels. Qiu et al. [186] prepared a decellularized periosteum extracellular matrix (PEM) hydrogel and showed that it promoted a M2 polarization of macrophages (upregulated expression of CD206 and Arg1) as well as increased osteogenic differentiation (upregulated expression of Runx2, ALP, Col1α1, OCN, and OPN) *in vitro,* compared with a Col I hydrogel. *In vivo*, PEM hydrogel recruited and promoted M1-M2 transition of macrophages and new bone formation.

Fibrinogen (Fg) is a blood pro-inflammatory and pro-healing protein involved in blood clotting. Fg-derived clot supports tissue regeneration, constituting the primordial extracellular matrix [187, 188], and has important roles in the inflammatory response to biomaterials [189, 190]. Fg is used in the clinic, together with thrombin, in the form of fibrin (Fb) sealants (e.g. fibrin glues, fibrin tissue adhesives) [191]. Santos Tde et al. [192] compared the potential of bone repair of collagen sponge with Fb glue in a rat calvarial defect model, with the later favoring higher bone formation. Kim et al. [193] demonstrated that Fg adsorption on biphasic CaP granules accelerated bone regeneration, when compared with biphasic CaP granules alone. Seebach et al. [194] revealed that MSC loaded Fb hydrogels fastened bone regeneration in comparison with cell free hydrogels. Systemic immune cell populations proportions, including the Mac-1 subpopulation, were modified by Fg [187, 195]. Importantly, Hsieh et al. [196] observed that distinct macrophage functions were elicited by Fg and Fb. Fg led to the secretion of pro-inflammatory cytokines (e.g. IL-6 and TNF-α) whereas Fb led to anti-inflammatory cytokine secretion (e.g. IL-10).

The structure of Fg is decorated with two RGD motifs which are related with improved cell adhesion [187, 197]. Multiple binding sites are also found for the leukocyte $\alpha_M\beta_2$ integrin (Mac-1). Mac-1 is an important receptor of immune cells, mediating a range of adhesive reactions during the inflammatory response [187, 198]. Low mechanical strength, high water solubility and rapid degradation are the biggest disadvantages of Fg [154]. The use of crosslinking agents revealed to be a suitable approach to improve Fg degradation rate and mechanical properties. Sell et al. [199] addressed the capacity of three different

crosslinkers (glutaraldehyde vapor, 1-ethyl-3-(3-dimethylaminopropyl) carbodiimide hydrochloride (EDC) and genipin) to enhance Fg mechanical properties and slow its degradation. Authors showed that Fg degradation rate was significantly reduced and mechanical properties were enhanced in EDC and genipin crosslinked scaffolds when compared to uncrosslinked scaffolds. Thus, the use of these crosslinkers rises as suitable approach to tailor Fg degradation rates together with long term mechanical stability. Our group and others have been researching Fg in the context of bone repair either alone [187], or combined with other biomaterials or cells [192-195, 200], in the presence/absence of thrombin. Peled et al. [200] used PEGylated fibrinogen hydrogels, with variable polyethylene glycol (PEG) compositions, to assess the potential of the Fg-based ingrowth matrices in promoting the osseous reconstruction of a segmental defect in the tibia of rats, in comparison with empty bone defects. Authors also attempted to analyze the synchronized hydrogel biodegradation in parallel with bone formation. Obtained results indicated that intermediate-degrading PEGylated Fg materials allowed for bone formation whereas fast-degrading PEGylated Fg materials or those that were untreated depicted non-unions. This indicated that PEG compositions governed the biodegradation rate of the material. In our group Fg was investigated first adsorbed to chitosan, and later alone. In our group, a study by Almeida et al. [68] showed that Fg adsorbed to chitosan films increased the capacity of MSC recruitment by NK cells. Later on, Maciel et al. [201] showed that Fg adsorption induces the production of osteogenic factors by monocytes/macrophages and Oliveira et al. [202] elucidated that the interaction between Fg and macrophages occurred via TLR-4. Besides this, adsorbed Fg was also shown to promote resorption of Ch by human OCs [203]. Also, *in vivo*, the study by Santos et al. [195] showed that adsorbed Fg potentiates the osteoconductive properties of Ch, inducing the formation of larger amounts of new bone. Then, Vasconcelos et al. [187] produced and implanted scaffolds entirely constituted of Fg (Fg-3D) in a femoral rat bone defect. The authors showed that Fg-3D scaffolds allowed for bone defect closure and periosteal repair faster than the empty group. Further *in vitro* work found that Fg scaffolds could be resorbed by OC, leading to the production of mediators capable of stimulating osteoblastogenesis [204].

3.1.2. BIOCERAMICS

Bioceramics consist of inorganic (i.e. not carbon based) nonmetallic compounds that harbor crystalline ceramics, amorphous glasses, and glass-ceramics - two-phase materials that share properties from both glasses and ceramics [205]. Bioactive ceramics are good bone grafts substitute materials. Most frequently used biodegradable ceramics include CaP-

based compounds (HA, tricalcium phosphate (TCP), dicalcium phosphate (DCP), biphasic calcium phosphate (BCP), calcium phosphates cements [205]. In fact, several CaP-based compounds are already commercially available (e.g. NanoBone Granulate (Artoss), In'Oss (Biomatlante), Mastergraft Strip (Medtronic)). CaP-based compounds have been shown to regulate macrophage secretion of inflammatory cytokines, chemokines and growth factors, favoring a pro-osteogenic microenvironment. Investigation of CaP-based compounds immunomodulatory properties towards macrophages as well as their impact on the macrophage-MSCs crosstalk between is being performed. Studies on this matter are summarized in Table 1.

Overall, the use of HA either in the form of nano sized HA particles [206], discs with nano needle topographies [207] or porous scaffolds [208] has been shown to modulate macrophages towards a M2 phenotype. The effect of the observed macrophage immunomodulation on MSCs has been translated into an increase in osteogenic differentiation [206-208]. For example, Mahon et al. [206] revealed that while micron sized HA particles modulated macrophages towards a M1 phenotype (increased levels of CD86, TNF-α, IL-6, IL-8 and IL-1β, and decreased levels of CD163 and CD206), nano sized HA particles had the opposite effect. Not only these particles promoted a M2 phenotype (increased levels CD163, CD206 and IL-10 and decreased levels of CD86) but also the conditioned media from macrophages preconditioned with them lead to increased osteogenic differentiation. *In vitro* findings were further corroborated *in vivo*.

β-TCP has been shown to promote mostly M1 macrophage polarization either in the form of particles [209] and powders and extracts [210]. Tai et al. [209] showed that β-TCP particles lead to an increased F4/80, CD11b and CD86 cell surface expression levels as well as increased levels of pro-inflammatory cytokines/chemokines including MCP-1, MIP-1α and IL-1ra. Similarly Chen et al. [210] showed that macrophages cultured with β-TCP extracts exhibited increased CCR7 cell surface levels together with increased levels of IL1β and IL6. *In vitro* results were further confirmed *in vivo*. β-TCP powder embedding in a rat femoral condyle modulated macrophages towards M1 (increased levels of CCR7, IL-1β, IFN**γ** and IL-6). β-TCP extracts further promoted, *in vitro*, MSCs osteogenic differentiation leading to increased ALP and OCN gene expression.

BCP has been shown to increase the fraction of M2 macrophages [211]. Chen et al. [211] demonstrated that BCP reduced macrophage secretion of TNF-α and IL-1β and increased the production of IL-10, BMP-2 and TGF-β1. Also, the macrophage/BCP conditioned medium lead to the upregulation of osteogenic specific genes and increased matrix mineralization. More recently, the authors showed that the osteoinductive potential of CaP-

based compounds (BCP, β-TCP and HA) was correlated with their immunomodulatory capacity. BCP increased the fraction of M2 macrophages and showed a superior osteoinductive potential, while β-TCP increased the fraction of M1 macrophages and had low osteoinductive potential, and HA showed an intermediate induction of both M1 and M2 macrophages [212].

Bioactive Glasses (BGs) (e.g.silicates, phosphate-based glasses and borate-based glasses) are also used as bone grafts (e.g. PerioGlas and NovaBone) and are reported to bond to bone quicker and elicit more bone regeneration than other ceramics like HA [213]. Still, some challenges regarding the use of BGs need to be tackled namely rapid degradation and mechanical weakness [214]. Ionic dissolution of the elements composing BGs (e.g. SiO2, Na2O, CaO and P2O5)soluble silica and calcium ions) is considered to be the basis of their osteogenic properties, stimulating osteogenic cells to produce bone matrix [213, 215, 216]. Based on this, BGs doping with ions have been assessed as a strategy to tailor BGs biological impact including modulation of macrophage polarization and MSCs differentiation [216, 217]. Like ceramics, BGs are also finding applications as immumodulatory biomaterials targeting macrophage phenotype. Table 1 summarizes existing research regarding BGs immunomodulatory properties towards the modulation of macrophage polarization and the effect on their crosstalk with MSCs. Overall, the use of BGs has been shown to modulate macrophages towards a M1 phenotype. However, when doped with ions (e.g. boron (B) [218], cerium (Ce) [219],) or immunomodulating drugs (e.g. FTY720 [220]) this phenotype can be reversed. Lu et al. [218] showed that B-incorporated calcium silicate coatings decreased M1 polarization and pro-inflammatory cytokine secretion and increased M2 polarization together with the secretion of anti-inflammatory cytokines, in comparison with calcium silicate coatings alone [218]. Zheng et al. [219] showed that Ce-doped mesoporous bioactive glass nanoparticles (MBGNs) reverted macrophage M1 polarization induced by MBGNs alone translated into decreased levels of IL-1β, NOS2 and MMP9. Similar results were obtained by Liu et al. [220] but through the use of FTY720-doped MBGNs here translated into decreased levels of IL-6, TNF-α. In both studies conditioned media from macrophages with doped MBGNs led to increased ALP activity, in comparison with MSCs that were not cultured in the presence of macrophage-biomaterial conditioned media.

Similarly to BGs, glass-ceramics are also ion-containing matrices [221], recognized for their osteoconductive and osteoinductive properties [222]. Macrophage immunomodulation by glass-ceramics materials appears to be at initial stages of investigation as, to our knowledge, only one study on this matter was found (Table 1). Briefly, cooper (Cu)-incorporated bioactive glass-ceramics (BGC) were developed and the effect of scaffolds ionic extracts on macrophages and chondrocytes was investigated [223]. Results showed that Cu incorporation into BGC promoted a M2 phenotype, leading to decreased the expression of pro-inflammatory cytokines TNF-α and IL-18 and increased expression of IL-10 anti-inflammatory cytokine. The expression of chondrocyte-associated genes was also increased by the addition of Cu to BGC. These results both in terms of cartilage and osteochondral interface regeneration as well as inflammatory response were not observed in BGC alone [223].

Table 1: Studies assessing the immunomodulatory properties of Ceramics, Bioactive Glasses and Glass-Ceramics towards macrophages and role of bioceramic-regulated macrophage response on osteogenic differentiation

Biomaterial	Monocytes/ Macrophages	MSCs	Inflammatory Stimuli in the presence of biomaterial	Main Findings	Year/ Ref.
BIOACTIVE CERAMICS					
Micron and nano sized HA particles	Human peripheral blood monocytes	Human BMSCs	n/a	· Promotion of a M1 phenotype (↑CD86, ↓CD163 and CD206, ↑TNF-α, IL-6, IL-8 and IL-1β) by micron sized HA · Promotion a M2 phenotype (↓CD86, ↑CD163 and CD206, ↑IL-10) by nano sized HA particles · Secretome from nano particle treated macrophages ↑MSC osteogenesis (↑BMP2 and ALP), in comparison with micron particle treated ones	2020 [206]
	n/a Biomaterial implantation in a rat femoral defect model			· ↑M1 macrophage markers expression (↑CD86 and INFγ) in micron sized HA functionalized scaffolds · ↑M2 macrophage markers (↑IL-10) and ↑bone volume in nano sized HA functionalized scaffolds	
Porous HA, BCP and β-TCP cilinders and discs	RAW264.7	Human BMSCs	n/a	· ↑CCR7+ M1 population in β-TCP cultured macrophages and ↓CD206+ M2 population in all tested CaP ceramics: higher in BCP and lower in β-TCP cultured macrophages · ↑IL-1β, MIP-1α and MIP1- β secretion levels in β-TCP cultured macrophages (HA was the intermediate material between β-TCP and BCP) · ↑Osteogenesis (↑Runx2, Alp) in BMSCs cultured with RAW264.7/BCP and RAW264.7/HA conditioned media	2020 [212]
	n/a Biomaterial implantation in a murine intramuscular implantation model			· Ectopic bone formation in 2/7 HA implants, 6/7 BCP implants and 0/7 β-TCP implants · ↑number of F4/80+ macrophages in β-TCP implants; ↑M1/M2 ratio and more M1 macrophages (↑iNOS) in β-TCP · ↓ M1/M2 ratio and more M2 macrophages (↑ARG) in BCP group	
HA discs (with microscale circular patterns: 4, 12 and 36μm and nano-needle, -sheet and -rod topographies)	RAW264.7	Human BMSCs	n/a	· ↓M1 macrophages (↓CD80) and ↑M2 macrophages (↑CD206) in nano, 12- and 36-nano than Flat and 4-nano HA discs · ↓CCR7, iNOS and TNF-α gene expression in macrophages cultured in nano, 12- and 36-nano HA discs · ↑ARG-1, CD206 and IL-10 gene expression in macrophages in all structures of HA discs, with exception for 4-nano structures · ↑Osteogenesis (↑BMP-2, COL-1 and RUNX2 gene expression) in MSCs cultured with macrophage preconditioned with all HA discs surface structures, with exception for 4-nano structures	2019 [207]
Porous HA scaffolds (with or without groove: HAS-G)	RAW264.7	BMSCs	n/a	· ↓TNF-α, IL-1β, IL-6 and ROS levels in macrophages cultured in HAS-G, without modifications in cell surface markers associated with M1 and M2 macrophage polarization · ↑ALP activity + Alizarin red staining and ↑Col I, OCN and RUNX2 gene expression in BMSCs cultured with RAW264.7/HAS-G conditioned media	2019 [208]

Table 1: (continuation)

Biomaterial	Monocytes/ Macrophages	MSCs	Inflammatory Stimuli in the presence of biomaterial	Main Findings	Year/ Ref.
Calcium deficient HA (CDHA) and β-TCP discs	RAW264.7	SaOS-2 and human BMSCs	LPS	· ↓Pro-inflammatory genes (IL-1β, IL-6, TNF-α and iNOS) in macrophages cultured in CDHA and β-TCP discs, under inflammatory conditions (LPS); decrease more pronounced for CDHA · SaOS-2:↑Runx2 and ↓BSP, OCN and ALP gene expression with RAW264.7/β-TCP conditioned media and ↑Runx2, ALP and OCN with RAW264.7/CDHA conditioned media · BMSCs: ↑Runx2 and BSP gene expression with RAW264.7/CDHA conditioned media and ↓Runx2, ALP, COLL I, BSP, OCN and BMP-2 with RAW264.7/β-TCP conditioned media	2019 [224]
Calcium deficient HA (CDHA) discs (particle size variation (coarse (C), fine (F)) & Liquid/Powder (L/P) ratio: 35:low, 65:high)	RAW264.7	SaOS-2	LPS	· ↑IL-1β and TNF-α gene expression and ↓iNOS and CD206 expression for all tested CDHA combinations (C35, C65, F35 and F65) · ↓IL-1β, IL-6 and TNF-α expression in LPS-stimulated macrophages cultured in CDHA substrates with lower L/P ratio (C35 and F35), in comparison with higher L/P ratios (C65 and F65); ↓IL-10 in LPS-stimulated macrophages cultured in needle-like substrates (F), when compared to plate-like substrates (C) · ↑Osteogenesis in SaOS-2 cultured with macrophages/CDHA F35 and 65 substrates (needle-like) conditioned media (↑BMP-2, BSP and COLL1); ↑Runx2 and OCN in F65 · ↓Osteogenesis in SaOS-2 cultured with LPS-stimulated macrophage/CDHA substrates conditioned media (particularly CDHA with lower L/P ratio)	2018 [225]
β-TCP discs (functionalized or not with heparin)	Human peripheral blood monocytes	rMSCs	n/a	· ↓TNF-α and IL-1β secretion levels in macrophages cultured in β-TCP discs with or without functionalization; higher decrease in heparin functionalized β-TCP · ↑COLL, BMP-2 and OPN in rMSCS cultured with macrophages/ heparin functionalized β-TCP	2018 [226]
TCP-HA Baghdadite Sr-HT-gahnite scaffolds	Human peripheral blood monocytes	n/a	n/a	· ↑M1-related genes (CCR7, IL1B, TNF and VEGF) by all scaffolds · ↓M2a- (CCL22, PDGFB, TIMP3) and M2c-related genes (MMP7, MMP9) by TCP-HA scaffolds · ↑M2c-related genes (CD163, MMP9, VCAN) by baghdadite scaffolds · Minimal effects over macrophage polarization induced by Sr-HT-gahnite scaffolds	2016 [227]
Biphasic calcium phosphate (BCP) discs	RAW264.7	MC3T3	n/a	· ↓IL-1β and TNF-α and ↑IL-6 and IL-10 secretion by BCP cultured macrophages · ↑ Runx2, Col-1 and OPN in MC3T3 cultured with macrophage/BCP conditioned media	2016 [211]
β-TCP particles	C57BL/6 mice BM-derived macrophages	n/a	n/a	· ↑F4/80 and CD11b and ↑CD86 in β-TCP-stimulated macrophages · ↑MCP-1, MIP-1α, IL-1ra in β-TCP-stimulated macrophages	2016 [209]

Table 1: (continuation)

Biomaterial	Monocytes/ Macrophages	MSCs	Inflammatory Stimuli in the presence of biomaterial	Main Findings	Year/ Ref.
β-TCP powders and extracts (with or without Cobalt (Co) incorportation) (CCP)	RAW264.7	hBMSCs	n/a	· ↑CCR7 in RAW264.7 cultured with CCP extracts (β-TCP + Co) · ↑IL1β and IL6 and ↓IL-1ra gene expression in RAW264.7 cultured with CCP extracts · ↑ALP and OCN gene expression and ↑ALP staining in BMSCS cultured with CCP extracts	2015 [210]
	n/a Powder embedding in rat femoral condyle defect model			· Fibrous inflammatory tissue formation in CCP group · ↑M1 macrophages (↑CCR7 and CD11c and ↑IL-1β, IFN**γ** and IL-6) in CCP group	
β-TCP extracts	RAW264.7	hBMSCs	n/a	· ↑IL-10and IL-1ra and ↓ IL-1β and IL-6 gene expression in macrophages stimulated with β-TCP extracts- · ↑Mineralization related-genes (OPN, OCN, COL1) and ↑nodule formation in BMSCs cultured with RAW264.7/β-TCP extracts conditioned media · ↑BMP2 signaling pathways related genes (BMPR2, SMAD5 and SMAD4) in BMSCs cultured with RAW264.7/β-TCP extracts conditioned media	2014 [228]
BIOACTIVE GLASSES					
Mesoporous bioactive glass nanoparticles (MBGNs) (doped or not with Cerium (Ce))	Murine macrophages J774a.1	SaOS-2	n/a	· ↑IL-1β, IL-6 and TNF-α gene expression in MBGN cultured macrophages; ↓IL-1β gene expression in Ce (0.05M and 0.2M)-MBGN cultured macrophages; ↓IL-6 gene expression in 0.2 M Ce-MBGN cultured macrophages · ↓Expression of oxidative stress-related genes (NOS2 and MMP9) in Ce (0.05M and 0.2M)-MBGN cultured macrophages · ↓RANKL, ↑COL1A1 SaOS-2 gene expression by J774a.1/Ce-MBGN conditioned media · ↑ALPSaOS-2 gene expression by J774a.1/MBGN conditioned media	2020 [219]
Mesoporous bioactive glass nanoparticles (MBGNs) (loaded or not with FTY720)	RAW264.7	mBMSCs	n/a	· ↑CD206, Arginase, IL-10, IL-1ra and ↓IL-6, TNF-α in FTY720-MBGNs cultured macrophages · ↑OPN, RUNX2, ALP mBMSCs gene expression by RAW264.7/FTY720-MBGNs conditioned media · ↑ALP in mBMSCs incubated with RAW264.7/FTY720-MBGNs conditioned media	2020 [220]
	n/a Biomaterial implantation in a rat femoral defect model			· ↑bone regeneration in FTY720-MBGNs implanted animals	
Calcium silicate (CS) coatings (with or without boron incorporation (B-CS))	RAW264.7	BMSCs	n/a	· ↓CD11c (M1) and ↑CD206 (M2) by B-CS · ↓CCR7 and CD11c and ↑CD206 gene expression by B-CS · ↑IL-10 and IL-1ra and ↓iNOS, IL-1β, IL-6, TNF-α and OSM gene expression by B-CS · ↑Runx2, Osterix, BSP, OPN, BMP2, VEGF and ↓RANKL gene expression in BMSCs cultured on B-CS coatings	2019 [218]

Table 1: (continuation)

Biomaterial	Monocytes/ Macrophages	MSCs	Inflammatory Stimuli in the presence of biomaterial	Main Findings	Year/ Ref.
Akermanite (AKT) Nagelschmidtite (NAGEL) discs, extracts (different concentrations) and particles (compared to β	RAW264.7	n/a	LPS	· ↑MCP-1, MIP-1α, TNF-α, IL-1β, IL-6 and IL-8 secretion levels in RAW264.7 seeded on AKT, NAGEL and β-TCP discs (lower in AKT and NAGEL) · ↓ERK, JNK, p38 and IkBα phosphorylation in LPS-stimulated RAW264.7 cultured with high concentration AKT and NAGEL extracts	2018 [229]
	n/a Particles implantation in a mice subcutaneous model		n/a	· Biomaterial encapsulation and FBGC formation and fibrosis and ↓Macrophage distribution in AKT and NAGEL implanted animals; ↓MCP-1, MIP-1α, TNF-α, IL-1β, IL-6 and IL-8 secretion levels in AKT and NAGEL implanted animals · ↑Apoptotic cells around implanted AKT and NAGEL	
Mesoporous silica nanospheres (MSNs) doped or not with Europium (Eu-MSNs)	RAW264.7	rBMSCs	n/a	· ↑IL-8, IL-6, IL-1β and OSM and ↓IkB expression in Eu-MSN cultured RAW264.7, as opposed to MSN cultured cells · ↑ALP, COL-I, OCN, OPN and RUNX2 gene expression and ↑COL-I and ALP protein expression in BMSCs cultured with RAW264.7/Eu-MSN conditioned media	2017 [230]
	n/a Implantation in a rat cranial defect model			· ↑Bone formation in Eu-MSN implanted group	
Sub-micron bioactive glasses (SBG) extracts (doped or not with Strontium (Sr))	RAW264.7	mMSCs	n/a	· ↑CD206 (M2), ↓CD11c (M1) and ↓IL-6 in macrophages cultured with Sr-SBG extracts · ↓iNOS, IL-1β, IL-6 and ↑IL1ra, Arg gene expression in macrophages cultured with Sr-SBG and SBG extracts (more pronounced effects observed with Sr-SBG extracts) · ↑BMP2, ALP, OCN, COL1 and RUNX2 mMSCs gene expression by RAW264.7/ Sr-SBG conditioned media · ↑Mineralized nodules in Sr-SBG group	2016 [231]
GLASS-CERAMICS					
*Bioactive glass ceramics (BGC) scaffolds and extracts (doped or not with Copper (Cu))	RAW264.7	n/a	n/a	· ↑IL-10, ↓TNF-α and IL-18 secretion levels in macrophages cultured with ionic extracts from Cu-BGC · ↓iNOS and ↑CD206 surface markers levels in macrophages cultured with ionic extracts from Cu-BGC · ↑Chondrocyte-related markers expression (COLLII, ACAN, SOX-9, HIF-1α) in chondrocytes cultured with ionic extracts from Cu-BGC extracts	2019 [223]

3.1.3. METALS

Biodegradable metals have been proposed as novel materials for bone grafting therapies as an alternative to the still conventionally used inert metals such as titanium (Ti), stainless still and chromium-cobalt (Cr-Co) alloys [232]. Degradable metals can be defined as pure metals, metal matrix or metal matrix composite capable of gradually degrade *in vivo* as they promote complete tissue healing with restoration of function [233]. Implants made with biodegradable metals greatly outperform their biodegradable polymers counterparts because they are significantly stronger [234].The central question when considering the use of biodegradable metals is the element chosen as the base metal, which should be nontoxic. Depending on the maximum concentration at which no adverse response is recognized, i.e. no observable adverse effect level (NOAEL), the base metal might be suitable for a large- or small-volume implants [235]. Another aspect to take into consideration is the corrosion rate. Metal corrosion processes should occur at a rate that provides necessary mechanical support until the complete healing of the tissue [235]. In the particular case of bone, a period of 6-18 months is desired for the remodeling process to be completed [236].

So far, three metallic systems, based on iron (Fe), zinc (Zn) and magnesium (Mg), as the base metal, have been most widely explored for the use in orthopedic implants [233, 235]. Upon implantation Fe, Zn and Mg ions are released from the implant to the surrounding environment. The ionic content/concentration will therefore impact the cellular responses and healing process and the biocompatibility of the implant [235]. In particular, inflammatory cells are sensitive to released metallic ions and/or particles released through corrosion processes [237, 238].

Fe is a transition metal (i.e. interchanges between divalent ferrous, Fe^{2+}, and trivalent ferric, Fe^{3+} ions) [239] and a trace element vital for humans due its crucial role in the blood for proper oxygen transport, oxidative metabolism, cellular proliferation, and many catalytic reactions [239]. The use of Fe-based biodegradable metals is attractive from a structural point of view. These metallic implants can provide both high strength (up to 1450 MPa) and ductility (up to 80% elongation) [235, 240, 241]. The suitability of iron as a biodegradable metal has been verified by Peuster et al. in preliminary *in vivo* studies in rabbits [242] and minipigs [243]. Results showed no evidence for local toxicity due to stent corrosion products, nor iron-related organ toxicity. However, the stents showed a slow degradation rate *in vivo*. Regarding the use of Fe-based biodegradable metals in osteosynthesis, Kraus et al. [244] investigated, over a period of 1 year, the degradation performance of three Fe-based materials in a growing rat skeleton. Degradation cues were showed by all tested materials but the degradation proceeded slowly. Also, the presence of oxygen is an

indispensable prerequisite for the degradation of iron [244]. More recently, Wegener et al. [236] developed a biodegradable porous iron-based implant for bone replacement. However, the use of these implants for the development of self-degrading and high load bearing bone replacement materials is compromised by their slow degradation rate in osteogenic environments [236]. Hence, research has focused on ways to increase the degradation rate of iron-based materials while maintaining their interesting mechanical properties [245, 246]. Fe ions (Fe^{2+}) are essential for immune function including macrophage polarization. Control of iron homeostasis is essential to regulate macrophage polarization into M1 and M2. As recently reviewed by Xia et al. [247], several studies indicate that Fe regulates macrophage polarization towards M1. For example, Zanganeh et al. [248] revealed that Fe nanoparticles induced M1 macrophage polarization, significantly upregulating CD86 and TNF-α. In agreement, Zhou et al. [249] showed that Fe overload induced M1 polarization, observed by the increased expression of IL-1β and TNF-α. Pereira et al. [250] exposed that Fe deprivation reduced IL-1β and TNF-α expression in human macrophages following LPS treatment. Contradictory results were shown by Wilkinson et al. [251]. Authors revealed that Fe administration led to a significant decrease in the M1 markers IL-1β and TNF-α and increased the expression of the M2 markers C-C Motif Chemokine Ligand 17 (CCL17) and C-C Motif Chemokine Ligand 22 (CCL22). As suggested by Xia and colleagues [247], these opposing results are thought to be context dependent and thus comparative studies on the effects of Fe on polarization of macrophage with distinct origins, tissues and species, are needed. Marycz et al. studied for the first time the effects of iron oxide nanoparticles in the presence/absence of magnetic field in both osteoblasts and osteoclasts activity. The effect of these nanoparticles on macrophage polarization was also studied together with macrophage-MSCs and macrophage-osteoclast co-culture. However, the role of iron-oxide modulated macrophages on osteogenic differentiation was not addressed. Briefly, iron oxide nanoparticles and magnetic field increased osteogenic differentiation, inhibited osteoclast activity and decreased inflammation in co-culture of macrophages with both osteoclasts and osteoblasts [252].

Zn is the second most abundant transition element in the human body [253]. It is an essential element as it serves as co-factor of several classes of regulatory proteins [240, 254] and enzymes [241, 255]. Zn ions (Zn^{2+}) are the main byproduct of zinc metal and play critical roles in several fundamental cellular processes [253]. Recently, Zn-based biodegradable metals have been proposed as promising alternatives to Fe and Mg. Zn overcomes the inherent limitations of Fe and Mg, both pure and alloyed, regarding corrosion

rates (which fall between those of Fe- and Mg-based biodegradable metals), and is easier to cast and process, when compared to Fe- and Mg-based biodegradable metals, [253, 256]. However, the use of Zn alone as a biodegradable metal is limited due to its insufficient strength, plasticity and hardness, inappropriate for most clinical devices [235, 241, 256]. Therefore, applying alloying elements such as Mg, Calcium (Ca), Sr, Aluminum (Al), among others, has been explored as a way to improve its mechanical properties and enhance corrosion [253, 257]. Although research on Zn-based alloys has focused mostly in the cardiovascular field [232], bone applications have also been under investigation. A recent study from Guo et al. [258] showed the feasibility of Zn membranes (with and without pores) to be used as guided bone regeneration membranes, both *in vitro* and *in vivo*. The most favorable osteogenic capacity was achieved through the use of Zn membranes with 300 μm pores, in comparison with membranes without pores and membranes with 1000 μm pores. In other study, Yang et al. [257] evaluated, *in vitro* and *in vivo,* the potential of binary Zn alloys with alloying elements as biodegradable bone implants in terms of mechanical properties, biodegradability and biocompatibility. Lithium (Li) and Mg were shown to be the most effective for strengthening Zn alloys (close to pure Ti), leading to accelerated but still moderate degradation, improved cytocompatibility, osteogenesis and osseointegration [257]. Zn ions (Zn^{2+}), either from Zn-containing materials/Zn-based biodegradable metals, or Zn coatings have been shown to fine-tune TLR signaling [259], enhance the expression of anti-inflammatory cytokines by T cells, maintain an anti-inflammatory environment [260, 261] and stimulate osteogenesis [261-265]. Zn has been shown to regulate macrophage polarization towards M1. Both Roy et al. [266] and Giovanni et al. [267] demonstrated that Zn oxide nanoparticles induced a pro-inflammatory response in macrophages. Dierichs et al. [268] showed that both Zn deficiency and Zn supplementation promoted M1 polarization and decreased M2 polarization. The immunomodulatory potential of Zn over macrophage polarization and subsequent effect on MSCs differentiation is still poorly understood and requires a more in-depth investigation. The impact of Zn surface topography (pure Zn plates with nano-, submicro-, and micro-topographies) on macrophage polarization and osteogenic differentiation was shown by Cockerill et al. [265]. Briefly, micro and submicro texture surfaces helped to rapidly decrease the inflammatory polarization of macrophages whereas micro texture surface displayed the superior performance in promoting osteogenic differentiation [265].

Mg is a cofactor in hundreds of enzymatic reactions particularly those that use nucleotides as cofactors or substrates; is required for protein and nucleic acid synthesis; and is

important for normal neurological and muscular function. Additionally, a considerable amount of Mg is present in bones and teeth [232, 269]. Mg-based biodegradable metals are more advantageous over Fe- and Zn-based ones. Albeit Fe, Zn and Mg are essential nutritional elements, the recommended daily intake for Mg is higher by one or two orders of magnitude than Fe and Zn, respectively [270]. Also, due to their excellent biocompatibility and mechanical properties, research on the development of biodegradable metals has focused mostly on Mg [232, 270]. Mg Young's Modulus is closer to that of cortical bone when compared with Fe or Zn [270], thus preventing stress shielding through the allowance of a natural load transfer to the surrounding bones to stimulated the bone remodeling process [232]. Despite such advantages, Mg mechanical strength is relatively low for an effective use as a heavy load-bearing implant. The greatest challenge of using pure Mg is to control the high corrosion rate, unpredictable in physiological environments, and potential toxicity associated with this corrosion process [232, 271-273]. Amounts of hydrogen gas generated exceed the permissible limit in human body, and is accompanied by substantial increases in pH and release of high amounts of metallic ions from the implant [232, 271-273]. Controlling the Mg degradation rate has been challenging, with implants degrading faster than tissue is able to repair. Use of alloying elements (e.g. Al, Zn, Ca, Fe, rare earth elements (REE)), followed by thermal and mechanical treatments and the use of different coating techniques can help to tailor degradation properties of Mg materials, leading to improved mechanical properties and corrosion behavior [232, 272, 273].

Recent clinical trials of Mg-based materials for orthopedic applications include: (1) MAGNEZIX®, to treat patients with mild hallux valgus [274] ; (2) RESOMET® (K-MET), for the treatment of hand fractures [275]; (3) pure magnesium, to treat patients with osteonecrosis of the femoral head [276].

The current knowledge of the immunomodulatory effects of Mg, either derived from Mg-containing materials/ Mg-based biodegradable metals, extracts or salts on macrophage phenotypic profile and subsequent effect of this immunomodulation on MSCs osteogenic differentiation is summarized in Table 2. Overall, the use of Mg has been shown to decrease macrophage M1 polarization, in some times accompanied by an up-regulation of M2-associated markers [277]. The effect of the observed macrophage immunomodulation on MSCs has been translated into an increase in osteogenic differentiation [277, 278] but also in enhanced chondrogenic activation [279].

When Mg implants degrade, Mg ions (Mg^{2+}) are released, which will affect the surrounding cells. The study of the inflammatory cells response to Mg^{2+} not only derived from Mg-containing materials [278, 280, 281] but also from Mg extracts [282, 283] and Mg salts

($MgSO_4$) [279, 284-286] has revealed interesting results. Yin et al. [280] showed that Mg oxide nanoparticles (MNPs) enhanced exacerbated macrophage M1 phenotype at the time point 6h (increased expression iNOS, CD11c and IL-27 expression) after being applied but then switched to the M2 phenotype at the time point 48h (decreased iNOS, CD86, IL-1β and IL-27 expression and increased expression of Arg-1 and IL-10). Furthermore, MNPs lead to a decreased osteogenic differentiation. Li et al. [278] showed that the Mg-containing Titanium dioxide (TiO_2) coatings suppressed macrophage inflammatory response upon LPS stimulation downregulated the expression of CD86, CD11c, iNOS, TNF-α and IL-1β and upregulated the expression of CD163, in comparison to TiO_2 alone . Macrophage gene expression of BMP-2, BMP-6 and VEGF was also up-regulated by Mg-containing TiO_2 coatings. Overall, authors showed that Mg switched macrophage phenotype from M1 to M2 and mediate osteogenesis by stimulating BMP-2, BMP-6 and VEGF expression in macrophage. Jin et al. [282] used high (100%), middle (50%) and low (10% or 20%) concentrated Mg-based alloy extracts to explore macrophage inflammatory response. For that, authors assessed TNF-α expression in these cells. A significant decrease in TNF-α expression was observed in macrophages cultured with low concentration extracts (10% and 20%), upon LPS stimulation. High and moderate concentrated extracts significantly induced apoptosis and necrosis. Similarly, Costantino et al. [283] also assessed macrophage inflammatory response to Mg-based materials using their extracts. Overall, there was an exacerbation of macrophage M2 profile (IL-1ra and IL-10) and inhibition of M1 (IL-1β and TNF-α) by Mg extracts, particularly Mg-2Ag and Mg-10Gd extracts). Hu et al. [279] investigated the potential of Mg supplementation ($MgSO_4$) to modulate macrophage polarization in the presence/absence of pro-inflammatory stimulation (LPS and IFN**γ**). In fact, Mg supplementation significantly reduced the expression of CCR7, IL-1β, IL-6, IL-10 and nuclear translocation of Nuclear factor kappa-light-chain-enhancer of activated B cells (NF-kB). Moreover, conditioned media from macrophages preconditioned with Mg extracts led to enhanced chondrogenic differentiation. These results were in agreement with previous studies where magnesium sulphate ($MgSO_4$) supplementation was shown to reduced macrophage pro-inflammatory stimulation [284, 285]. Also using Mg salts ($MgCl_2$), Diez-Tercero et al. [286] showed that stimulation with Mg decreased the expression of M1 associated markers (CCR7 and IL-1β) and increased the expression of M2 associated marker CD206).

There are also studies that support the ability of Mg ions to promote bone growth, activating the underlying mechanisms and signaling pathways. For instance, calcitonin gene-related polypeptide-α (CGRP) was shown to be involved in magnesium-induced bone formation in

rats [287] whereas in rabbits the canonical Wnt signaling pathway was shown to be involved in magnesium-induced bone regeneration [288].

Very recently, Qiao et al. [289] revealed a previously unknown time-dependent effect of Mg ions on bone regeneration by implanting an alginate-based hydrogel that allowed for a transient release of magnesium chloride ($MgCl_2$) in critical-sized tunnel defects created in rat femora. At the early phase of bone healing Mg exhibited osteo-promotive effects whereas at the later bone repair/remodeling phase osteo-inhibitory effects were detected. Thus, this study highlights for the need of development of new Mg-based materials with sustained and not extended Mg release in order to avoid unwanted effects such as the hindering of bone repair/regeneration.

Table 2: Studies assessing the immunomodulatory properties of Magnesium (Mg^{2+}) towards macrophages and role Mg^{2+}-regulated macrophage response on osteogenic differentiation

Mg^{2+} Source	Monocytes/ Macrophages	MSCs	Inflammatory Stimuli in the presence of Mg^{2+}	Main Findings	Year/ Ref.
Mg crosslinked Alg (Mg-Alg)	THP-1	Human MSCs	n/a	· Upregulation of M2-associated markers (↑CD163 and CD206) · Upregulation of osteogenesis favoring genes (↑CCL5, IL-1ra, IL-8, TGF-β, BMP2, VEGF and IL-10) and downregulation of osteoclastogenesis favoring genes (↓OSM, IL-6, IL-1β and TNF-α) · Upregulation of osteogenic markers (ALP, COL1A1, OPN, IBSP, BGLAP and Osterix) by Mg^{2+}/macrophages conditioned media	2021 [289]
	n/a Biomaterial implantation in a rat femur defect model			· Grafting on D0:↑Bone formation in Mg-Alg implant animals · Grafting on D7 and grafting on D0&D7: no significant differences in bone formation in Mg-Alg implant animals, compared with Alg alone	
$MgCl_2$ and tannic acid (TA) coating	RAW264.7	Rat BMSCs	LPS	· Downregulation of M1-associated markers (↓CD86, iNOS, IL-1β, IL-6 and TNF-α), an up-regulation of M2-associated markers (↑CD163, CD206, IL-4 and IL-10) in macrophages cultured on Ti plates coated with Mg and TA · ↑BMP2, OC, ALP, RUNX2, COL1, VEGF and OST gene expression in BMSCS cultured on Ti plates coated with Mg and TA	2021 [281]
$MgCl_2$	THP-1	n/a	LPS	· Downregulation of M1-associated markers (↓CCR7 and IL-1β), an up-regulation of M2-associated markers (↑CD206)	2021 [286]
MgO nanoparticles	RAW264.7	SaOS-2	LPS	· Up-regulation of M1-associated markers (↑iNOS, CD11c and IL-27), and downregulation of M2-associated markers (↓Arg-1 and IL-10) after nanoparticles treatment for 6h · Supression of M1-associated markers (↓iNOS, CD86, IL-1β and IL-27), and enhanced expression of M2-associated markers (↑Arg-1 and IL-10) after nanoparticles treatment for 48h · Decreased collagen synthesis and mineralization after nanoparticles application	2020 [280]
Pure Mg and Mg-10Gd	Macrophage differentiation from human leukocytes-enriched blood samples	HUCPV	n/a	· ↓TNF-α and IL-1β secretion in macrophages and HUCPV co-cultured with macrophage in Mg and Mg-10Gd · ↑ALP, OC and OPN expression in HUCPV co-cultured with macrophage in Mg and Mg-10Gd · Higher COLA1, SMAD1, SMAD4 and SMAD5 expression in HUCPV co-cultured with macrophage in Mg, in comparison Mg-10Gd;	2020 [290]
Micron-sized Mg particles (MgMPs) Extracts	THP-1	n/a	n/a	· Downregulation of M1-associated markers (↓CCR7, TNF-α and IL-1β), an up-regulation of M2-associated markers (↑CD206 and IL-10) and NF-kB activation reduction in macrophages exposed to Mg^{2+}	2020 [291]

Table 2: (continuation)

Mg^{2+} Source	Monocytes/ Macrophages	MSCs	Inflammatory Stimuli in the presence of Mg^{2+}	Main Findings	Year/ Ref.
$MgSO_4$	RAW264.7	Mice BMSCs	LPS	· Modulation of macrophage polarization towards a M2 phenotype (↑CD206, IL-10 and IL-1ra ; ↓CCR7 and TNF-α) · ↑ALP activity promoted by the presence of Mg^{2+}/RAW264.7 conditioned medium · Upregulation of osteogenic genes (Runx-2, ALP, OPN and OCN) in the presence of Mg^{2+}	2019 [277]
Mg-based alloy extract	THP-1	n/a	LPS	· ↓TNF-α production in macrophages cultured with low concentration extracts (10% and 20%) in the presence of LPS	2018 [282]
$MgSO_4$	RAW264.7	Human BMSCs	LPS and IFN-γ	· Macrophage activation inhibition: ↓CCR7, ↓CD206 (to a lesser degree); ↓IL-1β, IL-6 and IL-10; decreased nuclear translocation of NF-kB · Enhanced chondrogenic activation of human BMSCs in the presence of Mg^{2+}/macrophage conditioned medium	2018 [279]
[a] $MgSO_4$	RAW264.7	Murine C3H/10T1/2 MSCs	LPS or TNF-α	· ↓pNF-kB/NF-kB levels and ↑pSTAT-3/STAT-3 by Mg^{2+} · ↑MSCs proliferation rate by Mg^{2+} · Modulation of macrophage cytokine profile (↓IL-1β and IL-6; ↑IL-10 and PGE2) by Mg^{2+}/MSCs cells-conditioned media	2018 [292]

[a]Study concerning MSCs immunomodulation and subsequent effect on macrophage polarization

3.1.4. COMPOSITES

Composite materials are made by the combination of a minimum of two or more different materials such as polymers, ceramics and metals. The idea of combining different classes of materials aims to produce a material with improved properties that are not attainable by the use of a polymer a ceramic or a metal alone [293].

The term “matrix” is used to designate the major component of the composite, accounting for >50% by volume, forming the continuous phase and usually having relatively low stiffness and strength. On the other hand, the term “reinforcement” is used to designate the minor component of the composite, accounting for <50% by volume, which forms the discontinuous and dispersed phase and usually exhibits relatively high stiffness and strength [293].

Right after bioceramics, composites constitute the class of biodegradable materials where more studies have been reported regarding their potential as immunomodulatory materials. This is because these materials combine complementary advantages of different classes of materials, giving rise to distinct combinations. The use of polymer-ceramic composites constitutes a promising solution for bone tissue regeneration applications due to their good mechanical properties, osteoconductivity and bioactivity [294-296]. Besides polymer-ceramic combinations, other blends have been explored, also with promising results [297-299]. Table 3 summarizes the current knowledge of composites immunomodulatory potential towards macrophage polarization and the role of the observed immunomodulation on MSCs osteogenic differentiation.

In a general way, the use of composites has been shown to modulate macrophage towards a M2 phenotype. The effect of the observed macrophage immunomodulation on MSCs has been translated into an increase in osteogenic differentiation. For instance, Wang et al. [296] showed that magnetic lanthanum-doped HA/Chitosan scaffolds (MLaHA/CS) were able to modulate, *in vitro*, macrophage polarization into M2, promoting an increased in CD206 positive cells and a decrease in CCR7 positive cells. This was accompanied by a decrease in TNF-α and IL-6 secretion levels and an increase in TGF-β secretion levels. MSCs cultured with conditioned media from macrophages preconditioned with the aforementioned biomaterial showed increased expression of osteogenesis-related genes including ALP, BMP-2, OCN and RUNX-2. Additionally, bone repair ability of MLaHA/CS scaffolds was tested in a rat calvarial defect model and results showed more bone tissue formed in comparison with scaffolds only composed by HA/CS or LaHA/CS. In another study, Lin et al. [297] showed that macrophages cultured with PLGA/MgO-alendronate

microspheres exhibited an increased levels of CD206, decreased levels of CCR7 cell surface markers and augmented M2/M1 ratio. There was also a decrease in the secretion of pro-inflammatory cytokines (TNF-α and IL-1β) and an increase of anti-inflammatory ones (IL-10 and TGF-β), in comparison with PLGA/MgO and PLGA microspheres. Moreover, there was an increase in the expression of osteogenesis-related genes (ALP, OCN, Col I, Runx2 and OPN) in BMSCs cultured with macrophages-PLGA/MgO-alendronate conditioned media. Then, the inflammatory response to microspheres was further assessed *in vivo*, using a mouse air-pouch animal model. Results showed that animals implanted with PLGA/MgO-alendronate microspheres exhibited the highest M2 (Arg1) and the lowest M1 (iNOS) macrophage percentage as well as the thinnest fibrous layer, when compared with PLGA/MgO and PLGA groups. Lastly, microspheres were implanted in a rat intramedullary bone defect model. PLGA/MgO-alendronate implanted group showed the highest percentage of new bone volume, compared with PLGA/MgO and PLGA implanted groups. Using magnesium-enriched graphene oxide nanoscrolls decorated biomimetic scaffolds Zheng et al. [299] were also able to tune macrophage phenotype and promote bone regeneration. Besides enhancing bone formation, biomaterial implantation in rat calvaria led to a dynamic transformation on macrophage phenotype. Specifically, 3 days after implantation there was a predominance of M1 macrophages (CD68+, iNOS+), whereas at the 7^{th} and 14^{th} day after implantation macrophage phenotype switched towards M2 (CD68+, CD206+). Mechanistically it was shown that graphene-oxide induced inflammatory response was downregulated by magnesium, via NF-kB p65 nuclear translocation inhibition. Overall, authors demonstrated a synergistic immunomodulation, achieved through the integration of pro-inflammatory (graphene oxide (GO)) and anti-inflammatory (Mg) activators.

Table 3: Studies assessing the immunomodulatory properties of Composites focused on macrophages and role of ceramic-regulated macrophage response on osteogenic differentiation

Biomaterial	Monocytes/ Macrophages	MSCs	Inflammatory Stimuli in the presence of biomaterial	Main Findings	Year/ Ref.
PLGA/MgO-alendronate microsphoeres	RAW264.7	BMSCs	n/a	· ↑M2/M1 ratio (↑CD206 and ↓CCR7), ↓TNF-α, IL-1β and ↑IL-10, TGF-β and BMP-2 in macrophages cultured with PLGA/MgO-alendronate, comparing with PLGA/MgO and PLGA · ↑ALP, OCN, Col I, Runx2 and OPN in BMSCs cultured with macrophages- PLGA/MgO-alendronate conditioned media	2021 [297]
	n/a Biomaterial implantation in a mouse air pouch model and rat intramedullary bone defect model			· ↑M2 (Arg1), ↓M1 (iNOS) and ↓fibrous layers thickness in mouse implanted with PLGA/MgO-alendronate microspheres · ↑Percentage of bone volume in rats implanted with PLGA/MgO-alendronate microspheres	
AZ31 Mg alloy coated with PCL-based fibers loaded with coumarin and/or Zinc oxide (ZnO)NPs	RAW264.7	n/a	LPS	· ↓Percentage of macrophage fusion in Mg-PCL-ZnO samples upon LPS stimulation: Mg-PCL-ZnO (1.75%) < Mg-PCL-coumarin-ZnO (3.1%) < TCPS (8.1%) < Mg-PCL (8.9%) < Mg-PCL-CM (10.2%) < Mg (21.3%) · ↓IL-1β secretion levels in macrophages cultured in Mg samples and ↑IL-1β secretion secretion levels in macrophages cultured in Mg-PCL-ZnO samples, upon LPS stimulation · ↓NO secretion levels in macrophages cultured in all material combinations, upon LPS stimulation · ↓ROS levels in macrophages cultured in Mg-PCL-coumarin-ZnO samples and ↑ROS levels in macrophages cultured in Mg samples	2021 [300]
Zinc Silicate/nanoHA/ collagen (ZS/HA/Col) scaffolds (varying % of ZS: 0, 5, 10 and 15%)	Rat BM derived monocytes	Rat BMSCs	n/a	· Activation of p38 in monocytes cultured on 10ZA/HA/Col scaffolds; ↑TRAP+ cells by 10ZA/HA/Col scaffolds · ↑SDF-1, TGFβ1, VEGF-α and PDGF-BB by ZA/HA/Col scaffolds · ↑Bmp-2 and Osterix by ZA/HA/Col scaffolds	2020 [295]
	n/a Biomaterial implantation in a rat cranial defect model			· ↑Bone formation in 10ZA/HA/Col group	
Mg-enriched Graphene Oxide Nanoscrolls decorated biomimetic scaffolds (MgNPs@GNS/DBM)	RAW264.7	BMSCs	n/a	· ↓NF-kB p65 nuclear translocation and ↓ROS by GO+Mg^{2+} · ↑Runx2 and OCN gene expression in BMSCSs cultured with RAW264.7/GO+Mg^{2+} conditioned media · ↑ALP, Alizarin Red, Von Kossa and OCN staining in BMSCs cultured with RAW264.7/GO+Mg^{2+} conditioned media	2020 [299]
	n/a Biomaterial implantation in a rat cranial defect model			· ↑Bone regeneration in MgNPs@GNS/DBM group · ↑M1 macrophage (CD68+, iNOS+) in MgNPs@GNS/DBM group, 3 days after implantation · ↑M2 macrophage (CD68+, CD206+) in MgNPs@GNS/DBM group, 7 and 14 days after implantation	

Table 3: (continuation)

Biomaterial	Monocytes/ Macrophages	MSCs	Inflammatory Stimuli in the presence of biomaterial	Main Findings	Year/ Ref.
Zinc Silicate/ Poly(lactic-co-glycolic acid)/Calcium Phosphate cement (ZS/PLGA/CPC) (varying % of ZS: 0, 3, 5, 10 and 15))	RAW264.7	mBMSCs	n/a	· ↑CD206 (M2) by 3,10 and 15ZS/PLGA/CPC and ↓CD11c (M1) by 3 and 15ZS/PLGA/CPC · ↓IL-1β by 5 and 10ZS/PLGA/CPC, ↓IL-6 by 5-10ZS/PLGA/CPC, ↓TNF-α by 3-15ZS/PLGA/CPC · ↑ALP expression by RAW264.7/3 and 10ZS/PLGA/CPC conditioned material extracts · ↑BSP expression by RAW264.7/10ZS/PLGA/CPC conditioned material extracts · ↑OPN expression by RAW264.7/3-15ZS/PLGA/CPC conditioned material extracts	2020 [298]
	n/a	Biomaterial implantation (0 and 10ZS/PLGA/CPC) in a rat femoral defect model		· ↑Bone formation by 10ZS/PLGA/CPC	
Magnetic lanthanum-doped HA/Chitosan scaffolds (MLaHA/CS)	RAW264.7	rBMSCs	n/a	· ↓CCR7 (M1) and ↑CD206 (M2) in macrophages cultured on MLaHA/CS scaffolds · ↓TNF-α, IL-6 and ↑TGF-β in macrophages cultured on MLaHA/CS scaffolds · ↑ALP, BMP-2, OCN and RUNX-2 gene expression and ↑ALP staining in rBMSCs cultured on MLaHA/CS scaffolds	2020 [296]
	n/a	Biomaterial implantation in a rat calvarial defect model		· ↑Bone formation in MLaHA/CS implanted group	
Sr-crosslinked RGD-alginate hydrogel + Sr-doped HA (Sr-hybrid scaffold)	Human peripheral blood monocytes (for osteoclast differentiation)	Lonza hMSCs	n/a	· ↑ALP activity in hMSCs cultured on Sr-hybrid	2019 [301]
	n/a	Biomaterial implantation in a mice air-pouch model of inflammation		· ↑M2 macrophage polarization (F4/80+ CD206+) and ↓TNF-RI, MIP-1gamma and RANTES secretion in Sr-hybrid implanted animals	
Calcium phosphate/chitosan/ hyaluronic acid (CaP-CHI-HA) substrate	THP-1	n/a	LPS	· ↓TNF-α, MCP-1 secretion levels in macrophages cultured in CaP-CHI-HA substrates · ↓IL-6 and IL-8 secretion levels in macrophages cultured in CaP and CaP-CHI-HA substrates · ↑IL-10 secretion levels in macrophages cultured in CaP and CaP-CHI-HA substrates	2018 [302]
BioGide® collagen membrane with nanometer-sized BG coating	RAW264.7	hBMSCs	n/a	· ↓TNF-α, ↑IL-6, IL-1β and IL-1ra gene expression in RAW264.7 planted in BG-modified collagen membranes · ↑β-catenin, ALP, Runx2 and OPN gene expression in BMSCs cultured with RAW264.7/ BG-modified collagen membranes conditioned media	2018 [294]

Table 3: (continuation)

Biomaterial	Monocytes/ Macrophages	MSCs	Inflammatory Stimuli in the presence of biomaterial	Main Findings	Year/ Ref.
Silicified collagen scaffolds (SCSs)	C577BL6/6J mice bone-marrow derived monocytes	mBMSCs	n/a	· ↑SDF-1α, TGF-β, VEGFa and PDGF-BB gene and protein expression in monocytes cultured in SCS-conditioned culture medium · ↑BMSCs migration by SCS-conditioned monocytes	2017 [303]
	n/a Biomaterial implantation in a mouse calvarial defect model			· ↑SDF-1 and TGF-β expression in CD14+TRAP+ monocytes and ↑VEGF expression in SCS implanted group · ↑Alizarin red in SCS implanted group, and compared with demineralized cancellous sponge strip allograft (DSS) · ↑Bone formation in SCS implanted group and in comparison with DSS	
Magnesium-calcium phosphate cement (MCPC) scaffolds	RAW264.7	rBMSCs	n/a	· ↓M1 (CCR7) proportion of RAW264.7 cultured with MCPC extracts · ↓IL-6, IL-1β, iNOS, and ↑IL1-Ra, TGF-β1 and BMP-2 gene expression and ↓TNF-α and IL-6 secretion levels in RAW264.7 cultured with MCPC extracts · ↑ALP, BMP-2, COL 1 and Runx2 gene expression and ↑ALP activity in BMSCs cultured with RAW264.7/MCPC extracts conditioned media	2016 [304]
Chitosan-graft-poly(ε-caprolactone) copolymers (CS-g-PCL 50/50 and 80/20)	C577BL6/6J mice bone-marrow derived macrophages	n/a	LPS-IFNγ	· ↓iNOS gene expression in LPS-IFNγ stimulated macrophages cultured in CS-g-PCL 80/20 coated coverslips · CS-g-PCL 80/20 coated coverslips per se do not induce macrophage TNF- α gene expresion · ↑Arg1 gene expression in macrophages cultured in CS-g-PCL 50/50 coated coverslips in presence/absence of IL-4	2017 [305]
β-TCP coated Magnesium (Mg-β-TCP) scaffolds	RAW264.7	hBMSCs	n/a	· ↑TNF-α, IL-6, IL-1β and IFNγ gene expression in Mg-β-TCP cultured RAW264.7 · ↑IL1ra gene expression in Mg-β-TCP cultured RAW264.7 · ↑CD163 and ↓CCR7 in RAW264.7 stimulated with RAW264.7/ Mg-β-TCP scaffolds conditioned media ↑BMP2 and VEGF and ↓TGF-β3 and TRAP gene expression in Mg-β-TCP cultured RAW264.7 · ↑OPG, RANKL, ALP, OPN, OCN, IBSP and COL1 gene expression in BMSCs stimulated with RAW264.7/ Mg-β-TCP scaffolds conditioned media · ↑Alizarin red staining in BMSCs stimulated with RAW264.7/ Mg-β-TCP scaffolds conditioned media	2014 [306]

The literature discussed above, highlights the wide range of biodegradable biomaterials presently under investigation to promote fracture healing, and the contribution of immunomodulation, in particular the role of macrophages in the success of new biomaterial-based strategies. In the context of this thesis, Fg and Mg biomaterials will be further explored and investigated as to their capacity to modulate macrophage phenotype, in the context of bone repair/regeneration in healthy and inflammatory conditions.

4. AIMS OF THE THESIS

The main goal driving this thesis was to bioengineer a microenvironment that could modulate macrophages towards a bone healing phenotype, using biodegradable biomaterials.

Fg was combined with Magnesium (Mg)-based materials. The use of these materials on their own is still hindered by their poor mechanical properties and uncontrollable corrosion rates, respectively. Nonetheless, taking leverage of their immunomodulatory and pro-regenerative properties, it was hypothesized that their combination would act synergistically in modulating macrophage phenotype and their crosstalk with MSCs under physiological and pro-inflammatory conditions.

To test our hypothesis and accomplish our objective, the following aims were defined:

1) Combine Fg and Mg to obtain FgMg biomaterials and investigate their synergistic immunomodulatory potential towards macrophages and MSCs

Fg scaffolds were combined with Mg discs (multilayer constructs) and biomaterials extracts were prepared. Then, biomaterials extracts were tested for the potential of modulation macrophage phenotype and the impact of the secretome produced by macrophages exposed to biomaterials extracts on MSCs osteogenic differentiation. The results obtained are presented in chapter II.

2) Evaluate the effect of an FgMg combination biomaterial, as new Mg-incorporated Fg scaffolds, in vitro and in an in vivo model of inflammation

3D Fg scaffolds doped with increasing concentrations of Mg^{2+}, using $MgSO_4$ as the Mg^{2+} source, were produced ($FgMgSO_4$) and tested *in vitro* for their ability to modulate macrophage polarization and to promote MSC osteogenic differentiation. Best performing $FgMgSO_4$ scaffold was selected and tested *in vivo* for their potential to modulate macrophage response, using an air-pouch model of inflammation. The results obtained are presented in chapter III.

3) Perform non-viral transfection of monocytes/macrophages as an adjuvant tool to improve biomaterials ability to modulate macrophage polarization

nHA particles were synthesized, combined with siGLO or a fluorescently tagged siRNA MMP9 and then delivered to monolayered cultured monocytes. Fg and 10 mM FgMgSO4 scaffolds were crosslinked, disinfected, neutralized and soak-loaded on each side with particles nHA particles combined with siGLO. Monocytes were seeded on top of the scaffolds and internalization and transfection efficiency were assessed. First results obtained are described as supplementary work.

REFERENCES

[1] A.M.P. Magri, J.R. Parisi, A.L.M. de Andrade, A.C.M. Renno, Bone substitutes and photobiomodulation in bone regeneration: A systematic review in animal experimental studies, J Biomed Mater Res A (2021).

[2] F. Borgström, L. Karlsson, G. Ortsäter, N. Norton, P. Halbout, C. Cooper, M. Lorentzon, E.V. McCloskey, N.C. Harvey, M.K. Javaid, J.A. Kanis, C. Cooper, J.-Y. Reginster, S. Ferrari, P. Halbout, F. for the International Osteoporosis, Fragility fractures in Europe: burden, management and opportunities, Archives of Osteoporosis 15(1) (2020) 59.

[3] C. Xie, J. Ye, R. Liang, X. Yao, X. Wu, Y. Koh, W. Wei, X. Zhang, H. Ouyang, Advanced Strategies of Biomimetic Tissue-Engineered Grafts for Bone Regeneration, Adv Healthc Mater (2021) e2100408.

[4] P.V. Giannoudis, G.D. Chloros, Y.S. Ho, A historical review and bibliometric analysis of research on fracture nonunion in the last three decades, Int Orthop (2021).

[5] G.D. Chloros, A. Howard, V. Giordano, P.V. Giannoudis, Radiographic Long Bone Fracture Healing Scores: Can they predict non-union?, Injury 51(8) (2020) 1693-1695.

[6] R. Florencio-Silva, G.R. Sasso, E. Sasso-Cerri, M.J. Simoes, P.S. Cerri, Biology of Bone Tissue: Structure, Function, and Factors That Influence Bone Cells, Biomed Res Int 2015 (2015) 421746.

[7] Y. Liu, D. Luo, T. Wang, Hierarchical Structures of Bone and Bioinspired Bone Tissue Engineering, Small 12(34) (2016) 4611-32.

[8] B. Clarke, Normal bone anatomy and physiology, Clin J Am Soc Nephrol 3 Suppl 3 (2008) S131-9.

[9] H.K. Datta, W.F. Ng, J.A. Walker, S.P. Tuck, S.S. Varanasi, The cell biology of bone metabolism, J Clin Pathol 61(5) (2008) 577-87.

[10] S. Toosi, J. Behravan, Osteogenesis and bone remodeling: A focus on growth factors and bioactive peptides, Biofactors (2019).

[11] M. Unal, A. Creecy, J.S. Nyman, The Role of Matrix Composition in the Mechanical Behavior of Bone, Curr Osteoporos Rep 16(3) (2018) 205-215.

[12] R.J. Miron, D.D. Bosshardt, OsteoMacs: Key players around bone biomaterials, Biomaterials 82 (2016) 1-19.

[13] E. Bilgiç, Ö. Boyacıoğlu, M. Gizer, P. Korkusuz, F. Korkusuz, Chapter 6 - Architecture of bone tissue and its adaptation to pathological conditions, in: S. Angin, I.E. Şimşek (Eds.), Comparative Kinesiology of the Human Body, Academic Press2020, pp. 71-90.

[14] S. Donsante, B. Palmisano, M. Serafini, P.G. Robey, A. Corsi, M. Riminucci, From Stem Cells to Bone-Forming Cells, Int J Mol Sci 22(8) (2021).

[15] D.S. Amarasekara, S. Kim, J. Rho, Regulation of Osteoblast Differentiation by Cytokine Networks, Int J Mol Sci 22(6) (2021).

[16] I. Matic, B.G. Matthews, X. Wang, N.A. Dyment, D.L. Worthley, D.W. Rowe, D. Grcevic, I. Kalajzic, Quiescent Bone Lining Cells Are a Major Source of Osteoblasts During Adulthood, Stem Cells 34(12) (2016) 2930-2942.

[17] S.C. Miller, L. de Saint-Georges, B.M. Bowman, W.S. Jee, Bone lining cells: structure and function, Scanning Microsc 3(3) (1989) 953-60; discussion 960-1.

[18] J.M. Delaisse, T.L. Andersen, H.B. Kristensen, P.R. Jensen, C.M. Andreasen, K. Soe, Re-thinking the bone remodeling cycle mechanism and the origin of bone loss, Bone 141 (2020) 115628.

[19] C. Streicher, A. Heyny, O. Andrukhova, B. Haigl, S. Slavic, C. Schuler, K. Kollmann, I. Kantner, V. Sexl, M. Kleiter, L.C. Hofbauer, P.J. Kostenuik, R.G. Erben, Estrogen Regulates Bone Turnover by Targeting RANKL Expression in Bone Lining Cells, Sci Rep 7(1) (2017) 6460.

[20] C. Dierkes, M. Kreisel, A. Schulz, J. Steinmeyer, J.C. Wolff, L. Fink, Catabolic properties of microdissected human endosteal bone lining cells, Calcif Tissue Int 84(2) (2009) 146-55.

[21] F.G.F. Tresguerres, J. Torres, J. Lopez-Quiles, G. Hernandez, J.A. Vega, I.F. Tresguerres, The osteocyte: A multifunctional cell within the bone, Ann Anat 227 (2020) 151422.

[22] M.B. Schaffler, W.Y. Cheung, R. Majeska, O. Kennedy, Osteocytes: master orchestrators of bone, Calcif Tissue Int 94(1) (2014) 5-24.

[23] N. Sawa, H. Fujimoto, Y. Sawa, J. Yamashita, Alternating Differentiation and Dedifferentiation between Mature Osteoblasts and Osteocytes, Sci Rep 9(1) (2019) 13842.

[24] N. Udagawa, M. Koide, M. Nakamura, Y. Nakamichi, T. Yamashita, S. Uehara, Y. Kobayashi, Y. Furuya, H. Yasuda, C. Fukuda, E. Tsuda, Osteoclast differentiation by RANKL and OPG signaling pathways, J Bone Miner Metab 39(1) (2021) 19-26.

[25] W. Feng, J. Guo, M. Li, RANKL-independent modulation of osteoclastogenesis, J Oral Biosci 61(1) (2019) 16-21.

[26] T. Ono, M. Hayashi, F. Sasaki, T. Nakashima, RANKL biology: bone metabolism, the immune system, and beyond, Inflamm Regen 40 (2020) 2.

[27] M.K. Chang, L.J. Raggatt, K.A. Alexander, J.S. Kuliwaba, N.L. Fazzalari, K. Schroder, E.R. Maylin, V.M. Ripoll, D.A. Hume, A.R. Pettit, Osteal tissue macrophages are intercalated throughout human and mouse bone lining tissues and regulate osteoblast function in vitro and in vivo, J Immunol 181(2) (2008) 1232-44.

[28] L. Batoon, S.M. Millard, L.J. Raggatt, A.R. Pettit, Osteomacs and Bone Regeneration, Curr Osteoporos Rep 15(4) (2017) 385-395.

[29] L. Batoon, S.M. Millard, M.E. Wullschleger, C. Preda, A.C. Wu, S. Kaur, H.W. Tseng, D.A. Hume, J.P. Levesque, L.J. Raggatt, A.R. Pettit, CD169(+) macrophages are critical for osteoblast maintenance and promote intramembranous and endochondral ossification during bone repair, Biomaterials 196 (2019) 51-66.

[30] S.W. Cho, F.N. Soki, A.J. Koh, M.R. Eber, P. Entezami, S.I. Park, N. van Rooijen, L.K. McCauley, Osteal macrophages support physiologic skeletal remodeling and anabolic actions of parathyroid hormone in bone, Proc Natl Acad Sci U S A 111(4) (2014) 1545-50.

[31] S.F. Mohamad, L. Xu, J. Ghosh, P.J. Childress, I. Abeysekera, E.R. Himes, H. Wu, M.B. Alvarez, K.M. Davis, A. Aguilar-Perez, J.M. Hong, A. Bruzzaniti, M.A. Kacena, E.F. Srour, Osteomacs interact with megakaryocytes and osteoblasts to regulate murine hematopoietic stem cell function, Blood Adv 1(26) (2017) 2520-2528.

[32] I.G. Winkler, N.A. Sims, A.R. Pettit, V. Barbier, B. Nowlan, F. Helwani, I.J. Poulton, N. van Rooijen, K.A. Alexander, L.J. Raggatt, J.P. Levesque, Bone marrow macrophages maintain hematopoietic stem cell (HSC) niches and their depletion mobilizes HSCs, Blood 116(23) (2010) 4815-28.

[33] K.A. Alexander, M.K. Chang, E.R. Maylin, T. Kohler, R. Muller, A.C. Wu, N. Van Rooijen, M.J. Sweet, D.A. Hume, L.J. Raggatt, A.R. Pettit, Osteal macrophages promote in vivo intramembranous bone healing in a mouse tibial injury model, J Bone Miner Res 26(7) (2011) 1517-32.

[34] R. Bartl, C. Bartl, Modelling and Remodelling of Bone, Bone Disorders : Biology, Diagnosis, Prevention, Therapy, Springer International Publishing, Cham, 2017, pp. 21-30.

[35] M.R. Allen, D.B. Burr, Chapter 4 - Bone Modeling and Remodeling, in: D.B. Burr, M.R. Allen (Eds.), Basic and Applied Bone Biology, Academic Press, San Diego, 2014, pp. 75-90.

[36] P. Katsimbri, The biology of normal bone remodelling, Eur J Cancer Care (Engl) 26(6) (2017).

[37] N.E. Lassen, T.L. Andersen, G.G. Ploen, K. Soe, E.M. Hauge, S. Harving, G.E.T. Eschen, J.M. Delaisse, Coupling of Bone Resorption and Formation in Real Time: New Knowledge Gained From Human Haversian BMUs, J Bone Miner Res 32(7) (2017) 1395-1405.

[38] T.J. Martin, E. Seeman, Bone remodelling: its local regulation and the emergence of bone fragility, Best Pract Res Clin Endocrinol Metab 22(5) (2008) 701-22.

[39] F. Loi, L.A. Cordova, J. Pajarinen, T.H. Lin, Z. Yao, S.B. Goodman, Inflammation, fracture and bone repair, Bone 86 (2016) 119-30.

[40] M. Maruyama, C. Rhee, T. Utsunomiya, N. Zhang, M. Ueno, Z. Yao, S.B. Goodman, Modulation of the Inflammatory Response and Bone Healing, Front Endocrinol (Lausanne) 11 (2020) 386.

[41] M. Tsukasaki, H. Takayanagi, Osteoimmunology: evolving concepts in bone-immune interactions in health and disease, Nat Rev Immunol 19(10) (2019) 626-642.

[42] J.R. Arron, Y. Choi, Bone versus immune system, Nature 408(6812) (2000) 535-6.

[43] G. Mori, P. D'Amelio, R. Faccio, G. Brunetti, The Interplay between the bone and the immune system, Clin Dev Immunol 2013 (2013) 720504.

[44] P.J. Muire, L.H. Mangum, J.C. Wenke, Time Course of Immune Response and Immunomodulation During Normal and Delayed Healing of Musculoskeletal Wounds, Front Immunol 11 (2020) 1056.

[45] G.S. Baht, L. Vi, B.A. Alman, The Role of the Immune Cells in Fracture Healing, Curr Osteoporos Rep 16(2) (2018) 138-145.

[46] M. Maruyama, C. Rhee, T. Utsunomiya, N. Zhang, M. Ueno, Z. Yao, S.B. Goodman, Modulation of the Inflammatory Response and Bone Healing, Frontiers in Endocrinology 11(386) (2020).

[47] J.J. El-Jawhari, E. Jones, P.V. Giannoudis, The roles of immune cells in bone healing; what we know, do not know and future perspectives, Injury 47(11) (2016) 2399-2406.

[48] T.A. Einhorn, L.C. Gerstenfeld, Fracture healing: mechanisms and interventions, Nat Rev Rheumatol 11(1) (2015) 45-54.

[49] C.S. Bahney, R.L. Zondervan, P. Allison, A. Theologis, J.W. Ashley, J. Ahn, T. Miclau, R.S. Marcucio, K.D. Hankenson, Cellular biology of fracture healing, J Orthop Res 37(1) (2019) 35-50.

[50] K. Schmidt-Bleek, H. Schell, J. Lienau, N. Schulz, P. Hoff, M. Pfaff, G. Schmidt, C. Martin, C. Perka, F. Buttgereit, H.D. Volk, G. Duda, Initial immune reaction and angiogenesis in bone healing, J Tissue Eng Regen Med 8(2) (2014) 120-30.

[51] L. Claes, S. Recknagel, A. Ignatius, Fracture healing under healthy and inflammatory conditions, Nat Rev Rheumatol 8(3) (2012) 133-43.

[52] R. Marsell, T.A. Einhorn, The biology of fracture healing, Injury 42(6) (2011) 551-5.

[53] I. Könnecke, A. Serra, T. El Khassawna, C. Schlundt, H. Schell, A. Hauser, A. Ellinghaus, H.-D. Volk, A. Radbruch, G.N. Duda, K. Schmidt-Bleek, T and B cells participate in bone repair by infiltrating the fracture callus in a two-wave fashion, Bone 64 (2014) 155-165.

[54] G. Zhu, T. Zhang, M. Chen, K. Yao, X. Huang, B. Zhang, Y. Li, J. Liu, Y. Wang, Z. Zhao, Bone physiological microenvironment and healing mechanism: Basis for future bone-tissue engineering scaffolds, Bioact Mater 6(11) (2021) 4110-4140.

[55] K.E. Martin, A.J. Garcia, Macrophage phenotypes in tissue repair and the foreign body response: Implications for biomaterial-based regenerative medicine strategies, Acta Biomater (2021).

[56] S. Watanabe, M. Alexander, A.V. Misharin, G.R.S. Budinger, The role of macrophages in the resolution of inflammation, J Clin Invest 129(7) (2019) 2619-2628.

[57] L.J. Raggatt, M.E. Wullschleger, K.A. Alexander, A.C. Wu, S.M. Millard, S. Kaur, M.L. Maugham, L.S. Gregory, R. Steck, A.R. Pettit, Fracture healing via periosteal callus formation requires macrophages for both initiation and progression of early endochondral ossification, Am J Pathol 184(12) (2014) 3192-204.

[58] Y. Yao, X. Cai, F. Ren, Y. Ye, F. Wang, C. Zheng, Y. Qian, M. Zhang, The Macrophage-Osteoclast Axis in Osteoimmunity and Osteo-Related Diseases, Front Immunol 12 (2021) 664871.

[59] S.P. Nobs, M. Kopf, Tissue-resident macrophages: guardians of organ homeostasis, Trends Immunol (2021).

[60] A.C. Wu, L.J. Raggatt, K.A. Alexander, A.R. Pettit, Unraveling macrophage contributions to bone repair, Bonekey Rep 2 (2013) 373.

[61] C. Shi, E.G. Pamer, Monocyte recruitment during infection and inflammation, Nat Rev Immunol 11(11) (2011) 762-74.

[62] C. Schlundt, H. Fischer, C.H. Bucher, C. Rendenbach, G.N. Duda, K. Schmidt-Bleek, The multifaceted roles of macrophages in bone regeneration: A story of polarization, activation and time, Acta Biomater (2021).

[63] L. Vi, G.S. Baht, H. Whetstone, A. Ng, Q. Wei, R. Poon, S. Mylvaganam, M. Grynpas, B.A. Alman, Macrophages promote osteoblastic differentiation in-vivo: implications in fracture repair and bone homeostasis, J Bone Miner Res 30(6) (2015) 1090-102.

[64] E.A. Tonna, Fracture Callus Formation in Young and Old Mice Observed with Polarized Light Microscopy, Anat Rec 150 (1964) 349-61.

[65] G.S. Baht, D. Silkstone, L. Vi, P. Nadesan, Y. Amani, H. Whetstone, Q. Wei, B.A. Alman, Exposure to a youthful circulaton rejuvenates bone repair through modulation of beta-catenin, Nat Commun 6 (2015) 7131.

[66] L. Vi, G.S. Baht, E.J. Soderblom, H. Whetstone, Q. Wei, B. Furman, V. Puviindran, P. Nadesan, M. Foster, R. Poon, J.P. White, Y. Yahara, A. Ng, T. Barrientos, M. Grynpas, M.A. Mosely, B.A. Alman, Macrophage cells secrete factors including LRP1 that orchestrate the rejuvenation of bone repair in mice, Nat Commun 9(1) (2018) 5191.

[67] A.M. Silva, M.I. Oliveira, L. Sette, C.R. Almeida, M.J. Oliveira, M.A. Barbosa, S.G. Santos, Resveratrol as a natural anti-tumor necrosis factor-alpha molecule: implications to dendritic cells and their crosstalk with mesenchymal stromal cells, PLoS One 9(3) (2014) e91406.

[68] C.R. Almeida, D.P. Vasconcelos, R.M. Goncalves, M.A. Barbosa, Enhanced mesenchymal stromal cell recruitment via natural killer cells by incorporation of inflammatory signals in biomaterials, J R Soc Interface 9(67) (2012) 261-71.

[69] L. Gong, Y. Zhao, Y. Zhang, Z. Ruan, The Macrophage Polarization Regulates MSC Osteoblast Differentiation in vitro, Ann Clin Lab Sci 46(1) (2016) 65-71.

[70] P. Guihard, Y. Danger, B. Brounais, E. David, R. Brion, J. Delecrin, C.D. Richards, S. Chevalier, F. Redini, D. Heymann, H. Gascan, F. Blanchard, Induction of osteogenesis in mesenchymal stem cells by activated monocytes/macrophages depends on oncostatin M signaling, Stem Cells 30(4) (2012) 762-72.

[71] Y. Zhang, T. Bose, R.E. Unger, J.A. Jansen, C.J. Kirkpatrick, J. van den Beucken, Macrophage type modulates osteogenic differentiation of adipose tissue MSCs, Cell Tissue Res 369(2) (2017) 273-286.

[72] L.Y. Lu, F. Loi, K. Nathan, T.H. Lin, J. Pajarinen, E. Gibon, A. Nabeshima, L. Cordova, E. Jamsen, Z. Yao, S.B. Goodman, Pro-inflammatory M1 macrophages promote Osteogenesis by mesenchymal stem cells via the COX-2-prostaglandin E2 pathway, J Orthop Res 35(11) (2017) 2378-2385.

[73] K. Nathan, L.Y. Lu, T. Lin, J. Pajarinen, E. Jamsen, J.F. Huang, M. Romero-Lopez, M. Maruyama, Y. Kohno, Z. Yao, S.B. Goodman, Precise immunomodulation of the M1 to M2 macrophage transition enhances mesenchymal stem cell osteogenesis and differs by sex, Bone Joint Res 8(10) (2019) 481-488.

[74] J. Pajarinen, T. Lin, E. Gibon, Y. Kohno, M. Maruyama, K. Nathan, L. Lu, Z. Yao, S.B. Goodman, Mesenchymal stem cell-macrophage crosstalk and bone healing, Biomaterials 196 (2019) 80-89.

[75] C. Schlundt, T. El Khassawna, A. Serra, A. Dienelt, S. Wendler, H. Schell, N. van Rooijen, A. Radbruch, R. Lucius, S. Hartmann, G.N. Duda, K. Schmidt-Bleek, Macrophages in bone fracture healing: Their essential role in endochondral ossification, Bone 106 (2018) 78-89.

[76] P.J. Murray, J.E. Allen, S.K. Biswas, E.A. Fisher, D.W. Gilroy, S. Goerdt, S. Gordon, J.A. Hamilton, L.B. Ivashkiv, T. Lawrence, M. Locati, A. Mantovani, F.O. Martinez, J.L. Mege, D.M. Mosser, G. Natoli, J.P. Saeij, J.L. Schultze, K.A. Shirey, A. Sica, J. Suttles, I. Udalova, J.A. van Ginderachter, S.N. Vogel, T.A. Wynn, Macrophage activation and polarization: nomenclature and experimental guidelines, Immunity 41(1) (2014) 14-20.

[77] J.A. Ardura, G. Rackov, E. Izquierdo, V. Alonso, A.R. Gortazar, M.M. Escribese, Targeting Macrophages: Friends or Foes in Disease?, Front Pharmacol 10 (2019) 1255.

[78] A. Mantovani, S.K. Biswas, M.R. Galdiero, A. Sica, M. Locati, Macrophage plasticity and polarization in tissue repair and remodelling, J Pathol 229(2) (2013) 176-85.

[79] J. Loffler, F.A. Sass, S. Filter, A. Rose, A. Ellinghaus, G.N. Duda, A. Dienelt, Compromised Bone Healing in Aged Rats Is Associated With Impaired M2 Macrophage Function, Front Immunol 10 (2019) 2443.

[80] A. Ho-Shui-Ling, J. Bolander, L.E. Rustom, A.W. Johnson, F.P. Luyten, C. Picart, Bone regeneration strategies: Engineered scaffolds, bioactive molecules and stem cells current stage and future perspectives, Biomaterials 180 (2018) 143-162.

[81] D.M. Vasconcelos, S.G. Santos, M. Lamghari, M.A. Barbosa, The two faces of metal ions: From implants rejection to tissue repair/regeneration, Biomaterials 84 (2016) 262-275.

[82] A.R. Armiento, L.P. Hatt, G. Sanchez Rosenberg, K. Thompson, M.J. Stoddart, Functional Biomaterials for Bone Regeneration: A Lesson in Complex Biology, Advanced Functional Materials n/a(n/a) (2020) 1909874.

[83] G.L. Koons, M. Diba, A.G. Mikos, Materials design for bone-tissue engineering, Nature Reviews Materials 5(8) (2020) 584-603.

[84] L. Parisi, A. Toffoli, G. Ghiacci, G.M. Macaluso, Tailoring the Interface of Biomaterials to Design Effective Scaffolds, J Funct Biomater 9(3) (2018).

[85] M.E. Scarritt, R. Londono, B. S.F., Host Response to Implanted Materials and Devices: An Overview, in: B. Corradetti (Ed.), The Immune Response to Implanted Materials and Devices - The Impact of the Immune System on the Success of an Implant, Springer International Publishing2017, pp. 1-14.

[86] J. Anderson, S. Cramer, Chapter 2 - Perspectives on the Inflammatory, Healing, and Foreign Body Responses to Biomaterials and Medical Devices, in: S.F. Badylak (Ed.), Host Response to Biomaterials, Academic Press, Oxford, 2015, pp. 13-36.

[87] R. Londono, S.F. Badylak, Chapter 1 - Factors Which Affect the Host Response to Biomaterials, in: S.F. Badylak (Ed.), Host Response to Biomaterials, Academic Press, Oxford, 2015, pp. 1-12.

[88] D. Zhang, Q. Chen, C. Shi, M. Chen, K. Ma, J. Wan, R. Liu, Dealing with the Foreign-Body Response to Implanted Biomaterials: Strategies and Applications of New Materials, Advanced Functional Materials 31(6) (2021) 2007226.

[89] A. Carnicer-Lombarte, S.T. Chen, G.G. Malliaras, D.G. Barone, Foreign Body Reaction to Implanted Biomaterials and Its Impact in Nerve Neuroprosthetics, Front Bioeng Biotechnol 9 (2021) 622524.

[90] J.O. Abaricia, N. Farzad, T.J. Heath, J. Simmons, L. Morandini, R. Olivares-Navarrete, Control of innate immune response by biomaterial surface topography, energy, and stiffness(), Acta Biomater (2021).

[91] W.J. Geelhoed, L. Moroni, J.I. Rotmans, Utilizing the Foreign Body Response to Grow Tissue Engineered Blood Vessels in Vivo, J Cardiovasc Transl Res 10(2) (2017) 167-179.

[92] J.M. Anderson, S. Jiang, Implications of the Acute and Chronic Inflammatory Response and the Foreign Body Reaction to the Immune Response of Implanted Biomaterials, in: B.

Corradetti (Ed.), The Immune Response to Implanted Materials and Devices - The Impact of the Immune System on the Success of an Implant, Springer International Publishing2017, pp. 15-36.

[93] J.L. Brash, T.A. Horbett, R.A. Latour, P. Tengvall, The blood compatibility challenge. Part 2: Protein adsorption phenomena governing blood reactivity, Acta Biomater 94 (2019) 11-24.

[94] M.E. Bianchi, DAMPs, PAMPs and alarmins: all we need to know about danger, J Leukoc Biol 81(1) (2007) 1-5.

[95] E. Venereau, C. Ceriotti, M.E. Bianchi, DAMPs from Cell Death to New Life, Front Immunol 6 (2015) 422.

[96] S.N. Christo, K.R. Diener, A. Bachhuka, K. Vasilev, J.D. Hayball, Innate Immunity and Biomaterials at the Nexus: Friends or Foes, BioMed Research International 2015 (2015) 342304.

[97] R. Klopfleisch, F. Jung, The pathology of the foreign body reaction against biomaterials, J Biomed Mater Res A 105(3) (2017) 927-940.

[98] J. Wang, H. Arase, Regulation of immune responses by neutrophils, Ann N Y Acad Sci 1319 (2014) 66-81.

[99] E. Perez-Figueroa, P. Alvarez-Carrasco, E. Ortega, C. Maldonado-Bernal, Neutrophils: Many Ways to Die, Front Immunol 12 (2021) 631821.

[100] C.Y. Tsai, S.C. Hsieh, C.W. Liu, C.S. Lu, C.H. Wu, H.T. Liao, M.H. Chen, K.J. Li, C.Y. Shen, Y.M. Kuo, C.L. Yu, Cross-Talk among Polymorphonuclear Neutrophils, Immune, and Non-Immune Cells via Released Cytokines, Granule Proteins, Microvesicles, and Neutrophil Extracellular Trap Formation: A Novel Concept of Biology and Pathobiology for Neutrophils, Int J Mol Sci 22(6) (2021).

[101] Z. Sheikh, P.J. Brooks, O. Barzilay, N. Fine, M. Glogauer, Macrophages, Foreign Body Giant Cells and Their Response to Implantable Biomaterials, Materials (Basel) 8(9) (2015) 5671-5701.

[102] C.E. Witherel, D. Abebayehu, T.H. Barker, K.L. Spiller, Macrophage and Fibroblast Interactions in Biomaterial-Mediated Fibrosis, Adv Healthc Mater 8(4) (2019) e1801451.

[103] J. Ye, C. Xie, C. Wang, J. Huang, Z. Yin, B.C. Heng, X. Chen, W. Shen, Promoting musculoskeletal system soft tissue regeneration by biomaterial-mediated modulation of macrophage polarization, Bioact Mater 6(11) (2021) 4096-4109.

[104] J.N. Barbosa, D.P. Vasconcelos, Chapter 3 - Macrophage response to biomaterials, in: M. Mozafari (Ed.), Handbook of Biomaterials Biocompatibility, Woodhead Publishing2020, pp. 43-52.

[105] H. Knopf-Marques, L. Paiva, F. Prévot, J. Barthès, Macrophage-Based Immunomodulation for Biomaterial Applications, in: N.E. Vrana (Ed.), Biomaterials and Immune Response: Complications, Mechanisms and Immunomodulation - Complications, Mechanisms and Immunomodulation, CRC Press - Taylor & Francis Group2019, pp. 191-210.

[106] M. Hesketh, K.B. Sahin, Z.E. West, R.Z. Murray, Macrophage Phenotypes Regulate Scar Formation and Chronic Wound Healing, Int J Mol Sci 18(7) (2017).

[107] R. Klopfleisch, Macrophage reaction against biomaterials in the mouse model - Phenotypes, functions and markers, Acta Biomater 43 (2016) 3-13.

[108] P.L. Graney, S. Ben-Shaul, S. Landau, A. Bajpai, B. Singh, J. Eager, A. Cohen, S. Levenberg, K.L. Spiller, Macrophages of diverse phenotypes drive vascularization of engineered tissues, Sci Adv 6(18) (2020) eaay6391.

[109] F.O. Martinez, S. Gordon, The M1 and M2 paradigm of macrophage activation: time for reassessment, F1000Prime Rep 6 (2014) 13.

[110] D.V. Pechkovsky, A. Prasse, F. Kollert, K.M. Engel, J. Dentler, W. Luttmann, K. Friedrich, J. Muller-Quernheim, G. Zissel, Alternatively activated alveolar macrophages in pulmonary fibrosis-mediator production and intracellular signal transduction, Clin Immunol 137(1) (2010) 89-101.

[111] G. Raes, R. Van den Bergh, P. De Baetselier, G.H. Ghassabeh, C. Scotton, M. Locati, A. Mantovani, S. Sozzani, Arginase-1 and Ym1 are markers for murine, but not human, alternatively activated myeloid cells, J Immunol 174(11) (2005) 6561; author reply 6561-2.

[112] L.X. Wang, S.X. Zhang, H.J. Wu, X.L. Rong, J. Guo, M2b macrophage polarization and its roles in diseases, J Leukoc Biol 106(2) (2019) 345-358.

[113] E.B. Lurier, D. Dalton, W. Dampier, P. Raman, S. Nassiri, N.M. Ferraro, R. Rajagopalan, M. Sarmady, K.L. Spiller, Transcriptome analysis of IL-10-stimulated (M2c) macrophages by next-generation sequencing, Immunobiology 222(7) (2017) 847-856.

[114] S.A. Gharib, R.S. McMahan, W.E. Eddy, M.E. Long, W.C. Parks, M.L. Aitken, A.M. Manicone, Transcriptional and functional diversity of human macrophage repolarization, J Allergy Clin Immunol 143(4) (2019) 1536-1548.

[115] A. Sindrilaru, K. Scharffetter-Kochanek, Disclosure of the Culprits: Macrophages-Versatile Regulators of Wound Healing, Adv Wound Care (New Rochelle) 2(7) (2013) 357-368.

[116] C.J. Ferrante, G. Pinhal-Enfield, G. Elson, B.N. Cronstein, G. Hasko, S. Outram, S.J. Leibovich, The adenosine-dependent angiogenic switch of macrophages to an M2-like phenotype is independent of interleukin-4 receptor alpha (IL-4Ralpha) signaling, Inflammation 36(4) (2013) 921-31.

[117] V.A. Fadok, D.L. Bratton, A. Konowal, P.W. Freed, J.Y. Westcott, P.M. Henson, Macrophages that have ingested apoptotic cells in vitro inhibit proinflammatory cytokine production through autocrine/paracrine mechanisms involving TGF-beta, PGE2, and PAF, J Clin Invest 101(4) (1998) 890-8.

[118] J. Xue, S.V. Schmidt, J. Sander, A. Draffehn, W. Krebs, I. Quester, D. De Nardo, T.D. Gohel, M. Emde, L. Schmidleithner, H. Ganesan, A. Nino-Castro, M.R. Mallmann, L. Labzin, H. Theis, M. Kraut, M. Beyer, E. Latz, T.C. Freeman, T. Ulas, J.L. Schultze, Transcriptome-based network analysis reveals a spectrum model of human macrophage activation, Immunity 40(2) (2014) 274-88.

[119] S.D. Sommerfeld, C. Cherry, R.M. Schwab, L. Chung, D.R. Maestas, Jr., P. Laffont, J.E. Stein, A. Tam, S. Ganguly, F. Housseau, J.M. Taube, D.M. Pardoll, P. Cahan, J.H. Elisseeff, Interleukin-36gamma-producing macrophages drive IL-17-mediated fibrosis, Sci Immunol 4(40) (2019).

[120] M.J. Vassey, G.P. Figueredo, D.J. Scurr, A.S. Vasilevich, S. Vermeulen, A. Carlier, J. Luckett, N.R.M. Beijer, P. Williams, D.A. Winkler, J. de Boer, A.M. Ghaemmaghami, M.R. Alexander, Immune Modulation by Design: Using Topography to Control Human Monocyte Attachment and Macrophage Differentiation, Adv Sci (Weinh) 7(11) (2020) 1903392.

[121] K. Garg, N.A. Pullen, C.A. Oskeritzian, J.J. Ryan, G.L. Bowlin, Macrophage functional polarization (M1/M2) in response to varying fiber and pore dimensions of electrospun scaffolds, Biomaterials 34(18) (2013) 4439-51.

[122] K.M. Hotchkiss, G.B. Reddy, S.L. Hyzy, Z. Schwartz, B.D. Boyan, R. Olivares-Navarrete, Titanium surface characteristics, including topography and wettability, alter macrophage activation, Acta Biomater 31 (2016) 425-434.

[123] C.H. Lee, Y.J. Kim, J.H. Jang, J.W. Park, Modulating macrophage polarization with divalent cations in nanostructured titanium implant surfaces, Nanotechnology 27(8) (2016) 085101.

[124] K. Sadtler, M.T. Wolf, S. Ganguly, C.A. Moad, L. Chung, S. Majumdar, F. Housseau, D.M. Pardoll, J.H. Elisseeff, Divergent immune responses to synthetic and biological scaffolds, Biomaterials 192 (2019) 405-415.

[125] A. Vishwakarma, N.S. Bhise, M.B. Evangelista, J. Rouwkema, M.R. Dokmeci, A.M. Ghaemmaghami, N.E. Vrana, A. Khademhosseini, Engineering Immunomodulatory Biomaterials To Tune the Inflammatory Response, Trends Biotechnol 34(6) (2016) 470-482.

[126] M.E. Ogle, C.E. Segar, S. Sridhar, E.A. Botchwey, Monocytes and macrophages in tissue repair: Implications for immunoregenerative biomaterial design, Exp Biol Med (Maywood) 241(10) (2016) 1084-97.

[127] J.L. Dziki, S.F. Badylak, Immunomodulatory biomaterials, Current Opinion in Biomedical Engineering 6 (2018) 51-57.

[128] N.A. Hotaling, L. Tang, D.J. Irvine, J.E. Babensee, Biomaterial Strategies for Immunomodulation, Annu Rev Biomed Eng 17 (2015) 317-49.

[129] J. Lee, H. Byun, S.K. Madhurakkat Perikamana, S. Lee, H. Shin, Current Advances in Immunomodulatory Biomaterials for Bone Regeneration, Adv Healthc Mater 8(4) (2019) e1801106.

[130] Z. Chen, A. Bachhuka, S. Han, F. Wei, S. Lu, R.M. Visalakshan, K. Vasilev, Y. Xiao, Tuning Chemistry and Topography of Nanoengineered Surfaces to Manipulate Immune Response for Bone Regeneration Applications, ACS Nano 11(5) (2017) 4494-4506.

[131] L. Lv, Y. Xie, K. Li, T. Hu, X. Lu, Y. Cao, X. Zheng, Unveiling the Mechanism of Surface Hydrophilicity-Modulated Macrophage Polarization, Adv Healthc Mater 7(19) (2018) e1800675.

[132] Y. Zhu, H. Liang, X. Liu, J. Wu, C. Yang, T.M. Wong, K.Y.H. Kwan, K.M.C. Cheung, S. Wu, K.W.K. Yeung, Regulation of macrophage polarization through surface topography design to facilitate implant-to-bone osteointegration, Sci Adv 7(14) (2021).

[133] X. Yin, Y. Li, C. Yang, J. Weng, J. Wang, J. Zhou, B. Feng, Alginate/chitosan multilayer films coated on IL-4-loaded TiO2 nanotubes for modulation of macrophage phenotype, Int J Biol Macromol 132 (2019) 495-505.

[134] C. Yin, Q. Zhao, W. Li, Z. Zhao, J. Wang, T. Deng, P. Zhang, K. Shen, Z. Li, Y. Zhang, Biomimetic anti-inflammatory nano-capsule serves as a cytokine blocker and M2 polarization inducer for bone tissue repair, Acta Biomater 102 (2020) 416-426.

[135] I.M. Castano, R.M. Raftery, G. Chen, B. Cavanagh, B. Quinn, G.P. Duffy, F.J. O'Brien, C.M. Curtin, Rapid bone repair with the recruitment of CD206(+)M2-like macrophages using non-viral scaffold-mediated miR-133a inhibition of host cells, Acta Biomater 109 (2020) 267-279.

[136] B.N. Brown, J.E. Valentin, A.M. Stewart-Akers, G.P. McCabe, S.F. Badylak, Macrophage phenotype and remodeling outcomes in response to biologic scaffolds with and without a cellular component, Biomaterials 30(8) (2009) 1482-91.

[137] B.N. Brown, R. Londono, S. Tottey, L. Zhang, K.A. Kukla, M.T. Wolf, K.A. Daly, J.E. Reing, S.F. Badylak, Macrophage phenotype as a predictor of constructive remodeling following the implantation of biologically derived surgical mesh materials, Acta Biomater 8(3) (2012) 978-87.

[138] K. Sadtler, K. Estrellas, B.W. Allen, M.T. Wolf, H. Fan, A.J. Tam, C.H. Patel, B.S. Luber, H. Wang, K.R. Wagner, J.D. Powell, F. Housseau, D.M. Pardoll, J.H. Elisseeff, Developing a pro-regenerative biomaterial scaffold microenvironment requires T helper 2 cells, Science 352(6283) (2016) 366-70.

[139] A. Garcia-Garcia, I. Martin, Extracellular Matrices to Modulate the Innate Immune Response and Enhance Bone Healing, Front Immunol 10 (2019) 2256.

[140] K. Adu-Berchie, D.J. Mooney, Biomaterials as Local Niches for Immunomodulation, Accounts of Chemical Research 53(9) (2020) 1749-1760.

[141] Z. Chen, T. Klein, R.Z. Murray, R. Crawford, J. Chang, C. Wu, Y. Xiao, Osteoimmunomodulation for the development of advanced bone biomaterials, Materials Today 19(6) (2016) 304-321.

[142] Z. Peng, C. Wang, C. Liu, H. Xu, Y. Wang, Y. Liu, Y. Hu, J. Li, Y. Jin, C. Jiang, L. Liu, J. Guo, L. Zhu, 3D printed polycaprolactone/beta-tricalcium phosphate/magnesium peroxide oxygen releasing scaffold enhances osteogenesis and implanted BMSCs survival in repairing the large bone defect, J Mater Chem B 9(28) (2021) 5698-5710.

[143] N.H. Lee, M.S. Kang, T.H. Kim, D.S. Yoon, N. Mandakhbayar, S.B. Jo, H.S. Kim, J.C. Knowles, J.H. Lee, H.W. Kim, Dual actions of osteoclastic-inhibition and osteogenic-stimulation through strontium-releasing bioactive nanoscale cement imply biomaterial-enabled osteoporosis therapy, Biomaterials 276 (2021) 121025.

[144] A. Mostafavi, T. Abudula, C.S. Russell, E. Mostafavi, T.J. Williams, N. Salah, A. Alshahrie, S. Harris, S.M.M. Basri, Y.K. Mishra, T.J. Webster, A. Memic, A. Tamayol, In situ printing of scaffolds for reconstruction of bone defects, Acta Biomater 127 (2021) 313-326.

[145] A.K. Nasution, H. Hermawan, Degradable Biomaterials for Temporary Medical Implants, in: F. Mahyudin, H. Hermawan (Eds.), Biomaterials and Medical Devices: A Perspective from an Emerging Country, Springer International Publishing, Cham, 2016, pp. 127-160.

[146] S. Wei, J.X. Ma, L. Xu, X.S. Gu, X.L. Ma, Biodegradable materials for bone defect repair, Mil Med Res 7(1) (2020) 54.

[147] Z. Sheikh, S. Najeeb, Z. Khurshid, V. Verma, H. Rashid, M. Glogauer, Biodegradable Materials for Bone Repair and Tissue Engineering Applications, Materials (Basel) 8(9) (2015) 5744-5794.

[148] G. Bass, M.L. Becker, D.E. Heath, S.L. Cooper, 1.3.2 - Polymers: Basic Principles, in: W.R. Wagner, S.E. Sakiyama-Elbert, G. Zhang, M.J. Yaszemski (Eds.), Biomaterials Science (Fourth Edition), Academic Press2020, pp. 85-102.

[149] F. Donnaloja, E. Jacchetti, M. Soncini, M.T. Raimondi, Natural and Synthetic Polymers for Bone Scaffolds Optimization, Polymers (Basel) 12(4) (2020).

[150] Y. Song, L. Li, W. Zhao, Y. Qian, L. Dong, Y. Fang, L. Yang, Y. Fan, Surface modification of electrospun fibers with mechano-growth factor for mitigating the foreign-body reaction, Bioact Mater 6(9) (2021) 2983-2998.

[151] A.D. Schoenenberger, H. Tempfer, C. Lehner, J. Egloff, M. Mauracher, A. Bird, J. Widmer, K. Maniura-Weber, S.F. Fucentese, A. Traweger, U. Silvan, J.G. Snedeker, Macromechanics and polycaprolactone fiber organization drive macrophage polarization and regulate inflammatory activation of tendon in vitro and in vivo, Biomaterials 249 (2020) 120034.

[152] Y. Jia, W. Yang, K. Zhang, S. Qiu, J. Xu, C. Wang, Y. Chai, Nanofiber arrangement regulates peripheral nerve regeneration through differential modulation of macrophage phenotypes, Acta Biomater 83 (2019) 291-301.

[153] J. Zhang, B. Xie, Z. Xi, L. Zhao, L. Cen, Y. Yang, A comparable study of polyglycolic acid's degradation on macrophages' activation, Mater Sci Eng C Mater Biol Appl 109 (2020) 110574.

[154] M. Filippi, G. Born, M. Chaaban, A. Scherberich, Natural Polymeric Scaffolds in Bone Regeneration, Front Bioeng Biotechnol 8 (2020) 474.

[155] J.Y. Jo, S.I. Jeong, Y.M. Shin, S.S. Kang, S.E. Kim, C.M. Jeong, J.B. Huh, Sequential delivery of BMP-2 and BMP-7 for bone regeneration using a heparinized collagen membrane, Int J Oral Maxillofac Surg 44(7) (2015) 921-8.

[156] E.L. Durham, R.N. Howie, S. Hall, N. Larson, B. Oakes, R. Houck, Z. Grey, M. Steed, A.C. LaRue, R. Muise-Helmericks, J. Cray, Optimizing bone wound healing using BMP2 with absorbable collagen sponge and Talymed nanofiber scaffold, J Transl Med 16(1) (2018) 321.

[157] Q. Leng, L. Chen, Y. Lv, RNA-based scaffolds for bone regeneration: application and mechanisms of mRNA, miRNA and siRNA, Theranostics 10(7) (2020) 3190-3205.

[158] L. Sbricoli, R. Guazzo, M. Annunziata, L. Gobbato, E. Bressan, L. Nastri, Selection of Collagen Membranes for Bone Regeneration: A Literature Review, Materials (Basel) 13(3) (2020).

[159] F. Taraballi, B. Corradetti, S. Minardi, S. Powel, F. Cabrera, J.L. Van Eps, B.K. Weiner, E. Tasciotti, Biomimetic collagenous scaffold to tune inflammation by targeting macrophages, J Tissue Eng 7 (2016) 2041731415624667.

[160] C. Chu, L. Liu, Y. Wang, R. Yang, C. Hu, S. Rung, Y. Man, Y. Qu, Evaluation of epigallocatechin-3-gallate (EGCG)-modified scaffold determines macrophage recruitment, Mater Sci Eng C Mater Biol Appl 100 (2019) 505-513.

[161] R. Sridharan, E.J. Ryan, C.J. Kearney, D.J. Kelly, F.J. O'Brien, Macrophage Polarization in Response to Collagen Scaffold Stiffness Is Dependent on Cross-Linking Agent Used To Modulate the Stiffness, ACS Biomater Sci Eng 5(2) (2019) 544-552.

[162] A.M.H. Larsen, D.E. Kuczek, A. Kalvisa, M.S. Siersbaek, M.L. Thorseth, A.Z. Johansen, M. Carretta, L. Grontved, O. Vang, D.H. Madsen, Collagen Density Modulates the Immunosuppressive Functions of Macrophages, J Immunol 205(5) (2020) 1461-1472.

[163] B. Sultankulov, D. Berillo, K. Sultankulova, T. Tokay, A. Saparov, Progress in the Development of Chitosan-Based Biomaterials for Tissue Engineering and Regenerative Medicine, Biomolecules 9(9) (2019).

[164] S. Elkholy, S. Yahia, M. Awad, M. Elmessiery, In vivo evaluation of beta-CS/n-HA with different physical properties as a new bone graft material, Clin Implant Dent Relat Res 20(3) (2018) 416-423.

[165] F. Furlani, P. Sacco, E. Decleva, R. Menegazzi, I. Donati, S. Paoletti, E. Marsich, Chitosan Acetylation Degree Influences the Physical Properties of Polysaccharide

Nanoparticles: Implication for the Innate Immune Cells Response, ACS Appl Mater Interfaces 11(10) (2019) 9794-9803.

[166] I.F. Amaral, P. Sampaio, M.A. Barbosa, Three-dimensional culture of human osteoblastic cells in chitosan sponges: the effect of the degree of acetylation, J Biomed Mater Res A 76(2) (2006) 335-46.

[167] J.N. Barbosa, I.F. Amaral, A.P. Aguas, M.A. Barbosa, Evaluation of the effect of the degree of acetylation on the inflammatory response to 3D porous chitosan scaffolds, J Biomed Mater Res A 93(1) (2010) 20-8.

[168] D.P. Vasconcelos, A.C. Fonseca, M. Costa, I.F. Amaral, M.A. Barbosa, A.P. Aguas, J.N. Barbosa, Macrophage polarization following chitosan implantation, Biomaterials 34(38) (2013) 9952-9.

[169] D.P. Vasconcelos, M. Costa, I.F. Amaral, M.A. Barbosa, A.P. Aguas, J.N. Barbosa, Development of an immunomodulatory biomaterial: using resolvin D1 to modulate inflammation, Biomaterials 53 (2015) 566-73.

[170] D.P. Vasconcelos, C. de Torre-Minguela, A.I. Gomez, A.P. Aguas, M.A. Barbosa, P. Pelegrin, J.N. Barbosa, 3D chitosan scaffolds impair NLRP3 inflammasome response in macrophages, Acta Biomater 91 (2019) 123-134.

[171] A. Henriques Lourenco, N. Neves, C. Ribeiro-Machado, S.R. Sousa, M. Lamghari, C.C. Barrias, A. Trigo Cabral, M.A. Barbosa, C.C. Ribeiro, Injectable hybrid system for strontium local delivery promotes bone regeneration in a rat critical-sized defect model, Sci Rep 7(1) (2017) 5098.

[172] H. Zhang, Q. Cai, Y. Zhu, W. Zhu, A simple hydrogel scaffold with injectability, adhesivity and osteogenic activity for bone regeneration, Biomater Sci 9(3) (2021) 960-972.

[173] G. Choe, S. Oh, J.M. Seok, S.A. Park, J.Y. Lee, Graphene oxide/alginate composites as novel bioinks for three-dimensional mesenchymal stem cell printing and bone regeneration applications, Nanoscale 11(48) (2019) 23275-23285.

[174] J. Barros, M.P. Ferraz, J. Azeredo, M.H. Fernandes, P.S. Gomes, F.J. Monteiro, Alginate-nanohydroxyapatite hydrogel system: Optimizing the formulation for enhanced bone regeneration, Mater Sci Eng C Mater Biol Appl 105 (2019) 109985.

[175] S. Jain, T.H. Tran, M. Amiji, Macrophage repolarization with targeted alginate nanoparticles containing IL-10 plasmid DNA for the treatment of experimental arthritis, Biomaterials 61 (2015) 162-77.

[176] A. Kerschenmeyer, O. Arlov, V. Malheiro, M. Steinwachs, M. Rottmar, K. Maniura-Weber, G. Palazzolo, M. Zenobi-Wong, Anti-oxidant and immune-modulatory properties of sulfated alginate derivatives on human chondrocytes and macrophages, Biomater Sci 5(9) (2017) 1756-1765.

[177] G.S. Hussey, J.L. Dziki, S.F. Badylak, Extracellular matrix-based materials for regenerative medicine, Nature Reviews Materials 3(7) (2018) 159-173.

[178] D.N. Bracey, A.H. Jinnah, J.S. Willey, T.M. Seyler, I.D. Hutchinson, P.W. Whitlock, T.L. Smith, K.A. Danelson, C.L. Emory, B.A. Kerr, Investigating the Osteoinductive Potential of a Decellularized Xenograft Bone Substitute, Cells Tissues Organs 207(2) (2019) 97-113.

[179] M.S. Lee, D.H. Lee, J. Jeon, G. Tae, Y.M. Shin, H.S. Yang, Biofabrication and application of decellularized bone extracellular matrix for effective bone regeneration, Journal of Industrial and Engineering Chemistry 83 (2020) 323-332.

[180] J.L. Dziki, L. Huleihel, M.E. Scarritt, S.F. Badylak, Extracellular Matrix Bioscaffolds as Immunomodulatory Biomaterials<sup/>, Tissue Eng Part A 23(19-20) (2017) 1152-1159.

[181] B.M. Sicari, J.L. Dziki, B.F. Siu, C.J. Medberry, C.L. Dearth, S.F. Badylak, The promotion of a constructive macrophage phenotype by solubilized extracellular matrix, Biomaterials 35(30) (2014) 8605-12.

[182] L. Huleihel, J.L. Dziki, J.G. Bartolacci, T. Rausch, M.E. Scarritt, M.C. Cramer, T. Vorobyov, S.T. LoPresti, I.T. Swineheart, L.J. White, B.N. Brown, S.F. Badylak, Macrophage phenotype in response to ECM bioscaffolds, Semin Immunol 29 (2017) 2-13.

[183] P.F. Slivka, C.L. Dearth, T.J. Keane, F.W. Meng, C.J. Medberry, R.T. Riggio, J.E. Reing, S.F. Badylak, Fractionation of an ECM hydrogel into structural and soluble components reveals distinctive roles in regulating macrophage behavior, Biomaterials Science 2(10) (2014) 1521-1534.

[184] S.T. LoPresti, B.N. Brown, Effect of Source Animal Age upon Macrophage Response to Extracellular Matrix Biomaterials, J Immunol Regen Med 1 (2018) 57-66.

[185] R.X. Wu, X.T. He, J.H. Zhu, Y. Yin, X. Li, X. Liu, F.M. Chen, Modulating macrophage responses to promote tissue regeneration by changing the formulation of bone extracellular matrix from filler particles to gel bioscaffolds, Mater Sci Eng C Mater Biol Appl 101 (2019) 330-340.

[186] P. Qiu, M. Li, K. Chen, B. Fang, P. Chen, Z. Tang, X. Lin, S. Fan, Periosteal matrix-derived hydrogel promotes bone repair through an early immune regulation coupled with enhanced angio- and osteogenesis, Biomaterials 227 (2020) 119552.

[187] D.M. Vasconcelos, R.M. Goncalves, C.R. Almeida, I.O. Pereira, M.I. Oliveira, N. Neves, A.M. Silva, A.C. Ribeiro, C. Cunha, A.R. Almeida, C.C. Ribeiro, A.M. Gil, E. Seebach, K.L. Kynast, W. Richter, M. Lamghari, S.G. Santos, M.A. Barbosa, Fibrinogen scaffolds with immunomodulatory properties promote in vivo bone regeneration, Biomaterials 111 (2016) 163-178.

[188] M. Bessa-Goncalves, A.M. Silva, J.P. Bras, H. Helmholz, B.J.C. Luthringer-Feyerabend, R. Willumeit-Romer, M.A. Barbosa, S.G. Santos, Fibrinogen and magnesium combination biomaterials modulate macrophage phenotype, NF-kB signaling and crosstalk with mesenchymal stem/stromal cells, Acta Biomater 114 (2020) 471-484.

[189] L. Tang, J.W. Eaton, Fibrin(ogen) mediates acute inflammatory responses to biomaterials, J Exp Med 178(6) (1993) 2147-56.

[190] J. Zdolsek, J.W. Eaton, L. Tang, Histamine release and fibrinogen adsorption mediate acute inflammatory responses to biomaterial implants in humans, J Transl Med 5 (2007) 31.

[191] F. Scognamiglio, A. Travan, I. Rustighi, P. Tarchi, S. Palmisano, E. Marsich, M. Borgogna, I. Donati, N. de Manzini, S. Paoletti, Adhesive and sealant interfaces for general surgery applications, J Biomed Mater Res B Appl Biomater 104(3) (2016) 626-39.

[192] S. Santos Tde, R.P. Abuna, A.L. Almeida, M.M. Beloti, A.L. Rosa, Effect of collagen sponge and fibrin glue on bone repair, J Appl Oral Sci 23(6) (2015) 623-8.

[193] B.S. Kim, J. Lee, Enhanced bone healing by improved fibrin-clot formation via fibrinogen adsorption on biphasic calcium phosphate granules, Clin Oral Implants Res 26(10) (2015) 1203-10.

[194] E. Seebach, H. Freischmidt, J. Holschbach, J. Fellenberg, W. Richter, Mesenchymal stroma cells trigger early attraction of M1 macrophages and endothelial cells into fibrin hydrogels, stimulating long bone healing without long-term engraftment, Acta Biomater 10(11) (2014) 4730-4741.

[195] S.G. Santos, M. Lamghari, C.R. Almeida, M.I. Oliveira, N. Neves, A.C. Ribeiro, J.N. Barbosa, R. Barros, J. Maciel, M.C. Martins, R.M. Goncalves, M.A. Barbosa, Adsorbed fibrinogen leads to improved bone regeneration and correlates with differences in the systemic immune response, Acta Biomater 9(7) (2013) 7209-17.

[196] J.Y. Hsieh, T.D. Smith, V.S. Meli, T.N. Tran, E.L. Botvinick, W.F. Liu, Differential regulation of macrophage inflammatory activation by fibrin and fibrinogen, Acta Biomater 47 (2017) 14-24.

[197] B.J. Rybarczyk, S.O. Lawrence, P.J. Simpson-Haidaris, Matrix-fibrinogen enhances wound closure by increasing both cell proliferation and migration, Blood 102(12) (2003) 4035-43.

[198] V.K. Lishko, N.P. Podolnikova, V.P. Yakubenko, S. Yakovlev, L. Medved, S.P. Yadav, T.P. Ugarova, Multiple binding sites in fibrinogen for integrin alphaMbeta2 (Mac-1), J Biol Chem 279(43) (2004) 44897-906.

[199] S.A. Sell, M.P. Francis, K. Garg, M.J. McClure, D.G. Simpson, G.L. Bowlin, Cross-linking methods of electrospun fibrinogen scaffolds for tissue engineering applications, Biomed Mater 3(4) (2008) 045001.

[200] E. Peled, J. Boss, J. Bejar, C. Zinman, D. Seliktar, A novel poly(ethylene glycol)-fibrinogen hydrogel for tibial segmental defect repair in a rat model, J Biomed Mater Res A 80(4) (2007) 874-84.

[201] J. Maciel, M.I. Oliveira, E. Colton, A.K. McNally, C. Oliveira, J.M. Anderson, M.A. Barbosa, Adsorbed fibrinogen enhances production of bone- and angiogenic-related factors by monocytes/macrophages, Tissue Eng Part A 20(1-2) (2014) 250-63.

[202] M.I. Oliveira, M.L. Pinto, R.M. Goncalves, M.C.L. Martins, S.G. Santos, M.A. Barbosa, Adsorbed Fibrinogen stimulates TLR-4 on monocytes and induces BMP-2 expression, Acta Biomater 49 (2017) 296-305.

[203] A.L. Torres, S.G. Santos, M.I. Oliveira, M.A. Barbosa, Fibrinogen promotes resorption of chitosan by human osteoclasts, Acta Biomater 9(5) (2013) 6553-62.

[204] A.R. Almeida, M. Bessa-Goncalves, D.M. Vasconcelos, M.A. Barbosa, S.G. Santos, Osteoclasts degrade fibrinogen scaffolds and induce mesenchymal stem/stromal osteogenic differentiation, J Biomed Mater Res A 108(4) (2020) 851-862.

[205] J.R. Jones, I.R. Gibson, 1.3.4 - Ceramics, Glasses, and Glass-Ceramics: Basic Principles, in: W.R. Wagner, S.E. Sakiyama-Elbert, G. Zhang, M.J. Yaszemski (Eds.), Biomaterials Science (Fourth Edition), Academic Press2020, pp. 289-305.

[206] O.R. Mahon, D.C. Browe, T. Gonzalez-Fernandez, P. Pitacco, I.T. Whelan, S. Von Euw, C. Hobbs, V. Nicolosi, K.T. Cunningham, K.H.G. Mills, D.J. Kelly, A. Dunne, Nano-

particle mediated M2 macrophage polarization enhances bone formation and MSC osteogenesis in an IL-10 dependent manner, Biomaterials 239 (2020) 119833.

[207] C. Yang, C. Zhao, X. Wang, M. Shi, Y. Zhu, L. Jing, C. Wu, J. Chang, Stimulation of osteogenesis and angiogenesis by micro/nano hierarchical hydroxyapatite via macrophage immunomodulation, Nanoscale 11(38) (2019) 17699-17708.

[208] C. Li, L. Yang, X. Ren, M. Lin, X. Jiang, D. Shen, T. Xu, J. Ren, L. Huang, W. Qing, J. Zheng, Y. Mu, Groove structure of porous hydroxyapatite scaffolds (HAS) modulates immune environment via regulating macrophages and subsequently enhances osteogenesis, J Biol Inorg Chem 24(5) (2019) 733-745.

[209] S. Tai, J.Y. Cheng, H. Ishii, K. Shimono, V. Zangiacomi, T. Satoh, T. Hosono, E. Suzuki, K. Yamaguchi, K. Maruyama, Effects of beta-tricalcium phosphate particles on primary cultured murine dendritic cells and macrophages, Int Immunopharmacol 40 (2016) 419-427.

[210] Z. Chen, J. Yuen, R. Crawford, J. Chang, C. Wu, Y. Xiao, The effect of osteoimmunomodulation on the osteogenic effects of cobalt incorporated beta-tricalcium phosphate, Biomaterials 61 (2015) 126-38.

[211] X. Chen, J. Wang, J. Wang, X. Zhu, X. Yang, Y. Fan, X. Zhang, The positive role of macrophage secretion stimulated by BCP ceramic in the ceramic-induced osteogenic differentiation of pre-osteoblasts via Smad-related signaling pathways, RSC Advances 6(104) (2016) 102134-102141.

[212] X. Chen, M. Wang, F. Chen, J. Wang, X. Li, J. Liang, Y. Fan, Y. Xiao, X. Zhang, Correlations between macrophage polarization and osteoinduction of porous calcium phosphate ceramics, Acta Biomater 103 (2020) 318-332.

[213] J.R. Jones, Reprint of: Review of bioactive glass: From Hench to hybrids, Acta Biomater 23 Suppl (2015) S53-82.

[214] F. Baino, S. Hamzehlou, S. Kargozar, Bioactive Glasses: Where Are We and Where Are We Going?, J Funct Biomater 9(1) (2018).

[215] L.L. Hench, J.M. Polak, Third-generation biomedical materials, Science 295(5557) (2002) 1014-7.

[216] I. Cacciotti, Bivalent cationic ions doped bioactive glasses: the influence of magnesium, zinc, strontium and copper on the physical and biological properties, Journal of Materials Science 52(15) (2017) 8812-8831.

[217] A. Hoppe, A.R. Boccaccini, Biological Impact of Bioactive Glasses and Their Dissolution Products, Front Oral Biol 17 (2015) 22-32.

[218] X. Lu, K. Li, Y. Xie, S. Qi, Q. Shen, J. Yu, L. Huang, X. Zheng, Improved osteogenesis of boron incorporated calcium silicate coatings via immunomodulatory effects, J Biomed Mater Res A 107(1) (2019) 12-24.

[219] K. Zheng, E. Torre, A. Bari, N. Taccardi, C. Cassinelli, M. Morra, S. Fiorilli, C. Vitale-Brovarone, G. Iviglia, A.R. Boccaccini, Antioxidant mesoporous Ce-doped bioactive glass nanoparticles with anti-inflammatory and pro-osteogenic activities, Mater Today Bio 5 (2020) 100041.

[220] L. Liu, F. Zhao, X. Chen, M. Luo, Z. Yang, X. Cao, G. Miao, D. Chen, X. Chen, Local delivery of FTY720 in mesoporous bioactive glass improves bone regeneration by synergistically immunomodulating osteogenesis and osteoclastogenesis, J Mater Chem B 8(28) (2020) 6148-6158.

[221] J.S. Fernandes, P. Gentile, R.A. Pires, R.L. Reis, P.V. Hatton, Multifunctional bioactive glass and glass-ceramic biomaterials with antibacterial properties for repair and regeneration of bone tissue, Acta Biomater 59 (2017) 2-11.

[222] M.N. Rahaman, 3 - Bioactive ceramics and glasses for tissue engineering, in: A.R. Boccaccini, P.X. Ma (Eds.), Tissue Engineering Using Ceramics and Polymers (Second Edition), Woodhead Publishing2014, pp. 67-114.

[223] R. Lin, C. Deng, X. Li, Y. Liu, M. Zhang, C. Qin, Q. Yao, L. Wang, C. Wu, Copper-incorporated bioactive glass-ceramics inducing anti-inflammatory phenotype and regeneration of cartilage/bone interface, Theranostics 9(21) (2019) 6300-6313.

[224] J.M. Sadowska, F. Wei, J. Guo, J. Guillem-Marti, Z. Lin, M.P. Ginebra, Y. Xiao, The effect of biomimetic calcium deficient hydroxyapatite and sintered beta-tricalcium phosphate on osteoimmune reaction and osteogenesis, Acta Biomater 96 (2019) 605-618.

[225] J.M. Sadowska, F. Wei, J. Guo, J. Guillem-Marti, M.P. Ginebra, Y. Xiao, Effect of nano-structural properties of biomimetic hydroxyapatite on osteoimmunomodulation, Biomaterials 181 (2018) 318-332.

[226] A. Diez-Escudero, M. Espanol, M. Bonany, X. Lu, C. Persson, M.P. Ginebra, Heparinization of Beta Tricalcium Phosphate: Osteo-immunomodulatory Effects, Adv Healthc Mater 7(5) (2018).

[227] P.L. Graney, S.I. Roohani-Esfahani, H. Zreiqat, K.L. Spiller, In vitro response of macrophages to ceramic scaffolds used for bone regeneration, J R Soc Interface 13(120) (2016).

[228] Z. Chen, C. Wu, W. Gu, T. Klein, R. Crawford, Y. Xiao, Osteogenic differentiation of bone marrow MSCs by beta-tricalcium phosphate stimulating macrophages via BMP2 signalling pathway, Biomaterials 35(5) (2014) 1507-18.

[229] Y. Huang, C. Wu, X. Zhang, J. Chang, K. Dai, Regulation of immune response by bioactive ions released from silicate bioceramics for bone regeneration, Acta Biomater 66 (2018) 81-92.

[230] M. Shi, L. Xia, Z. Chen, F. Lv, H. Zhu, F. Wei, S. Han, J. Chang, Y. Xiao, C. Wu, Europium-doped mesoporous silica nanosphere as an immune-modulating osteogenesis/angiogenesis agent, Biomaterials 144 (2017) 176-187.

[231] W. Zhang, F. Zhao, D. Huang, X. Fu, X. Li, X. Chen, Strontium-Substituted Submicrometer Bioactive Glasses Modulate Macrophage Responses for Improved Bone Regeneration, ACS Appl Mater Interfaces 8(45) (2016) 30747-30758.

[232] H.-S. Han, S. Loffredo, I. Jun, J. Edwards, Y.-C. Kim, H.-K. Seok, F. Witte, D. Mantovani, S. Glyn-Jones, Current status and outlook on the clinical translation of biodegradable metals, Materials Today 23 (2019) 57-71.

[233] Y. Liu, Y. Zheng, X.-H. Chen, J.-A. Yang, H. Pan, D. Chen, L. Wang, J. Zhang, D. Zhu, S. Wu, K.W.K. Yeung, R.-C. Zeng, Y. Han, S. Guan, Fundamental Theory of Biodegradable Metals—Definition, Criteria, and Design, Advanced Functional Materials 29(18) (2019) 1805402.

[234] H.S. Han, I. Jun, H.K. Seok, K.S. Lee, K. Lee, F. Witte, D. Mantovani, Y.C. Kim, S. Glyn-Jones, J.R. Edwards, Biodegradable Magnesium Alloys Promote Angio-Osteogenesis to Enhance Bone Repair, Adv Sci (Weinh) 7(15) (2020) 2000800.

[235] F. Witte, 1.3.3D - Biodegradable Metals, in: W.R. Wagner, S.E. Sakiyama-Elbert, G. Zhang, M.J. Yaszemski (Eds.), Biomaterials Science (Fourth Edition), Academic Press2020, pp. 271-287.

[236] B. Wegener, A. Sichler, S. Milz, C. Sprecher, K. Pieper, W. Hermanns, V. Jansson, B. Nies, B. Kieback, P.E. Müller, V. Wegener, P. Quadbeck, Development of a novel biodegradable porous iron-based implant for bone replacement, Scientific Reports 10(1) (2020) 9141.

[237] R. Tsaryk, K. Peters, R.E. Unger, D. Scharnweber, C.J. Kirkpatrick, The effects of metal implants on inflammatory and healing processes, International Journal of Materials Research 98(7) (2007) 622-629.

[238] M.P. Staiger, A.M. Pietak, J. Huadmai, G. Dias, Magnesium and its alloys as orthopedic biomaterials: a review, Biomaterials 27(9) (2006) 1728-34.

[239] A. Yiannikourides, G.O. Latunde-Dada, A Short Review of Iron Metabolism and Pathophysiology of Iron Disorders, Medicines (Basel) 6(3) (2019).

[240] H. Li, Y. Zheng, L. Qin, Progress of biodegradable metals, Progress in Natural Science: Materials International 24(5) (2014) 414-422.

[241] Y.F. Zheng, X.N. Gu, F. Witte, Biodegradable metals, Materials Science and Engineering: R: Reports 77 (2014) 1-34.

[242] M. Peuster, P. Wohlsein, M. Brugmann, M. Ehlerding, K. Seidler, C. Fink, H. Brauer, A. Fischer, G. Hausdorf, A novel approach to temporary stenting: degradable cardiovascular stents produced from corrodible metal-results 6-18 months after implantation into New Zealand white rabbits, Heart 86(5) (2001) 563-9.

[243] M. Peuster, C. Hesse, T. Schloo, C. Fink, P. Beerbaum, C. von Schnakenburg, Long-term biocompatibility of a corrodible peripheral iron stent in the porcine descending aorta, Biomaterials 27(28) (2006) 4955-62.

[244] T. Kraus, F. Moszner, S. Fischerauer, M. Fiedler, E. Martinelli, J. Eichler, F. Witte, E. Willbold, M. Schinhammer, M. Meischel, P.J. Uggowitzer, J.F. Loffler, A. Weinberg, Biodegradable Fe-based alloys for use in osteosynthesis: outcome of an in vivo study after 52 weeks, Acta Biomater 10(7) (2014) 3346-53.

[245] M. Moravej, D. Mantovani, Biodegradable metals for cardiovascular stent application: interests and new opportunities, Int J Mol Sci 12(7) (2011) 4250-70.

[246] M. Schinhammer, A.C. Hänzi, J.F. Löffler, P.J. Uggowitzer, Design strategy for biodegradable Fe-based alloys for medical applications, Acta Biomaterialia 6(5) (2010) 1705-1713.

[247] Y. Xia, Y. Li, X. Wu, Q. Zhang, S. Chen, X. Ma, M. Yu, Ironing Out the Details: How Iron Orchestrates Macrophage Polarization, Front Immunol 12 (2021) 669566.

[248] S. Zanganeh, G. Hutter, R. Spitler, O. Lenkov, M. Mahmoudi, A. Shaw, J.S. Pajarinen, H. Nejadnik, S. Goodman, M. Moseley, L.M. Coussens, H.E. Daldrup-Link, Iron oxide

nanoparticles inhibit tumour growth by inducing pro-inflammatory macrophage polarization in tumour tissues, Nat Nanotechnol 11(11) (2016) 986-994.

[249] Y. Zhou, K.T. Que, Z. Zhang, Z.J. Yi, P.X. Zhao, Y. You, J.P. Gong, Z.J. Liu, Iron overloaded polarizes macrophage to proinflammation phenotype through ROS/acetyl-p53 pathway, Cancer Med 7(8) (2018) 4012-4022.

[250] M. Pereira, T.D. Chen, N. Buang, A. Olona, J.H. Ko, M. Prendecki, A.S.H. Costa, E. Nikitopoulou, L. Tronci, C.D. Pusey, H.T. Cook, S.P. McAdoo, C. Frezza, J. Behmoaras, Acute Iron Deprivation Reprograms Human Macrophage Metabolism and Reduces Inflammation In Vivo, Cell Rep 28(2) (2019) 498-511 e5.

[251] H.N. Wilkinson, E.R. Roberts, A.R. Stafford, K.L. Banyard, P. Matteucci, K.A. Mace, M.J. Hardman, Tissue Iron Promotes Wound Repair via M2 Macrophage Polarization and the Chemokine (C-C Motif) Ligands 17 and 22, Am J Pathol 189(11) (2019) 2196-2208.

[252] K. Marycz, P. Sobierajska, M. Roecken, K. Kornicka-Garbowska, M. Kepska, R. Idczak, J.M. Nedelec, R.J. Wiglusz, Iron oxides nanoparticles (IOs) exposed to magnetic field promote expression of osteogenic markers in osteoblasts through integrin alpha-3 (INTa-3) activation, inhibits osteoclasts activity and exerts anti-inflammatory action, J Nanobiotechnology 18(1) (2020) 33.

[253] G.K. Levy, J. Goldman, E. Aghion, The Prospects of Zinc as a Structural Material for Biodegradable Implants—A Review Paper, Metals 7(10) (2017) 402.

[254] J.M. Berg, Y. Shi, The Galvanization of Biology: A Growing Appreciation for the Roles of Zinc, Science 271(5252) (1996) 1081.

[255] J.E. Coleman, Zinc enzymes, Curr Opin Chem Biol 2(2) (1998) 222-34.

[256] H. Kabir, K. Munir, C. Wen, Y. Li, Recent research and progress of biodegradable zinc alloys and composites for biomedical applications: Biomechanical and biocorrosion perspectives, Bioact Mater 6(3) (2021) 836-879.

[257] H. Yang, B. Jia, Z. Zhang, X. Qu, G. Li, W. Lin, D. Zhu, K. Dai, Y. Zheng, Alloying design of biodegradable zinc as promising bone implants for load-bearing applications, Nat Commun 11(1) (2020) 401.

[258] H. Guo, D. Xia, Y. Zheng, Y. Zhu, Y. Liu, Y. Zhou, A pure zinc membrane with degradability and osteogenesis promotion for guided bone regeneration: In vitro and in vivo studies, Acta Biomater 106 (2020) 396-409.

[259] A. Brieger, L. Rink, H. Haase, Differential regulation of TLR-dependent MyD88 and TRIF signaling pathways by free zinc ions, J Immunol 191(4) (2013) 1808-17.

[260] S. Hojyo, T. Fukada, Roles of Zinc Signaling in the Immune System, J Immunol Res 2016 (2016) 6762343.

[261] W. Liu, J. Li, M. Cheng, Q. Wang, K.W.K. Yeung, P.K. Chu, X. Zhang, Zinc-Modified Sulfonated Polyetheretherketone Surface with Immunomodulatory Function for Guiding Cell Fate and Bone Regeneration, Adv Sci (Weinh) 5(10) (2018) 1800749.

[262] Y. Qiao, W. Zhang, P. Tian, F. Meng, H. Zhu, X. Jiang, X. Liu, P.K. Chu, Stimulation of bone growth following zinc incorporation into biomaterials, Biomaterials 35(25) (2014) 6882-97.

[263] J. Yu, L. Xu, K. Li, N. Xie, Y. Xi, Y. Wang, X. Zheng, X. Chen, M. Wang, X. Ye, Zinc-modified Calcium Silicate Coatings Promote Osteogenic Differentiation through TGF-beta/Smad Pathway and Osseointegration in Osteopenic Rabbits, Sci Rep 7(1) (2017) 3440.

[264] G. Cama, S. Nkhwa, B. Gharibi, A. Lagazzo, R. Cabella, C. Carbone, P. Dubruel, H. Haugen, L. Di Silvio, S. Deb, The role of new zinc incorporated monetite cements on osteogenic differentiation of human mesenchymal stem cells, Mater Sci Eng C Mater Biol Appl 78 (2017) 485-494.

[265] I. Cockerill, Y. Su, J.H. Lee, D. Berman, M.L. Young, Y. Zheng, D. Zhu, Micro-/Nanotopography on Bioresorbable Zinc Dictates Cytocompatibility, Bone Cell Differentiation, and Macrophage Polarization, Nano Lett 20(6) (2020) 4594-4602.

[266] R. Roy, V. Parashar, L.K. Chauhan, R. Shanker, M. Das, A. Tripathi, P.D. Dwivedi, Mechanism of uptake of ZnO nanoparticles and inflammatory responses in macrophages require PI3K mediated MAPKs signaling, Toxicol In Vitro 28(3) (2014) 457-67.

[267] M. Giovanni, J. Yue, L. Zhang, J. Xie, C.N. Ong, D.T. Leong, Pro-inflammatory responses of RAW264.7 macrophages when treated with ultralow concentrations of silver, titanium dioxide, and zinc oxide nanoparticles, J Hazard Mater 297 (2015) 146-52.

[268] L. Dierichs, V. Kloubert, L. Rink, Cellular zinc homeostasis modulates polarization of THP-1-derived macrophages, Eur J Nutr 57(6) (2018) 2161-2169.

[269] N.E. Saris, E. Mervaala, H. Karppanen, J.A. Khawaja, A. Lewenstam, Magnesium. An update on physiological, clinical and analytical aspects, Clin Chim Acta 294(1-2) (2000) 1-26.

[270] Y. Chen, Z. Xu, C. Smith, J. Sankar, Recent advances on the development of magnesium alloys for biodegradable implants, Acta Biomater 10(11) (2014) 4561-4573.

[271] T. Kraus, S.F. Fischerauer, A.C. Hanzi, P.J. Uggowitzer, J.F. Loffler, A.M. Weinberg, Magnesium alloys for temporary implants in osteosynthesis: in vivo studies of their degradation and interaction with bone, Acta Biomater 8(3) (2012) 1230-8.

[272] D. Zhao, F. Witte, F. Lu, J. Wang, J. Li, L. Qin, Current status on clinical applications of magnesium-based orthopaedic implants: A review from clinical translational perspective, Biomaterials 112 (2017) 287-302.

[273] M. Razavi, Y. Huang, Assessment of magnesium-based biomaterials: from bench to clinic, Biomaterials Science 7(6) (2019) 2241-2263.

[274] H. Windhagen, K. Radtke, A. Weizbauer, J. Diekmann, Y. Noll, U. Kreimeyer, R. Schavan, C. Stukenborg-Colsman, H. Waizy, Biodegradable magnesium-based screw clinically equivalent to titanium screw in hallux valgus surgery: short term results of the first prospective, randomized, controlled clinical pilot study, BioMedical Engineering OnLine 12(1) (2013) 62.

[275] J.W. Lee, H.S. Han, K.J. Han, J. Park, H. Jeon, M.R. Ok, H.K. Seok, J.P. Ahn, K.E. Lee, D.H. Lee, S.J. Yang, S.Y. Cho, P.R. Cha, H. Kwon, T.H. Nam, J.H. Han, H.J. Rho, K.S. Lee, Y.C. Kim, D. Mantovani, Long-term clinical study and multiscale analysis of in vivo biodegradation mechanism of Mg alloy, Proc Natl Acad Sci U S A 113(3) (2016) 716-21.

[276] D. Zhao, S. Huang, F. Lu, B. Wang, L. Yang, L. Qin, K. Yang, Y. Li, W. Li, W. Wang, S. Tian, X. Zhang, W. Gao, Z. Wang, Y. Zhang, X. Xie, J. Wang, J. Li, Vascularized bone grafting fixed by biodegradable magnesium screw for treating osteonecrosis of the femoral head, Biomaterials 81 (2016) 84-92.

[277] X. Zhang, Q. Chen, X. Mao, Magnesium Enhances Osteogenesis of BMSCs by Tuning Osteoimmunomodulation, BioMed Research International 2019 (2019) 7908205.

[278] X. Li, Q. Huang, L. Liu, W. Zhu, T.A. Elkhooly, Y. Liu, Q. Feng, Q. Li, S. Zhou, Y. Liu, H. Wu, Reduced inflammatory response by incorporating magnesium into porous TiO2 coating on titanium substrate, Colloids Surf B Biointerfaces 171 (2018) 276-284.

[279] T. Hu, H. Xu, C. Wang, H. Qin, Z. An, Magnesium enhances the chondrogenic differentiation of mesenchymal stem cells by inhibiting activated macrophage-induced inflammation, Sci Rep 8(1) (2018) 3406.

[280] Y. Yin, Q. Huang, M. Yang, J. Xiao, H. Wu, Y. Liu, Q. Li, W. Huang, G. Lei, K. Zhou, MgO Nanoparticles Protect against Titanium Particle-Induced Osteolysis in a Mouse Model Because of Their Positive Immunomodulatory Effect, ACS Biomater Sci Eng 6(5) (2020) 3005-3014.

[281] M. He, X. Gao, Y. Fan, L. Xie, M. Yang, W. Tian, Tannic acid/Mg(2+)-based versatile coating to manipulate the osteoimmunomodulation of implants, J Mater Chem B 9(4) (2021) 1096-1106.

[282] L. Jin, J. Wu, G. Yuan, T. Chen, In vitro study of the inflammatory cells response to biodegradable Mg-based alloy extract, PLoS One 13(3) (2018) e0193276.

[283] M.D. Costantino, A. Schuster, H. Helmholz, A. Meyer-Rachner, R. Willumeit-Romer, B.J.C. Luthringer-Feyerabend, Inflammatory response to magnesium-based biodegradable implant materials, Acta Biomater 101 (2020) 598-608.

[284] J. Sugimoto, A.M. Romani, A.M. Valentin-Torres, A.A. Luciano, C.M. Ramirez Kitchen, N. Funderburg, S. Mesiano, H.B. Bernstein, Magnesium decreases inflammatory cytokine production: a novel innate immunomodulatory mechanism, J Immunol 188(12) (2012) 6338-46.

[285] F. Gao, B. Ding, L. Zhou, X. Gao, H. Guo, H. Xu, Magnesium sulfate provides neuroprotection in lipopolysaccharide-activated primary microglia by inhibiting NF-kappaB pathway, J Surg Res 184(2) (2013) 944-50.

[286] L. Diez-Tercero, L.M. Delgado, E. Bosch-Rue, R.A. Perez, Evaluation of the immunomodulatory effects of cobalt, copper and magnesium ions in a pro inflammatory environment, Sci Rep 11(1) (2021) 11707.

[287] Y. Zhang, J. Xu, Y.C. Ruan, M.K. Yu, M. O'Laughlin, H. Wise, D. Chen, L. Tian, D. Shi, J. Wang, S. Chen, J.Q. Feng, D.H. Chow, X. Xie, L. Zheng, L. Huang, S. Huang, K. Leung, N. Lu, L. Zhao, H. Li, D. Zhao, X. Guo, K. Chan, F. Witte, H.C. Chan, Y. Zheng, L. Qin, Implant-derived magnesium induces local neuronal production of CGRP to improve bone-fracture healing in rats, Nat Med 22(10) (2016) 1160-1169.

[288] C.C. Hung, A. Chaya, K. Liu, K. Verdelis, C. Sfeir, The role of magnesium ions in bone regeneration involves the canonical Wnt signaling pathway, Acta Biomater 98 (2019) 246-255.

[289] W. Qiao, K.H.M. Wong, J. Shen, W. Wang, J. Wu, J. Li, Z. Lin, Z. Chen, J.P. Matinlinna, Y. Zheng, S. Wu, X. Liu, K.P. Lai, Z. Chen, Y.W. Lam, K.M.C. Cheung, K.W.K.

Yeung, TRPM7 kinase-mediated immunomodulation in macrophage plays a central role in magnesium ion-induced bone regeneration, Nat Commun 12(1) (2021) 2885.

[290] Q. Wang, L. Xu, R. Willumeit-Romer, B.J.C. Luthringer-Feyerabend, Macrophage-derived oncostatin M/bone morphogenetic protein 6 in response to Mg-based materials influences pro-osteogenic activity of human umbilical cord perivascular cells, Acta Biomater (2020).

[291] L. Sun, X. Li, M. Xu, F. Yang, W. Wang, X. Niu, In vitro immunomodulation of magnesium on monocytic cell toward anti-inflammatory macrophages, Regen Biomater 7(4) (2020) 391-401.

[292] F. da Silva Lima, A.B. da Rocha Romero, A. Hastreiter, A. Nogueira-Pedro, E. Makiyama, C. Colli, R.A. Fock, An insight into the role of magnesium in the immunomodulatory properties of mesenchymal stem cells, J Nutr Biochem 55 (2018) 200-208.

[293] G. Zhang, H. Lu, S. Mamidwar, M. Wang, 1.3.7 - Composites, in: W.R. Wagner, S.E. Sakiyama-Elbert, G. Zhang, M.J. Yaszemski (Eds.), Biomaterials Science (Fourth Edition), Academic Press2020, pp. 415-429.

[294] Z. Chen, L. Chen, R. Liu, Y. Lin, S. Chen, S. Lu, Z. Lin, Z. Chen, C. Wu, Y. Xiao, The osteoimmunomodulatory property of a barrier collagen membrane and its manipulation via coating nanometer-sized bioactive glass to improve guided bone regeneration, Biomater Sci 6(5) (2018) 1007-1019.

[295] Y. Song, H. Wu, Y. Gao, J. Li, K. Lin, B. Liu, X. Lei, P. Cheng, S. Zhang, Y. Wang, J. Sun, L. Bi, G. Pei, Zinc Silicate/Nano-Hydroxyapatite/Collagen Scaffolds Promote Angiogenesis and Bone Regeneration via the p38 MAPK Pathway in Activated Monocytes, ACS Appl Mater Interfaces 12(14) (2020) 16058-16075.

[296] Q. Wang, Y. Tang, Q. Ke, W. Yin, C. Zhang, Y. Guo, J. Guan, Magnetic lanthanum-doped hydroxyapatite/chitosan scaffolds with endogenous stem cell-recruiting and immunomodulatory properties for bone regeneration, J Mater Chem B 8(24) (2020) 5280-5292.

[297] Z. Lin, D. Shen, W. Zhou, Y. Zheng, T. Kong, X. Liu, S. Wu, P.K. Chu, Y. Zhao, J. Wu, K.M.C. Cheung, K.W.K. Yeung, Regulation of extracellular bioactive cations in bone tissue microenvironment induces favorable osteoimmune conditions to accelerate in situ bone regeneration, Bioact Mater 6(8) (2021) 2315-2330.

[298] G. Qian, T. Lu, J. Zhang, R. Liu, Z. Wang, B. Yu, H. Li, H. Shi, J. Ye, Promoting bone regeneration of calcium phosphate cement by addition of PLGA microspheres and zinc silicate via synergistic effect of in-situ pore generation, bioactive ion stimulation and macrophage immunomodulation, Applied Materials Today 19 (2020) 100615.

[299] Z. Zheng, Y. Chen, H. Hong, Y. Shen, Y. Wang, J. Sun, X. Wang, The "Yin and Yang" of Immunomodulatory Magnesium-Enriched Graphene Oxide Nanoscrolls Decorated Biomimetic Scaffolds in Promoting Bone Regeneration, Adv Healthc Mater (2020) e2000631.

[300] A.M. Negrescu, M.G. Necula, A. Gebaur, F. Golgovici, C. Nica, F. Curti, H. Iovu, M. Costache, A. Cimpean, In Vitro Macrophage Immunomodulation by Poly(epsilon-caprolactone) Based-Coated AZ31 Mg Alloy, Int J Mol Sci 22(2) (2021).

[301] A.H. Lourenco, A.L. Torres, D.P. Vasconcelos, C. Ribeiro-Machado, J.N. Barbosa, M.A. Barbosa, C.C. Barrias, C.C. Ribeiro, Osteogenic, anti-osteoclastogenic and immunomodulatory properties of a strontium-releasing hybrid scaffold for bone repair, Mater Sci Eng C Mater Biol Appl 99 (2019) 1289-1303.

[302] H. Rammal, C. Bour, M. Dubus, L. Entz, L. Aubert, S.C. Gangloff, S. Audonnet, N.B. Bercu, F. Boulmedais, C. Mauprivez, H. Kerdjoudj, Combining Calcium Phosphates with Polysaccharides: A Bone-Inspired Material Modulating Monocyte/Macrophage Early Inflammatory Response, Int J Mol Sci 19(11) (2018).

[303] J.L. Sun, K. Jiao, L.N. Niu, Y. Jiao, Q. Song, L.J. Shen, F.R. Tay, J.H. Chen, Intrafibrillar silicified collagen scaffold modulates monocyte to promote cell homing, angiogenesis and bone regeneration, Biomaterials 113 (2017) 203-216.

[304] M. Wang, Y. Yu, K. Dai, Z. Ma, Y. Liu, J. Wang, C. Liu, Improved osteogenesis and angiogenesis of magnesium-doped calcium phosphate cement via macrophage immunomodulation, Biomater Sci 4(11) (2016) 1574-1583.

[305] L. Papadimitriou, M. Kaliva, M. Vamvakaki, M. Chatzinikolaidou, Immunomodulatory Potential of Chitosan-graft-poly(ε-caprolactone) Copolymers toward the Polarization of Bone-Marrow-Derived Macrophages, ACS Biomaterials Science & Engineering 3(7) (2017) 1341-1349.

[306] Z. Chen, X. Mao, L. Tan, T. Friis, C. Wu, R. Crawford, Y. Xiao, Osteoimmunomodulatory properties of magnesium scaffolds coated with beta-tricalcium phosphate, Biomaterials 35(30) (2014) 8553-65.

CHAPTER II

ORIGINAL RESEARCH WORK

Fibrinogen and magnesium combination biomaterials modulate macrophage phenotype, NF-kB signaling and crosstalk with mesenchymal stem/stromal cells. *Acta Biomaterialia*. 114 (2020) 471–484

Fibrinogen and magnesium combination biomaterials modulate macrophage phenotype, NF-kB signaling and crosstalk with mesenchymal stem/stromal cells

Bessa-Gonçalves M[a,b], Silva AM[a,b],, Brás JP[a,b], Helmholz H[c], Luthringer-Feyerabend BJC[c], Willumeit-Römer R[c], Barbosa MA[a,b], Santos SG[a,b*]

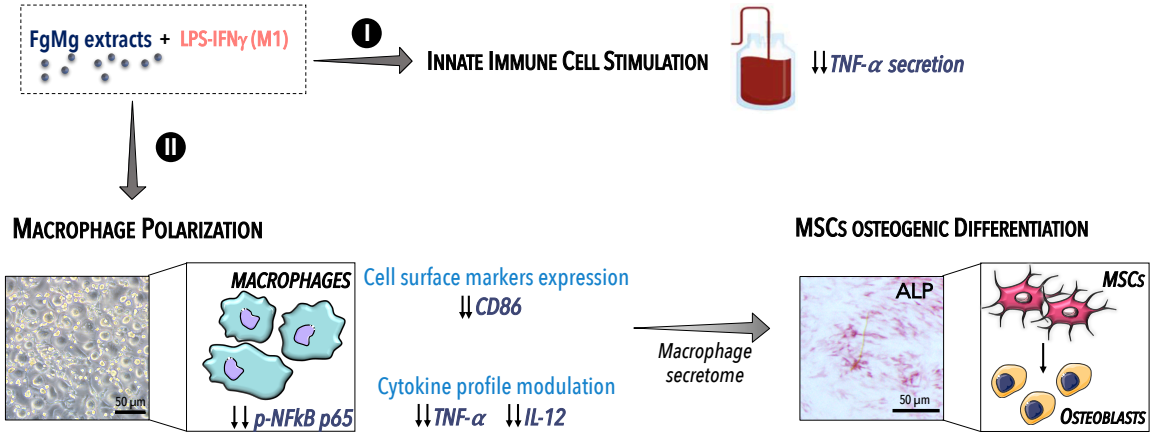
[a]*i3S – Instituto de Investigação e Inovação em Saúde, and INEB - Instituto de Engenharia Biomédica, Universidade do Porto, Rua Alfredo Allen 208, 4200-135 Porto, Portugal*

[b]*Instituto Ciências Biomédicas Abel Salazar da Universidade do Porto, Rua de Jorge Viterbo Ferreira 228, 4050-313 Porto, Portugal.*

[c]*Helmholtz-Center Geesthacht, Centre for Materials and Coastal Research, Institute of Materials Research, Division for Metallic Biomaterials, Max-Planck-St.1, D-21502, Geesthacht, Germany*

ABSTRACT

Macrophage behavior upon biomaterial implantation conditions the inflammatory response and subsequent tissue repair. The hypothesis behind this work was that fibrinogen (Fg) and magnesium (Mg) biomaterials, used in combination (FgMg) could act synergistically to modulate macrophage activation, promoting a pro-regenerative phenotype. Materials were characterized by scanning electron microscopy, Fg and Mg degradation products were quantified by atomic absorption spectroscopy and ELISA. Whole blood immune cells and primary human monocyte-derived macrophages were exposed to the biomaterials extracts in unstimulated (M0) or pro-inflammatory LPS or LPS-IFNγ (M1) conditions. Macrophage phenotype was evaluated by flow cytometry, cytokines secreted by whole blood cells and macrophages were measured by ELISA, and signaling pathways were probed by Western blotting. The secretomes of macrophages preconditioned with biomaterials extracts were incubated with human mesenchymal stem/stromal cells (MSC) and their effect on osteogenic differentiation was evaluated *via* Alkaline Phosphatase (ALP) activity and alizarin red staining. Scaffolds of Fg, alone or in the FgMg combination, presented similar 3D porous architectures. Extracts from FgMg materials reduced LPS-induced TNF-α secretion by innate immune cells, and macrophage M1 polarization upon LPS-IFNγ stimulation, resulting in lower cell surface CD86 expression, lower NF-kB p65 phosphorylation and reduced TNF-α secretion. Moreover, while biomaterial extracts *per se* did not enhance MSC osteogenic differentiation, macrophage secretome, particularly from cells exposed to FgMg extracts, increased MSC ALP activity and alizarin red staining, compared with extracts alone. These findings suggest that the combination of Fg and Mg synergistically influences macrophage pro-inflammatory activation and crosstalk with MSC.



Keywords: biomaterials; fibrinogen; magnesium; macrophages; mesenchymal stem/stromal cells

1. INTRODUCTION

Inflammation is necessary for adequate and complete bone healing upon injury, but exacerbated inflammation underlies most musculoskeletal diseases [1]. While fracture-related injury elicits a beneficial acute inflammatory response, chronic inflammation impairs bone health and repair [1].

Thus, biomaterials capable of modulating the inflammatory response have been increasingly explored to promote tissue repair/regeneration [2]. Monocytes/macrophages are a central cell population in biomaterials response, conditioning inflammatory and regenerative processes, by transitioning between pro- (M1) and anti-inflammatory (M2) phenotypes [3]. Polarizing macrophages towards an M2 phenotype is strategy that impacts on recruitment of Mesenchymal Stem/Stromal Cells (MSCs) via paracrine factors [4, 5], leading to their osteogenic differentiation [4, 5].

Fibrinogen (Fg) is a protein with essential roles in coagulation, wound healing and inflammation. Its healing properties are well known and are the basis for wide use of fibrin glue [6]. On the other hand, its pro-inflammatory impact has been described in several diseases, like Alzheimer's, Stroke, or Rheumatoid Arthritis [7]. Previous work from our group showed that Fg adsorbed to chitosan interacts with monocytes through TLR4 [8], enhances the production of osteogenic factors by macrophage [9], and MSC recruitment by natural killer (NK) cells [10]. In addition, in a femoral bone defect model, Fg adsorbed to chitosan [11] or as pure Fg scaffolds [12] modulated local and systemic response to injury, both at 6 days (end of acute inflammation) and 8 weeks (repair/remodeling stage) post-injury, improving bone repair [12].

On the other hand, Magnesium (Mg) alloys are promising biomaterials for orthopedic applications, due to their mechanical properties similar to human bone, degradability and the physiological role of Mg in bone [13]. However, the use of Mg alloys is limited by their fast degradation rate, which leads to the release of high amounts of metallic ions, substantial pH increase and generation of hydrogen gas, all with adverse tissue effects. This destabilizes the bone-implant interface and hinders healing [13, 14]. Interestingly, at low concentration Mg degradation products may have beneficial effects in modulating the immune response, and promoting MSC proliferation and osteogenic differentiation [15, 16]. To tailor Mg biomaterials degradation rate and biocompatibility, alloying elements and subsequent thermal or mechanical treatment have been explored [17, 18]. Also, combining Mg biomaterials with degradable polymers could be an attractive option, to gain greater

control over biodegradability and promotion of fully functional remodeled bone tissue [14, 18].

Herein, we hypothesize that the combination of Fg and Mg into the same biomaterial can act synergistically to modulate macrophage activation and their crosstalk with MSC. To test this hypothesis, pure fibrinogen scaffold (denoted as “Fg”), Mg discs (“Mg”) and multilayer constructs combining Fg and Mg (“FgMg”) were prepared. Instead of seeding cells directly on these biomaterials we have used their extracts. The potential of Fg, Mg and FgMg extracts to modulate the phenotype of macrophages, and the impact of their secretome on MSC differentiation were evaluated. Results show, for the first time, that FgMg material extracts were capable of reducing M1 polarization in primary macrophages, leading them to produce a secretome that promoted MSCs osteogenic differentiation.

2. MATERIALS AND METHODS

2.1. Biomaterial formulations

2.1.1. Fg scaffolds: Fg 3D scaffolds (12 mm diameter x 9 mm thickness) (Supplementary Fig. 1) were prepared by freeze-drying, as previously described [12]. Briefly, a solution of Fg 60 mg/mL (from human plasma, Grifols, Barcelona, Spain) was prepared from an 80 mg/mL Fg stock solution, in water, and cast into 48-well plates (1000 µL/well), frozen overnight (o.n.) at −20 °C, and freeze-dried for 48 h, at −80 °C. Resulting scaffolds were chemically crosslinked o.n. with N-(3-Dimethylaminopropyl)-N′ - ethylcarbodiimide hydrochloride (EDC, E1769, Sigma-Aldrich Co., St Louis, MO, USA) at 8.8 mM, prepared in ethanol, as described [19]. Then, scaffolds were removed from the plate, neutralized and disinfected, through impregnation under vacuum in a gradient of ethanol solutions (99.9%, 70%, 50% and 25%), followed by three washes in cell culture media.

2.1.2. Mg discs: Pure Mg ingots (Mg; 99.95%) were prepared by permanent mold gravity casting at Helmholtz Zentrum Geesthacht (Geesthacht, Germany). After extrusion, 10 mm diameter x 1.5 mm thickness discs were cut from rods, as described in [20]. The discs (Supplementary Fig. 1) were cleaned by sonication for 20 min in n-hexane (Merck, Darmstadt, Germany), for 20 min in acetone (Merck, Darmstadt, Germany) and for 3 min in 100% ethanol. Lastly, specimens were sterilized in 70% ethanol (20 min with sonication) and dried under sterile conditions [20]. Degradation rate of the current batch of Mg discs (Mg pure 16614) was determined prior to in vitro tests. The degradation rate, 0.32 mm/year,

was measured in media supplemented with FBS, during 7 days immersion, and under cell culture conditions (37 °C, 21% O2, 5% CO2, 95% RH), as previously described in [21].

2.1.3. Fg scaffolds combined with Mg discs (multilayer constructs): a solution of Fg 60 mg/mL (from human plasma, Grifols, Barcelona, Spain) prepared as above was cast into 48-well plates (500 µL/well) and frozen o.n. at −20 °C. Mg discs were cleaned as above, cooled (−20 °C), and placed on top of the Fg layer. Then, another layer of Fg (500 µL) was added on top of the Mg disc. Resulting multilayer constructs (Supplementary Fig. 1) (a total of three layers (Fg-Mg-Fg), with combined 12 mm diameter x 10,5 mm thickness (each Fg layer with 4,5 mm thickness and Mg disc with 1,5 mm thickness)) were frozen, freeze-dried and then chemically crosslinked and processed as described above for Fg scaffolds.

2.2 Scanning electron microscopy (SEM) and energy dispersive spectroscopy (EDS) characterization

Microstructure/surface morphology of Fg alone or in the FgMg combination was analysed by SEM/EDS using a high resolution (Schottky) environmental EM with X-ray microanalysis and electron backscattered diffraction analysis (Quanta 400 FEG ESEM / EDAX Genesis X4M). Cross-sections of approximately 1 mm thickness were cut and mounted with carbon tape. Samples were coated with a gold (Au)/ palladium (Pd) thin film, by sputtering for 80 s with 15 mA current, to provide conductivity, using the SPI module sputter coater equipment [12]. EDS coupled to SEM was used for elemental analysis.

2.3. Extracts preparation and characterization

Extracts were prepared according to EN ISO standards 10993:5 (ISO 10993-5:2009) and 10993:12 (ISO 10993-12:2012), using 0.1 g material/mL extraction medium for Fg and 0.2 g material/mL extraction medium for Mg and FgMg. After sterilization, samples were incubated in extraction media (Roswell Park Memorial Institute (RPMI) 1640 media with L-glutamine, Corning, Manassas, USA), supplemented with 10% fetal bovine serum (FBS) (Biowest, Riverside, MO, USA) for 72 h at 37 ºC with 120 rpm agitation. pH measurements were performed using an ArgusX pH Meter (Sentron Europe BV, Roden, the Netherlands) for pure Fg, Mg, and FgMg extracts, and RPMI cell culture media, as control. Mg content on elutes (mg/L) was measured *via* atomic absorption spectroscopy (AAS; Agilent 240 AA, Waldbronn, Germany). An external calibration was performed for quantification, which uses

Mg reference solution to cover the targeted analyte range (element-specific detections at absorbance 285.2 nm). Air/Acetylene flame type together with pre-read delay time of 3 seconds and a read time of three seconds with three replicates were used. Fg degradation product D-dimer was quantified by enzyme-linked immunosorbent assay (ELISA), using RayBio® Human D-Dimer ELISA Kit (RayBiotech, Norcross, GA, USA), according to manufacturer's instructions. A calibration curve using standards was used to quantify the relative amount of D-Dimer in each sample. Before being used for cell culture experiments, pure extracts were diluted (1:10) in fresh RPMI 1640 media, complete with L-glutamine (Corning, Manassas, USA), and supplemented with 10% fetal bovine serum (FBS, Biowest, Riverside, MO, USA), using methods adapted from [15], and pH measurements upon extracts dilution were performed as above.

2.4. Ethics statement

All obtained human samples and procedures were performed in agreement with the principles of the Declaration of Helsinki. Monocytes were isolated from surplus buffy coats (BC) from healthy blood donors, kindly donated by Serviço de Imunohemoterapia, Centro Hospitalar Universitário de São João (CHUSJ), Porto. Human mesenchymal stem/stromal cells (MSC) were obtained from healthy human bone marrow from patients undergoing knee ligament surgery, kindly donated by Serviço de Ortopedia, CHUSJ, Porto. All experimental protocols were conducted following the approval and recommendations of the CHUSJ Ethics Committee for Health (references 90/19 and 260/11). Buffy coats and bone marrow samples were provided anonymized and patient identification was not provided to researchers.

2.5. Whole blood innate immune stimulation

Buffy coats from peripheral blood of healthy blood donors were cultured for 24 h (200 µl per well) with Fg, Mg and FgMg extracts (diluted 1:10, as described in 2.3), in presence or absence of 10 ng/mL LPS, Escherichia coli O55:B5 (Sigma-Aldrich Co., St Louis, MO, USA), following protocols adapted from [22]. After incubation, the bloods were centrifuged for 2 min, 10,000 g, RT (Heraeus™ Fresco™ 21 Microcentrifuge, ThermoFisher Scientific, Waltham, MA, USA) and supernatants were collected. The effect on Human tumor necrosis factor α (TNF-α), secretion was investigated by ELISA (ELISA Max™ Deluxe, BioLegend, San Diego, CA, USA) according to manufacturer's instructions [12].

2.6. Primary human monocyte isolation and macrophage differentiation

Human monocytes were isolated from peripheral blood of healthy blood donors by negative selection, using methods described in [8]. Briefly, BC were centrifuged at room temperature (RT) for 20 min at 1200 g (Eppendorf Centrifuge 5810R, VWR International LLC, Radnor, PA, USA), without active acceleration or brake, for blood components separation. Peripheral blood mononuclear cells (PBMC) were collected and incubated with RosetteSep^{TM} Human Monocyte Enrichment Cocktail (Stem-Cell Technologies, Vancouver, Canada) at RT for 20 min under gentle mixing. The mixture was then diluted at a 1:1 ratio with 2% heat inactivated FBS (Biowest, Riverside, MO, USA) in PBS, gently layered over Histopaque-1077 (Sigma-Aldrich Co., St Louis, MO, USA) and centrifuged as previous. The enriched monocyte layer was collected and washed three times with PBS by centrifugation at 17 min, 700 rpm, RT (Eppendorf Centrifuge 5810R, VWR International LLC, Radnor, PA, USA).

For macrophage differentiation, 0,5 × 10^6 monocytes were seeded on glass coverslips in 24-well plates, and cultured for 7 days in RPMI 1640 media with L-glutamine (Corning, Manassas, VA, USA) supplemented with 10% heat-inactivated FBS (Biowest, Riverside, MO, USA), 100 U mL^{-1} penicillin and 100 µg/mL^{-1} streptomycin (P/S, both from Invitrogen, Carlsbad, CA, USA), in the presence of 50 ng/mL of recombinant human macrophage colony-stimulating factor (rh M-CSF, ImmunoTools, Friesoythe, Germany). After 7 days, cell culture media was replaced and M-CSF was removed. At day 10, media was replaced and monocytes/macrophages were stimulated with 10 ng/mL LPS, (as above) and 50 ng/mL IFN**γ** (ImmunoTools, Friesoythe, Germany), for M1, in presence or absence of Fg, Mg and FgMg extracts (diluted 1:10, as described in 2.3), for 72 h. Supernatants were collected under sterile conditions at day 13, centrifuged at 13,000 rpm, 5 min, 4 °C (Eppendorf Centrifuge 5810R, VWR International LLC, Radnor, PA, USA), to remove any cellular debris, and stored at −20 °C until further analysis, or used to prepare conditioned media for MSC cultures. Macrophages were then incubated with PBS - 50 mM ethylenediaminetetraacetic acid (EDTA, VWR International LLC, Radnor, PA, USA) during 15 min at 4 °C and gently harvested for further experiments. The complete experimental procedure is described in Fig. 1.

2.7. Macrophage polarization evaluation by flow cytometry

Macrophages collected at day 13, were washed, resuspended in FACS buffer (PBS, 2% FBS, 0.01% sodium azide (Sigma-Aldrich Co., St Louis, MO, USA) and stained with specific fluorochrome-conjugated antibodies, in the dark, for 30 min at 4 °C. Macrophages were incubated with the following antibodies: anti-human CD14-APC (clone MEM-18), CD86-FITC (clone BU63) (all from ImmunoTools, Friesoythe, Germany) and CD163-PE (clone GHI/61) (BD Biosciences, San Jose, CA, USA). Isotype-matched antibodies were used as negative controls, to define background staining. After additional washes, 10,000 cells, gated according to forward and side scatter parameters, were acquired using a BD FACSCanto II™ flow cytometer (Becton Dickinson) using FACSDiva™ software (both from BD Biosciences, San Jose, CA, USA). Data were analysed using FlowJo software (BD Biosciences, San Jose, CA, USA, version 10) and the percentage of CD14, CD86 and CD163 positive cells was calculated by subtracting the corresponding isotype control.

2.8. Western blot analysis

Macrophages were treated with Fg, Mg and FgMg biomaterial extracts (diluted 1:10, as described in 2.3) in the presence/absence of M1 stimulation (as above), for 30 min. Using methods described in [8], cells were harvested and washed twice with cold PBS, before cell lysis with RIPA buffer (1% NP-40 (Sigma-Aldrich Co., St Louis, MO, USA), 150 mM NaCl (VWR International LLC, Radnor, PA, USA), 50 mM Tris-HCl (pH 7.5) (Sigma-Aldrich Co., St Louis, MO, USA), 2 mM EDTA (VWR International LLC, Radnor, PA, USA)) supplemented with a mixture of phosphatase and protease inhibitors (10 µg/mL NaF (VWR International LLC, Radnor, PA, USA), 20 µg/mL Na_3VO_4, 10 µg/mL PMSF, 10 µg/mL aprotinin, 10 µg/mL leupeptin and 50 µg/mL $Na_4P_2O_7$ (all from Sigma-Aldrich Co., St Louis, MO, USA)) for 30 min, on ice, with frequent shaking. Lysates were collected, centrifuged at 14,000 rpm, 10 min, 4 °C (Eppendorf Centrifuge 5810R, VWR International LLC, Radnor, PA, USA), and supernatants were recovered and stored at −80 °C until protein quantification using DC protein assay kit (Bio-Rad Laboratories, Irvine, CA, USA). The same amount of protein per sample (30 µg/lane) was resolved by SDS-PAGE in reducing conditions using 10% polyacrylamide gels, and transferred to nitrocellulose membranes (GE Healthcare, Chicago, IL, USA). Membranes were blocked in a solution of 5% bovine serum albumin (BSA, VWR International LLC, Radnor, PA, USA) in Tris-buffered saline (TBS)-Tween 0.1%, and then probed o.n. at 4 °C, using the following primary antibodies: phospho-p38 MAPK (dilution 1:1000; cat. no.4511); phospho-p44/42 MAPK (Erk1/2)

(dilution 1:2000; cat. no.4370); phospho-SAPK/JNK (dilution 1:1000; cat. no.4668); phospho-NF-kB p65 (dilution 1:1000; cat. no.3033), glyceraldehyde 3-phosphate dehydrogenase (GAPDH - used as protein loading control; dilution 1:1000; cat. no.5174) (all from Cell Signalling Technology, Danvers, MA, USA). The secondary antibody used for signal detection was horseradish peroxidase (HRP)-conjugated goat anti-rabbit immunoglobulin (IgG) (dilution 1:2000; cat. no.7074, Cell Signalling Technology, Danvers, MA, USA). Blots were visualized using a chemiluminescent substrate ECL Prime (GE Healthcare, Chicago, IL, USA) and exposure to X-ray films [8]. The films were scanned in a Molecular Imager GS-800 calibrated densitometer (Bio-Rad Laboratories, Irvine, CA, USA), and quantitative results were obtained using Image Lab (Bio-Rad Laboratories, Irvine, CA, USA, version 6.0.1), normalizing the values of each sample with the values of GAPDH.

2.9. Macrophage cytokine secretion profile by ELISA

The relative concentration of different cytokines was quantified (pg/mL) in macrophage culture supernatants from 72 h stimulation, using commercially available ELISA kits. Human tumor necrosis factor α (TNF-α), interleukin (IL) −6, IL-1β, IL-12p70 and IL-10 (ELISA Max™ Deluxe, BioLegend, San Diego, CA, USA) [12], and human transforming growth factor β1 (TGF-β1) (DuoSet® ELISA development system, R&D systems, Minneapolis, Minnesota, USA) [23] ELISA were performed according to manufacturer's instructions.

2.10. Primary human mesenchymal stem/stromal cells isolation, culture and osteogenic differentiation

Primary human MSC were isolated from bone marrow by density gradient centrifugation followed by selection of adherent cells, and characterization according to the international stem cell society criteria, as previously described [10]. Bone marrow was collected from patients undergoing orthopaedic surgery. After lymphoprep gradient centrifugation at 1100 g, 30 min, 20ºC, without brake (Eppendorf Centrifuge 5810R, VWR International LLC, Radnor, PA, USA), cells were collected and plated in MSC growth medium (Dulbecco's modified Eagle's medium (DMEM) supplemented with 10% FBS Gibco MSC qualified (Fisher Scientific, Hampton, New Hampshire, USA) and 1% P/S) [10]. For MSC culture and maintenance, cells were seeded in 175 cm^2 tissue culture flasks (Falcon, Corning, Manassas, USA) with Dulbecco's modified Eagle's medium (DMEM; low-glucose with

glutamax Corning, Manassas, USA) supplemented with 10% FBS Gibco MSC qualified (Fisher Scientific, Hampton, New Hampshire, USA) and 1% P/S. Media was changed twice a week. Cells were passaged at 80% confluence by washing with warm PBS and detaching cells by using Gibco trypsin-EDTA 0.05% (Fisher Scientific, Hampton, New Hampshire, USA) for 5 min at 37 °C. The viable cells were counted using trypan blue (Sigma-Aldrich Co., St Louis, MO, USA) exclusion dye and seeded at a density of 3000 cells/cm^2 in 175 cm^2 tissue culture flasks (Falcon, Corning, Manassas, USA).

For osteogenic differentiation assays MSC were used at passage 7 and a total of 6000 cells/cm^2 were seeded on 96-well plates and incubated at 37 °C in DMEM supplemented with 10% FBS and 1% P/S. After reaching confluence, media was changed for: (i) negative control (basal media: DMEM (with 10% FBS and 1% P/S); (ii) positive control (osteogenic media: DMEM with 10% FBS (Biowest, Riverside, MO, USA), 1% P/S, 100 mM dexamethasone (Sigma- Aldrich Co., St Louis, MO, USA), 0.05 mM ascorbic acid (Sigma-Aldrich Co., St Louis, MO, USA) and 10 mM β-glycerophosphate (Sigma-Aldrich Co., St Louis, MO, USA)); (iii) biomaterials extracts controls (Fg, Mg and FgMg extracts diluted 1:10, as described in 2.3, and then diluted 1:2 in basal media to have similar conditions as for conditioned media); and (iv) conditioned media from day 13 macrophages preconditioned with biomaterials extracts in presence/absence of M1 stimulation (as described in 2.6), diluted in basal media 1:2. For each condition, two replicates were made for colorimetric evaluation of ALP activity and calcium deposition (alizarin red staining). Media was changed twice a week maintaining the respective stimulation, until day 14.

2.11. ALP and Alizarin Red staining

Before ALP staining at day 14, MSC were washed twice with PBS and fixed with 4% paraformaldehyde (Sigma-Aldrich Co., St Louis, MO, USA). Then, fixed MSC were incubated with ALP substrate, composed by 4% naphtol AS-MX phosphate alkaline solution in Fast Violet B solution (both from Sigma-Aldrich Co., St Louis, MO, USA) for 45 min at RT [24]. Calcium deposition was assessed by staining fixed MSC with Alizarin Red S (AZ) (Sigma-Aldrich Co., St Louis, MO, USA) for 10 min at room temperature [24]. Samples were washed twice in PBS at 4 °C and kept in water until being photographed under a stereomicroscope (Olympus SZX10, Shinjuku, Tokyo, Japan). The acquired images were analysed using an algorithm developed in MATLAB (Mathworks, Natick, MA, USA, version R2017b) to quantify ALP and AZ staining, as previously described [25]. In detail, ALP and AZ intensities were quantified after thresholding color images on the total area of each well

(ALP: red > 0.1; red > 0.9 x green; green< 0.92 x blue; AZ: red > 1.4 x green; red > 1.3 x blue).

2.12. Statistical analysis

Statistical analysis was performed using GraphPad Prism software (San Diego, CA, USA, version 7). Data were tested for normality using D'Agostino & Pearson normality test. To compare multiple groups Friedman's or Kruskal-Wallis tests were performed, followed by Dunn's multiple comparisons test for non-parametric data, while for parametric data ANOVA followed by Sidak's multiple comparisons test were used, as specified in figure legends. Data are represented as arithmetic mean ± standard deviation (SD) from at least three independent experiments. Error bars on box-and-whiskers plots indicate the minimum and maximum values obtained in the analysis. Statistical significance was considered for *p<0.05; **p<0.01; ***p<0.001; ****p<0.0001.

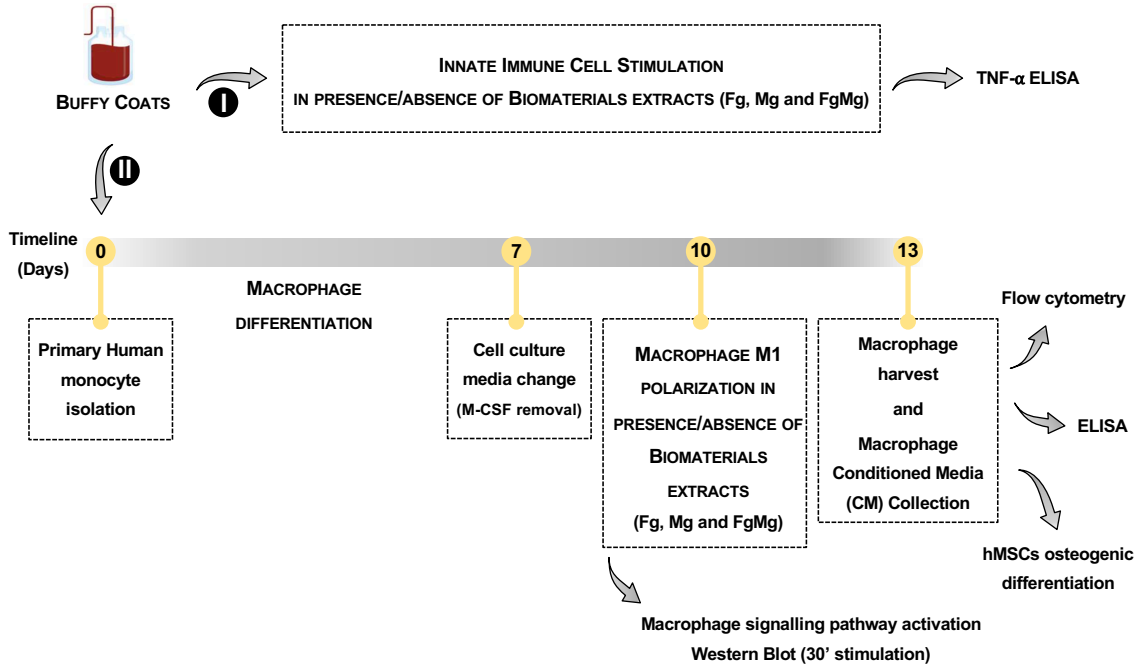


Fig. 1. Experimental timeline and readouts.

3. RESULTS

3.1. Fg scaffolds and their combination with Mg discs: 3D architecture and extract composition

Fg scaffolds were produced by freeze-drying, as described before [12], and combined with Mg discs. First, we analyzed the morphology of the Fg layer (Fig. 2). The SEM analysis revealed that the interconnected porous structure of Fg was largely maintained in the FgMg materials (Fig. 2A). As expected, EDS analysis showed the presence of detectable amounts of Mg in the Fg layer, only when analysing the FgMg combination (Fig. 2B).

Next, material extracts were produced and their Mg and Fg composition was evaluated. AAS was used to measure Mg concentration, and results (Fig. 2C) showed, as expected, that extracts from Fg materials had only residual Mg content, and significantly less than those from Mg and FgMg materials, which contained an average of 122.8 ± 10.11 and 205.8 ± 30.05 mg/L of Mg, respectively. The presence of Fg degradation products was measured using the d-Dimer quantification kit. Extracts from Fg materials had slightly higher levels of d-Dimer than those from FgMg materials, and both had significantly more d-Dimer than the residual amounts detected in Mg materials extracts (Fig. 2D). The pH of the extract solutions was also determined and was higher in the extracts of Mg-containing biomaterials when compared with Fg-only ones, Fg (8.29 ± 0.02), Mg (9.80 ± 0.11) and FgMg (9.94 ± 0.02), and with RPMI cell culture media (7.81 ± 0.09). Upon 1:10 dilution, the pH of all extracts was in the physiologic range, 7.93 ± 0.15 for Fg, 8.31 ± 0.04 for Mg and 8.32 ± 0.02 for FgMg.

Overall, these results indicated that the presence of Mg discs still allows the formation of a porous 3D structure characteristic of Fg, but Mg is released and found in the Fg layer of combination materials. Concentrations of degradation products for Mg and Fg were not statistically different between the single material extract and the extract of the combination.

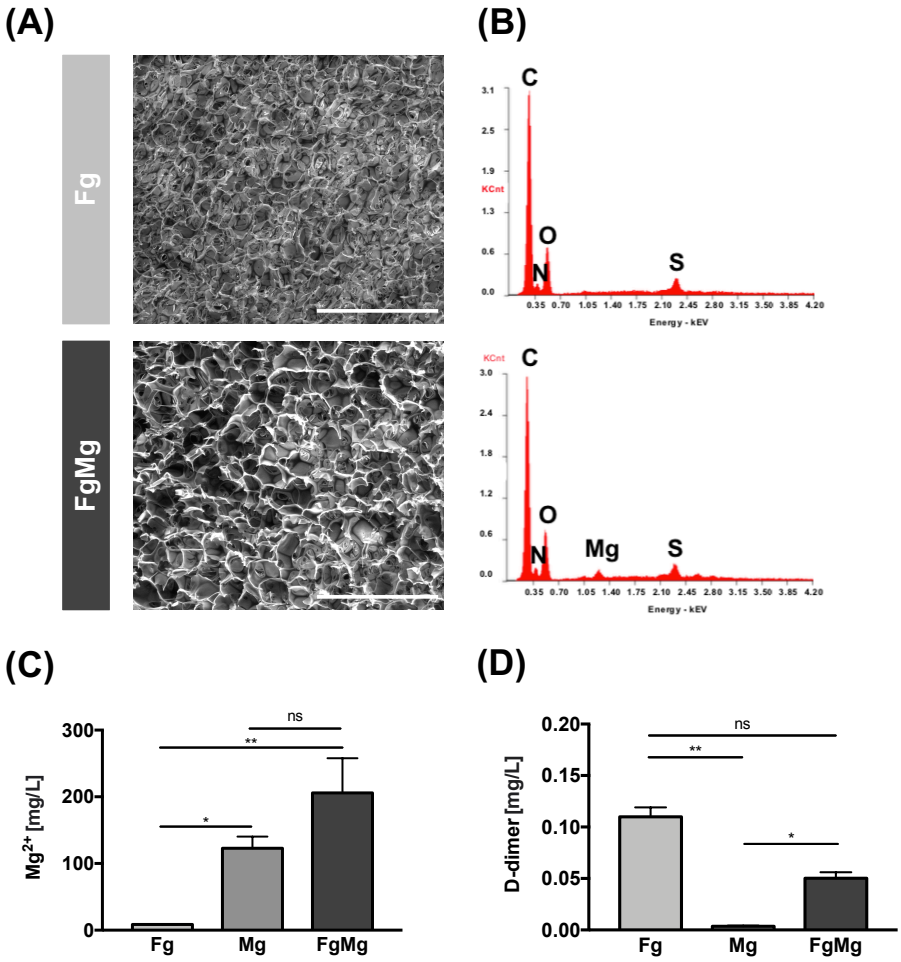


Fig. 2. Morphology of Fg alone or combined with Mg discs and biomaterials extracts composition. (A) SEM evaluation of the porous structure and **(B)** surface elemental composition of Fg alone or from FgMg combination (C: carbon, N: nitrogen, O: oxygen, Mg: magnesium, S: sulfur). Magnification: 250x. Scale bar: 400 µm. **(C)** Concentration of Mg^{2+} ions and **(D)** Fg-derived d-Dimer in pure extracts. Data represent arithmetic mean ± SD, analyzed by Kruskal-Wallis test followed by uncorrected Dunn's test (n = 3). *p<0.05; **p<0.01.

3.2. FgMg biomaterial extracts decreased LPS-stimulated TNF-α secretion

To evaluate the activation of innate immune cells and the potential for biomaterial extracts to act as immune-modulators, we first analyzed the impact of Fg, Mg and FgMg extracts, alone or upon endotoxin (i.e. LPS) stimulation, on concentrated whole blood, containing all peripheral blood immune cell populations. Results illustrated in Fig. 3 show that, none of the biomaterial extracts per se led to TNF-α secretion. As expected, secretion levels of TNF-α were significantly up-regulated in blood samples stimulated with LPS, comparing to non-stimulated samples. All extracts have shown the capacity to reduce TNF-α secretion levels, in response to LPS stimulation, but only extracts from the FgMg combination led to significantly less TNF-α secretion, when compared to the LPS stimulated control.

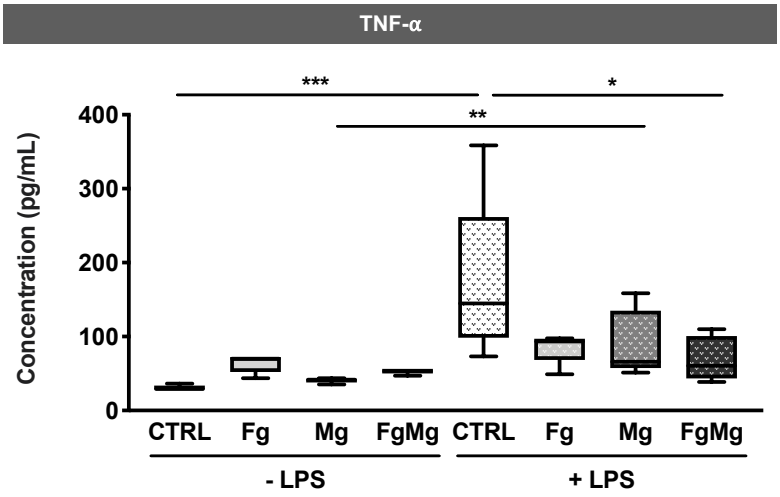


Fig. 3. TNF-α secretion levels in buffy coats stimulated with Fg, Mg and FgMg extracts alone or in the presence of LPS. Innate immune cells in buffy coats were left unstimulated or stimulated with LPS in presence/absence of biomaterials extracts (Fg, Mg and FgMg extracts). TNF-α secretion was determined by ELISA. Graphs are minimum to maximum box-and-whiskers plots, with median representation (n = 5 independent donors). Friedman's test followed by uncorrected Dunn's test were performed. *p<0.05; **p<0.01; ***p<0.001.

3.3. FgMg biomaterial extracts impaired macrophage M1 polarization

As macrophages play a central role in biomaterials response, next we sought to investigate in more detail whether macrophage polarization could be modulated by the degradation products from Fg, Mg or FgMg biomaterials. Macrophages were exposed to the materials extracts and either left unstimulated, or stimulated towards M1 pro-inflammatory phenotype, by the addition of LPS and IFN**γ**. Cell surface markers associated to M1 (CD86) and M2 phenotypes (CD163) were analyzed in relation to the lineage marker CD14, at day 13. Dot plots illustrating macrophage phenotype in the different conditions are presented in Fig. 4A. When the percentage of positive cells for each marker was quantified across different donors, high percentages of CD14 positive cells were found, as expected. M1 stimulation increased the percentage of CD14 cells, particularly when combined with the presence of FgMg extracts, leading that increase to be statistically significant, compared to the respective M0 control (Fig. 4B). The biomaterial extracts per se did not increased CD86 cell surface expression, as all M0 conditions show similar and low percentages of CD86 positive cells. M1 stimulation, with LPS-IFN**γ**, increased the percentage of cells expressing CD86 in control (CTRL) culture conditions and in the presence of extracts of Fg and Mg materials separately. Interestingly, in presence of extracts from the FgMg combination biomaterial, the percentage of CD86 positive cells was no longer significantly different from M0 unstimulated conditions (Fig. 4C). As expected, the percentage of cells expressing CD163

(M2 marker) decreased when cells were stimulated towards M1 polarization and results showed that the presence of the different biomaterial extracts did not have a significant impact on CD163 expression (Fig. 4D). The decrease in CD86 levels in M1 stimulated macrophages exposed to FgMg extracts suggests that this combination impairs M1 polarization.

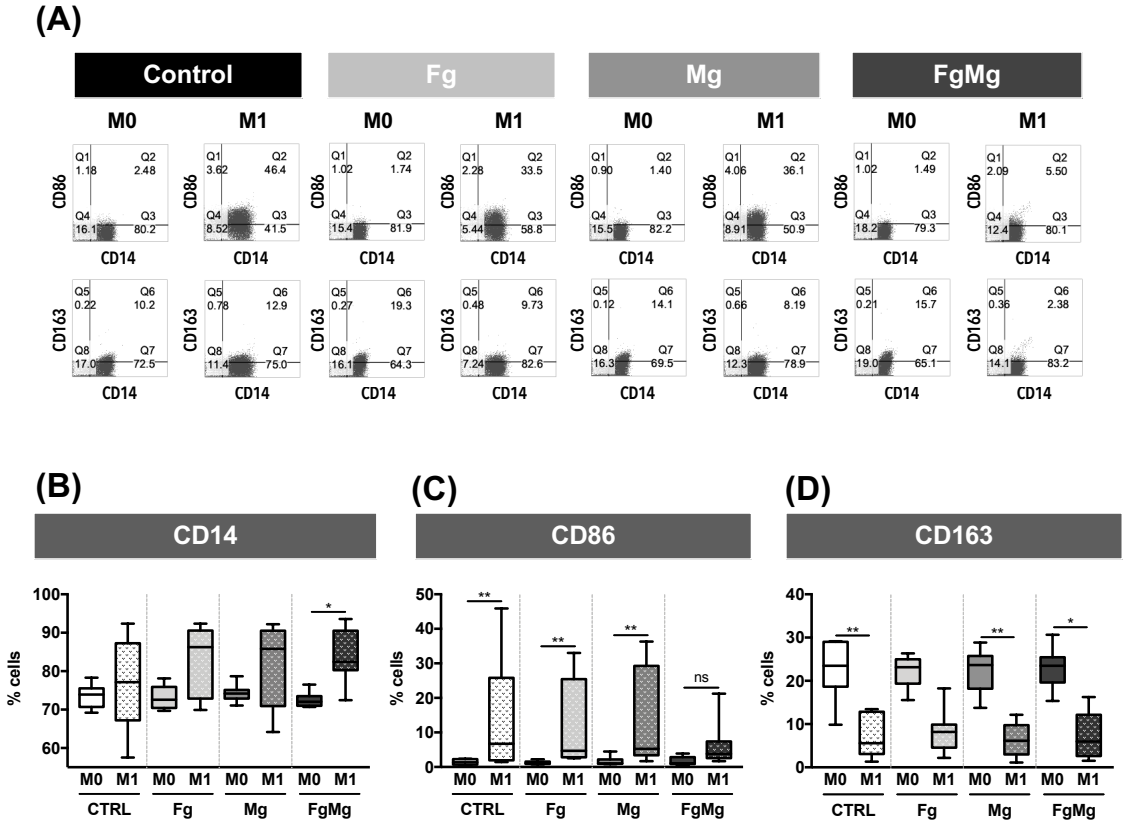


Fig. 4. Macrophage cell surface receptor profile upon preconditioning with Fg, Mg and FgMg extracts in the presence/absence of M1 stimulation. Macrophages were cultured with Fg, Mg and FgMg extracts with or without M1 stimulation (LPS-IFN**γ**) for 72 h, before being harvested, stained for the indicated cell surface markers and analyzed by flow cytometry. (A) Dot plots of a representative blood donor, where values in each quadrant represent percentage of cells in that quadrant. (B) Percentage of CD14+ cells (n = 8). (C) Percentage of double-positive cells, CD14+CD86+ (n = 8). (D) Percentage of double-positive cells, CD14+CD163+ (n = 8). Isotype controls were used to define background staining. M0=naïve/unstimulated macrophages; M1=LPS-IFN**γ** stimulated macrophages. Graphs are minimum to maximum box-and-whiskers plots, with median representation. Friedman's test followed by corrected Dunn's test were performed. *p<0.05; **p<0.01.

3.4. FgMg biomaterial extracts decreased NF-kB p65 phosphorylation, following M1 stimulation

To uncover the mechanism by which the FgMg extract could be impairing the M1 activation of macrophages, the MAPK signaling pathways (JNK, ERK and p38) and NF-kB p65 phosphorylation, known to be stimulated in monocytes/macrophages in response to M1

stimulation [8, 26-28], were probed by Western blotting. Results depicted in Fig. 5 highlighted that biomaterial extracts per se did not induce activation of MAPK pathways or NF-kB p65 phosphorylation. As expected, activation of all MAPK pathways occurred in response to M1 stimulation. When results were quantified across different donors, we could observe a tendency for FgMg extracts to increase ERK and decrease p38 phosphorylation levels in the presence of M1 stimulation, albeit this observation was not statistically significant. Interestingly, the presence of materials extracts reduced phosphorylation levels of NF-kB p65, activated in response to M1 stimulation, reaching statistical significance for the FgMg combination extract. In conclusion, results showed that FgMg extracts lead to the downregulation of NF-kB p65 phosphorylation, suggesting that this combination may have an impact over the inflammatory signalling pathways.

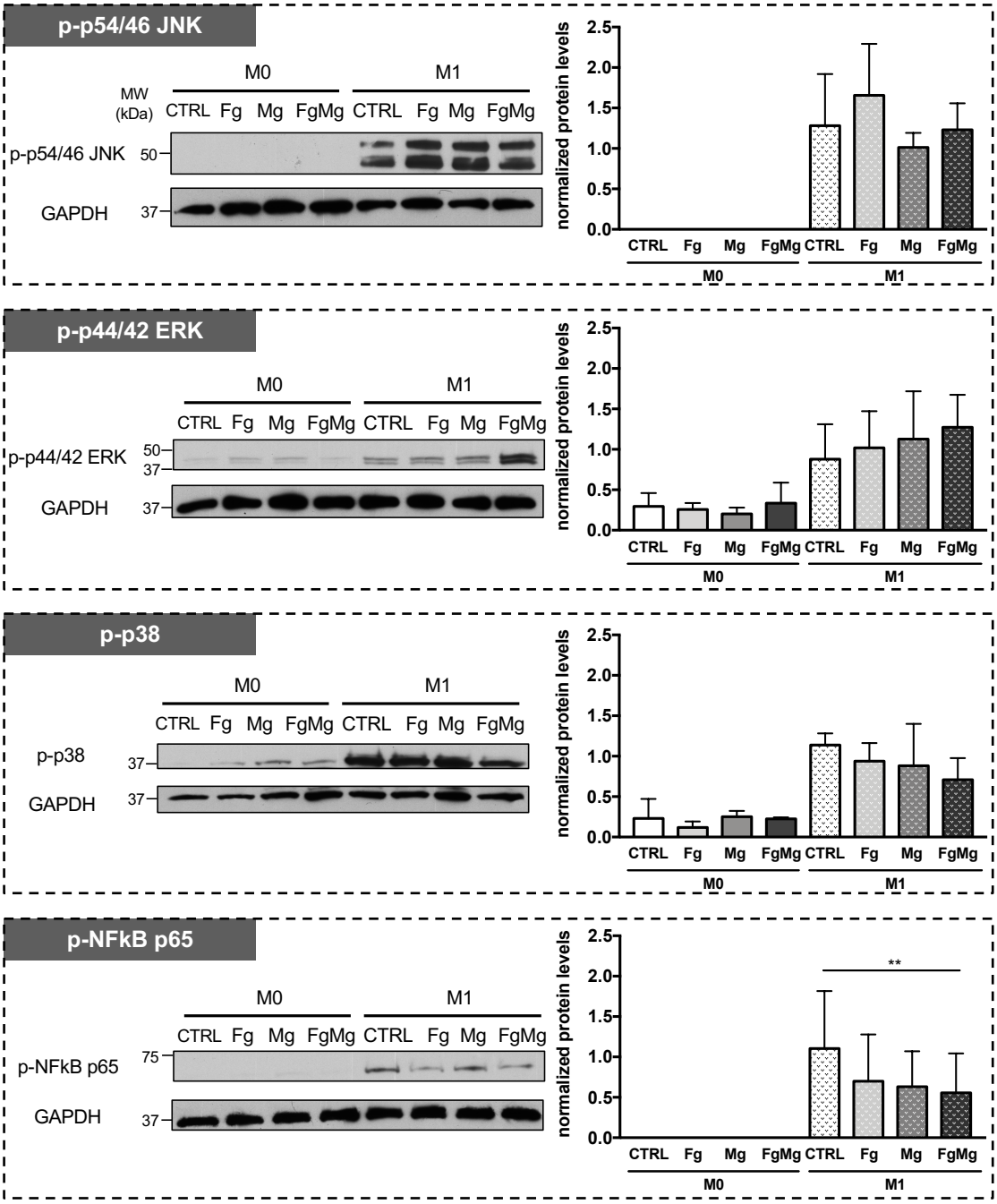


Fig. 5. Activation of MAPK (JNK, ERK, p38) and NF-kB p65 signaling pathways in macrophages preconditioned with Fg, Mg and FgMg extracts with or without M1 stimulation. Western blot shows protein levels of p54/46 JNK, p44/42 ERK, p38 and NF-kB p65 phosphorylated forms in macrophages preconditioned with or without (CTRL) biomaterials extracts (Fg, Mg and FgMg extracts) in the presence/absence (M0) of M1 stimulation (LPS-IFN**γ**). p-p54/46 JNK (n = 3), p-p44/42 ERK (n = 3), p-p38 (n = 3) and p-NF-kB p65 (n = 4). Relative protein levels were quantified using Image Lab software. GAPDH was used as normalizer. Data are mean ± SD. Friedman's test followed by corrected Dunn's test were performed. $^{**}p<0.01$.

3.5. Fg, Mg and FgMg biomaterials extracts influenced cytokine secretion by M1 stimulated macrophages

Cytokines are important players in the inflammatory response to biomaterials and important regulators of its progression and resolution [29]. To explore the functional consequences of Fg, Mg and FgMg extracts on M0 and M1-stimulated macrophages, cytokine secretion profiles were assessed. Results presented in Fig. 6 show that biomaterial extracts per se had no significant impact on the secretion levels of TNF-α, IL-6, IL-1β, IL-12 p70, IL-10 or TGF-β1. As expected, in control conditions secretion levels of TNF-α, IL- 6, IL-1 β, IL-12p70 and IL-10 were up-regulated in M1 stimulated macrophages, comparing to their M0 counterparts. Interestingly, material extracts impacted cytokine secretion levels in response to M1 stimulation. While all material extracts reduced TNF-α secretion levels upon M1 stimulation, with loss of the statistically significant increase between M0 and M1 in presence of Fg and FgMg extracts, IL-6 secretion was only impacted by Mg material extract. Moreover, Fg extracts impaired the increased IL-1β secretion in response to LPS-IFN**γ** stimulation, compared to the respective M0, and showed significantly lower secretion, when compared with M1 in CTRL conditions. Secretion levels of IL-12p70 were not significantly increased by M1 stimulation when macrophages were in presence of Mg and FgMg extracts. Materials extracts did not impact the increased IL-10 secretion upon M1 stimulation, when compared with respective M0 macrophages. In addition, FgMg extracts significantly increased macrophage TGF-β1 secretion in response to M1 stimulation, when compared to their M0 counterparts. Overall, Fg, Mg and FgMg extracts led to decreased secretion of specific cytokines by M1-stimulated macrophages which might point towards distinct immunomodulatory effect upon different cytokines.

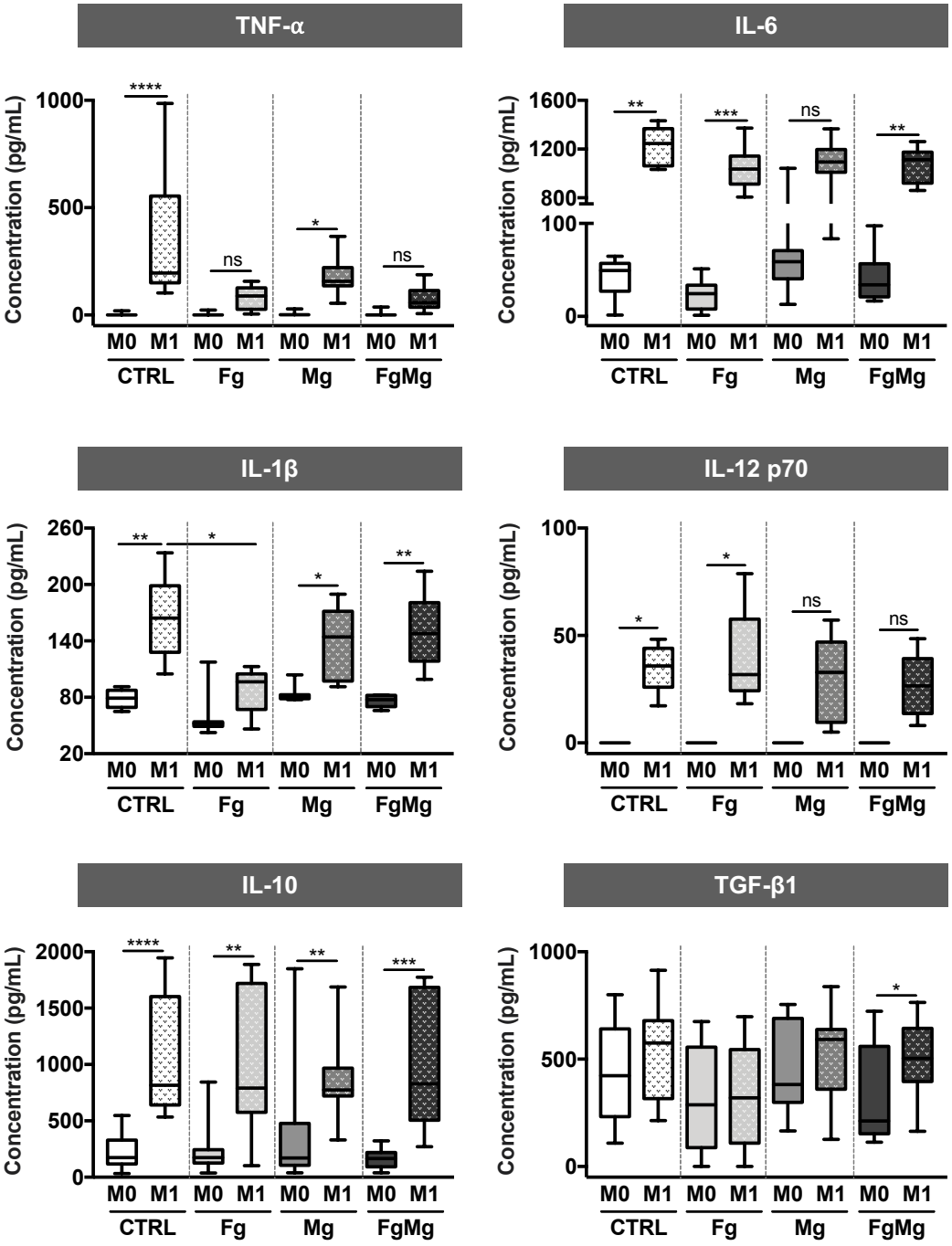


Fig. 6. Macrophage cytokine production upon preconditioning with Fg, Mg and FgMg extracts alone or in the presence of M1 stimulation. TNF-α, IL-6, IL-1β, IL-12p70, IL-10 and TGF-β1 release were determined by ELISA using macrophages secretome at day 13, from the following conditions: M0=naïve/unstimulated macrophages; M1=LPS-IFNγ stimulated macrophages; and macrophages preconditioned with Fg, Mg and FgMg extracts in the presence/absence of M1 stimulation. Graphs are minimum to maximum box-and-whiskers plots, with median representation. Friedman's test followed by corrected Dunn's multiple comparisons were performed for TNF-α, IL-6, IL-1β (all n = 8), IL-12p70 (n = 5) and IL-10 (n = 11). One-way ANOVA followed by Sidak's multiple comparisons test were performed for TGF-β1 (n = 11). *p<0.05; **p<0.01; ***p<0.001; ****p<0.0001.

3.6. Secretome from macrophages preconditioned with FgMg biomaterial extracts increased MSC ALP activity and calcium deposition

Next we wanted to evaluate the impact of the observed macrophage immunomodulation by the biomaterials extracts, on their crosstalk with MSC. So, the secretome produced by macrophages preconditioned with biomaterials extracts in the presence/absence of M1 stimulation, was used for promoting MSC osteogenic differentiation in the absence of osteoinductive stimulation (ascorbic acid, β-glycerophosphate and dexamethasone). MSC cultured in presence of Fg, Mg and FgMg extracts were used as controls, for the potential direct effect of biomaterials extracts on osteogenesis. Osteogenesis in presence of chemical inductors was used as positive control. ALP activity staining was performed at day 14, as an indicator of early osteogenesis. Results illustrated in Fig. 7A show the quantification of ALP-stained areas across the different experiments. In general, secretome from M1 stimulated macrophages promoted higher ALP activity than those of M0 macrophages, although the differences were not statistically significant. Interestingly, the secretome of macrophages exposed to FgMg extracts promoted the highest ALP activity, with that of M0 macrophages, inducing significantly higher ALP activity than the one from CTRL M0 macrophages, or from M0 exposed to Fg material extracts. When macrophage secretomes were compared to the biomaterial extracts per se, the secretome of M0 macrophages exposed to Mg extracts induced significantly higher ALP activity than Mg extracts, and secretomes of macrophages (M0 and M1) exposed to FgMg extracts induced higher ALP activity than FgMg extract.

Moreover, the effect of macrophages secretome on mineral deposition was analysed by alizarin red staining. Results presented in Fig. 7B show that, similarly to ALP activity, materials extracts per se did not increase calcium deposition significantly, while more alizarin red staining could be observed in MSC stimulated by the secretome of macrophages. In general, macrophage exposure to biomaterials extracts led to secretomes that induced significant increases in alizarin red staining in MSC cultures, when compared to those exposed to extracts alone. Albeit, MSC cultured with secretome of M0 macrophages not exposed to any extract led to a significant increase in the alizarin red staining, compared to their M1 counterparts.

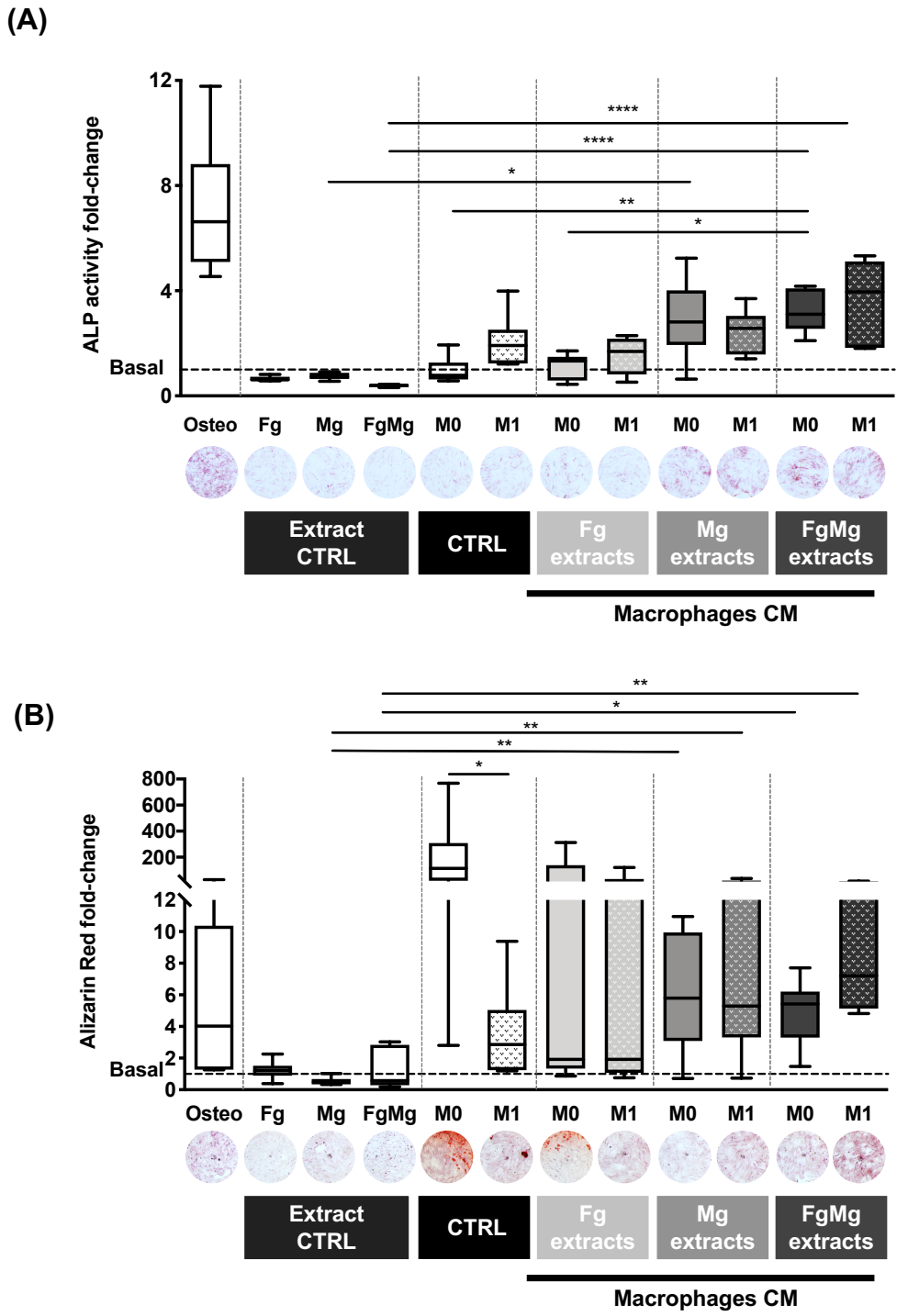


Fig. 7. Effect of macrophage secretome on MSC osteogenic differentiation. MSC were incubated for 14 days with biomaterial extracts (extract CTRL=Fg, Mg and FgMg biomaterials extracts) or the secretome of macrophages unstimulated (M0), or LPS-IFNγ stimulated (M1), in presence/absence of biomaterial extracts (CTRL=conditioned media from macrophages not exposed to extracts; Fg, Mg and FgMg extracts=conditioned media from macrophages preconditioned with Fg, Mg and FgMg extracts alone), as indicated. Basal and osteogenic (osteo) media were used as controls. ALP **(A)** and Alizarin Red **(B)** stainings were performed and stained areas were quantified using MATLAB. Values were normalized by the basal condition (n = 6). Representative pictures (Zoom=1.6x) are shown for each condition. Error bars on box-and-whiskers plots indicate the minimum and maximum values, with median representation. Friedman's test followed by uncorrected Dunn's test were performed. *p<0.05; **p<0.01; ****p<0.0001.

To determine the contribution of the materials degradation products, contained in macrophage secretome, for ALP activity and mineral deposition the concentration of Mg ions and Fg degradation product, d-Dimer, in conditioned media was evaluated. The results obtained are presented in Fig. 8, and show similar Mg concentrations in the conditioned media of macrophages exposed to all extracts and control conditions, while Fg degradation product d-Dimer was more concentrated in conditioned media from macrophages exposed to Fg and FgMg biomaterials. Together, these results indicated that the macrophage secretion products induced ALP activity and mineral deposition on MSC, while direct exposure to biomaterial degradation products did not have the same impact.

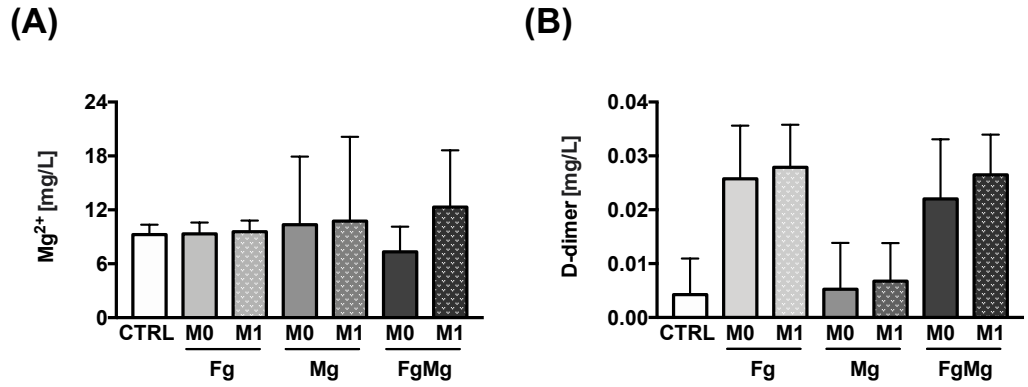


Fig. 8. Magnesium and fibrinogen degradation products content in conditioned media from macrophages cultured with Fg, Mg and FgMg extracts in the presence/absence of M1 stimulation. (A) Mg content and **(B)** Fg degradation products (d-Dimer) in conditioned media from macrophages preconditioned with biomaterials extracts (Fg, Mg and FgMg) alone or in the presence of M1 stimulation (LPS-IFN**γ**). Data are mean ± SD. Friedman's test followed by corrected Dunn's test were performed for conditioned media measurements (n = 8).

4. DISCUSSION

Macrophages are key players in the inflammatory response to injury and to biomaterial implantation [2], and their modulation is an increasingly sought-after strategy [2, 30].

Development and clinical application of Mg-based materials is impaired by Mg unpredictable corrosion in aqueous environments, hydrogen gas formation and pH alkalization during degradation [17, 18, 31]. Mg combination with polymers, may improve Mg corrosion resistance [32], and Fg regenerative properties, render it an attractive interface for Mg-based materials and host tissue. Thus, in this study Fg and Mg were combined for the first time to make FgMg. The rational underlying this biomaterial combination was that Fg and Mg could act synergistically to modulate macrophage polarization and promote a pro-regenerative microenvironment. Herein, the Mg disc was

surrounded by an upper and a lower Fg layer, aiming to provide a protective coating to Mg. The presence of Mg material did not alter the Fg layer porosity, which was similar to that previously reported for Fg scaffolds [12]. In the current work *in vitro* degradation rates of Fg, Mg and FgMg were indirectly evaluated, via the concentration of Mg^{2+} and d-Dimer (Fg degradation product) in their extracts. Fg scaffolds were previously reported to be more susceptible to *in vitro* hydrolysis, than proteolysis [12]. For Mg-based biomaterials, correlations between *in vivo* and *in vitro* degradation rates are reported to be better achieved when biomaterials are immersed in cell culture media under physiological conditions (37 ºC, 21% O2, 5% CO2, 95% RH) [33]. Importantly, comparison between *in vitro* and *in vivo* degradation rates is not straightforward. Degradation rates determined *in vitro* allow only to infer a potential *in vivo* degradation pattern [34]. Protein adsorption upon biomaterial implantation, is known to condition the host inflammatory response and interactions with immune cells [35]. Fg is one of the most studied proteins for adsorption to biomaterials [36], being able to interact with other proteins. The Fg layer in FgMg is expected to facilitate interaction with host proteins and cells.

The current study used biomaterial extracts to evaluate the immunomodulatory impact of Fg, Mg and FgMg degradation products, particularly on primary human macrophages. This approach has been previously reported to evaluate the impact of Mg-based materials on different cell populations [15, 20, 37, 38], including on THP1-derived macrophages [39], but not primary human macrophages. Here, biomaterial extracts were diluted 10-fold, achieving a physiological pH, in agreement with previous recommendation on improving conditions for *in vitro* testing Mg-based materials [31, 40].

Stimulation of immune cells in buffy coats from peripheral blood of healthy blood donors was evaluated based on TNF-α secretion, as TNF-α is reported to be secreted in response to endotoxins, like LPS, in a concentration dependent-manner [22]. The biomaterial extracts *per se* did not promote TNF-α secretion, supporting low endotoxin content. When cells were stimulated with LPS, TNF-α secretion was impaired by the presence of biomaterials extracts, particularly for FgMg. These results were further supported by the cytokine profile observed herein for macrophages.

Depending on microenvironmental cues, macrophages can polarize towards a range of phenotypes, from pro-inflammatory M1 to anti-inflammatory M2 [3]. The classical pro-inflammatory LPS-IFNγ M1 stimulation [41] was performed for 72h, which leads to full cell maturation [16]. Cell surface expression of M1 marker (CD86) showed that extracts from FgMg combination materials impaired macrophage M1 polarization, more efficiently than

those from Fg or Mg separately. None of the extracts promoted increased M2 macrophage marker CD163, suggesting a reduction of M1 polarization, but that is not accompanied by increased M2 phenotype. Previous work using RAW 264.7-derived macrophages on Mg-treated titanium materials showed that release of Mg^{2+} led to decreased pro-inflammatory markers (CD86), but the authors report also increased anti-inflammatory molecules (CD163 and CD206), in non-stimulated or LPS-stimulated conditions[42, 43].

Moreover, Mg ions from materials containing Mg [42, 43], their extracts [39] or Mg salts ($MgSO_4$) [44-46], have also been associated with decreased pro-inflammatory cytokines production, including TNF-α and IL-6. Similarly, we observed a tendency for Mg-containing biomaterials extracts, to reduce IL-6 and IL-12p70 secretion levels.

In line with results presented here, previous work from our group showed that Fg adsorbed to chitosan reduced macrophage activation and pro-inflammatory cytokine secretion, stimulating release of pro-osteogenic and angiogenic factors [9]. Conversely, soluble Fg has been reported to stimulate macrophages towards a pro-inflammatory profile [47], and increase pro-inflammatory cytokines secretion by human monocytes [48], and mouse macrophages [47]. Interestingly, here macrophage response to Fg-biomaterials extracts was closer to the one observed for adsorbed Fg, rather than for its soluble form. Of the anti-inflammatory cytokines tested, IL-10 has been described as a M2 cytokine [49-51]. Nevertheless, in this work and previous ones [52-54], M1 polarized macrophages were shown as important IL-10 producers, which has been suggested as a regulatory mechanism [55]. Additionally, FgMg extracts promoted an increased TGF-β1 secretion, upon M1 stimulation. However, the role of this cytokine in regulating macrophages responses remains incompletely established [56].

Macrophage polarization depends on activation of signaling pathways involving MAPK and NF-kB, downstream of LPS-mediated TLR4 engagement [28, 57, 58]. Our previous work indicated that adsorbed Fg induced MAPK phosphorylation, and that LPS induced a phosphorylation peak 30 min upon stimulation [8]. However, herein Fg-biomaterial extracts did not promote JNK, ERK and p38 phosphorylation, or modify phosphorylation levels upon M1 stimulation. Although soluble Fg was reported to increased monocyte NF-kB p65 activity [48], we did not find Fg extract-mediated NF-kB p65 phosphorylation. Also, Mg^{2+} supplementation (Mg salts), has been shown to reduce NF-kB activation, with subsequent reduction of pro-inflammatory cytokine secretion, upon LPS stimulation with or without IFN**γ**, in RAW 264.7 cell line [46] and cord blood monocytes [44]. Among NF-kB family members, p65 is typically involved in inflammatory response, with increased

phosphorylation of NF-kB p65 being associated to the pathogenesis of several chronic inflammatory diseases [59]. NF-kB inhibition studies have shown that p65 silencing reduced secretion of pro-inflammatory mediators, like IL-6 [60]. The current work showed that FgMg combination extracts inhibit M1-stimulated NF-kB p65 to a greater extent than those of individual materials, indicating a synergistic impact of Fg and Mg on macrophages.

To address the functional implication of exposure to the biomaterials extracts on macrophages, their crosstalk with MSC was probed. MSC can be isolated from several sources, including bone marrow, adipose tissue, peripheral blood, placenta or umbilical cord blood. However, the amount of MSC obtained, their proliferation and differentiation capacity differ [61]. Herein, MSC were isolated from bone marrow, the most widely used source, due to their involvement in the bone repair microenvironment. Macrophages are reported to influence MSC osteogenic differentiation, through cytokine secretion [4, 62-64]. ALP activity was used as a marker for osteogenesis differentiation, as this enzyme activity is transiently increased when MSCs commit to the osteogenic lineage, peaking at 14 days of differentiation [65]. While some studies highlight the role of pro-inflammatory M1 macrophages [62, 63] in stimulating MSCs osteogenic differentiation, others attribute this role to anti-inflammatory M2 macrophages [4, 64]. In the current study, macrophage exposure to biomaterial extracts had a greater impact than M1 polarization in their secretome promoting MSC ALP activity and mineral deposition. Interestingly, gene expression analysis at day 7 was not in agreement with ALP activity and alizarin red staining at day 14, showing low transcription activation of *RUNX2* and *ALP* by the secretome of macrophages in all conditions tested (Supplementary Fig. 2). Although the impact of the selected time point cannot be ruled out, this might also be dependent on different mechanisms of regulation of protein translation and activity [66], as reported by Rescigno et al., where short exposures to low frequency magnetic fields induced higher ALP activity, when compared with its mRNA expression [67].

Together, the results presented here provide a proof-of-concept of Fg and Mg synergistic impact on macrophage M1 response, and their crosstalk with MSC, supporting the potential of FgMg combination biomaterials to be further developed for bone tissue repair. Nevertheless, some important questions should be addressed in future work. In the biomaterial development, analyzing the implications of changing the proportions between Fg and Mg in the final biomaterial or the presence of alloying elements in the Mg component could further improve the outcomes reported here. Also, the angiogenic potential of the FgMg combination should be investigated. Interestingly, previous work showed that

incorporation of Fg in Ch materials stimulated angiogenesis in a critical size bone defect model, although an increased number of blood vessels did not directly correlate with bone repair [11]. Also, Mg extracts have been reported to increase human umbilical vein endothelial cells proliferation, under hypoxic conditions [20]. This effect was concentration-dependent, with low Mg concentrations (10 mM) increasing vascular smooth muscle cell proliferation and migration rate, and higher Mg concentrations (40-60 mM) inducing coagulation and inflammation [68]. Finally, future evaluation of this combination biomaterial *in vivo* will be essential to understand its capacity to dampen inflammation and promote bone repair, particularly in inflammatory conditions.

5. CONCLUSION

In conclusion, the present study reports, for the first time, the combination of Fg and Mg biomaterials and the impact of their degradation products on macrophages. The results presented support the hypothesis that Fg and Mg can act synergistically to reduce macrophage pro-inflammatory stimulation, and lead macrophages to promote MSC osteogenic differentiation. Hence, the combination of Fg and Mg rises as an interesting strategy to tune the initial inflammatory response, dampening the M1 macrophage response, to support bone repair.

ACKNOWLEDGMENTS

This work was funded by NORTE-01-0145-FEDER-000012, NORTE 2020, under PORTUGAL 2020 Partnership Agreement, through ERDF; Mafalda Bessa-Gonçalves and João Paulo Brás are funded by FCT PhD Programmes and by Programa Operacional Potencial Humano (POCH), BiotechHealth Programme (Doctoral Programme on Cellular and Molecular Biotechnology Applied to Health Sciences – reference PD/BI/128355/2017 and PD/BI/128356/2017, respectively), and through the PhD studentship PD/BD/135489/2018 and PD/BD/135490/2018, respectively. The authors thank Grifols SA for donating clinical grade fibrinogen; Daniela Silva for the technical and scientific support with SEM analysis (CEMUP); i3S Scientific Platform Translational Cytometry, member of the PPBI (PPBI-POCI-01-0145-FEDER-022122); Serviço de Ortopedia and Serviço de Imunohemoterapia, Centro Hospitalar Universitário de São João for donating bone marrow samples and buffy coats, respectively; Monika Lucszak (HZG) for their expert technical assistance in extracts characterization; Maria Inês Almeida for her help with gene expression analysis.

REFERENCES

[1] F. Loi, L.A. Cordova, J. Pajarinen, T.H. Lin, Z. Yao, S.B. Goodman, Inflammation, fracture and bone repair, Bone 86 (2016) 119-30.

[2] Z. Julier, A.J. Park, P.S. Briquez, M.M. Martino, Promoting tissue regeneration by modulating the immune system, Acta Biomater 53 (2017) 13-28.

[3] E. Mariani, G. Lisignoli, R.M. Borzi, L. Pulsatelli, Biomaterials: Foreign Bodies or Tuners for the Immune Response?, Int J Mol Sci 20(3) (2019).

[4] L. Gong, Y. Zhao, Y. Zhang, Z. Ruan, The Macrophage Polarization Regulates MSCS Osteoblast Differentiation in vitro, Ann Clin Lab Sci 46(1) (2016) 65-71.

[5] L. Vi, G.S. Baht, H. Whetstone, A. Ng, Q. Wei, R. Poon, S. Mylvaganam, M. Grynpas, B.A. Alman, Macrophages promote osteoblastic differentiation in-vivo: implications in fracture repair and bone homeostasis, J Bone Miner Res 30(6) (2015) 1090-102.

[6] F. Scognamiglio, A. Travan, I. Rustighi, P. Tarchi, S. Palmisano, E. Marsich, M. Borgogna, I. Donati, N. de Manzini, S. Paoletti, Adhesive and sealant interfaces for general surgery applications, J Biomed Mater Res B Appl Biomater 104(3) (2016) 626-39.

[7] D. Davalos, K. Akassoglou, Fibrinogen as a key regulator of inflammation in disease, Semin Immunopathol 34(1) (2012) 43-62.

[8] M.I. Oliveira, M.L. Pinto, R.M. Goncalves, M.C.L. Martins, S.G. Santos, M.A. Barbosa, Adsorbed Fibrinogen stimulates TLR-4 on monocytes and induces BMP-2 expression, Acta Biomater 49 (2017) 296-305.

[9] J. Maciel, M.I. Oliveira, E. Colton, A.K. McNally, C. Oliveira, J.M. Anderson, M.A. Barbosa, Adsorbed fibrinogen enhances production of bone- and angiogenic-related factors by monocytes/macrophages, Tissue Eng Part A 20(1-2) (2014) 250-63.

[10] C.R. Almeida, D.P. Vasconcelos, R.M. Goncalves, M.A. Barbosa, Enhanced mesenchymal stromal cell recruitment via natural killer cells by incorporation of inflammatory signals in biomaterials, J R Soc Interface 9(67) (2012) 261-71.

[11] S.G. Santos, M. Lamghari, C.R. Almeida, M.I. Oliveira, N. Neves, A.C. Ribeiro, J.N. Barbosa, R. Barros, J. Maciel, M.C. Martins, R.M. Goncalves, M.A. Barbosa, Adsorbed fibrinogen leads to improved bone regeneration and correlates with differences in the systemic immune response, Acta Biomater 9(7) (2013) 7209-17.

[12] D.M. Vasconcelos, R.M. Goncalves, C.R. Almeida, I.O. Pereira, M.I. Oliveira, N. Neves, A.M. Silva, A.C. Ribeiro, C. Cunha, A.R. Almeida, C.C. Ribeiro, A.M. Gil, E. Seebach, K.L. Kynast, W. Richter, M. Lamghari, S.G. Santos, M.A. Barbosa, Fibrinogen scaffolds with immunomodulatory properties promote in vivo bone regeneration, Biomaterials 111 (2016) 163-178.

[13] B.J. Luthringer, F. Feyerabend, R. Willumeit-Romer, Magnesium-based implants: a mini-review, Magnes Res 27(4) (2014) 142-54.

[14] D.M. Vasconcelos, S.G. Santos, M. Lamghari, M.A. Barbosa, The two faces of metal ions: From implants rejection to tissue repair/regeneration, Biomaterials 84 (2016) 262-275.

[15] B.J. Luthringer, R. Willumeit-Romer, Effects of magnesium degradation products on mesenchymal stem cell fate and osteoblastogenesis, Gene 575(1) (2016) 9-20.

[16] M.D. Costantino, A. Schuster, H. Helmholz, A. Meyer-Rachner, R. Willumeit-Romer, B.J.C. Luthringer-Feyerabend, Inflammatory response to magnesium-based biodegradable implant materials, Acta Biomater 101 (2020) 598-608.

[17] M. Razavi, Y. Huang, Assessment of magnesium-based biomaterials: from bench to clinic, Biomater Sci 7(6) (2019) 2241-2263.

[18] D. Zhao, F. Witte, F. Lu, J. Wang, J. Li, L. Qin, Current status on clinical applications of magnesium-based orthopaedic implants: A review from clinical translational perspective, Biomaterials 112 (2017) 287-302.

[19] S.A. Sell, M.P. Francis, K. Garg, M.J. McClure, D.G. Simpson, G.L. Bowlin, Cross-linking methods of electrospun fibrinogen scaffolds for tissue engineering applications, Biomed Mater 3(4) (2008) 045001.

[20] L. Xu, R. Willumeit-Romer, B.J.C. Luthringer-Feyerabend, Effect of magnesium-degradation products and hypoxia on the angiogenesis of human umbilical vein endothelial cells, Acta Biomater (2019).

[21] N.A. Agha, F. Feyerabend, B. Mihailova, S. Heidrich, U. Bismayer, R. Willumeit-Romer, Magnesium degradation influenced by buffering salts in concentrations typical of in vitro and in vivo models, Mater Sci Eng C Mater Biol Appl 58 (2016) 817-25.

[22] M. Daneshian, S. von Aulock, T. Hartung, Assessment of pyrogenic contaminations with validated human whole-blood assay, Nat Protoc 4(12) (2009) 1709-21.

[23] A.R. Almeida, M. Bessa-Goncalves, D.M. Vasconcelos, M.A. Barbosa, S.G. Santos, Osteoclasts degrade fibrinogen scaffolds and induce mesenchymal stem/stromal osteogenic differentiation, Journal of biomedical materials research. Part A (2019).

[24] M.I. Almeida, A.M. Silva, D.M. Vasconcelos, C.R. Almeida, H. Caires, M.T. Pinto, G.A. Calin, S.G. Santos, M.A. Barbosa, miR-195 in human primary mesenchymal stromal/stem cells regulates proliferation, osteogenesis and paracrine effect on angiogenesis, Oncotarget 7(1) (2016) 7-22.

[25] D.M. Vasconcelos, C. Falentin-Daudre, D. Blanquaert, D. Thomas, P.L. Granja, V. Migonney, Role of protein environment and bioactive polymer grafting in the S. epidermidis response to titanium alloy for biomedical applications, Mater Sci Eng C Mater Biol Appl 45 (2014) 176-83.

[26] J.P. Bras, A.M. Silva, G.A. Calin, M.A. Barbosa, S.G. Santos, M.I. Almeida, miR-195 inhibits macrophages pro-inflammatory profile and impacts the crosstalk with smooth muscle cells, PLoS One 12(11) (2017) e0188530.

[27] A.F. Valledor, E. Sanchez-Tillo, L. Arpa, J.M. Park, C. Caelles, J. Lloberas, A. Celada, Selective roles of MAPKs during the macrophage response to IFN-gamma, J Immunol 180(7) (2008) 4523-9.

[28] K.M. Rao, MAP kinase activation in macrophages, J Leukoc Biol 69(1) (2001) 3-10.

[29] S.E. Headland, L.V. Norling, The resolution of inflammation: Principles and challenges, Semin Immunol 27(3) (2015) 149-60.

[30] R. Sridharan, A.R. Cameron, D.J. Kelly, C.J. Kearney, F.J. O'Brien, Biomaterial based modulation of macrophage polarization: a review and suggested design principles, Materials Today 18(6) (2015) 313-325.

[31] J. Wang, F. Witte, T. Xi, Y. Zheng, K. Yang, Y. Yang, D. Zhao, J. Meng, Y. Li, W. Li, K. Chan, L. Qin, Recommendation for modifying current cytotoxicity testing standards for biodegradable magnesium-based materials, Acta Biomater 21 (2015) 237-49.

[32] L.Y. Li, L.Y. Cui, R.C. Zeng, S.Q. Li, X.B. Chen, Y. Zheng, M.B. Kannan, Advances in functionalized polymer coatings on biodegradable magnesium alloys - A review, Acta Biomater 79 (2018) 23-36.

[33] A.H. Martinez Sanchez, B.J. Luthringer, F. Feyerabend, R. Willumeit, Mg and Mg alloys: how comparable are in vitro and in vivo corrosion rates? A review, Acta Biomater 13 (2015) 16-31.

[34] J.M. Anderson, Future challenges in the in vitro and in vivo evaluation of biomaterial biocompatibility, Regen Biomater 3(2) (2016) 73-7.

[35] R.M. Visalakshan, M.N. MacGregor, S. Sasidharan, A. Ghazaryan, A.M. Mierczynska-Vasilev, S. Morsbach, V. Mailander, K. Landfester, J.D. Hayball, K. Vasilev, Biomaterial Surface Hydrophobicity-Mediated Serum Protein Adsorption and Immune Responses, ACS Appl Mater Interfaces 11(31) (2019) 27615-27623.

[36] T.A. Horbett, Fibrinogen adsorption to biomaterials, Journal of biomedical materials research. Part A 106(10) (2018) 2777-2788.

[37] A.H. Martinez Sanchez, F. Feyerabend, D. Laipple, R. Willumeit-Romer, A. Weinberg, B.J.C. Luthringer, Chondrogenic differentiation of ATDC5-cells under the influence of Mg and Mg alloy degradation, Mater Sci Eng C Mater Biol Appl 72 (2017) 378-388.

[38] F. Cecchinato, N.A. Agha, A.H. Martinez-Sanchez, B.J. Luthringer, F. Feyerabend, R. Jimbo, R. Willumeit-Romer, A. Wennerberg, Influence of Magnesium Alloy Degradation on Undifferentiated Human Cells, PLoS One 10(11) (2015) e0142117.

[39] L. Jin, J. Wu, G. Yuan, T. Chen, In vitro study of the inflammatory cells response to biodegradable Mg-based alloy extract, PLoS One 13(3) (2018) e0193276.

[40] J. Fischer, D. Pröfrock, N. Hort, R. Willumeit, F. Feyerabend, Reprint of: Improved cytotoxicity testing of magnesium materials, Materials Science and Engineering: B 176(20) (2011) 1773-1777.

[41] M. Orecchioni, Y. Ghosheh, A.B. Pramod, K. Ley, Macrophage Polarization: Different Gene Signatures in M1(LPS+) vs. Classically and M2(LPS-) vs. Alternatively Activated Macrophages, Front Immunol 10 (2019) 1084.

[42] B. Li, H. Cao, Y. Zhao, M. Cheng, H. Qin, T. Cheng, Y. Hu, X. Zhang, X. Liu, In vitro and in vivo responses of macrophages to magnesium-doped titanium, Sci Rep 7 (2017) 42707.

[43] X. Li, Q. Huang, L. Liu, W. Zhu, T.A. Elkhooly, Y. Liu, Q. Feng, Q. Li, S. Zhou, Y. Liu, H. Wu, Reduced inflammatory response by incorporating magnesium into porous TiO2 coating on titanium substrate, Colloids Surf B Biointerfaces 171 (2018) 276-284.

[44] J. Sugimoto, A.M. Romani, A.M. Valentin-Torres, A.A. Luciano, C.M. Ramirez Kitchen, N. Funderburg, S. Mesiano, H.B. Bernstein, Magnesium decreases inflammatory cytokine production: a novel innate immunomodulatory mechanism, J Immunol 188(12) (2012) 6338-46.

[45] F. Gao, B. Ding, L. Zhou, X. Gao, H. Guo, H. Xu, Magnesium sulfate provides neuroprotection in lipopolysaccharide-activated primary microglia by inhibiting NF-kappaB pathway, J Surg Res 184(2) (2013) 944-50.

[46] T. Hu, H. Xu, C. Wang, H. Qin, Z. An, Magnesium enhances the chondrogenic differentiation of mesenchymal stem cells by inhibiting activated macrophage-induced inflammation, Sci Rep 8(1) (2018) 3406.

[47] J.Y. Hsieh, T.D. Smith, V.S. Meli, T.N. Tran, E.L. Botvinick, W.F. Liu, Differential regulation of macrophage inflammatory activation by fibrin and fibrinogen, Acta Biomater 47 (2017) 14-24.

[48] D.B. Kuhns, D.A. Priel, J.I. Gallin, Induction of human monocyte interleukin (IL)-8 by fibrinogen through the toll-like receptor pathway, Inflammation 30(5) (2007) 178-88.

[49] F.O. Martinez, S. Gordon, The M1 and M2 paradigm of macrophage activation: time for reassessment, F1000Prime Rep 6 (2014) 13.

[50] J.P. Edwards, X. Zhang, K.A. Frauwirth, D.M. Mosser, Biochemical and functional characterization of three activated macrophage populations, J Leukoc Biol 80(6) (2006) 1298-307.

[51] F.O. Martinez, A. Sica, A. Mantovani, M. Locati, Macrophage activation and polarization, Front Biosci 13 (2008) 453-61.

[52] F. Raggi, S. Pelassa, D. Pierobon, F. Penco, M. Gattorno, F. Novelli, A. Eva, L. Varesio, M. Giovarelli, M.C. Bosco, Regulation of Human Macrophage M1-M2 Polarization Balance by Hypoxia and the Triggering Receptor Expressed on Myeloid Cells-1, Front Immunol 8 (2017) 1097.

[53] A.A. Tarique, J. Logan, E. Thomas, P.G. Holt, P.D. Sly, E. Fantino, Phenotypic, functional, and plasticity features of classical and alternatively activated human macrophages, Am J Respir Cell Mol Biol 53(5) (2015) 676-88.

[54] M. Jaguin, N. Houlbert, O. Fardel, V. Lecureur, Polarization profiles of human M-CSF-generated macrophages and comparison of M1-markers in classically activated macrophages from GM-CSF and M-CSF origin, Cell Immunol 281(1) (2013) 51-61.

[55] W.A. Baseler, L.C. Davies, L. Quigley, L.A. Ridnour, J.M. Weiss, S.P. Hussain, D.A. Wink, D.W. McVicar, Autocrine IL-10 functions as a rheostat for M1 macrophage glycolytic commitment by tuning nitric oxide production, Redox Biol 10 (2016) 12-23.

[56] A. Kelly, S. Gunaltay, C.P. McEntee, E.E. Shuttleworth, C. Smedley, S.A. Houston, T.M. Fenton, S. Levison, E.R. Mann, M.A. Travis, Human monocytes and macrophages regulate immune tolerance via integrin alphavbeta8-mediated TGFbeta activation, J Exp Med 215(11) (2018) 2725-2736.

[57] H. Chi, S.P. Barry, R.J. Roth, J.J. Wu, E.A. Jones, A.M. Bennett, R.A. Flavell, Dynamic regulation of pro- and anti-inflammatory cytokines by MAPK phosphatase 1 (MKP-1) in innate immune responses, Proc Natl Acad Sci U S A 103(7) (2006) 2274-9.

[58] M.G. Dorrington, I.D.C. Fraser, NF-kappaB Signaling in Macrophages: Dynamics, Crosstalk, and Signal Integration, Front Immunol 10 (2019) 705.

[59] S. Giridharan, M. Srinivasan, Mechanisms of NF-kappaB p65 and strategies for therapeutic manipulation, J Inflamm Res 11 (2018) 407-419.

[60] U.J. Lee, S.R. Choung, K.V. Prakash, E.J. Lee, M.Y. Lee, Y.J. Kim, C.W. Han, Y.C. Choi, Dual knockdown of p65 and p50 subunits of NF-kappaB by siRNA inhibits the induction of inflammatory cytokines and significantly enhance apoptosis in human primary synoviocytes treated with tumor necrosis factor-alpha, Mol Biol Rep 35(3) (2008) 291-8.

[61] R. Hass, C. Kasper, S. Bohm, R. Jacobs, Different populations and sources of human mesenchymal stem cells (MSCs): A comparison of adult and neonatal tissue-derived MSCs, Cell Commun Signal 9 (2011) 12.

[62] P. Guihard, Y. Danger, B. Brounais, E. David, R. Brion, J. Delecrin, C.D. Richards, S. Chevalier, F. Redini, D. Heymann, H. Gascan, F. Blanchard, Induction of osteogenesis in mesenchymal stem cells by activated monocytes/macrophages depends on oncostatin M signaling, Stem Cells 30(4) (2012) 762-72.

[63] L.Y. Lu, F. Loi, K. Nathan, T.H. Lin, J. Pajarinen, E. Gibon, A. Nabeshima, L. Cordova, E. Jamsen, Z. Yao, S.B. Goodman, Pro-inflammatory M1 macrophages promote Osteogenesis by mesenchymal stem cells via the COX-2-prostaglandin E2 pathway, J Orthop Res 35(11) (2017) 2378-2385.

[64] Y. Zhang, T. Bose, R.E. Unger, J.A. Jansen, C.J. Kirkpatrick, J. van den Beucken, Macrophage type modulates osteogenic differentiation of adipose tissue MSCs, Cell Tissue Res 369(2) (2017) 273-286.

[65] E. Birmingham, G.L. Niebur, P.E. McHugh, G. Shaw, F.P. Barry, L.M. McNamara, Osteogenic differentiation of mesenchymal stem cells is regulated by osteocyte and osteoblast cells in a simplified bone niche, Eur Cell Mater 23 (2012) 13-27.

[66] C. Vogel, E.M. Marcotte, Insights into the regulation of protein abundance from proteomic and transcriptomic analyses, Nat Rev Genet 13(4) (2012) 227-32.

[67] T. Rescigno, A. Capasso, B. Bisceglia, M.F. Tecce, Short Exposures to an Extremely Low-Frequency Magnetic Field (ELF MF) Enhance Protein but not mRNA Alkaline Phosphatase Expression in Human Osteosarcoma Cells, Open Biochem J 12 (2018) 65-77.

[68] J. Ma, N. Zhao, D. Zhu, Biphasic responses of human vascular smooth muscle cells to magnesium ion, Journal of biomedical materials research. Part A 104(2) (2016) 347-56.

SUPPLEMENTARY MATERIAL

Supplementary Methods

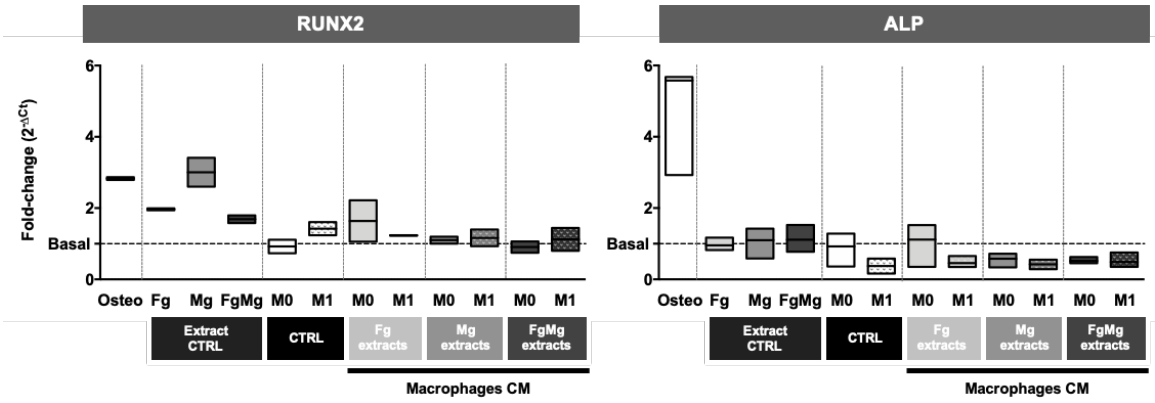
Gene Expression Analysis

MSCs were homogenized at day 7 and total RNA was extracted using TRIzol® Reagent (Invitrogen, Carlsbad, CA, USA), according to the manufacturer's instructions. The amount and quality of extracted total RNA were evaluated by Nanodrop Spectrophotometer ND-1000 (Thermo Fisher Scientific, Wilmington, DE, USA). RNA integrity was evaluated by gel electrophoresis. Samples were then treated with TURBO DNA-free™ kit (Invitrogen, Carlsbad, CA, USA) to remove contaminating DNA from RNA preparations. Complementary DNA (cDNA) was synthetized using random hexamers (Invitrogen, Carlsbad, CA, USA), dNTPs (Bioline Meridian Bioscience, Cincinnati, OH, USA) and Superscript® III Reverse Transcriptase kit (Invitrogen, Carlsbad, CA, USA) according to manufacturer instructions. qPCR reactions were performed using cDNA, primers (ALP_Human, Fw: GACGGACCCGTCACTCTC, Rv: GTGCCCGTGGTCAATTCT; RUNX2_Human, Fw: CCTGAACTCTGCACCAAGTC, Rv: GAGGTGGCAGTGTCATCATC; GAPDH_Human, Fw: CGTCTTCACCACCATGGAGA, Rv:CGGCCATCACGCCACAGTTT and iTaq Universal SYBR Green Supermix (Bio-Rad, Irvine, CA, USA) in a CFX Real-Time PCR Detection System (Bio-Rad, Irvine, CA, USA) with the following conditions: 3 min at 95 °C and 40 cycles of 30 s at 95 °C, 30 s at 58 °C and 30 s at 72 °C. GAPDH was used as a reference gene. Relative gene expression levels were calculated using the quantification cycle (Cq) method, according to MIQE guidelines [1]. Data was analysed using Bio-Rad CFX Manager software and all the reactions were performed in duplicate [2].

Supplementary Figures



Supplementary Fig.1. Macroscopic view of Fibrinogen (Fg) scaffolds, Magnesium (Mg) discs and Fg scaffolds combined with Mg discs (FgMg)



Supplementary Fig.2. *RUNX2* and *ALP* gene expression during osteogenic differentiation of hMSCs stimulated with the secretome from macrophage cultured with Fg, Mg and FgMg extracts in the presence/absence of M1 stimuli. MSCs were incubated for 7 days with biomaterial extracts (extract CTRL= Fg, Mg and FgMg biomaterials extracts) or the secretome of macrophages unstimulated (M0), or LPS-IFNγ stimulated (M1), in presence/absence of biomaterial extracts (CTRL=conditioned media from macrophages not exposed to extracts; Fg, Mg and FgMg extracts=conditioned media from macrophages preconditioned with Fg, Mg and FgMg extracts alone), as indicated. Basal and osteogenic (osteo) media were used as controls. *RUNX2* (A) and *ALP* (B) mRNA levels were measured by Reverse transcription and real-time quantitative polymerase chain reaction (RT-qPCR), and normalized for GAPDH gene expression for each sample. Graphs are box-and-whiskers plots, with median representation. Friedman's test followed by uncorrected Dunn's test were performed for conditioned media measurements (n=2-3).

REFERENCES

[1] S.A. Bustin, V. Benes, J.A. Garson, J. Hellemans, J. Huggett, M. Kubista, R. Mueller, T. Nolan, M.W. Pfaffl, G.L. Shipley, J. Vandesompele, C.T. Wittwer, The MIQE guidelines: minimum information for publication of quantitative real-time PCR experiments, Clin Chem 55(4) (2009) 611-22.

[2] M.I. Almeida, A.M. Silva, D.M. Vasconcelos, C.R. Almeida, H. Caires, M.T. Pinto, G.A. Calin, S.G. Santos, M.A. Barbosa, miR-195 in human primary mesenchymal stromal/stem cells regulates proliferation, osteogenesis and paracrine effect on angiogenesis, Oncotarget 7(1) (2016) 7-22.

CHAPTER III

ORIGINAL RESEARCH WORK

Fibrinogen scaffolds incorporating magnesium ions modulate macrophages towards a M2 phenotype *in vitro* and *in vivo*

(submitted)

Fibrinogen scaffolds incorporating magnesium ions modulate macrophages towards a M2 phenotype *in vitro* and *in vivo*

M Bessa-Gonçalves[a,b], C Ribeiro-Machado[a], M Costa[b], CC Ribeiro[a,c], JN Barbosa[a,b], MA Barbosa[a,b], SG Santos[a*]

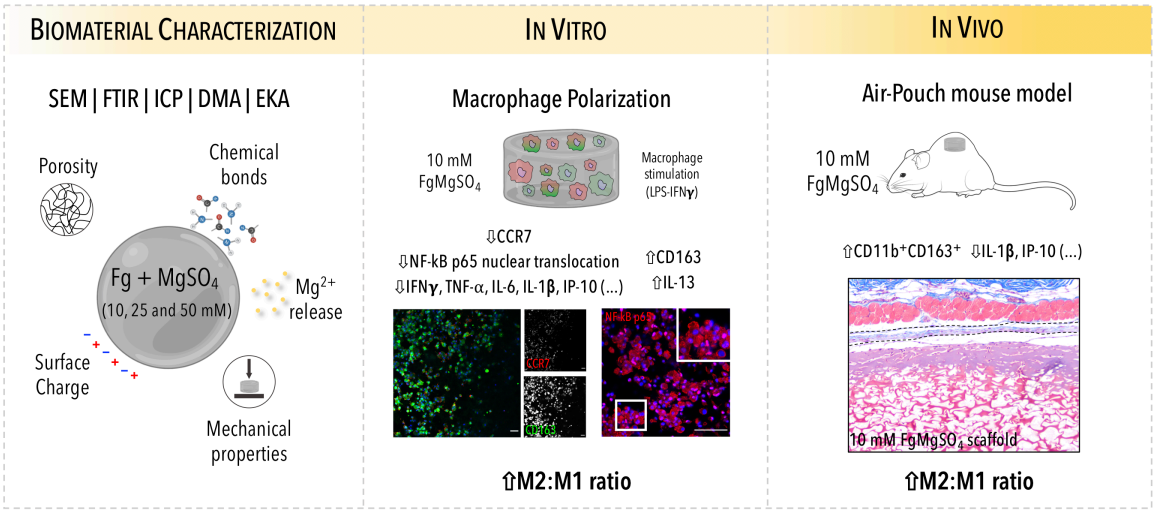
[a]*i3S – Instituto de Investigação e Inovação em Saúde, Universidade do Porto, Rua Alfredo Allen 208, 4200-135 Porto, Portugal; INEB - Instituto de Engenharia Biomédica, Universidade do Porto, Rua Alfredo Allen 208, 4200-135 Porto, Portugal*

[b]*Instituto Ciências Biomédicas Abel Salazar da Universidade do Porto, Rua de Jorge Viterbo Ferreira 228, 4050-313 Porto, Portugal.*

[c]*ISEP – Instituto Superior de Engenharia do Porto, Instituto Politécnico do Porto, Rua Dr. António Bernardino de Almeida 431, 4249-015, Porto, Portugal.*

ABSTRACT

Biomaterials that modulate macrophage activation will impact the inflammatory and regenerative responses. The current work aims to develop a fibrinogen (Fg) and magnesium (Mg) biomaterial combination, to modulate macrophage polarization in naïve and inflammatory conditions. Scaffolds of Fg alone or incorporating precise amounts of $MgSO_4$ (10, 25 and 50 mM) were produced and characterized. All scaffolds presented a 3D network of interconnected pores, but porosity decreased with increasing $MgSO_4$ concentrations. Also, incorporation of $MgSO_4$ increased surface charge and loss and storage modulus of Fg scaffolds, particularly for the 10 mM $FgMgSO_4$ combination. Importantly, only 10 mM $FgMgSO_4$ scaffolds were able to modulate macrophage activation, increasing the percentage of $CD163^+$ M2 cells, and decreasing that of $CCR7^+$ M1 cells. The mechanism involves NF-kB p65 nuclear translocation, which was significantly decreased in macrophages cultured on 10 mM $FgMgSO_4$ scaffolds. Analysis of cytokine/chemokine panel showed that M1 cells on 10 mM $FgMgSO_4$ secreted significantly less pro-inflammatory mediators (IFN**γ**, IL-6, IL-12p40, TNF-α, Groα, IP-10, MIP-1α) than those on Fg scaffolds. Notably, 10 mM $FgMgSO_4$ scaffolds also increased the percentage of $CD11b^+CD163^+$ cells, M2 macrophages, *in vivo*, in inflammatory exudates. A cytokine/chemokine panel showed that both scaffolds decreased pro-inflammatory cytokines, when compared to Sham-operated animals, but only 10 mM $FgMgSO_4$ was able to significantly decrease IL-1β, IP-10, MIP-2, MDC and MIP-3α. Overall, our findings demonstrate that 10 mM $FgMgSO_4$ scaffolds modulate the inflammatory response both *in vitro* and *in vivo,* promoting M2 macrophage polarization.



Keywords: 3D scaffolds, fibrinogen, magnesium, immunomodulation, macrophages

1. INTRODUCTION

Biomaterial implantation triggers an inflammatory reaction, leading often to a foreign body reaction (FBR). Macrophages are among the earliest arrivals to interact with the implanted materials, initiating and mediating the host FBR. These cells have pivotal roles in regulating the resolution of inflammation and promoting tissue repair/regeneration [1, 2]. Although different roles are played by M1 and M2 macrophages, they are equally vital for the success of tissue repair/regeneration [2]. The presence of pro-inflammatory M1 macrophages at early stages of inflammation is required for complete healing. However, their excessive and prolonged activation leads to an exacerbated inflammatory response, that impairs tissue repair/regeneration and can lead to implant failure [3]. In this context, modulating macrophage fate from pro-inflammatory M1 to anti-inflammatory M2 phenotype is an increasingly explored strategy in biomaterial development [3, 4]. Biomaterial-based macrophage modulation approaches include the modification of materials composition, surface properties, surface topography and mechanical properties [5]. For instance, the use of hybrid biomaterials composed of a material that is combined with metallic ions (e.g. magnesium, zinc, strontium) has been explored as an approach to modulate macrophage immune responses, as some bioactive ions have immunoregulatory effects [6-8].

Biodegradable polymers are widely used as scaffolding materials for tissue repair/regeneration [9]. Fibrinogen (Fg) is a protein involved in the healing process, and is clinically applied as fibrin sealant, upon thrombin crosslinking [10]. Fg has been investigated in our group either adsorbed to chitosan (Ch) or as 3D scaffold. Previous work showed that Ch/Fg substrates promote pro-regenerative responses on immune cells: increasing natural killer (NK) cells capacity to recruit mesenchymal stem/stromal cells (MSCs) [11]; interacting with monocytes/macrophages via TLR-4 [12]; and up-regulating the production of osteogenic factors by monocytes/macrophages [13]. Additionally, Ch scaffolds incorporating adsorbed Fg and pure Fg-3D scaffolds modulated local and systemic inflammatory/immune cell response to injury, and improved bone repair [14, 15].

The use of Magnesium (Mg) alloys has been attracting interest due to their best trade-off between biodegradability, biological and mechanical properties, similarity to human bone and natural presence in bone [16]. Recent clinical trials of Mg-based materials for orthopedic applications include: MAGNEZIX®, to treat patients with mild hallux valgus [17]; RESOMET® (K-MET), for the treatment of hand fractures [18]; and pure magnesium, to treat patients with osteonecrosis of the femoral head [19]. However, difficulties still need to be overcome regarding Mg fast corrosion in body fluids [16]. Notwithstanding, the released

metal ions from biodegradable magnesium alloys (Mg^{2+}) have shown to induce beneficial effects in the process of bone healing as they were shown to be immunomodulatory, reducing pro-inflammatory macrophage polarization [20, 21], and osteopromotive, inducing osteogenic differentiation [20, 22]. Magnesium supplementation has already been tested in clinical practice for common health conditions (e.g. osteoporosis, depression, cardiac diseases) [23] and is being tested towards improved tissue engineering strategies [24, 25]. Hence, the incorporation of these natural bioactive ions within scaffolds may constitute a promising approach to promote tissue repair/regeneration [26, 27].

A previous study of our group addressed the combination between Fg and metallic Mg materials. Results revealed that the extracts of these materials were able to reduce macrophage pro-inflammatory phenotype and stimulate their capacity to promote MSCs osteogenic differentiation [20]. In the current work, we took this one step further and developed a new biomaterial combination by incorporating precise amounts of Mg^{2+} ions into Fg-3D porous scaffolds, in order to determine the best Mg concentration for immunomodulation. Fg-3D scaffolds with 0, 10, 25 and 50 mM of magnesium sulphate ($MgSO_4$) ($FgMgSO_4$) were prepared and characterized. Only the 10 mM $FgMgSO_4$ combination was able to significantly change Fg mechanical properties and direct macrophages towards an M2 phenotype. This combination reduced NF-kB p65 nuclear translocation after M1 stimulation and significantly reduced secretion levels of important pro-inflammatory mediators like IFN**γ**, IL-6, IL-12p40, TNF-α, and IP-10, when compared with M1-stimulated macrophages cultured on Fg scaffolds. When implanted *in vivo*, 10 mM $FgMgSO_4$ scaffolds still increased the percentage of M2 ($CD11b^+CD163^+$) macrophages in inflammatory exudates. While both scaffolds decreased pro-inflammatory cytokines when compared to Sham-operated animals, only 10 mM FgMgSO4 was able to significantly decrease important mediators, like IL-1β and IP-10. Taken together, the results presented here show that $MgSO_4$ incorporation in Fg scaffolds at 10 mM concentration improved scaffold performance and ability to modulate macrophage phenotype *in vitro* and *in vivo.*

2. MATERIALS AND METHODS

2.1. Biomaterials formulations: Fg scaffolds alone or combined with $MgSO_4$ ($FgMgSO_4$)

Fg-3D and $MgSO_4$ incorporated-Fg 3D scaffolds (12 mm diameter x 9 mm thickness) were prepared by freeze-drying [20, 28]. Briefly, Fg scaffolds were prepared by diluting, in PBS,

a Fg stock solution at 80 mg/mL (Grifols S.A., Barcelona, Spain) to a final concentration of 60 mg/mL. $FgMgSO_4$ scaffolds were prepared by mixing a Fg stock solution at 80 mg/mL with 200 mM $MgSO_4$ concentrate stock solution, prepared in PBS, to have final concentrations of 60 mg/mL Fg and 10, 25 or 50 mM of $MgSO_4$. Solutions were casted into 48-well plates (800 µL/well), frozen overnight at -20 ºC and freeze-dried for 72 h, at -80 ºC. Resulting scaffolds were cut with appropriate cutters/molds into cylinders and chemically crosslinked o.n. with N-(3-Dimethylaminopropyl)-N′-ethylcarbodiimide hydrochloride (EDC, E1769, Sigma-Aldrich Co., St Louis, MO, USA) at 8.8 mM, prepared in ethanol, as previous [20, 29]. Then, scaffolds were neutralized and disinfected, through impregnation under vacuum in a gradient of ethanol solutions (99%, 70%, 50% and 25%), followed by three washes in sterile PBS. Scaffolds were allowed to incubate at 37 ºC in complete media for 1h, prior to cell seeding, as formerly described [28].

2.2. Fg and $FgMgSO_4$ scaffolds characterization

2.2.1. *Scanning Electron Microscopy (SEM) and energy dispersive spectroscopy (EDS)*

Microstructure/surface morphology of Fg and $FgMgSO_4$ (10, 25 and 50 mM) scaffolds were analysed by SEM/EDS using a high resolution (Schottky) environmental EM with X-ray microanalysis and electron backscattered diffraction analysis (Quanta 400 FEG ESEM / EDAX Genesis X4M). Cross-sections of approximately 1 mm thickness were cut and mounted with carbon tape. Samples were then coated with a gold (Au)/ palladium (Pd) thin film, by sputtering for 80 sec with 15 mA current, to provide conductivity, using the SPI module sputter coater equipment [20]. The acquired images were analysed using an algorithm developed in MATLAB (Mathworks, Natick, MA, USA, version R2017b) to quantify SEM images porosity [30]. EDS coupled to SEM was used for elemental analysis.

2.2.2. *Fourier Transform Infrared Spectroscopy (FTIR)*

The chemical composition of crosslinked Fg and $FgMgSO_4$ (10, 25 and 50 mM) scaffolds was analysed by FTIR. Fg and $FgMgSO_4$ scaffolds were reduced to powder and analysed as KBr pellets using a spectrometer (Spectrum 2000, PerkinElmer, Waltham, MA, USA), as previously described [31]. 32 scans were collected with 4 cm^{-1} resolution. Peak analysis was performed through spectra analysis.

2.2.3. *Inductively Coupled Plasma – Atomic Emission Spectroscopy (ICP-AES)*

Mg^{2+} levels released from $FgMgSO_4$ (10, 25 and 50 mM) scaffolds to cell culture medium were quantified by ICP-AES. The analysis was carried out on a Horiba Jobin Yvon ULTIMA sequential ICP (generator RF of 40.68 MHz, Palaiseau, France), using the Horiba Jobin Yvon ICP Analyst 5.4 software. A monochromator with a Czerny Turner spectrometer was used. The gas used was Argon. For the element Mg, the following wavelength was chosen: 279.553 nm. Scaffolds were maintained for up to 13 days in complete medium (RPMI 1640 media with L-glutamine (Corning, Manassas, VA, USA) supplemented with 10% heat-inactivated FBS (Biowest, Riverside, MO, USA) and 100 U mL^{-1} penicillin and 100 µg mL^{-1} streptomycin (1% P/S, both from Invitrogen, Carlsbad, CA, USA)), at 37 °C under a humidified atmosphere of 5% v/v CO2 in air, in order to simulate the conditions subsequently used for cell culture studies. Fg was used as control to account for Mg^{2+} levels from complete medium. Cell culture medium was renewed at day 7 and 10, to match with the time points from *in vitro* studies with macrophages, and stored at -20 ºC until further analysis. Five samples from each material per time point were analysed. Three determinations were performed for each sample and average results were reported.

2.2.4. *Dynamic Mechanical Analysis (DMA)*

DMA (DMA 8000, PerkinElmer, Waltham, MA, USA) compression mode was used to study the viscoelastic properties of crosslinked Fg and $FgMgSO_4$ (10, 25 and 50 mM) scaffolds (4 mm diameter x 3 mm height). This analysis consists of a parallel-plate measuring system that compresses the samples between the plates. A frequency of oscillation of 1 Hz and displacement amplitude of 1% of the thickness of the samples was used throughout the experiments, as previously described [31].

2.2.5. *Electro Kinetic Analysis (EKA)*

Zeta potential of crosslinked Fg and $FgMgSO_4$ (10, 25 and 50 mM) scaffolds (8 mm diameter x 3 mm height) was determined from streaming potential measurements with a commercial electrokinetic analyzer (EKA, Anton Paar, Graz, Austria) using a special powder cell adapted inside a cylindrical cell, as described in [31]. Samples were mounted inside the powder cell and streaming potential was measured using Ag/AgCl electrodes installed at both ends of the streaming channel – the cylindrical cell. The electrolyte used was 1 mM KCl (Sigma-Aldrich Co., St Louis, MO, USA) and adjusted to physiological pH values (~7,2

– 7,4). Experiments were performed at room temperature (RT). The streaming potential was measured while applying an electrolyte flow in alternating directions and pressure ramps from 0 to 200 mbar. For each scaffold twelve pressure ramps were performed, six in each flow direction, in order to cope with the asymmetric potential fluctuations.

2.3. In vitro studies

2.3.1. *Ethics Statement*

Human primary monocytes were isolated from surplus buffy coats (BC) from healthy blood donors, kindly donated by Serviço de Imunohemoterapia, Centro Hospitalar Universitário de São João (CHUSJ), Porto. Human mesenchymal stem/stromal cells (MSCs) were obtained from healthy human bone marrow from patients undergoing knee ligament surgery, kindly donated by Serviço de Ortopedia, CHUSJ, Porto. All obtained human samples and procedures were performed in agreement with the principles of the Declaration of Helsinki and all experimental protocols were conducted following the approval and recommendations of the CHUSJ Ethics Committee for Health (references 90/19 and 260/11). A written informed consent was obtained from all subjects before sample collection. Buffy coats and bone marrow samples were provided anonymized and patient identification was not provided to researchers.

2.3.2. *Human primary monocyte isolation and macrophage differentiation*

Human monocytes were isolated from peripheral blood of healthy blood donors by negative selection using RosetteSep™ Human Monocyte Enrichment Cocktail (StemCell Technologies, Vancouver, Canada), as previously described [12, 20]. For macrophage differentiation, 0,5 x 10^6 monocytes were resuspended in a 10 µL aliquot of complete medium (RPMI 1640 media with L-glutamine (Corning, Manassas, VA, USA) supplemented with 10% heat-inactivated FBS (Biowest, Riverside, MO, USA) and 100 U mL^{-1} penicillin and 100 µg mL^{-1} streptomycin (1% P/S, both from Invitrogen, Carlsbad, CA, USA)), seeded directly on top of Fg and $FgMgSO_4$ (10, 25 and 50 mM) scaffolds (0,5 x 10^6 monocytes/scaffold) and left to adhere for 3h. Complete medium supplemented with 50 ng/mL of recombinant human macrophage colony-stimulating factor (rh M-CSF, ImmunoTools, Friesoythe, Germany) was then added to immerse the scaffolds with the seeded cells. Cell culture media was replaced after 7 days and M-CSF was removed. At the 10^{th} day media was replaced and monocytes/macrophages were stimulated with 10

ng/mL LPS, Escherichia coli O55:B5 (Sigma-Aldrich Co., St Louis, MO, USA) and 50 ng/mL IFNγ (ImmunoTools, Friesoythe, Germany), for M1 stimulation, for 30 min (NF-kB p65 translocation assay assessment) or for 72h (cell surface marker and cytokine profile assessment). Controls were left unstimulated. Supernatants were collected at the end of the experiment, under sterile conditions and centrifuged at 13,000 rpm, 5 min, 4 ºC (Eppendorf Centrifuge 5810R, VWR International LLC, Radnor, PA, USA), to remove any cellular debris, and stored at -20 ºC until further analysis.

2.3.3. *Resazurin reduction assay and Lactate dehydrogenase (LDH)*

Macrophage metabolic activity was determined through resazurin reduction assay. Briefly, 13 days after macrophage culture on Fg and $FgMgSO_4$ (10, 25 and 50 mM) scaffolds samples were incubated with resazurin redox dye (0.1 mg/mL) (Sigma-Aldrich Co., St Louis, MO, USA) for 2 h, as described in [28]. The multi-mode microplate reader Synergy MX (BioTek, Winnoski, VT, USA) was used to measure fluorescence intensity (530 nm Excitation/590 nm Emission) and data presented in relative fluorescence units (RFU).

Cell death was assessed by the CytoTox96® assay (Promega, Madison, WI, USA), which measures the release of lactate dehydrogenase (LDH) from dying cells [32], following the manufacturer's instructions. The presence of LDH was measured in cell free-supernatants and absorbance (490 nm) recorded in a microplate reader Synergy MX (BioTek, Winnoski, VT, USA). Total LDH release was achieved by using LDH positive Control provided by the CytoTox96® assay. Percent cytotoxicity was defined as the percentage of released LDH compared with maximal LDH activity from LDH positive Control.

2.3.4. *Macrophage polarization evaluation by immunofluorescence staining*

Macrophages cultured on Fg and $FgMgSO_4$ (10, 25 and 50 mM) scaffolds in the presence/absence of M1 stimulation were collected at day 13, fixed for 15 min with 4% paraformaldehyde (PFA) at RT, and then washed three times with PBS. Immunofluorescent staining for CCR7 and CD163 cell surface markers was performed following protocols adapted from [33]. Briefly, for cell membrane permeabilization, scaffolds were incubated for 20 min with 0.2% Triton X-100 (Sigma-Aldrich Co., St Louis, MO, USA) in PBS. Nonspecific binding was blocked with 1% bovine serum albumin (BSA, Sigma-Aldrich Co., St Louis, MO, USA) in PBS. Then, samples were sequentially incubated in the following solutions: (1) primary antibody rabbit anti-human CCR7 (1:100, ab32527, Abcam, Cambridge, UK),

overnight (o.n) at 4 ºC; (2) fluorescent-conjugated secondary antibody Alexa fluor 647 goat anti-rabbit (1:300, A-21245, ThermoFisher Scientific, Waltham, MA, USA), for 1h at RT; (3) blocking with 1% BSA (Sigma-Aldrich Co., St Louis, MO, USA) in PBS, for 1h at RT; (4) primary antibody mouse anti-human CD163 (1:100, MCA1853T, Bio-Rad, CA, USA), o.n at 4 ºC; (5) fluorescent-conjugated secondary antibody Alexa fluor 488 goat anti-mouse (1:300, A-11017, ThermoFisher Scientific, Waltham, MA, USA), for 1h at RT. Three rinses for 5 minutes in PBS were performed between antibodies solutions. Samples were mounted on µ-Dish 35 mm (Ibidi, Gräfelfing, Germany), with Fluoroshield with DAPI (F6057, Sigma-Aldrich Co., St Louis, MO, USA) and observed with confocal microscopy (TCS, SP5, Leica Microsystems, Wetzlar, Germany). The amount of $CCR7^+$ and $CD163^+$ cells in Fg and $FgMgSO_4$ (10, 25 and 50 mM) scaffolds was quantified using ImageJ software (U.S. National Institutes of Health, MD, USA), counting immune-positive cells on a minimum of 5 fields at 20x magnification per scaffold. Macrophage M2:M1 polarization ratio quantification was obtained dividing the number of $CD163^+$ positive cells by the number of $CCR7^+$ positive cells.

2.3.5. *Macrophage NF-kB p65 translocation evaluation by immunofluorescence staining*

Macrophages were cultured on Fg and $FgMgSO_4$ (10, 25 and 50 mM) scaffolds in the presence/absence of M1 stimulation, for 30 min. Immunofluorescent staining for NF-kB p65 was performed following steps abovementioned, using rabbit anti-human NF-kB p65 (dilution 1:400; #8242, Cell Signalling Technology, MA, USA) and fluorescent-conjugated secondary antibody Alexa fluor 647 goat anti-rabbit (1:300, A-21245, ThermoFisher Scientific, Waltham, MA, USA). Three rinses for 5 minutes in PBS were performed between antibodies solutions. Samples were mounted on µ-Dish 35 mm (Ibidi, Gräfelfing, Germany), with Fluoroshield with DAPI (F6057, Sigma-Aldrich Co., St Louis, MO, USA) and observed with confocal microscopy (TCS, SP5, Leica Microsystems, Wetzlar, Germany). The number of NF-kB p65 cells positive for nuclear and cytoplasmatic signal, in Fg and 10 mM $FgMgSO_4$ scaffolds, was quantified using ImageJ software (U.S. National Institutes of Health, MD, USA), on a minimum of 5 fields at 20x magnification per scaffold. NF-kB p65 nuclear:cytoplasm ratio was obtained dividing the number of NF-kB p65 cells positive for nuclear signal by the number of NF-kB p65 cells positive for cytoplasmatic signal.

2.3.6. *Macrophage cytokine quantification*

Cytokines present in conditioned media from macrophages cultured, for 13 days, in Fg and $FgMgSO_4$ (10, 25 and 50 mM scaffolds) (in the presence/absence of M1 stimulation) were quantified at Eve Technologies Corp. (Calgary, AB, Canada) using the Human Cytokine Array/Chemokine Array 48-Plex: soluble CD40 ligand (sCD40L), epidermal growth factor (EGF), Eotaxin/CCL11, fibroblast growth factor 2 (FGF-2), FMS-related tyrosine kinase 3 ligand (Flt-3 ligand), Fractalkine/CX3CL1, granulocyte colony-stimulating factor (G-CSF), granulocyte-macrophage colony-stimulating factor (GM-CSF), growth-regulated on alpha protein (GRO-α/CXCL1), interferon alpha-2 (IFNα2), interferon gamma (IFN**γ**), interleukin (IL)-1α, IL-1β, IL-1ra, IL-2, IL-3, IL-4, IL-5, IL-6, IL-7, IL-8, IL-9, IL-10, IL-12 (p40), IL-12 (p70), IL-13, IL-15, IL-17A, IL-17E/IL-25, IL-17F, IL-18, IL-22, IL-27, interferon induced protein 10 (IP-10/CXCL10), monocyte chemoattractant protein (MCP)-1/CCL2, MCP-3/CCL7, macrophage colony-stimulating factor (M-CSF), macrophage-derived chemokine (MDC/CCL22), monokine induced by interferon gamma (MIG/CXCL9), macrophage inflammatory protein -1 alpha (MIP-1α/CCL3), macrophage inflammatory protein -1 beta (MIP-1β/CCL4), platelet derived growth factor (PDGF)-AA, PDGF-AB/BB, regulated upon activation, normal T cell expressed, and decreted (RANTES/CCL5), transforming growth factor alpha (TGFα), tumor necrosis factor (TNF)α, TNFβ and vascular endothelial growth factor A (VEGF-A).

The sensitivity of the assay for the analysed markers ranged from 0.14 to 50.78 pg/mL.

2.4. In vivo studies

2.4.1. *Mouse air-pouch model*

The air-pouch model of inflammation was established as described in [8, 34]. All animal experiments, using male BALB/c mice with 7-8 weeks (Charles River Laboratories, Barcelona, Spain), were conducted following protocols approved by the Ethics Committee of the Portuguese Official Authority on Animal Welfare and Experimentation (DGAV). Briefly, sterile air (5 mL) was subcutaneously injected in the dorsal area of the mice, for air-pouch formation. A second injection of sterile air (3 mL) was performed 5 days later, to reinforce the air-pouch. After 24h, Fg and 10 mM $FgMgSO_4$ scaffolds (8 mm diameter x 3 mm height) were implanted inside the air pouch. Animals were randomly divided into three groups: Sham-operated animals, animals implanted with Fg scaffolds and animals

implanted with 10 mM $FgMgSO_4$ scaffolds. 6 animals were used for each experimental group.

2.4.2. *Inflammatory exudates collection, explants recovery and organs retrieval*

Three days after implantation, exudates were harvested from the mice air-pouches by washing the air-pouch cavity with PBS, as previously described [34]. Mice were euthanized by anaesthetic overdose with isoflurane followed by application of cervical displacement as a confirmatory method. Explants and adjacent tissues were recovered immediately after the recovery of the inflammatory exudates. The sutures were cut, wound edged separated and scaffolds together with skin were carefully removed from the air-pouch cavity. Spleen, lymph nodes and kidneys were also retrieved.

2.4.3. Fluorescence-activated cell sorting (FACS)

The exudates were filtered through 100 µm nylon mesh (Fisher Scientific, Hampton, NH, USA) to remove cell clumps and centrifuged at 300 g for 5 min at 4 ºC. Supernatants were collected and stored at -20 ºC until further cytokine analysis and cell pellets resuspended in FACS buffer (PBS, 2% FBS, 0.01% sodium azide (Sigma-Aldrich Co., St Louis, MO, USA). Single-cell suspensions were pre-incubated with Fc-receptor-blocking antibody anti-mouse CD16 (clone 93, Biolegend, San Diego, CA, USA) for 5 min at 4 ºC. The following antibodies were used: PE anti-mouse Ly-6G/Ly-6C (Gr-1) (3:50 µl, clone RB6-8C5, Biolegend, San Diego, CA, USA), APC anti-mouse CD11c (5:50 µl, clone HL3, BD Pharmigen, San Jose, CA, USA), PE Cyanine7 (Cy7) anti-mouse/human CD11b (2:50 µl, clone M1/70, Biolegend, San Diego, CA, USA), Alexa Fluor 488 anti-mouse CD197 (CCR7) (2:50 µl, clone 4B12; Biolegend, San Diego, CA, USA) and Brilliant Violet 421 anti-mouse CD163 (2:50 µl, clone S15049I, Biolegend, San Diego, CA, USA). Fluorescence Minus One (FMO) Controls (PE, APC, PE*Cy7, Alexa Fluor 488 and Brilliant Violet 421 FMO control) were used for gating analyses to distinguish positively from negatively staining cell populations. Compensation was performed using single colour controls prepared from BD Comp Beads (BD Biosciences, San Jose, CA, USA) for cell surface staining. Fluorescence was measured using BD FACSCanto II™ flow cytometer (Becton Dickinson) using FACSDiva™ software (both from BD Biosciences, San Jose, CA, USA) and 10,000 events, gated according to forward and side scatter parameters, were collected for each sample. Data were analysed using FlowJo software (BD Biosciences, San Jose, CA, USA, version 10)

2.4.4. *Cytokine production*

Cytokines present in supernatants recovered from inflammatory exudates were quantified at Eve Technologies Corp. (Calgary, AB, Canada) using the using the Mouse Cytokine Array/Chemokine Array 44-Plex: Eotaxin/CCL11, Erythropoietin, 6Ckine/CCL21, Fractalkine/CX3CL1, G-CSF, GM-CSF, interferon beta 1 (IFNB1), IFN**γ**, IL-1α, IL-1β, IL-2, IL-3, IL-4, IL-5, IL-6, IL-7, IL-9, IL-10, IL-11, IL-12 (p40), IL-12 (p70), IL-13, IL-15, IL-16, IL-17, IL-20, IP-10, keratinocyte chemoattractant (KC), leukemia inhibitor factor (LIF), lipopolysaccharide-induced CXC chemokine (LIX/CXCL5), MCP-1/CCL2, MCP-5/CCL12, M-CSF, MDC/CCL22, MIG/CXCL9, MIP-1α/CCL3, MIP-1β/CCL4, MIP-2/CXCL2, MIP-3α/CCL20, MIP-3B/CCL19, RANTES, thymus- and activation-regulated chemokine (TARC/CCL17), tissue inhibitor of metalloproteinase (TIMP)-1, TNFα, and VEGF.

The sensitivity of the assay for the analysed markers ranged from 0.1 to 33.3 pg/mL.

2.4.5. *Histological analysis*

Implanted materials and adjacent skin, spleen, lymph nodes and kidneys were retrieved 72h after biomaterial implantation for histological evaluation. Samples were fixed in 10% neutral buffered formalin (Bio-Optica) and processed for paraffin embedding. Sections of 3 µm were stained for Hematoxylin and Eosin (HE) and Masson's Trichrome (MT, Sigma Aldrich), following protocols previously described in [8]. All tissues were stained for HE, while only implanted materials/adjacent skin was stained for MT. Briefly, for HE sections were stained with Hematoxylin for 3 min, washed and stained with Eosin Y for 1 min. For MT, HT15 – Trichrome Stain (Masson) kit (Sigma) manufacter's instructions were followed. The stained sections were visualized using light microscopy (Zeiss, Axiovert 200M). MT MosaicX sections were used for capsule thickness quantification using Image J software, where a total of 20 measurements were considered.

2.5. Statistical analysis

Statistical analysis was performed using GraphPad Prism software (San Diego, CA, USA, version 9). Data were tested for normality using Shapiro-Wilk normality test. To compare data from multiple groups Kruskal-Wallis tests followed by Dunn's multiple comparisons test were performed for non-parametric data, while ANOVA followed by Sidak's multiple comparisons test were used for parametric data. Error bars on box-and-whiskers plots

indicate the minimum and maximum values obtained in the analysis. Data are represented as arithmetic mean ± standard deviation (SD) from at least three independent experiments. Statistical significance was considered for *p<0.05; **p<0.01; ***p<0.001; ****p<0.0001.

3. RESULTS

3.1. $MgSO_4$ is incorporated into the structure of Fg, increasing its mechanical properties and zeta potential

3D scaffolds of Fg with 0, 10, 25 and 50 mM of $MgSO_4$ were produced by freeze-drying methodologies [20, 28]. To assess the effect of $MgSO_4$ supplementation on Fg-3D architecture SEM analysis was performed. Results showed that the 3D network of interconnected pores that characterizes Fg scaffolds was maintained upon incorporation of increased concentrations of $MgSO_4$ (Fig. 1A). Scaffolds porosity was between 33% and 69% and no significant differences in porosity were induced by the presence of EDC crosslinking agent. However, 50 mM $FgMgSO_4$ exhibited significantly decreased porosity when compared to scaffolds of Fg alone and with10 and 25 mM $FgMgSO_4$, in the presence or absence of EDC (Fig. 1B). As expected, EDS analysis showed the presence of detectable amounts of Mg in all $MgSO_4$-incorporated Fg scaffolds (Fig. 1C). Overall, these results indicated that albeit $MgSO_4$ incorporation allowed for the maintenance of Fg-3D porous interconnected structure, 50 mM concentration reduced porosity.

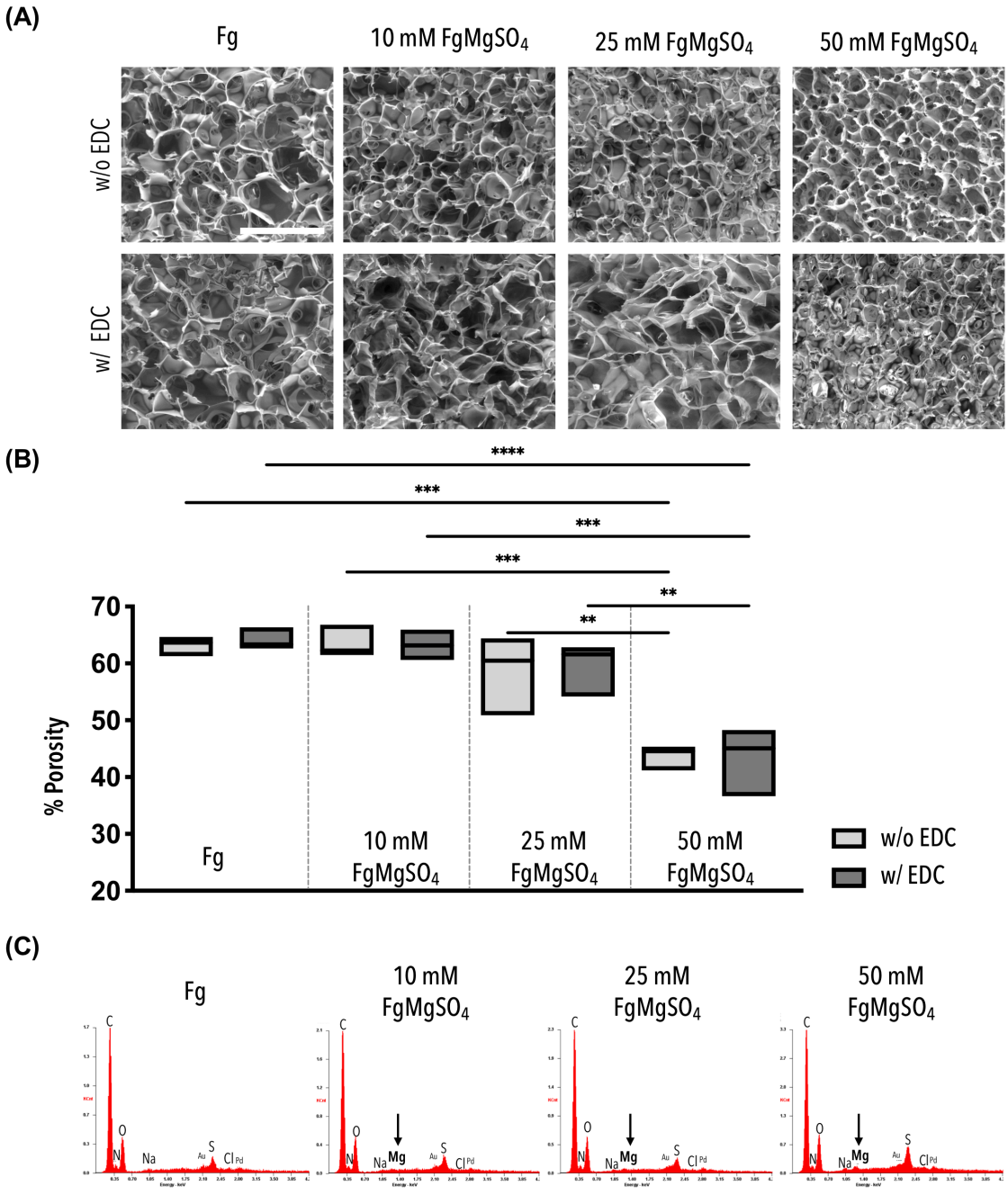


Fig. 1. Morphology of Fg alone or combined with increasing concentrations of $MgSO_4$. (A) Evaluation of the porous structure by SEM analysis and quantification of the percentage of porosity of non-crosslinked (w/o EDC) and crosslinked (w/EDC) Fg and $FgMgSO_4$ (10, 25 and 50 mM) 3D scaffolds. Magnification: 500x. Scale bar: 200 µm. **(C)** surface elemental composition of Fg and $FgMgSO_4$ (10, 25 and 50 mM) scaffolds (C: carbon, N: nitrogen, O: oxygen, Mg: magnesium, S: sulfur, Na: sodium, Cl: chloride, Au: gold, Pd: palladium). Graphs are minimum to maximum floating-bars, with median representation (n=3). **p<0.01, ***p<0.001, ****p<0.0001 using one-way ANOVA followed by Sidak's multiple comparisons test.

To further explore the effects of $MgSO_4$ incorporation on Fg, FTIR analysis was performed. Fg characteristic vibration modes from amines at 3371-3419 cm^{-1} and 2954-2965 cm^{-1} (N-H stretching) and amides at 1639-1654 cm^{-1} (C=O stretching) were detected [15, 35, 36].

The peak at 1385 cm^{-1} (C-H bending) was sharpened in $MgSO_4$-incorporated Fg scaffolds which could be attributed to sulphate binding (S=O stretching). Finally, the peaks at 1135-1138 cm^{-1} and 620-623 cm^{-1}, sharpened (increased relative intensity) in $MgSO_4$-incorporated Fg scaffolds, also indicate specific sulphate binding sites, in agreement with reported values [37] (Fig. 2A). The release profile of Mg^{2+} was then assessed by ICP-AES. Mg^{2+} levels measured in Fg scaffolds were used as negative control and subtracted to the ones measured in $FgMgSO_4$ 10, 25 and 50 mM scaffolds. Release results showed that 10 mM $FgMgSO_4$ have a linear increase in Mg^{2+} release along time, while 25 and 50 mM $FgMgSO_4$ have significantly higher Mg^{2+} amounts release, and that appear to have reached a plateau by day 13 (Fig. 2B).

The scaffolds mechanical properties were evaluated by DMA analysis, and results are shown in Fig. 2C. A significant increase of both storage and loss modulus was observed for 10 mM $FgMgSO_4$ scaffolds, in comparison to Fg alone, and to 25 mM $FgMgSO_4$. The storage modulus of 10 mM $FgMgSO_4$ scaffolds was also significantly higher than that of their 50 mM counterpart. Finally, electrokinetic analysis showed a statistically significant increase in the zeta potential at physiological pH in all $FgMgSO_4$ scaffolds, in comparison to Fg alone (Fig. 2D).

Taken together these results showed that $MgSO_4$ was successfully incorporated into the Fg chemical structure, increasing the zeta potential of the scaffolds. For 10 mM $FgMgSO_4$, scaffolds maintained Fg porosity levels, but significantly increased scaffolds mechanical properties, showing low and linear cumulative Mg release along the 13 days.

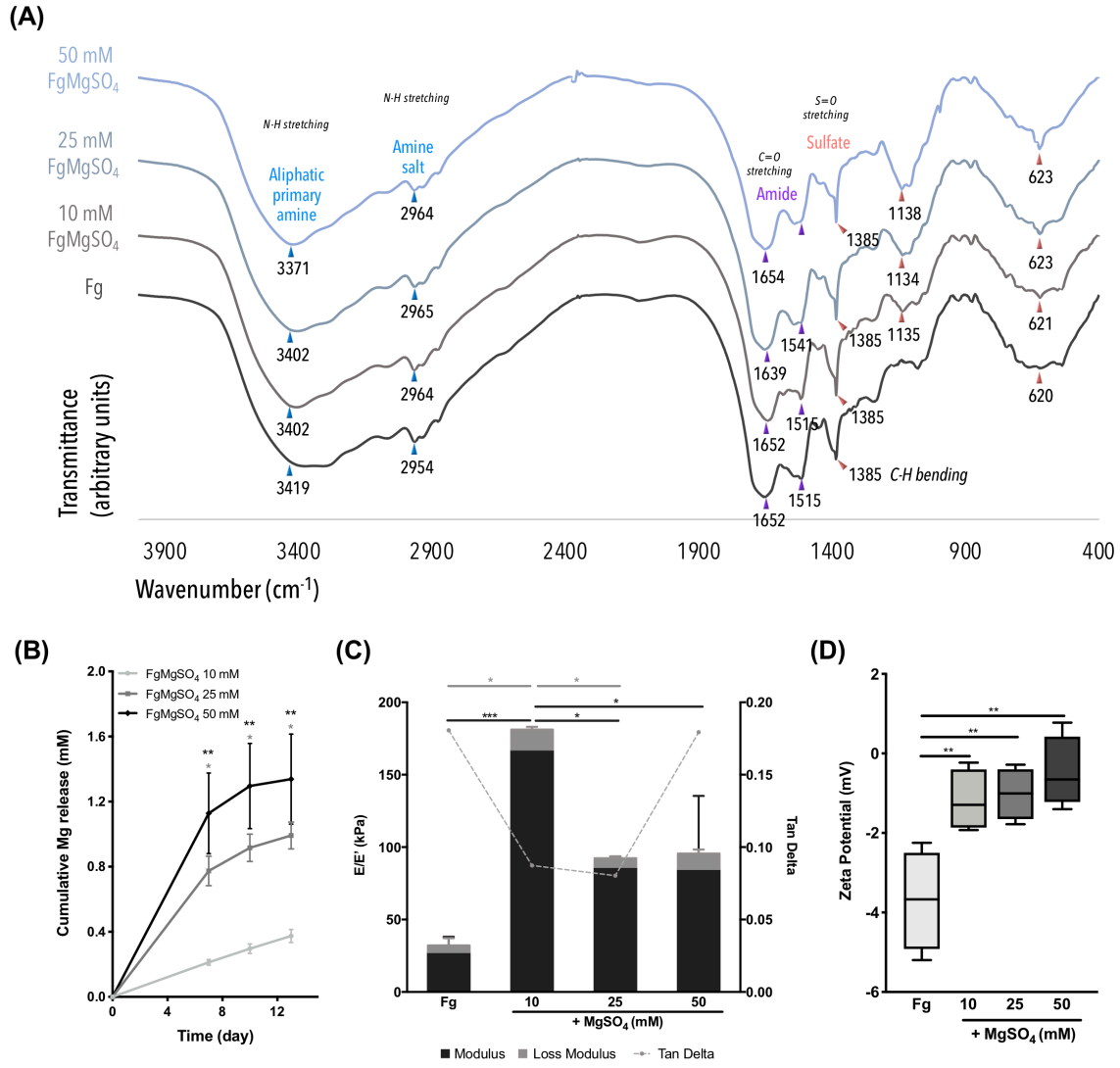


Fig. 2. Characterization of 3D Fg and $FgMgSO_4$ scaffolds. (A) FTIR spectra of crosslinked Fg and $FgMgSO_4$ (10, 25 and 50 mM) scaffolds with the most relevant peaks identified. **(B)** Cumulative Mg^{2+} release from $FgMgSO_4$ (10, 25 and 50 mM) scaffolds along 13 days, mimicking cell culture conditions. Statistical significance in relation to 10 mM $FgMgSO_4$ scaffolds **(C)** Mean values of storage (E′), loss modulus (E″), and tan delta δ for crosslinked Fg and $FgMgSO_4$ (10, 25 and 50 mM) scaffolds, obtained by DMA. Data are mean ± SD (n=3). **(D)** Zeta potential of crosslinked Fg and $FgMgSO_4$ (10 mM, 25 mM and 50 mM) scaffolds determined using EKA (n=4). Graphs are minimum to maximum box-and-whiskers plots, with median representation. *p<0.05, **p<0.01, ***p<0.001 using one-way ANOVA followed by Sidak's multiple comparisons test.

3.2. 10 mM $FgMgSO_4$ scaffolds promote M2 macrophage polarization without cytotoxicity

Mg^{2+} is a major element in the human body, however high concentrations negatively impact cellular responses. In particular, macrophages are sensitive to ionic concentration and/or particles released from biomaterials [38] (Fig.3A). First, we investigated whether macrophage viability would be affected by $MgSO_4$ increasing concentrations. For that, macrophage metabolic activity was assessed by resazurin reduction assay. Results

showed a tendency for reduced metabolic activity for cells cultured on scaffolds with 50 mM $MgSO_4$, but no significant differences were observed between the groups (Fig. 3B). To further understand if increased $MgSO_4$ caused toxicity on macrophages, LDH cytotoxicity assay was performed. Macrophages cultured on 25 and 50 mM $FgMgSO_4$ scaffolds showed significant increases on LDH release, either in unstimulated conditions and under M1 pro-inflammatory stimulation, and when compared to 10 mM $FgMgSO_4$ scaffolds (Fig. 3C).

To explore macrophage polarization and the potential of the FgMg combinations with increasing $MgSO_4$ to modulate this process, CCR7 and CD163, were evaluated as M1 and M2 phenotypic markers, respectively. Results are illustrated in Fig. 3D, and show that 10 mM $FgMgSO_4$ scaffolds significantly increased the number of cells positive for CD163 and decreased CCR7 positive ones, either in unstimulated (M0) conditions and in response to M1 stimulation. Conversely, Fg alone, 25 and 50 mM $FgMgSO_4$ scaffolds showed a predominance of cells positive for CCR7 both in M0 and M1 conditions (Fig. 3D). When the numbers of cells expressing CCR7 and CD163 were quantified across different donors results showed that M2:M1 ratio was significantly increased by 10 mM $FgMgSO_4$ scaffolds either in M0 and M1 conditions, when compared with Fg alone, and 25 and 50 mM $FgMgSO_4$ scaffolds (Fig. 3E).

Together, these results demonstrated that the 10 mM $FgMgSO_4$ scaffolds significantly induced M2 polarization and reduced M1 macrophage polarization. Thus, these scaffolds were selected for the following experiments.

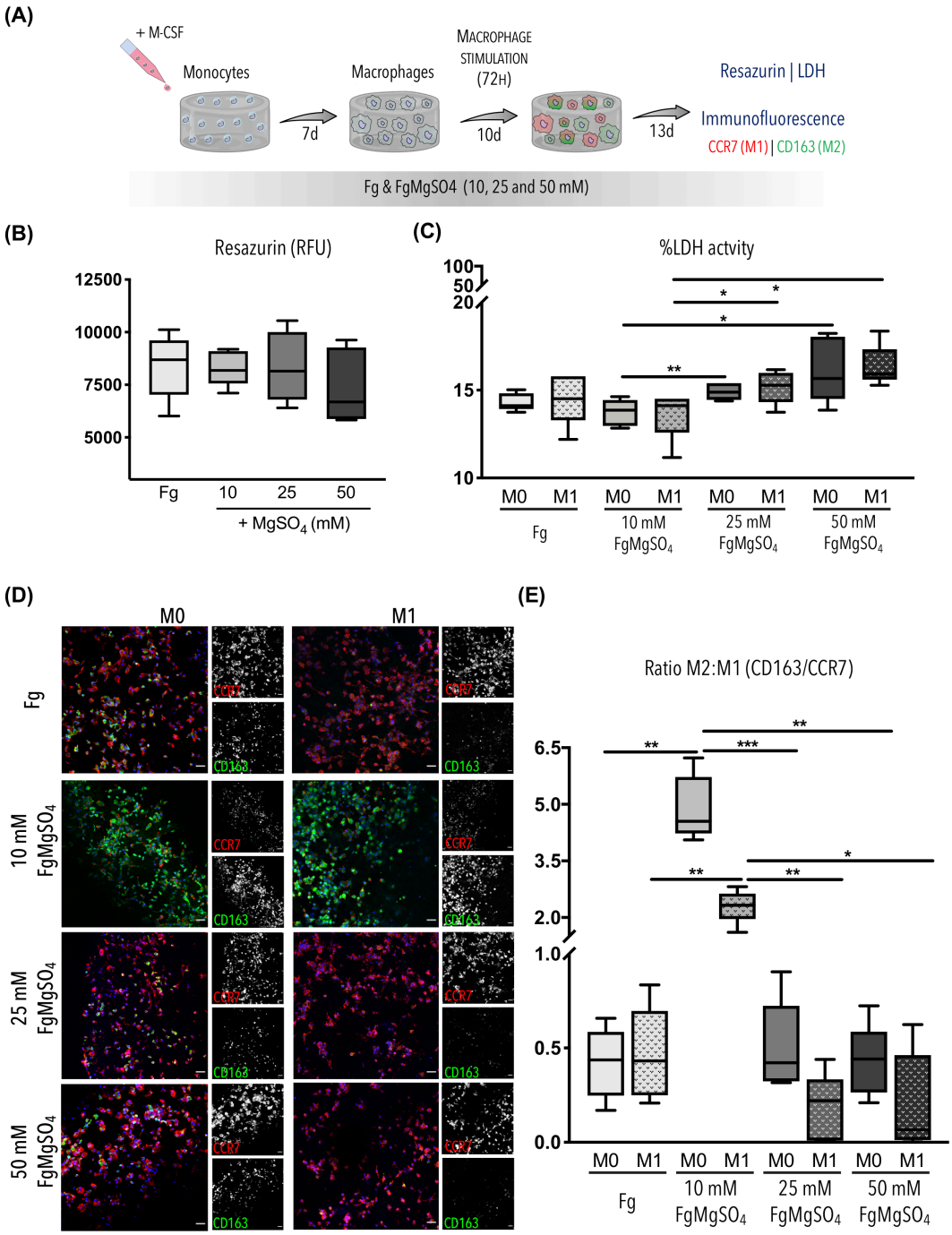


Fig. 3. Effect of Fg and $FgMgSO_4$ scaffolds on macrophages metabolic activity, LDH and M1 versus M2 polarization. (A) Schematic representation of the experimental approach. **(B)** Metabolic activity of macrophages cultured in Fg and $FgMgSO_4$ (10, 25 and 50 mM) scaffolds (n=5). Results are presented as relative fluorescence units (RFU). **(C)** Percentage of LDH activity, normalized to LDH positive control, in conditioned media from human macrophages cultured in Fg and $FgMgSO_4$ (10, 25 and 50 mM) scaffolds with or without M1 stimulation (LPS-IFNγ) (n=5). **(D)** Representative images of immunostaining for CCR7 (M1, in red) and CD163 (M2, in green) markers in human macrophages cultured on Fg and $FgMgSO_4$ (10, 25 and 50 mM) scaffolds, with or without M1 stimulation for 72h, analysed by confocal microscopy. Scale bar: 100 μm. **(E)** Quantification across different donors of the M2:M1 ratio (CD163/CCR7), calculated from the number of macrophages expressing each marker, after culture on Fg and $FgMgSO_4$ (10, 25 and 50 mM) scaffolds (n=5 independent donors). Graphs are minimum to maximum box-and-whiskers plots, with median representation. *p<0.05, **p<0.01, ***p<0.001 using one-way ANOVA followed by Sidak's multiple comparisons test.

3.3. 10 mM $FgMgSO_4$ scaffolds reduce NF-kB p65 nuclear translocation and pro-inflammatory cytokine secretion

We subsequently set out to explore the underlying mechanism of macrophage phenotype modulation by 10 mM $FgMgSO_4$ scaffolds. For that purpose, the activation of nuclear factor-kB (NF-kB) p65, known to be a critical signal transduction pathway related to M1 polarization [39] was probed. NF-kB p65 activation leads to its nuclear translocation, while in resting conditions this transcription factor is found sequestered by a protein complex, in the cytoplasm [39]. Briefly, macrophages cultured in Fg and 10 mM $FgMgSO_4$ scaffolds, were stimulated with LPS-IFN**γ** for 30 min and immunofluorescent staining for NF-kB p65 was performed (Fig. 4A). As expected, M1 stimulation significantly promoted the nuclear translocation of NF-kB p65, as seen by the pink nuclear staining of combined DAPI (blue) and NF-kB p65 (red), when compared with unstimulated M0 conditions (Fig. 4B). Cells with NF-kB p65 in the nucleus and in the cytoplasm were counted across different conditions and different donors and a ratio of nuclear:cytoplasmatic NF-kB p65 was calculated (Fig. 4C). As expected, M1 stimulation increased the nuclear:cytoplasmatic NF-kB p65 ratio for cells cultured on both scaffolds. However, M1 cells cultured on 10 mM $FgMgSO_4$ scaffolds showed a significantly decreased nuclear:cytoplasmatic NF-kB p65 ratio, when compared with those on Fg scaffolds (Fig. 4C). These results suggest a partial inhibition of the NF-kB pathway, which is involved in pro-inflammatory cytokine secretion.

Thus, next the cytokine/chemokine profile of macrophages cultured on Fg or 10 mM $FgMgSO_4$ scaffolds, left unstimulated, M0, or stimulated, M1, for 72h was evaluated. As the material being developed here is new, a broad array including cytokines, chemokines and growth factors was selected.

The factors that showed statistically significant differences between groups are depicted in Fig. 5, and the remaining ones are presented in Supplementary Fig. 1. As expected, secretion levels of several pro-inflammatory mediators (FLT-3L, G-CSF, IFN**γ**, IL-6, IL-12p40, IL-15, IL-17F, IL-27, TGF-α, TNF-α, TNF-β, Groα, IP-10, MCP-3, MIG/CXCL9, MIP-1α, MIP-1β, RANTES and VEGF) were up-regulated in M1-stimulated macrophages cultured either in Fg and 10 mM $FgMgSO_4$ scaffolds, comparing to their M0 counterparts.

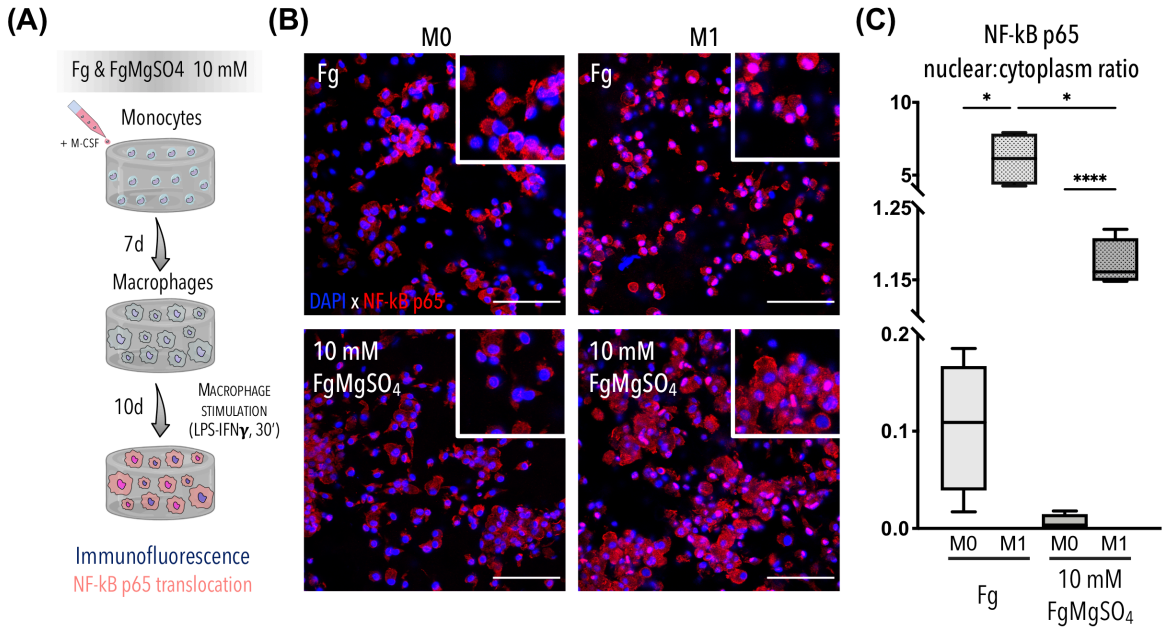


Fig. 4. NF-kB p65 nuclear translocation in macrophages cultured on Fg and 10 mM $FgMgSO_4$ scaffolds. **(A)** Schematic representation of experimental approach used for NF-kB p65 nuclear translocation assessment. **(B)** Representative images of macrophages cultured on Fg or 10 mM $FgMgSO_4$ scaffolds, in unstimulated M0 conditions, or after 30 minutes of M1 stimulation (LPS-IFN**γ**). Cells were stained for nuclei (DAPI, in blue) and NF-kB p65 (in red) and analysed by confocal microscopy. Nuclear translocation of NF-kB is detectable as pink staining, resulting of combined DAPI, blue, and NF-kB, red signals. Scale bar: 100 μm. Insert shows further detail of nuclear staining **(C)** Quantification of images as those illustrated in (B) for different donors, counting the number of macrophages cultured on Fg and 10 mM $FgMgSO_4$ scaffolds, with nuclear or cytoplasmic NF-kB p65 staining, expressed as nuclear:cytoplasm NF-kB p65 ratio (n=4). Graphs are minimum to maximum box-and-whiskers plots, with median representation. *p<0.05, ****p<0.0001 using one-way ANOVA followed by Sidak's multiple comparisons test.

Importantly, 10 mM $FgMgSO_4$ scaffolds significantly reduced secretion levels of IFN**γ**, IL-6, IL-12p40, TNF-α, Groα, IP-10 and MIP-1α, when compared with M1-stimulated macrophages cultured on Fg scaffolds. Also, Eotaxin, FGF-2, GM-CSF, IL-1α, IL-1β, IL-8, IL-9, IL12p70, IL-17A and IL-17E/IL-25 secretion levels were significantly up-regulated in M1-stimulated macrophages cultured on Fg, but their increase was not statistically significant between M0 and M1 conditions on 10 mM $FgMgSO_4$ scaffolds. Some anti-inflammatory mediators were also increased in M1 conditions, both on Fg and on 10 mM $FgMgSO_4$ scaffolds, including IL-4, IL-10 and IL-22, whereas IL-13 secretion levels were only increased in M1-stimulated macrophages cultured on 10 mM $FgMgSO_4$. Overall, 10 mM $FgMgSO_4$ led to an impaired secretion of pro-inflammatory mediators, in response to M1 stimulation, and increased secretion of anti-inflammatory ones.

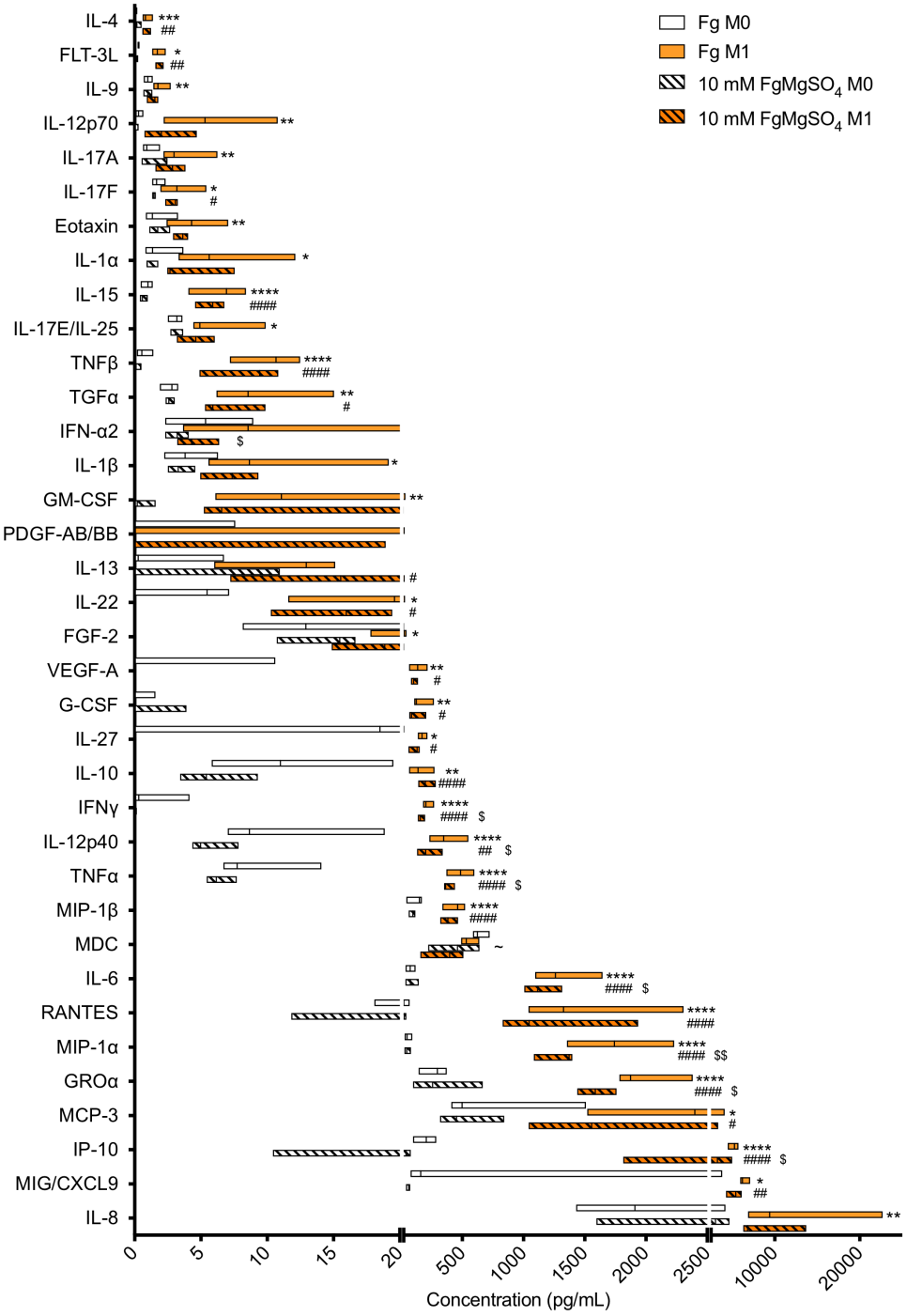


Fig. 5. Cytokine secretion by human macrophages cultured Fg and 10 mM $FgMgSO_4$ scaffolds in the presence/absence of M1 stimulation. Cytokine levels in supernatants of macrophage cultured on Fg (plain bars) or 10 mM $FgMgSO_4$ (patterned bars) scaffolds and left unstimulated (white) or M1 stimulated (orange) for 72h. Box-plots represent min-to-max distribution (n=5). Kruskal-Wallis test followed by corrected Dunn's multiple comparisons were performed for FLT-3L, IL-1α, IL-17E/IL-25, TGF-α, PDGF-AB/BB, IL-13, IL-22, VEGF-A, G-CSF, IL-27, IFN-γ, MCP-3, MIG/CXCL9 and IL-8. One-way ANOVA followed by Sidak's multiple comparisons test were performed for IL-4, IL-9, IL-12p70, IL-17A, IL-17F, eotaxin, IL-15, TNF- β, INF-α2, IL-1β, GM-CSF, FGF-2, IL-10, IL-12p40, TNF-α, MIP-1β, MDC, IL-6, RANTES, MIP-1α, Gro-α and IP10. Statistical significance is indicated as follows: *p<0.05, **p<0.01, ***p<0.001 and ****p<0.0001 for Fg M0 versus Fg M1; $^{\#}$p<0.05, $^{\#\#}$p<0.01 and $^{\#\#\#\#}$p<0.0001 for 10 mM for $FgMgSO_4$ M0 versus 10 mM $FgMgSO_4$ M1; $^{\$}$p<0.05 and $^{\$\$}$p<0.01 for Fg M1 versus 10 mM $FgMgSO_4$ M1; ~p<0.05 for Fg M0 versus 10 mM $FgMgSO_4$ M0.

3.4. 10 mM $FgMgSO_4$ scaffolds promote M2 macrophage polarization in vivo

Finally, we wanted to ascertain if 10 mM $FgMgSO_4$ scaffolds could modulate inflammation and macrophage polarization in vivo. The subcutaneous air pouch in vivo model of inflammation was used to evaluate the inflammatory response to the developed biomaterials (Fig. 6A). Three different animal groups were performed: Sham-operated, Fg and 10 mM $FgMgSO_4$ implanted animals.

Animals were sacrificed 3 days after implantation, implanted scaffolds and surrounding skin were retrieved for histological analysis and results are illustrated in Fig. 6B. Normal skin tissue architecture was observed in Sham-operated animals, while a thin capsule, accompanied with a low infiltration of inflammatory cells were present at the periphery of implanted materials (Fig. 6C). Capsule measurements revealed no significant differences between Fg and 10 mM $FgMgSO_4$ groups (Fig. 6D). To assess possible systemic effects of Mg ions, organs were processed for histological analysis, namely lymph nodes, spleen, and kidney. No morphological alterations at either macro or microscopic level were observed, compared to Sham group (Supplementary Fig. 2).

To analyse the inflammatory response in detail, inflammatory exudates were collected, cells were separated and analysed by flow cytometry. Macrophages were detected using CD11b [40], and the M1 and M2 subpopulations of macrophages were identified by CCR7 and CD163 markers, respectively [40, 41]. The gating strategy is depicted in Fig. 6E. When data for all animals was analysed (Fig. 6F), there was a tendency for decreased percentage of $CD11b^+$ cells recruited to the Fg and 10 mM $FgMgSO_4$ implant site, when compared to Sham-operated animals, but this was not statistically significant (Fig. 6F i). No differences were observed in the percentage of $CD11b^+CCR7^+$ cells (M1 macrophages) between groups (Fig. 6F ii). However, the percentage of $CD11b^+CD163^+$ cells (M2 macrophages) was significantly higher in the group implanted with 10 mM $FgMgSO_4$, when compared with those implanted with Fg and with Sham-operated animals (Fig. 6F iii), resulting also in significantly higher M2:M1 ratio (Fig. 6F iv). Besides macrophages, other immune cell populations were analysed in the exudates, namely neutrophils and dendritic cells. These were detected using Ly-6G/Ly-6C and Cd11c, respectively, but there were no significant differences in the percentage of Ly-6G/Ly-$6C^+$, or the percentage of $CD11c^+$ between groups (Supplementary Fig. 3). Altogether, the data indicates that 10 mM $FgMgSO_4$ scaffolds induce an M2 macrophage phenotypic response.

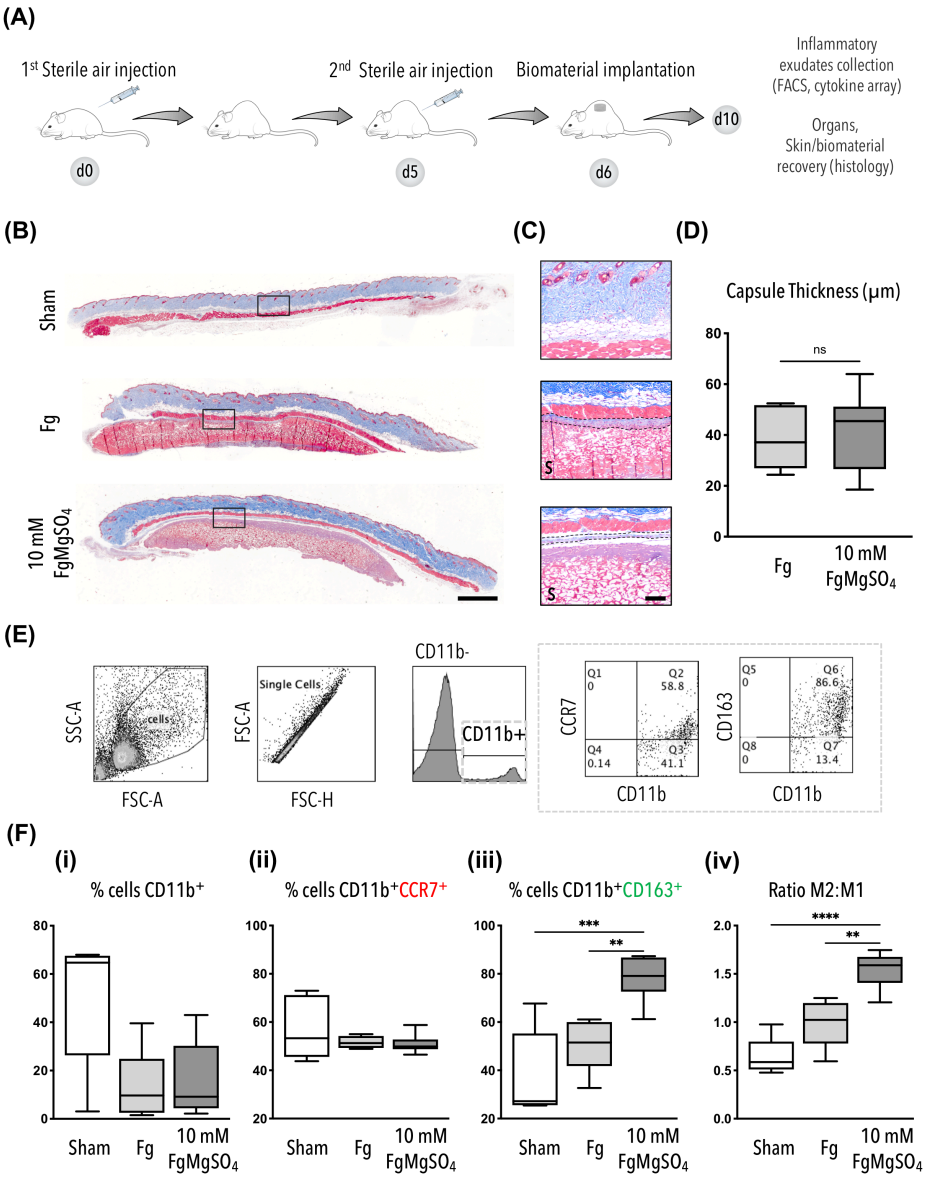


Fig. 6. Characterization of the *in vivo* inflammatory response to Fg and 10 mM $FgMgSO_4$ scaffolds implantation. (A) Schematic representation of experimental approach. **(B)** Masson trichrome (MT) stained mosaic of the air pouch site of Sham-operated animals and Fg and $FgMgSO_4$ implanted animals. Collagen can be seen in blue (scale bar = 500 µm). **(C)** Detailed image of the implanted scaffold, showing inflammatory cells around and within (scale bar = 250 µm). Scaffold is represented with a (S) and a thin fibrous capsule indicated within the dotted lines, in both Fg and 10 mM $FgMgSO_4$ scaffolds. **(D)** Quantification of the fibrous capsule thickness surrounding the implants after 3 days of implantation. MT MosaicX sections from (C) were used for capsule thickness quantification using Image J software, where a total of 20 measurements were considered (n=6). **(E)** Flow cytometry gating strategy. Side scatter-area (SSC-A) and forward scatter-area (FSC-A) gating was used for excluding debris. Forward scatter area (FSC-A) versus forward scatter height (FSC-H) density plot was used to exclude doublets. CD11b single parameter histogram was used to identify macrophages ($CD11b^+$). Two parameter density plots were used to determine double positive cells $CD11b^+CCR7^+$ (M1 macrophages) and $CD11b^+CD163^+$ (M2 macrophages). **(F)** Cell percentages quantified across all animals in each group, showing: **(i)** Percentage of $CD11b^+$ cells. **(ii)** Percentage of double positive cells, $CD11b^+CCR7^+$. **(iii)** Percentage of double positive cells, $CD11b^+CD163^+$. **(iv)** M2/M1 ratio. Graphs are minimum to maximum box-and-whiskers plots, with median representation (n=5-6). **p<0.01, ***p<0.001, ****p<0.0001 using one-way ANOVA followed by Sidak's multiple comparisons test.

The inflammatory exudates were also analysed for the levels of inflammatory mediators, by a cytokine/chemokine array. The molecules exhibiting statistically significant differences between groups are depicted in Fig. 7. The remainders are presented in Supplementary Fig. 4. The results obtained show that implantation of either Fg or 10 mM $FgMgSO_4$ caused a general decrease in pro-inflammatory cytokines, when compared to Sham-operated animals. Results show that IL-6, LIF, TNF-α, KC, MCP-1, MIP-1α and MIP-1β were decreased in Fg and 10 mM $FgMgSO_4$ groups, in comparison with Sham-operated. However, their reduction was more pronounced in animals implanted with 10 mM $FgMgSO_4$ than those implanted with Fg. Secretion levels of IL-5 and Eotaxin were exclusively reduced by Fg scaffolds, while levels of IL-1β, IP-10, MIP-2, MDC and MIP-3α were reduced exclusively in the 10 mM $FgMgSO_4$ group.

Together, these results show that 10 mM $FgMgSO_4$ scaffolds modulate inflammation and macrophage polarization in vivo.

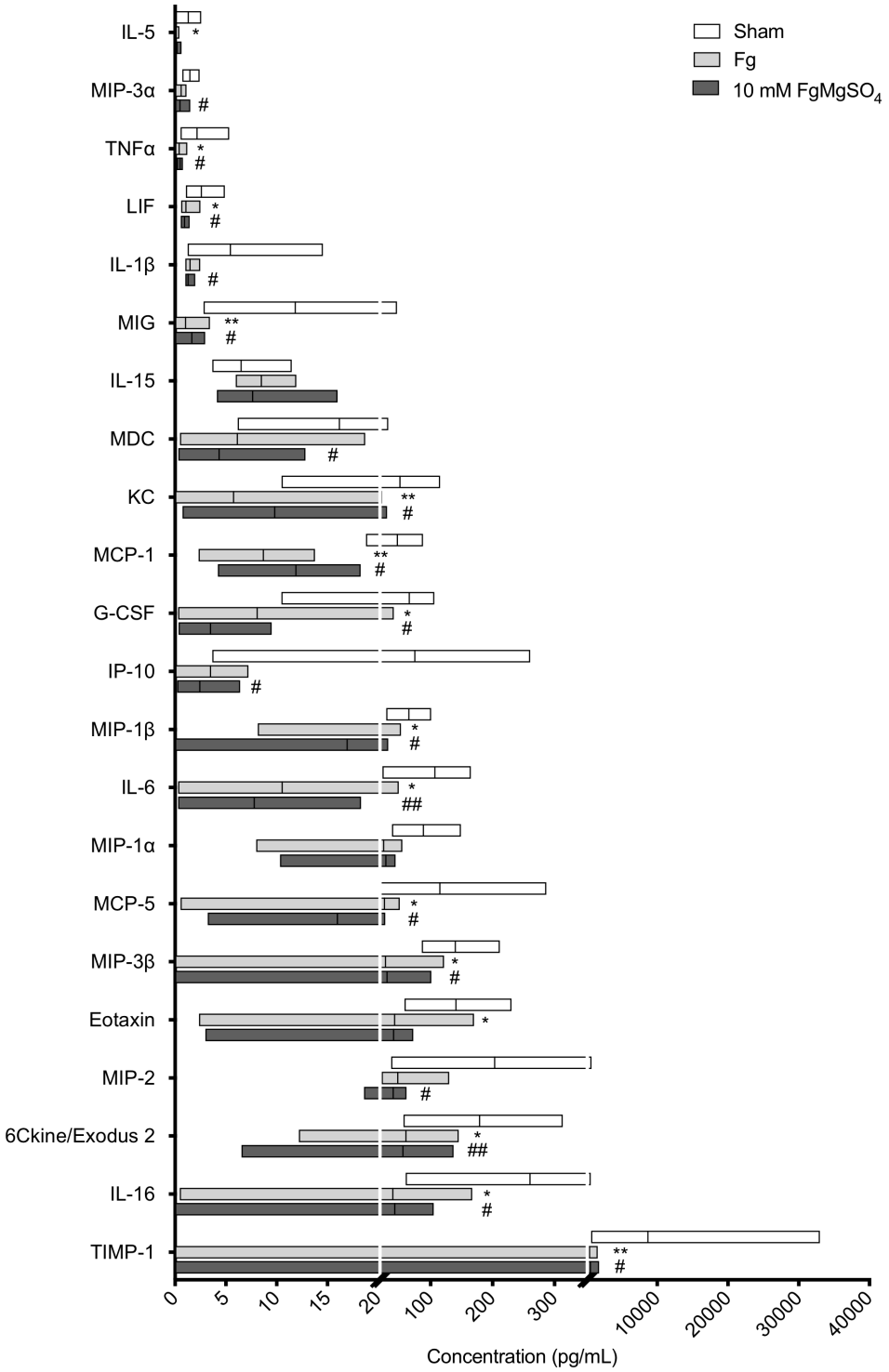


Fig.7. Cytokine production by inflammatory cells on the recovered exudates 3 days after implantation in an air-pouch mouse model. Cytokine levels in inflammatory exudates collected from the mouse air pouches of Sham-operated (white bars), Fg (light gray bars) and 10 mM $FgMgSO_4$ (dark gray bars) implanted animals. Box-plots represent min-to-max distribution (n=6). Kruskal-Wallis test followed by corrected Dunn's multiple comparisons were performed for IL-5, LIF, MIG, KC, MCP-1, G-CSF, IP10, MIP-1β, IL-6, MIP-3β, eotaxin, MIP-2, IL16 and TIMP-1. One-way ANOVA followed by Sidak's multiple comparisons test were performed for MIP-3α, TNF-α, IL-1β, IL-15, MDC, MIP-1α, MCP-5 and 6Ckine/Exodus. Statistical significance is indicated as follows: *$p<0.05$, **$p<0.01$ for Sham versus Fg; $^{\#}p<0.05$ and $^{\#\#}p<0.01$ for Sham versus 10 mM $FgMgSO_4$

4. DISCUSSION

Bioengineering immunomodulatory microenvironments using biomaterials capable of controlling the inflammatory response after injury is an attractive approach for regenerative medicine. Macrophages are one of the first responders to biomaterial implantation, conditioning inflammation and the regeneration processes. The high plasticity of these immune cells has fostered the development of different strategies to control macrophage polarization [2].

An ion-enriched environment may modulate the response of immune cells to pro-inflammatory stimuli as well as inducing osteogenic differentiation of MSCs [42]. Thus, incorporation of different ions within polymeric, ceramic and metallic matrices has been explored to tune/improve the biological properties of the resultant material and further enhance the regenerative process [43].

In this study, 3D $MgSO_4$-incorporated Fg scaffolds were developed and tested for their potential to target macrophage polarization towards the M2 phenotype. The combination between Fg and Mg has been previously explored by us, showing that the extracts from FgMg multilayer construct acted synergistically to reduce macrophage inflammatory activation [20]. In the current study we take that combination to the next level, by controlling the concentration of Mg in Fg scaffolds we found the optimal Mg concentration and developed a novel functional biomaterial capable of inducing a M2-macrophage polarization both *in vitro* and *in vivo*.

Fg-based 3D scaffolds with 0, 10, 25 and 50 mM of $MgSO_4$ ($FgMgSO_4$) were produced by freeze-drying and characterized. All combinations presented a 3D network of interconnected pores, reported to act as an important regulatory cue for cell adhesion and viability [44]. Interestingly, the incorporation of 50 mM of $MgSO_4$ into Fg lead to a significant decrease on the porosity of the scaffolds. Garg et al. [44] reported that higher porosity facilitated macrophage infiltration in the 3D space, and promoted the expression of M2 macrophage markers, whereas materials with lower porosity showed to hinder the infiltration of these cells and enhanced the expression of M1 markers. Besides porosity, other biomaterial surface properties, like surface charge, chemical composition, stiffness, also have an important contribution in regulating cell responses [45]. FTIR analysis indicated the presence of sulphate in the Fg structure. DMA analysis showed that for all tested combinations, storage modulus was higher than loss modulus. This indicates that the elastic behavior is dominant over the viscous one. Adhikari et al. [46] showed that

magnesium gluconate (MgG) addition significantly increased chitosan mechanical properties. Similarly, we observed higher mechanical properties in $MgSO_4$-incorporated Fg scaffolds, particularly for 10 mM $FgMgSO_4$ scaffolds when compared to Fg alone. We found a cumulative release of Mg that was lower for 10 mM than 25 and 50 mM, and that was linear for the lower Mg concentration, plateauing for the other 2 concentrations. Moreover, $FgMgSO_4$ scaffolds exhibited a significant increase in surface charge in comparison with Fg alone. We hypothesize this increase to be due to the addition of the positively charged cation Mg^{2+} in the Fg structure. These alterations induced by the incorporation of $MgSO_4$ are expected to affect the ionic exchange with the cell culture media, which influences cell behavior, as reported in previous studies [47, 48].

In order to investigate the immunomodulatory effects of the different Mg concentrations and mechanical properties of $FgMgSO_4$ scaffolds, human monocytes were isolated and seeded on top of the materials. Cells were allowed to differentiate into macrophages and then left unstimulated (M0) or stimulated with LPS-IFN**γ** (M1), a pro-inflammatory stimulation commonly used in inflammation related studies [20, 49, 50]. Magnesium ions (Mg^{2+}) are reported to modulate macrophage phenotype [51]. However, excessive concentrations can be related to cytotoxicity. Here, we found a cytotoxic effect for 25 and 50 mM $FgMgSO_4$ scaffolds, either in unstimulated conditions and under M1 pro-inflammatory stimulation. This is in agreement with findings by Jin et al. [52], who found, in the THP-1 cell line, that the 600 mg/L (approximately 25 mM) magnesium concentration of a Mg-based alloy was cytotoxic. In this same cell line, Sun et al. [51] showed that Mg^{2+} modulated THP-1-derived macrophages towards M2 phenotype in a time and concentration dependent manner, expressing less CCR7 and more CD206. Both *in vitro* and *in vivo*, the evaluation of macrophage polarization was performed using antibodies against CCR7 and CD163, often used as markers of polarized M1 and M2 macrophages, respectively [33, 53, 54]. Our results showed increased M2:M1 ratio for the cells cultured on 10 mM $FgMgSO_4$ scaffolds and reduced M2:M1 ratios for those on 25 and 50 mM $FgMgSO_4$ scaffolds. We hypothesize that the enhanced percentage of $CCR7^+$ cells in 25 and 50 mM $FgMgSO_4$ scaffolds may be correlated with their increased toxicity, as showed by LDH results. We previously showed that extracts of a combination between Fg and metallic Mg reduced macrophage M1 activation, but did not increase M2 cells [20], which might be related to the extract concentration of Mg resulting from the metal degradation.

The inflammatory activation of macrophages is normally associated with the activation of signaling pathways involving MAPK and NF-kB. In line with our previous results, showing

that FgMg combination extracts reduced phosphorylation levels of NF-kB p65 in response to M1 stimulation [20], we showed here that 10 mM $FgMgSO_4$ scaffolds impaired NF-kB p65 nuclear translocation, in comparison with Fg alone. Our results were also in accordance with the evidences reported by Hu et al. [55]. Authors showed that 5 and 10 mM Mg supplementation, prior to the application of M1 pro-inflammatory stimulation with LPS-IFN**γ** to RAW cells, significantly decreased the translocation of NF-kB p65 into the nucleus, reducing the nuclear:cytoplasmatic ratio. Also, it is known that NF-kB activation mediates the expression of several inflammatory cytokine genes such as TNF-α, IL-1β and IL-6 [56].

To further explore the functional implications of biomaterial-mediated regulation of macrophage polarization, a broad quantitative analysis of cytokines, chemokines and growth factors was performed in M0 and M1 macrophages cultured on Fg and 10 mM $FgMgSO_4$ scaffolds. Our data supports the anti-inflammatory impact of 10 mM $FgMgSO_4$ scaffolds, showing a downregulation of inflammatory mediators, like IFN**γ**, IL-6, IL-12p40, TNF-α, and also impairing the increase of others, like IL-1β, IL-8, IL12p70, in response to M1-stimulation, when compared with Fg scaffolds. Additionally, IL-13 was significantly increased in 10 mM $FgMgSO_4$ cultured macrophages in presence of M1 stimulation. IL-13 is described as an anti-inflammatory cytokine able to downregulate LPS mediated inflammatory responses (together with IL-4) [57], inhibiting the secretion of pro-inflammatory mediators including IL-6, IL-1β, IL12 and TNF-α, as confirmed by us and others [58].

In this study, we also investigated the inflammatory response to Fg and 10 mM $FgMgSO_4$ *in vivo* for the first time, using the mouse air-pouch model, and maintaining particular attention on the M1 and M2 macrophage polarization. These are key players of the biological response to biomaterial implantation [59]. Fg scaffolds were previously studied in an *in vivo* rat bone defect model and shown to modulate local and systemic response to injury and improved bone repair [15]. Here, the inflammatory exudates were collected and analysed by flow cytometry and obtained results revealed significantly higher percentage of $CD11b^+CD163^+$ cells in animals implanted with 10 mM $FgMgSO_4$ scaffolds, in comparison with Fg implanted animals and Sham-operated ones. The levels of some cytokines in the retrieved inflammatory exudates were investigated using a cytokine/chemokine array. Overall, we have found a general decrease in several pro-inflammatory cytokines both in animals implanted with Fg and 10 mM $FgMgSO_4$ scaffolds. Still, 10 mM $FgMgSO_4$ scaffolds were more efficient in suppressing inflammatory response by exclusively reducing the secretion of key inflammation-related cytokines like IL-1β, IP-10 and chemokines like MIP-

2, MDC and MIP-3α. Within the cytokine/chemokine panels that were analysed, some mediators were affected/modulated both *in vitro* and *in vivo* as is the case of IL-1β and IP-10. IL-1β is a pro-inflammatory cytokine produced by LPS-activated macrophages via NF-kB activation [60]. This cytokine is an important mediator of the inflammatory response shown to contribute to pathophysiological alterations of inflammatory osteoarticular disorders including osteoarthritis [61] and rheumatoid arthritis [62]. In accordance with our results, other studies have also demonstrated that Mg down-regulated IL-1β secretion levels [55, 56, 63]. IP-10 is a pro-inflammatory chemokine whose secretion is induced and increased by pro-inflammatory stimuli such as INF**γ** and TNF-α, in a TLR4-NFkB dependent manner [64]. It has been described to be involved in chemotaxis and recruitment of inflammatory cells and production of osteoclastogenic cytokines [65, 66], with pathogenic roles in inflammatory osteoarticular disorders such as rheumatoid arthritis [66]. Contrary to what has been demonstrated by us, Cross et al. [67] showed that $MgSO_4$ increased LPS-induced IP-10 secretion levels. However, their study was conducted on fetal membranes using 5 mM $MgSO_4$, thus it may be related to the Mg concentration used.

Beyond the immune reaction, macrophages are also known to control osteogenesis, via the release of a wide range of cytokines/chemokines. The macrophage-MSCs crosstalk is essential to resolve the inflammation stage and initiate new bone formation [68]. Thus, in the current work we also investigated the effect of secreted molecules from macrophages cultured on 10 mM $FgMgSO_4$ scaffolds on the osteogenic differentiation of bone marrow-derived MSCs, as a functional impact, important for regeneration. The exposure of MSCs to the secretome from M0 and M1 macrophages, cultured in Fg and 10 mM $FgMgSO_4$ scaffolds, lead to an increased mineral deposition, albeit not significantly different from Fg and 10 mM $FgMgSO_4$ scaffolds extracts (Supplementary Fig. 5). When MSCs were cultured directly on Fg and on 10 mM $FgMgSO_4$ scaffolds, the later enhanced their osteogenic differentiation (Supplementary Fig. 5). The effect of Mg^{2+} on MSCs has been previously studied, showing to improve osteogenesis in a dose-dependent manner [69]. Lower Mg^{2+} concentrations were more prone to induce MSCs mineralization, instead of higher concentrations, due to cytotoxicity [24, 70-72]. For instance, Zhang et al. [71] showed that 1.8, 2.3 and 3.8 mM of magnesium chloride ($MgCl_2$) were effective in significantly inhibiting BMSCs mineralization. Similarly, Zhang et al. [72] revealed that higher BMSCs mineralization was achieved in medium supplemented with 0-0.5 mM of $MgCl_2$. Concentrations above 0.5 mM (1-16 mM) lead to decreased BMSCs mineralization. In line with our results, Yoshizawa et al. [24] demonstrated that BMSCs osteogenic differentiation

was significantly enhanced in medium containing 10 mM $MgSO_4$, inducing higher mineral deposition, and inhibited at 100 mM $MgSO_4$.

Taken together, our *in vitro* and *in vivo* findings show that the developed 10 mM $FgMgSO_4$ scaffolds have improved mechanical properties, and are able to modulate macrophage polarization and cytokine secretion towards a M2, anti-inflammatory phenotype.

5. CONCLUSION

The present study reports, for the first time, the development and the use of $MgSO_4$-incorporated Fg scaffolds ($FgMgSO_4$) to modulate macrophage phenotype both *in vitro* and *in vivo*. The results presented revealed a regulatory effect of Mg^{2+} in the concentration of 10 mM, modulating macrophage polarization towards a M2 anti-inflammatory phenotype. Hence, these findings support that 10 mM $FgMgSO_4$ scaffolds can modulate inflammation and promote a pro-regenerative microenvironment.

ACKNOWLEDGMENTS

Mafalda Bessa-Gonçalves funded by FCT PhD Programmes and by Programa Operacional Potencial Humano (POCH), BiotechHealth Programme (Doctoral Programme on Cellular and Molecular Biotechnology Applied to Health Sciences – reference PD/BI/128355/2017), and through the PhD studentship PD/BD/135489/2018. The authors thank Grifols SA for donating clinical grade fibrinogen; Daniela Silva for the technical and scientific support with SEM analysis (CEMUP); i3S Scientific Platform Translational Cytometry, member of the PPBI (PPBI-POCI-01-0145-FEDER-022122); Serviço de Ortopedia and Serviço de Imunohemoterapia, Centro Hospitalar Universitário de São João for donating bone marrow samples and buffy coats, respectively. The authors would like to thank *Serviço do Imunohemoterapia* and *Departamento de Ortopedia*, at *Centro Hospitalar de São João (CHSJ)*, for kindly donating the buffy coats and bone marrow samples, the advanced light microscopy unit at i3S for confocal analysis, and CEMUP for the SEM analysis.

REFERENCES

[1] C. Schlundt, H. Fischer, C.H. Bucher, C. Rendenbach, G.N. Duda, K. Schmidt-Bleek, The multifaceted roles of macrophages in bone regeneration: A story of polarization, activation and time(), Acta Biomater (2021).

[2] K.E. Martin, A.J. Garcia, Macrophage phenotypes in tissue repair and the foreign body response: Implications for biomaterial-based regenerative medicine strategies, Acta Biomater (2021).

[3] L. Davenport Huyer, S. Pascual-Gil, Y. Wang, S. Mandla, B. Yee, M. Radisic, Advanced Strategies for Modulation of the Material–Macrophage Interface, Advanced Functional Materials 30(44) (2020) 1909331.

[4] R. Sridharan, A.R. Cameron, D.J. Kelly, C.J. Kearney, F.J. O'Brien, Biomaterial based modulation of macrophage polarization: a review and suggested design principles, Materials Today 18(6) (2015) 313-325.

[5] J. Li, X. Jiang, H. Li, M. Gelinsky, Z. Gu, Tailoring Materials for Modulation of Macrophage Fate, Advanced Materials n/a(n/a) (2021) 2004172.

[6] W. Liu, J. Li, M. Cheng, Q. Wang, K.W.K. Yeung, P.K. Chu, X. Zhang, Zinc-Modified Sulfonated Polyetheretherketone Surface with Immunomodulatory Function for Guiding Cell Fate and Bone Regeneration, Adv Sci (Weinh) 5(10) (2018) 1800749.

[7] M. Wang, Y. Yu, K. Dai, Z. Ma, Y. Liu, J. Wang, C. Liu, Improved osteogenesis and angiogenesis of magnesium-doped calcium phosphate cement via macrophage immunomodulation, Biomater Sci 4(11) (2016) 1574-1583.

[8] A.H. Lourenco, A.L. Torres, D.P. Vasconcelos, C. Ribeiro-Machado, J.N. Barbosa, M.A. Barbosa, C.C. Barrias, C.C. Ribeiro, Osteogenic, anti-osteoclastogenic and immunomodulatory properties of a strontium-releasing hybrid scaffold for bone repair, Mater Sci Eng C Mater Biol Appl 99 (2019) 1289-1303.

[9] S.S. Soni, C.B. Rodell, Polymeric materials for immune engineering: Molecular interaction to biomaterial design, Acta Biomater (2021).

[10] I.V. Roberts, D. Bukhary, C.Y.L. Valdivieso, N. Tirelli, Fibrin Matrices as (Injectable) Biomaterials: Formation, Clinical Use, and Molecular Engineering, Macromol Biosci 20(1) (2020) e1900283.

[11] C.R. Almeida, D.P. Vasconcelos, R.M. Goncalves, M.A. Barbosa, Enhanced mesenchymal stromal cell recruitment via natural killer cells by incorporation of inflammatory signals in biomaterials, J R Soc Interface 9(67) (2012) 261-71.

[12] M.I. Oliveira, M.L. Pinto, R.M. Goncalves, M.C.L. Martins, S.G. Santos, M.A. Barbosa, Adsorbed Fibrinogen stimulates TLR-4 on monocytes and induces BMP-2 expression, Acta Biomater 49 (2017) 296-305.

[13] J. Maciel, M.I. Oliveira, E. Colton, A.K. McNally, C. Oliveira, J.M. Anderson, M.A. Barbosa, Adsorbed fibrinogen enhances production of bone- and angiogenic-related factors by monocytes/macrophages, Tissue Eng Part A 20(1-2) (2014) 250-63.

[14] S.G. Santos, M. Lamghari, C.R. Almeida, M.I. Oliveira, N. Neves, A.C. Ribeiro, J.N. Barbosa, R. Barros, J. Maciel, M.C. Martins, R.M. Goncalves, M.A. Barbosa, Adsorbed fibrinogen leads to improved bone regeneration and correlates with differences in the systemic immune response, Acta Biomater 9(7) (2013) 7209-17.

[15] D.M. Vasconcelos, R.M. Goncalves, C.R. Almeida, I.O. Pereira, M.I. Oliveira, N. Neves, A.M. Silva, A.C. Ribeiro, C. Cunha, A.R. Almeida, C.C. Ribeiro, A.M. Gil, E. Seebach, K.L. Kynast, W. Richter, M. Lamghari, S.G. Santos, M.A. Barbosa, Fibrinogen scaffolds with immunomodulatory properties promote in vivo bone regeneration, Biomaterials 111 (2016) 163-178.

[16] B.J. Luthringer, F. Feyerabend, R. Willumeit-Romer, Magnesium-based implants: a mini-review, Magnes Res 27(4) (2014) 142-54.

[17] H. Windhagen, K. Radtke, A. Weizbauer, J. Diekmann, Y. Noll, U. Kreimeyer, R. Schavan, C. Stukenborg-Colsman, H. Waizy, Biodegradable magnesium-based screw clinically equivalent to titanium screw in hallux valgus surgery: short term results of the first prospective, randomized, controlled clinical pilot study, Biomed Eng Online 12 (2013) 62.

[18] J.-W. Lee, H.-S. Han, K.-J. Han, J. Park, H. Jeon, M.-R. Ok, H.-K. Seok, J.-P. Ahn, K.E. Lee, D.-H. Lee, S.-J. Yang, S.-Y. Cho, P.-R. Cha, H. Kwon, T.-H. Nam, J.H.L. Han, H.-J. Rho, K.-S. Lee, Y.-C. Kim, D. Mantovani, Long-term clinical study and multiscale analysis of in vivo biodegradation mechanism of Mg alloy, Proceedings of the National Academy of Sciences 113(3) (2016) 716.

[19] D. Zhao, S. Huang, F. Lu, B. Wang, L. Yang, L. Qin, K. Yang, Y. Li, W. Li, W. Wang, S. Tian, X. Zhang, W. Gao, Z. Wang, Y. Zhang, X. Xie, J. Wang, J. Li, Vascularized bone

grafting fixed by biodegradable magnesium screw for treating osteonecrosis of the femoral head, Biomaterials 81 (2016) 84-92.

[20] M. Bessa-Goncalves, A.M. Silva, J.P. Bras, H. Helmholz, B.J.C. Luthringer-Feyerabend, R. Willumeit-Romer, M.A. Barbosa, S.G. Santos, Fibrinogen and magnesium combination biomaterials modulate macrophage phenotype, NF-kB signaling and crosstalk with mesenchymal stem/stromal cells, Acta Biomater 114 (2020) 471-484.

[21] M.D. Costantino, A. Schuster, H. Helmholz, A. Meyer-Rachner, R. Willumeit-Romer, B.J.C. Luthringer-Feyerabend, Inflammatory response to magnesium-based biodegradable implant materials, Acta Biomater 101 (2020) 598-608.

[22] C. Liu, X. Fu, H. Pan, P. Wan, L. Wang, L. Tan, K. Wang, Y. Zhao, K. Yang, P.K. Chu, Biodegradable Mg-Cu alloys with enhanced osteogenesis, angiogenesis, and long-lasting antibacterial effects, Sci Rep 6 (2016) 27374.

[23] G.K. Schwalfenberg, S.J. Genuis, The Importance of Magnesium in Clinical Healthcare, Scientifica (Cairo) 2017 (2017) 4179326.

[24] S. Yoshizawa, A. Brown, A. Barchowsky, C. Sfeir, Magnesium ion stimulation of bone marrow stromal cells enhances osteogenic activity, simulating the effect of magnesium alloy degradation, Acta Biomater 10(6) (2014) 2834-42.

[25] C. Janning, E. Willbold, C. Vogt, J. Nellesen, A. Meyer-Lindenberg, H. Windhagen, F. Thorey, F. Witte, Magnesium hydroxide temporarily enhancing osteoblast activity and decreasing the osteoclast number in peri-implant bone remodelling, Acta Biomater 6(5) (2010) 1861-8.

[26] Y. Xie, C. Hu, Y. Feng, D. Li, T. Ai, Y. Huang, X. Chen, L. Huang, J. Tan, Osteoimmunomodulatory effects of biomaterial modification strategies on macrophage polarization and bone regeneration, Regen Biomater 7(3) (2020) 233-245.

[27] E. Bosch-Rué, L. Diez-Tercero, B. Giordano-Kelhoffer, L.M. Delgado, B.M. Bosch, M. Hoyos-Nogués, M.A. Mateos-Timoneda, P.A. Tran, F.J. Gil, R.A. Perez, Biological Roles and Delivery Strategies for Ions to Promote Osteogenic Induction, Frontiers in Cell and Developmental Biology 8(1809) (2021).

[28] A.R. Almeida, M. Bessa-Goncalves, D.M. Vasconcelos, M.A. Barbosa, S.G. Santos, Osteoclasts degrade fibrinogen scaffolds and induce mesenchymal stem/stromal osteogenic differentiation, J Biomed Mater Res A 108(4) (2020) 851-862.

[29] S.A. Sell, M.P. Francis, K. Garg, M.J. McClure, D.G. Simpson, G.L. Bowlin, Cross-linking methods of electrospun fibrinogen scaffolds for tissue engineering applications, Biomed Mater 3(4) (2008) 045001.

[30] A. Rabbani, S. Salehi, Dynamic modeling of the formation damage and mud cake deposition using filtration theories coupled with SEM image processing, Journal of Natural Gas Science and Engineering 42 (2017) 157-168.

[31] N. Neves, B.B. Campos, I.F. Almeida, P.C. Costa, A.T. Cabral, M.A. Barbosa, C.C. Ribeiro, Strontium-rich injectable hybrid system for bone regeneration, Mater Sci Eng C Mater Biol Appl 59 (2016) 818-827.

[32] T. Riss, A. Niles, R. Moravec, N. Karassina, J. Vidugiriene, Cytotoxicity Assays: In Vitro Methods to Measure Dead Cells, in: S. Markossian, G.S. Sittampalam, A. Grossman, K. Brimacombe, M. Arkin, D. Auld, C.P. Austin, J. Baell, J.M.M. Caaveiro, T.D.Y. Chung, N.P. Coussens, J.L. Dahlin, V. Devanaryan, T.L. Foley, M. Glicksman, M.D. Hall, J.V. Haas, S.R.J. Hoare, J. Inglese, P.W. Iversen, S.D. Kahl, S.C. Kales, S. Kirshner, M. Lal-Nag, Z. Li, J. McGee, O. McManus, T. Riss, P. Saradjian, O.J. Trask, Jr., J.R. Weidner, M.J. Wildey, M. Xia, X. Xu (Eds.), Assay Guidance Manual, Bethesda (MD), 2004.

[33] V. Ballotta, A. Driessen-Mol, C.V. Bouten, F.P. Baaijens, Strain-dependent modulation of macrophage polarization within scaffolds, Biomaterials 35(18) (2014) 4919-28.

[34] D.P. Vasconcelos, A.C. Fonseca, M. Costa, I.F. Amaral, M.A. Barbosa, A.P. Aguas, J.N. Barbosa, Macrophage polarization following chitosan implantation, Biomaterials 34(38) (2013) 9952-9.

[35] S.Y. Lin, Y.S. Wei, T.F. Hsieh, M.J. Li, Pressure dependence of human fibrinogen correlated to the conformational alpha-helix to beta-sheet transition: an Fourier transform infrared study microspectroscopic study, Biopolymers 75(5) (2004) 393-402.

[36] R.I. Litvinov, D.A. Faizullin, Y.F. Zuev, J.W. Weisel, The alpha-helix to beta-sheet transition in stretched and compressed hydrated fibrin clots, Biophys J 103(5) (2012) 1020-7.

[37] F. Ovalles, M. Gallignani, R. Rondón, M.R. Brunetto, R. Luna, Determination of sulphate for measuring magnesium sulphate in pharmaceuticals by flow analysis-fourier transforms infrared spectroscopy, Latin American Journal of Pharmacy 28 (2009) 173-182.

[38] D.M. Vasconcelos, S.G. Santos, M. Lamghari, M.A. Barbosa, The two faces of metal ions: From implants rejection to tissue repair/regeneration, Biomaterials 84 (2016) 262-275.

[39] T. Liu, L. Zhang, D. Joo, S.-C. Sun, NF-κB signaling in inflammation, Signal Transduction and Targeted Therapy 2(1) (2017) 17023.

[40] K.A. Jablonski, S.A. Amici, L.M. Webb, D. Ruiz-Rosado Jde, P.G. Popovich, S. Partida-Sanchez, M. Guerau-de-Arellano, Novel Markers to Delineate Murine M1 and M2 Macrophages, PLoS One 10(12) (2015) e0145342.

[41] B. Li, Y. Hu, Y. Zhao, M. Cheng, H. Qin, T. Cheng, Q. Wang, X. Peng, X. Zhang, Curcumin Attenuates Titanium Particle-Induced Inflammation by Regulating Macrophage Polarization In Vitro and In Vivo, Front Immunol 8 (2017) 55.

[42] A. Przekora, Current Trends in Fabrication of Biomaterials for Bone and Cartilage Regeneration: Materials Modifications and Biophysical Stimulations, Int J Mol Sci 20(2) (2019).

[43] P. Kazimierczak, J. Kolmas, A. Przekora, Biological Response to Macroporous Chitosan-Agarose Bone Scaffolds Comprising Mg- and Zn-Doped Nano-Hydroxyapatite, Int J Mol Sci 20(15) (2019).

[44] K. Garg, N.A. Pullen, C.A. Oskeritzian, J.J. Ryan, G.L. Bowlin, Macrophage functional polarization (M1/M2) in response to varying fiber and pore dimensions of electrospun scaffolds, Biomaterials 34(18) (2013) 4439-51.

[45] M. Rahmati, E.A. Silva, J.E. Reseland, A.H. C, H.J. Haugen, Biological responses to physicochemical properties of biomaterial surface, Chem Soc Rev 49(15) (2020) 5178-5224.

[46] U. Adhikari, N.P. Rijal, S. Khanal, D. Pai, J. Sankar, N. Bhattarai, Magnesium incorporated chitosan based scaffolds for tissue engineering applications, Bioact Mater 1(2) (2016) 132-139.

[47] W.G. Brodbeck, Y. Nakayama, T. Matsuda, E. Colton, N.P. Ziats, J.M. Anderson, Biomaterial surface chemistry dictates adherent monocyte/macrophage cytokine expression in vitro, Cytokine 18(6) (2002) 311-9.

[48] E. Engel, S. Del Valle, C. Aparicio, G. Altankov, L. Asin, J.A. Planell, M.P. Ginebra, Discerning the role of topography and ion exchange in cell response of bioactive tissue engineering scaffolds, Tissue Eng Part A 14(8) (2008) 1341-51.

[49] S. Han, Z. Chen, P. Han, Q. Hu, Y. Xiao, Activation of Macrophages by Lipopolysaccharide for Assessing the Immunomodulatory Property of Biomaterials<sup/>, Tissue Eng Part A 23(19-20) (2017) 1100-1109.

[50] M. Orecchioni, Y. Ghosheh, A.B. Pramod, K. Ley, Macrophage Polarization: Different Gene Signatures in M1(LPS+) vs. Classically and M2(LPS-) vs. Alternatively Activated Macrophages, Front Immunol 10 (2019) 1084.

[51] L. Sun, X. Li, M. Xu, F. Yang, W. Wang, X. Niu, In vitro immunomodulation of magnesium on monocytic cell toward anti-inflammatory macrophages, Regen Biomater 7(4) (2020) 391-401.

[52] L. Jin, C. Chen, Y. Li, F. Yuan, R. Gong, J. Wu, H. Zhang, B. Kang, G. Yuan, H. Zeng, T. Chen, A Biodegradable Mg-Based Alloy Inhibited the Inflammatory Response of THP-1 Cell-Derived Macrophages Through the TRPM7-PI3K-AKT1 Signaling Axis, Front Immunol 10 (2019) 2798.

[53] S.F. Badylak, J.E. Valentin, A.K. Ravindra, G.P. McCabe, A.M. Stewart-Akers, Macrophage phenotype as a determinant of biologic scaffold remodeling, Tissue Eng Part A 14(11) (2008) 1835-42.

[54] A. Mantovani, S. Sozzani, M. Locati, P. Allavena, A. Sica, Macrophage polarization: tumor-associated macrophages as a paradigm for polarized M2 mononuclear phagocytes, Trends Immunol 23(11) (2002) 549-55.

[55] T. Hu, H. Xu, C. Wang, H. Qin, Z. An, Magnesium enhances the chondrogenic differentiation of mesenchymal stem cells by inhibiting activated macrophage-induced inflammation, Sci Rep 8(1) (2018) 3406.

[56] C. Xie, X. Li, J. Zhu, J. Wu, S. Geng, C. Zhong, Magnesium isoglycyrrhizinate suppresses LPS-induced inflammation and oxidative stress through inhibiting NF-kappaB and MAPK pathways in RAW264.7 cells, Bioorg Med Chem 27(3) (2019) 516-524.

[57] A.H. Bryant, S. Spencer-Harty, S.E. Owens, R.H. Jones, C.A. Thornton, Interleukin 4 and interleukin 13 downregulate the lipopolysaccharide-mediated inflammatory response by human gestation-associated tissues, Biol Reprod 96(3) (2017) 576-586.

[58] N. Kolosowska, M.H. Keuters, S. Wojciechowski, V. Keksa-Goldsteine, M. Laine, T. Malm, G. Goldsteins, J. Koistinaho, H. Dhungana, Peripheral Administration of IL-13 Induces Anti-inflammatory Microglial/Macrophage Responses and Provides Neuroprotection in Ischemic Stroke, Neurotherapeutics 16(4) (2019) 1304-1319.

[59] J.N. Barbosa, D.P. Vasconcelos, Chapter 3 - Macrophage response to biomaterials, in: M. Mozafari (Ed.), Handbook of Biomaterials Biocompatibility, Woodhead Publishing2020, pp. 43-52.

[60] J. Rex, U. Albrecht, C. Ehlting, M. Thomas, U.M. Zanger, O. Sawodny, D. Haussinger, M. Ederer, R. Feuer, J.G. Bode, Model-Based Characterization of Inflammatory Gene Expression Patterns of Activated Macrophages, PLoS Comput Biol 12(7) (2016) e1005018.

[61] Y. Jia, W. He, H. Zhang, L. He, Y. Wang, T. Zhang, J. Peng, P. Sun, Y. Qian, Morusin Ameliorates IL-1beta-Induced Chondrocyte Inflammation and Osteoarthritis via NF-kappaB Signal Pathway, Drug Des Devel Ther 14 (2020) 1227-1240.

[62] D. Dragoljevic, M.K.S. Lee, C. Louis, W. Shihata, M.J. Kraakman, J. Hansen, S.L. Masters, B.Y. Hanaoka, P.R. Nagareddy, G.I. Lancaster, I.P. Wicks, A.J. Murphy, Inhibition of interleukin-1beta signalling promotes atherosclerotic lesion remodelling in mice with inflammatory arthritis, Clin Transl Immunology 9(11) (2020) e1206.

[63] Q. Wang, L. Xu, H. Helmholz, R. Willumeit-Romer, B.J.C. Luthringer-Feyerabend, Effects of degradable magnesium on paracrine signaling between human umbilical cord perivascular cells and peripheral blood mononuclear cells, Biomater Sci 8(21) (2020) 5969-5983.

[64] Y. Ohmori, T.A. Hamilton, Cooperative interaction between interferon (IFN) stimulus response element and kappa B sequence motifs controls IFN gamma- and lipopolysaccharide-stimulated transcription from the murine IP-10 promoter, J Biol Chem 268(9) (1993) 6677-88.

[65] T. Kuranobu, S. Mokuda, K. Oi, T. Tokunaga, K. Yukawa, H. Kohno, Y. Yoshida, S. Hirata, E. Sugiyama, Activin A Expressed in Rheumatoid Synovial Cells Downregulates TNFalpha-Induced CXCL10 Expression and Osteoclastogenesis, Pathobiology 87(3) (2020) 198-207.

[66] J.H. Lee, B. Kim, W.J. Jin, H.H. Kim, H. Ha, Z.H. Lee, Pathogenic roles of CXCL10 signaling through CXCR3 and TLR4 in macrophages and T cells: relevance for arthritis, Arthritis Res Ther 19(1) (2017) 163.

[67] S.N. Cross, R.A. Nelson, J.A. Potter, E.R. Norwitz, V.M. Abrahams, Magnesium sulfate differentially modulates fetal membrane inflammation in a time-dependent manner, Am J Reprod Immunol 80(1) (2018) e12861.

[68] Y. Niu, Z. Wang, Y. Shi, L. Dong, C. Wang, Modulating macrophage activities to promote endogenous bone regeneration: Biological mechanisms and engineering approaches, Bioact Mater 6(1) (2021) 244-261.

[69] S. Onder, A.C. Calikoglu-Koyuncu, K. Kazmanli, M. Urgen, F.N. Kok, G. Torun-Kose, Magnesium doping on TiN coatings affects mesenchymal stem cell differentiation and proliferation positively in a dose-dependent manner, Biomed Mater Eng 29(4) (2018) 427-438.

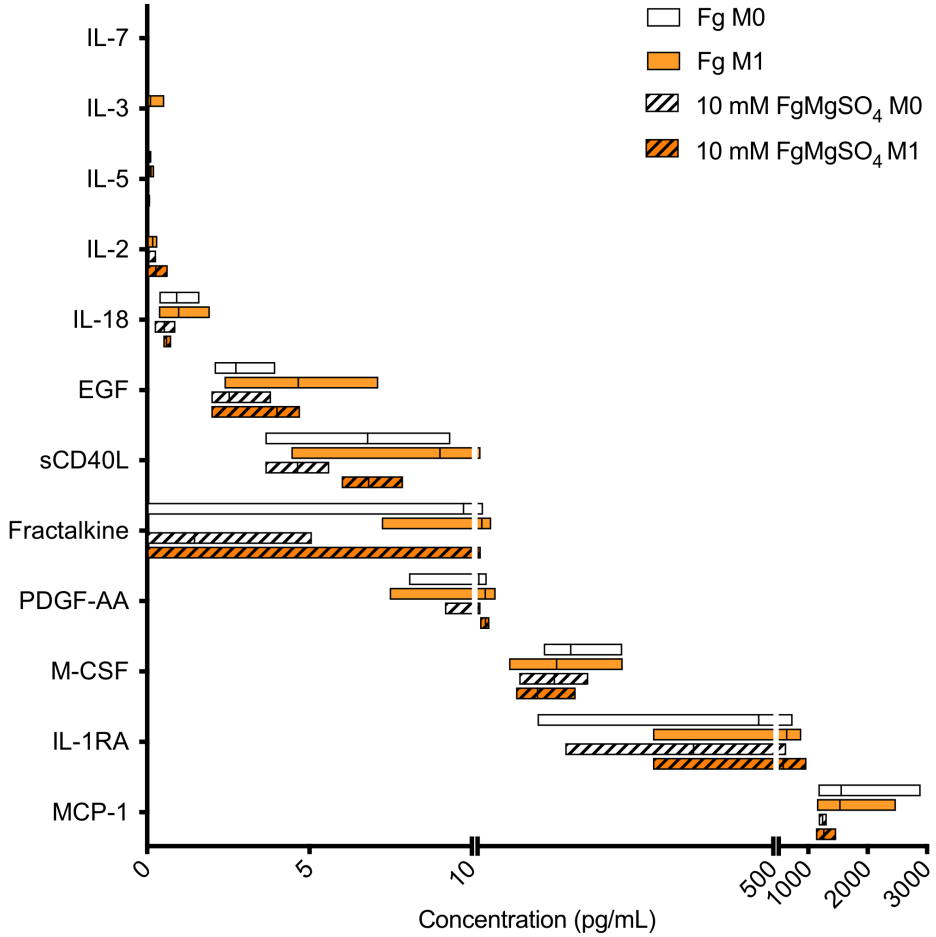
[70] Y. Li, J. Wang, J. Yue, Y. Wang, C. Yang, Q. Cui, High magnesium prevents matrix vesicle-mediated mineralization in human bone marrow-derived mesenchymal stem cells via mitochondrial pathway and autophagy, Cell Biol Int 42(2) (2018) 205-215.

[71] L. Zhang, C. Yang, J. Li, Y. Zhu, X. Zhang, High extracellular magnesium inhibits mineralized matrix deposition and modulates intracellular calcium signaling in human bone marrow-derived mesenchymal stem cells, Biochem Biophys Res Commun 450(4) (2014) 1390-5.

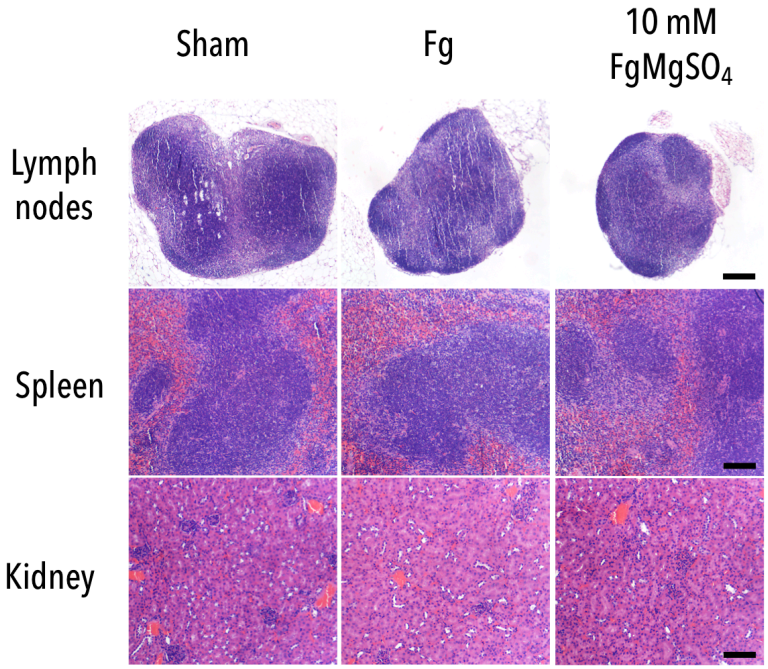
[72] J. Zhang, L. Tang, H. Qi, Q. Zhao, Y. Liu, Y. Zhang, Dual Function of Magnesium in Bone Biomineralization, Adv Healthc Mater 8(21) (2019) e1901030.

SUPPLEMENTARY MATERIAL

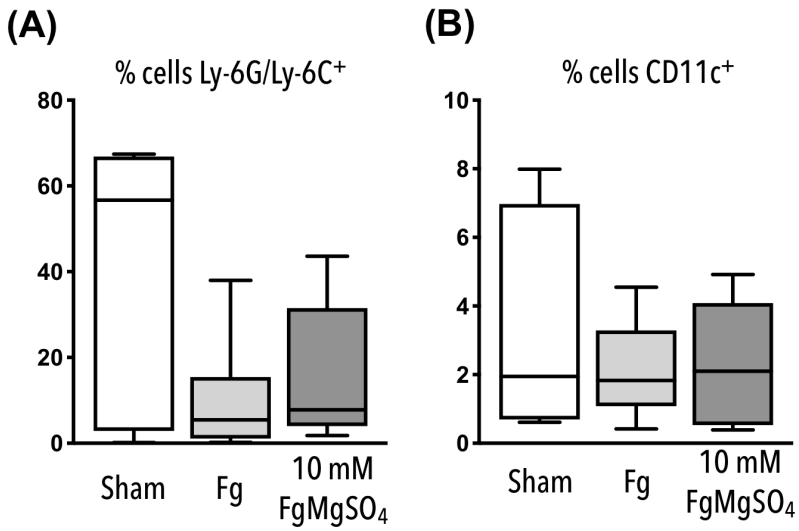
Supplementary Figures



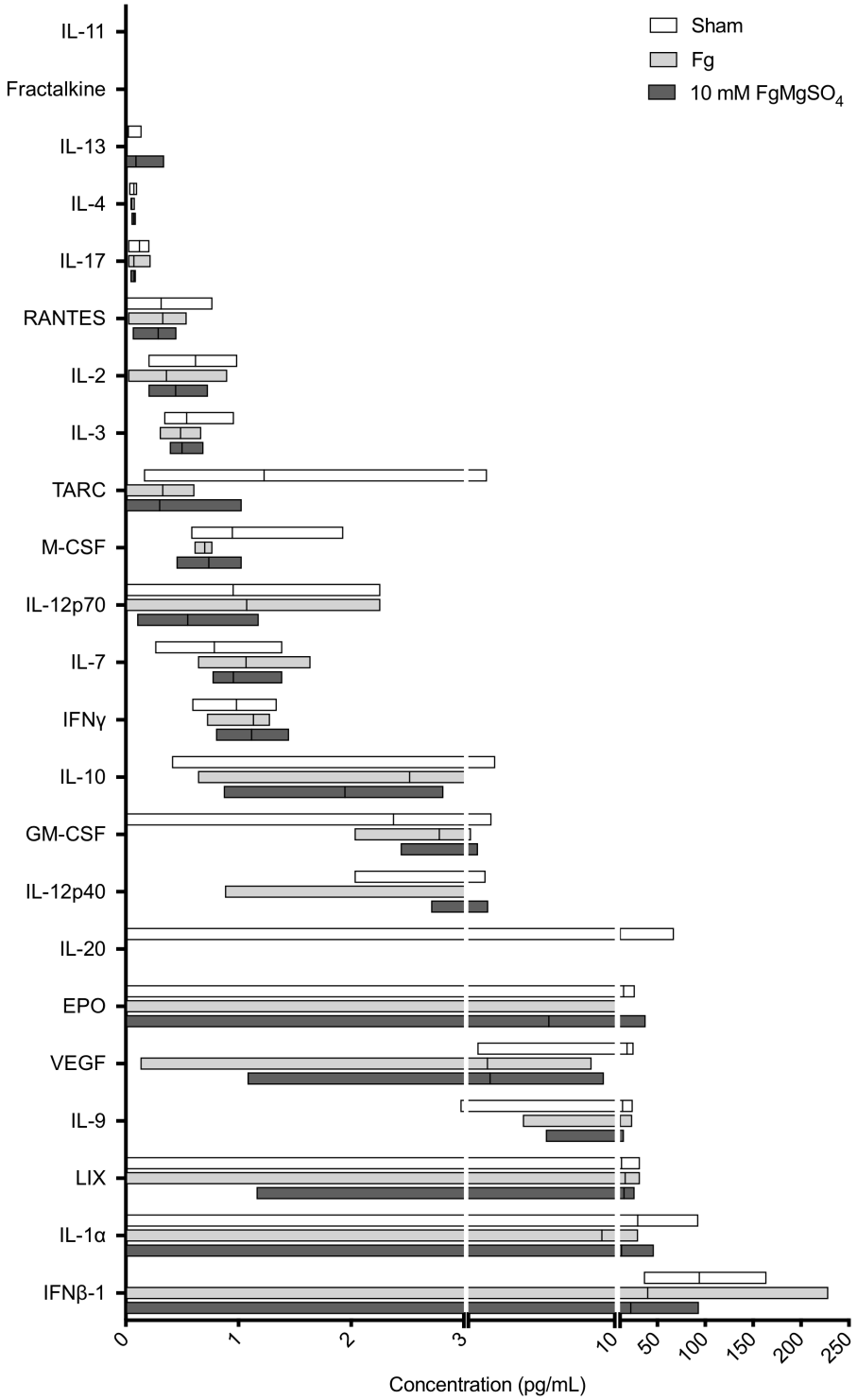
Supplementary Fig. 1. (related to Fig.5) Cytokine secretion by human macrophages cultured Fg and 10 mM $FgMgSO_4$ scaffolds in the presence/absence of M1 stimulation. Cytokine levels (that did not showed statistically significant differences between groups) in supernatants of macrophage cultured on Fg (plain bars) or 10 mM $FgMgSO_4$ (patterned bars) scaffolds and left unstimulated (white) or M1 stimulated (orange) for 72h. Box-plots represent min-to-max distribution (n=5). Kruskal-Wallis test followed by corrected Dunn's multiple comparisons were performed for IL-7, IL-3, IL-5, IL-2, EGF, fractalkine, PDGF-AA and MCP-1. One-way ANOVA followed by Sidak's multiple comparisons test were performed for IL-18, sCD40L, M-CSF and IL-1RA.



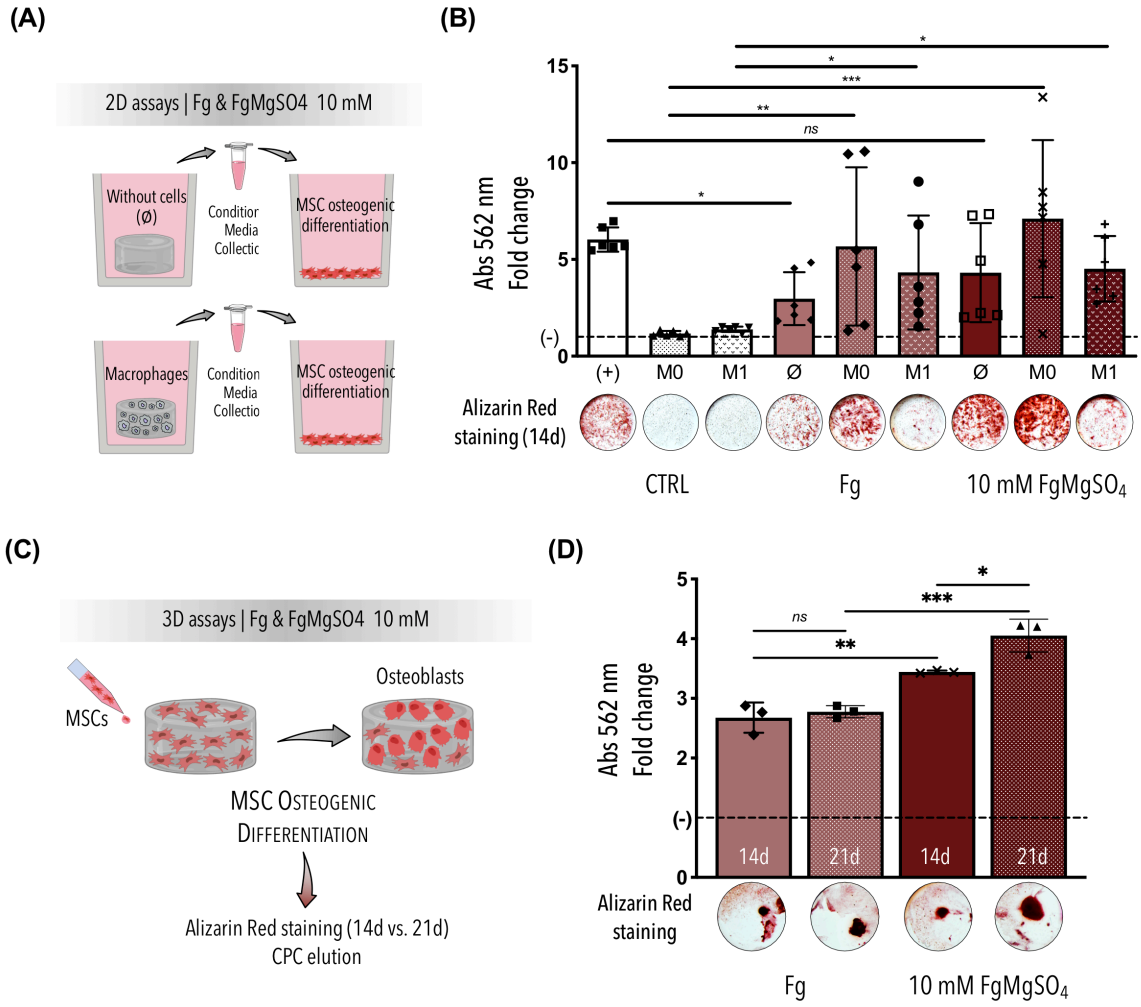
Supplementary Fig. 2. Histological analysis of mouse lymph nodes, spleen and kidneys of the animals retrieved 3 days after implantation. Representative HE stained sections of the lymph nodes, spleen and kidney from Sham-operated and Fg and 10 mM $FgMgSO_4$ implanted animals (scale bar = 100 μm).



Supplementary Fig. 3. Percentage of neutrophils and dendritic cells on the recovered exudates 3 days after implantation in an air-pouch mouse model. Cell percentages quantified across all animals in each group, showing **(A)** Percentage of Ly-6G/Ly-6C$^+$ cells and **(B)** Percentage of CD11c$^+$ cells. Kruskal-Wallis test followed by corrected Dunn's multiple comparisons were performed for Ly-6G/Ly-6C$^+$. One-way ANOVA followed by Sidak's multiple comparisons test were performed for CD11c+



Supplementary Fig. 4. (related to Fig.7) Cytokine production by inflammatory cells on the recovered exudates 3 days after implantation in an air-pouch mouse model. Cytokine levels (that did not showed statistically significant differences between groups) in inflammatory exudates collected from the mouse air pouches of Sham-operated (white bars), Fg (light gray bars) and 10 mM $FgMgSO_4$ (dark gray bars) implanted animals. Box-plots represent min-to-max distribution (n=6). Kruskal-Wallis test followed by corrected Dunn's multiple comparisons were performed for IL-11, fractalkine, IL-13, IL-17, IL-5, TARC, M-CSF, INF-**γ**, IL-10, IL12-p40, IL-20, EPO, VEGF, IL-1α and IFN-β1. One-way ANOVA followed by Sidak's multiple comparisons test were performed for IL-4, RANTES, IL-2, IL-3, IL-12p70, IL-7, GM-CSF, IL-9 and LIX.



Supplementary Fig. 5. Effect of macrophage-Fg/10 mM $FgMgSO_4$ secretome and Fg and 10 mM $FgMgSO_4$ scaffolds on MSC osteogenic differentiation. (A) Schematic representation of experimental approach used for 2D studies with conditioned medium from macrophages cultured on Fg and 10 mM $FgMgSO_4$ scaffolds. **(B)** MSC were incubated for 14 days with the secretome of unstimulated (M0) or LPS-IFNγ (M1) stimulated macrophages, Fg and 10 mM FgMgSO4 biomaterials extracts (Ø) or the secretome of macrophages cultured in Fg and $FgMgSO_4$ (10 mM) scaffolds in presence/absence of M1 stimulation. Basal (-) and osteogenic (osteo) (+) media were used as controls. Alizarin Red staining was performed and stained areas quantified by measuring the absorbance at 562 nm upon calcium deposits elution with CPC. Values were normalized by the basal condition (-). Representative pictures are shown for each condition (n=6). **(C)** Schematic representation of experimental approach used for 3D studies. **(D)** MSC were cultured for 14 and 21 days on Fg and $FgMgSO_4$ (10 mM) scaffolds. Alizarin Red staining was performed and stained areas quantified by measuring the absorbance at 562 nm upon calcium deposits elution with CPC. Scaffolds without cells were used as staining controls and values were normalized by these basal conditions (-). Representative pictures are shown for each condition (n=3). Data are represented as arithmetic mean ± standard deviation (SD). **p<0.05, **p<0.01, ***p<0.001 using one-way ANOVA followed by Sidak's multiple comparisons test.

CHAPTER IV

GENERAL DISCUSSION / FUTURE PERSPECTIVES

1. GENERAL DISCUSSION

Bone-related diseases and injuries account as one of the main causes of disability, affecting millions of people and representing a significant burden for health-care systems worldwide. The natural bone self-repair capacity is impaired when injury is extensive or in disease scenarios [1, 2]. Bone healing after injury is an intricate process, characterized by three partially overlapping phases: inflammation, repair and remodeling [1, 3]. Successful bone healing is highly dependent on the initial inflammatory phase [1, 3, 4]. The fine regulation of the inflammatory phase, driven by several mediators and immune cells, is determinant to enable the transition to the repair and ultimately the remodeling phase [5]. While an overactive inflammatory response can result in chronic inflammation a weak inflammatory response has potential consequences like infections [6], both leading to impaired or delayed fracture healing [7, 8]. Specifically, modulation of macrophage polarization from M1 to M2 is relevant for bone healing, both in healthy and inflammatory conditions, promoting inflammation resolution and endogenous tissue repair/regeneration.

In recent years, scaffold-based tissue engineering for bone regenerative medicine has been intensely researched to provide an alternative to autografts, the current gold standard bone substitutes, because of their limited availability and high morbidity at the donor site [9, 10]. Over the last years, we have perceived a change in the concept of an ideal biomaterial. Until recently, biomaterials were designed to “not trigger an inflammatory response”. More recently, this paradigm has started to switch from immune evasion to immune modulation.

On this basis, the work of this Doctoral dissertation was focused on bioengineering an immunomodulatory microenvironment for bone healing. A combination between fibrinogen (Fg) and magnesium (Mg) was proposed, as a biodegradable biomaterial to bioengineer a microenvironment capable of modulating macrophage phenotype as well as their crosstalk with MSCs, crucial for tissue repair/regeneration (Chapters II and III). The potential of this combination to act synergistically to modulate macrophage M1 pro-inflammatory activation was investigated first in the form of biomaterial extracts (Chapter II), and then as new Mg-incorporated Fg scaffolds (Chapter III). Finally, the biomaterials from Chapter III were used to develop gene-activated scaffolds, that can be used in the future to fine tune macrophage modulation (Supplementary results).

The natural polymer Fg constitutes a promising material to be used for tissue engineering scaffolds due to its biocompatibility and biodegradability, but also pro-inflammatory and pro-healing properties [11]. Our group has been exploring Fg either adsorbed to Ch [12] or as a 3D scaffold [13]. We previously showed that Fg enhances bone regeneration [12, 13] and

impacts the immune and inflammatory responses [14-16]. Despite Fg pro-inflammatory role [17], depending on the applied dose and protein conformation it may also act as an immunomodulatory influence [13, 18]. Thus, herein the focus was on the study of the immunomodulatory properties of Fg scaffolds to modulate macrophage behavior, particularly in pro-inflammatory conditions.

On the other hand, Mg and its alloys are already used in the clinic as regenerative biomaterials for osteoarticular applications [19-21]. Moreover, Mg, and particularly Mg ions, are also reported as immunomodulatory [18, 22]. Despite being osteopromotive and having mechanical properties close to those of bone, the applicability of biodegradable Mg-based materials is still hindered by their fast and uncontrolled degradation rate, and the potential toxicity associated with the corrosion process [23, 24]. Use of alloying element can help to tailor degradation properties of Mg materials. Various Mg alloys have been developed, and the choice of alloying elements is of importance to control the release of potentially toxic elements [24]. Also, combination of Mg-based materials with biodegradable polymeric coatings is also being explored as a strategy to control Mg degradation/corrosion rate [25]. The combination between Mg and the Fg degradable polymer had not been explored before, and it might represent an appealing approach to tune Mg biodegradability and combine the immunomodulatory and regenerative properties of both materials.

As previously discussed, the bone healing process involves multiple stages, that are overlapping-in-time and regulation, requiring the participation of various immune cell types [2, 26]. Among immune cells, macrophages have attracted much interest as key participants in all stages of tissue repair. Macrophages plasticity allows them to respond to different stimuli transitioning between pro-inflammatory (M1) and anti-inflammatory (M2) phenotypes [27, 28]. The microenvironment created by M1 and/or M2 macrophages has been reported to impact bone healing (e.g. tune macrophages for inflammation resolution and osteogenesis), with macrophage immunomodulation rising as an indispensable tool to assess biomaterials immune compatibility and overall performance [29, 30].

Hence, the first main goal here proposed was to combine Fg and Mg to obtain FgMg biomaterials and investigate their synergistic immunomodulatory potential towards macrophages and MSCs. Particularly we investigated the hypothesis that the combination of the two materials could act synergistically, and that, by modulating macrophages, we could impact MSCs differentiation. In chapter II, we report for the first time a biomaterial combining Fg and Mg. The first approach was to build a multilayer construct, using metallic Mg discs and layers of Fg polymerized by freeze drying and investigate the impact of its degradation products on macrophages and MSCs. We demonstrate for the first time that

extracts from FgMg combination material impaired LPS-IFN**γ**-driven macrophage M1 polarization, decreasing the percentage of CD86 positive cells, in a NF-kB p65 dependent-mechanism. Fg and Mg alone are reported to increase and decrease NF-kB activation, respectively. Soluble Fg is reported to induce MAPK phosphorylation [16] and to increase NF-kB activation [31]. In contrast to what is described in the literature, we did not find Fg extract mediated MAPK activation nor NF-kB activation. These observations stress out that the conformation of the Fg molecule influences the host response. In contrast to Fg, Mg is associated with reduced NF-kB activation, as shown by us and others [32, 33]. Our results also showed that FgMg extracts modulated macrophage cytokine secretion namely TNF-α and IL-12, in response to M1 stimulation. Furthermore, secretome from unstimulated macrophages preconditioned with FgMg extracts significantly increased MSCs ALP activity. It is worth noting that the most favorable phenotype (M1 and/or M2 phenotype) for osteogenesis as well the underlying signaling pathways behind this process are still matter of debate [34]. Therefore, results must be cautiously interpreted. Depending on the adopted experimental setup – *in vitro* vs. *in vivo* experiments; cell line vs. primary cells; co-culture systems vs. conditioned media; conditioned media dilutions; different biomaterial forms (e.g. extracts vs. powder vs. bulk material) – it is expected that distinct and often contradictory results arise. For instance, while Sadowska et al. [35] did not report increased osteogenesis of BMSCs upon incubation with conditioned media from RAW cells cultured on β-TCP surfaces, the opposite trend was reported by Chen et al. [36], using RAW cells cultured with β-TCP extracts.

Overall, results from Chapter II indicate a synergistic effect between Fg and Mg over the macrophage-MSC crosstalk. These outcomes provide an important understanding of the immunological properties of Fg and Mg, which will dictate a favorable fate for biomaterial integration.

Bearing in mind that Mg-based biomaterials therapeutic/beneficial effects are due to the release of Mg ions, we proceeded with the direct incorporation of precise amounts of Mg ions (Mg^{2+}) on Fg scaffolds. Ion doping was shown to improve the efficiency of bone regeneration aiming for a faster, more controlled and predictable outcome [37]. This led to the second main aim of this work, focused on evaluating the effect of a FgMg combination biomaterial, as new Mg-incorporated Fg scaffolds, on i*n vitro* and *in vivo* models of inflammation (Chapter III). To explore this matter, 3D scaffolds incorporated with increasing concentrations of Mg^{2+} were produced and tested for their ability to modulate macrophage polarization, *in vitro* and *in vivo*. As described in chapter III, $MgSO_4$ incorporation into Fg-3D structure (10, 25 and 50 mM $FgMgSO_4$) allowed for the maintenance of Fg-3D

characteristic porous structure and increased scaffolds mechanical properties as well as surface charge. Yet, cytotoxic analysis revealed that higher concentrations presented higher cytotoxicity. Considering our findings on the capacity of 10 mM $FgMgSO_4$ scaffolds to modulate macrophages phenotype *in vitro*, we questioned if there was also an impact on their osteoinductive potential and ultimately on the modulation of macrophage phenotype *in vivo*. Chen et al. hypothesized and demonstrated that CaP ceramics biomaterial immunomodulatory capacity was closely associated with their osteoinductive potential [38]. This correlation was not thoroughly replicated by our work. We verified that the secretome of macrophages cultured both in Fg and 10 mM $FgMgSO_4$ scaffolds, either in M0 or M1 conditions, increased MSC osteogenic differentiation, when compared with secretome of plastic-cultured M0 and M1 macrophages. However, when MSC were cultured directly on 10 mM $FgMgSO_4$ scaffolds, they showed significantly increased calcium deposits, in comparison with those cultured on Fg scaffolds. The topic on the possible correlations and role of implant-modulated macrophage polarization on osteogenic differentiation is also a matter of debate and requires further investigation [38].

As biodegradable materials, both Fg and Mg avoid FBR in the long term, improving integration and promoting tissue regeneration. *In vivo*, and in agreement with *in vitro* studies, 10 mM $FgMgSO_4$ scaffolds increased the percentage of M2 macrophages, when compared with Fg implanted and sham operated animals. This was also accompanied by a significant increase in the M2:M1 ratio and an overall decrease in the secretion of key inflammation-related cytokines. Albeit a higher M2:M1 ratio has been associated with an improvement in tissue repair [39], more research is needed to fully understand the phenotype that macrophages adopt during the stages of FBR and the way it varies along this process [40]. While some studies report the M1-like macrophages as the predominant phenotype at all FBR stages [41], others report a shift in the macrophage phenotype along the FBR (initial M1 activation followed by an M2 activation and increased M2:M1 ratio at later stages) [39, 42]. Moreover, the existence of a dual M1/M2 macrophage associated with FBR, i.e. co-expression of M1 and M2 markers associated, has also been reported [43-45]. Moreover, it should always be taken into consideration the existence of other macrophage phenotypes besides the traditional M1/M2 paradigm. For instance, the scaffold associated macrophage phenotype (SAM), reported to express $CD11b^+$, $F4/80^+$, $CD11c^{+/-}$, CD206hi, $CD86^+$, $MHCII^+$, mixed M1/M2 phenotype with antigen presentation capabilities ($MHCII^+$), was defined by Sadtler et al. [46, 47], when analyzing the immune microenvironments upon biomaterial implantation *in vivo*.

Overall, Chapter III provided evidence of the promising features of 10 mM $FgMgSO_4$ scaffolds for inflammation and macrophage modulation, both *in vitro* and *in vivo*. Also, supplementary data to this chapter shows the positive impact of these scaffolds on MSC osteogenic differentiation. To our knowledge this was the first study using $MgSO_4$ incorporated into 3D Fg scaffolds as an immunomodulatory biomaterial that allowed the modulation of macrophage phenotype towards a M2 phenotype.

Still in the context of this thesis, we proposed to explore the potential of the materials developed in Chapter III, crosslinked Fg and 10 mM $FgMgSO_4$ scaffolds, as biomaterial-based miRNA delivery systems capable of fine tuning inflammation resolution in the context of bone repair and regeneration. miRNAs are important regulators of macrophage activation and polarization [48, 49], and thus an attractive route to modulate macrophage phenotype and their crosstalk with MSCs. Transfection of RNA based products is an advantageous alternative over DNA based ones to achieve target protein expression [50]. Unlike DNA, RNA does not need to enter the cell nucleus to be functional, thus allowing the transfection in both mitotic and non-mitotic cells, which is the case of monocytes and macrophages [50]. The CaP based gene delivery vectors, namely nHA particles, used herein provide an attractive alternative to other transfection viral or non-viral transfection vectors because they are cost-effective, biocompatible and bioresorbable [51]. Viral transfection, using adenovirus or lentivirus shows high transfection efficiency but major *in vivo* safety concerns, while non-viral methods, like lipid and polymer-based delivery, have moderate transfection efficiency. Here, a non-viral transfection methodology was briefly explored, as complementary strategy to modulate macrophage phenotype, and consequently impact their crosstalk with MSCs. Previous studies from our group uncovered miR-195/anti-miR195 [52, 53] as interesting targets that could be further explored to tune inflammation resolution in the context of bone repair and regeneration. Preliminary results presented in this thesis, using nHA particles (synthesized following an *in situ* precipitation protocol established by Cunniffe et al. [54]) demonstrated that we were able to deliver these particles loaded with siGLO and fluorescently tagged siRNA MMP9 to monocytes in monolayer. When applied to 3D Fg and 10 mM $FgMgSO_4$ scaffolds, siGLO loaded nHA particles were also successfully delivered to monocytes, demonstrating that these 3D scaffolds have the potential to act as GAMs (Gene-activated matrix).

Taken together, the findings stemming from this thesis on the combination between Fg and Mg suggest this combination as new immunomodulatory biomaterial to be further tested for improved bone repair and regeneration. Indeed, as described in chapter II we confirmed that Fg and Mg act synergistically in modulating macrophage phenotype, subsequently

impacting on MSC osteogenic differentiation. It was achieved an impairment on LPS-IFNγ-driven macrophage M1 polarization. Yet, this was not accompanied by modifications in M2 phenotype. Thus, in chapter III we took a leap further on the combination between Fg and Mg, with a Mg-incorporated Fg scaffold being developed. By incorporating Mg^{2+}, it was possible to increase the biomaterial mechanical properties and gain greater control over the modulation of macrophage polarization. Working with Mg-incorporated Fg scaffolds, we were able to increase M2 polarization while still impacting/impairing M1 polarization.

Overall, in the scope of this thesis, we brought new insights on the potential of combination materials to bioengineer immunomodulatory microenvironments, to promote tissue repair/regeneration. We reported for the first time the combination of Fg and Mg, showing their synergistic effect in modulating macrophage phenotype and promoting a pro-regenerative phenotype, either when this combination was used in the form of extracts or as 3D scaffolds, but with a different Mg source. Moreover, the potential of this combination material to act as a GAM deserves further exploration.

2. FUTURE PERSPECTIVES

In chapter II we described our studies regarding the combination between Fg and Mg and the impact of its extracts on macrophage polarization, following pro-inflammatory stimulation, and their crosstalk with MSCs. Following our outcomes, we believe that the combination of these materials requires further optimization, to obtain a true combinatory material. For instance, on the Fg/Mg ratios and on Mg surface treatments that allowed a better integration with Fg. Despite the several strategies for the Mg surface treatment currently under development, it is our belief that they are still in their infancy. Several alloying elements have been used to improve Mg corrosion resistance. Yet, a lot remains unknown, particularly concerning their possible cytotoxic side effects. Moreover, despite the promises that the technique of ion implantation may bring, when using Mg in the form of discs this technique is not able to uniformly cover all the faces and thus, uneven corrosion rates can be expected.

The results obtained in Chapter III showed that the 10mM $FgMgSO_4$ scaffolds were able to modulate macrophages towards a M2 phenotype *in vitro* and *in vivo*. The *in vivo* inflammatory response, and particularly macrophage polarization, in response to the biomaterials were studied in the air pouch model, at 3 days after implantation. Given the results obtained it would be of great interest to explore different time points, and evaluate the effect of 10 mM $FgMgSO_4$ scaffolds at different stages of the foreign body response.

The significant changes regarding mechanical properties, achieved by incorporating Mg^{2+} might be worth exploring further as a strategy/trend to improve mechanical properties of polymers, even for other than Fg. Importantly, the use of the FgMg combination in the context of bone applications must be carefully planned. This material would not be suitable for load-bearing applications as its mechanical properties, albeit increased by Mg incorporation, are still far from those encountered in bone. However, for non-load-bearing applications (i.e. calvaria lesions), this combination might be well suited.

Moreover, as the process of bone regeneration depends on the coupling of angiogenesis and osteogenesis [55], the study of these processes would be interesting to be pursued. Revascularization and angiogenesis are necessary not only to re-establish the blood supply to the bone but also to bring minerals, growth factors and osteoprogenitor cells necessary for healing and remodeling after injury. On the other hand, MSCs can directly influence the formation of new vessels through the secretion of cytokines and growth factors, including VEGF and fibroblast growth factor (FGF) [55]. *In vitro*, co-culture studies between endothelial cells and MSCs could be used to study the crosstalk between these cells [56]. *In vivo*, a critical size bone defect could be used. Previous work from our group using the critical size bone defect model showed that, although angiogenesis is important, and is stimulated by Fg incorporation in Ch materials, the number of new blood vessels found *in vivo* did not correlate directly with bone repair [12]. Accumulating evidence supports that Mg influences the process of angiogenesis, despite its effects on the underlying mechanisms needing to be further explored. Xu et al. showed that Mg extracts increased the proliferation of human umbilical vein endothelial cells, under hypoxic conditions [57]. In another study, low Mg concentrations (10 mM) were shown to increase vascular smooth muscle cell proliferation and migration rate, whereas higher Mg concentrations (40-60 mM) had the opposite effect and induced coagulation and inflammation [58]. Also, it is widely known that angiogenesis can be associated with the inflammatory response, and be increased in exacerbated inflammation. Lastly, it would be equally important to assess the potential of this biomaterial combination to improve bone tissue healing.

We believe there is still space for this combination to be explored and upgraded, particularly at the molecular level, as showed by the supplementary results chapter, where we showed that non-viral transfection of monocytes/macrophages can be performed using Fg and 10 mM $FgMgSO_4$ scaffolds. Further studies addressing its functional transfection efficiencies will be valuable, as well as the assessment of the effect that this procedure *per se* induces on macrophage polarization. Our previous results showed that miR-195-5p acts as a regulator of macrophage M1 polarization, favoring an anti-inflammatory phenotype [52]. The

group also showed that miR-195-5p inhibits MSCs osteogenic differentiation and proliferation [53]. Thus, miR-195 is an interesting target for the development of local bone regeneration therapies. Next steps would be to load Fg and 10 mM $FgMgSO_4$ scaffolds with nHA particles combined with miR-195/anti-miR-195 mimic or scrambled miR mimic and address their effectiveness in delivering miR-mimics/miR-inhibitors. Moreover, the macrophage phenotype modulation and impact of macrophage secretome on MSC proliferation and differentiation are relevant questions to further explore in future works. Ultimately, an *in vivo* proof-of-concept would be of interest to be also performed.

Although much more research would be required, we envisage the clinical application of this combination not limited to the context of bone. Taking into account that Fg is clinically applied crosslinked with thrombin, in the form of fibrin glue, this FgMg combination might also find application as an adhesive for skin wounds, intervening in the modulation of the macrophage phenotype in that context. We also foresee potential for this combination to be used as coating to functionally optimize biomedical properties of the non-biodegradable biomaterials currently used in the clinic .

Thus, we consider that this work is of interest for a wide range of researchers, including those developing new biomaterials for tissue repair/regeneration and those exploring the modulation of macrophage phenotype for promoting a regenerative microenvironment.

REFERENCES

[1] L. Claes, S. Recknagel, A. Ignatius, Fracture healing under healthy and inflammatory conditions, Nat Rev Rheumatol 8(3) (2012) 133-43.

[2] K. Schmidt-Bleek, B.J. Kwee, D.J. Mooney, G.N. Duda, Boon and Bane of Inflammation in Bone Tissue Regeneration and Its Link with Angiogenesis, Tissue Eng Part B Rev 21(4) (2015) 354-64.

[3] M. Maruyama, C. Rhee, T. Utsunomiya, N. Zhang, M. Ueno, Z. Yao, S.B. Goodman, Modulation of the Inflammatory Response and Bone Healing, Front Endocrinol (Lausanne) 11 (2020) 386.

[4] S.A. Eming, M. Hammerschmidt, T. Krieg, A. Roers, Interrelation of immunity and tissue repair or regeneration, Semin Cell Dev Biol 20(5) (2009) 517-27.

[5] K.T. Feehan, D.W. Gilroy, Is Resolution the End of Inflammation?, Trends Mol Med 25(3) (2019) 198-214.

[6] E. Seebach, K.F. Kubatzky, Chronic Implant-Related Bone Infections-Can Immune Modulation be a Therapeutic Strategy?, Front Immunol 10 (2019) 1724.

[7] A.E. Rapp, R. Bindl, S. Recknagel, A. Erbacher, I. Muller, H. Schrezenmeier, C. Ehrnthaller, F. Gebhard, A. Ignatius, Fracture Healing Is Delayed in Immunodeficient NOD/scidIL2Rgammacnull Mice, PLoS One 11(2) (2016) e0147465.

[8] L. Shen, Y. Xiao, H. Xie, H. Zhao, T. Luo, L. Liu, X. Pan, A naturally derived small molecule NDSM253 inhibits IKK1 to suppress inflammation response and promote bone healing after fracture, Am J Transl Res 13(1) (2021) 24-37.

[9] T.M. De Witte, L.E. Fratila-Apachitei, A.A. Zadpoor, N.A. Peppas, Bone tissue engineering via growth factor delivery: from scaffolds to complex matrices, Regen Biomater 5(4) (2018) 197-211.

[10] L. Roseti, V. Parisi, M. Petretta, C. Cavallo, G. Desando, I. Bartolotti, B. Grigolo, Scaffolds for Bone Tissue Engineering: State of the art and new perspectives, Mater Sci Eng C Mater Biol Appl 78 (2017) 1246-1262.

[11] J.Y. Joo, M.L. Amin, T. Rajangam, S.S.A. An, Fibrinogen as a promising material for various biomedical applications, Molecular & Cellular Toxicology 11(1) (2015) 1-9.

[12] S.G. Santos, M. Lamghari, C.R. Almeida, M.I. Oliveira, N. Neves, A.C. Ribeiro, J.N. Barbosa, R. Barros, J. Maciel, M.C. Martins, R.M. Goncalves, M.A. Barbosa, Adsorbed

fibrinogen leads to improved bone regeneration and correlates with differences in the systemic immune response, Acta Biomater 9(7) (2013) 7209-17.

[13] D.M. Vasconcelos, R.M. Goncalves, C.R. Almeida, I.O. Pereira, M.I. Oliveira, N. Neves, A.M. Silva, A.C. Ribeiro, C. Cunha, A.R. Almeida, C.C. Ribeiro, A.M. Gil, E. Seebach, K.L. Kynast, W. Richter, M. Lamghari, S.G. Santos, M.A. Barbosa, Fibrinogen scaffolds with immunomodulatory properties promote in vivo bone regeneration, Biomaterials 111 (2016) 163-178.

[14] C.R. Almeida, D.P. Vasconcelos, R.M. Goncalves, M.A. Barbosa, Enhanced mesenchymal stromal cell recruitment via natural killer cells by incorporation of inflammatory signals in biomaterials, J R Soc Interface 9(67) (2012) 261-71.

[15] J. Maciel, M.I. Oliveira, E. Colton, A.K. McNally, C. Oliveira, J.M. Anderson, M.A. Barbosa, Adsorbed fibrinogen enhances production of bone- and angiogenic-related factors by monocytes/macrophages, Tissue Eng Part A 20(1-2) (2014) 250-63.

[16] M.I. Oliveira, M.L. Pinto, R.M. Goncalves, M.C.L. Martins, S.G. Santos, M.A. Barbosa, Adsorbed Fibrinogen stimulates TLR-4 on monocytes and induces BMP-2 expression, Acta Biomater 49 (2017) 296-305.

[17] J.K. Ryu, M.A. Petersen, S.G. Murray, K.M. Baeten, A. Meyer-Franke, J.P. Chan, E. Vagena, C. Bedard, M.R. Machado, P.E.R. Coronado, T. Prod'homme, I.F. Charo, H. Lassmann, J.L. Degen, S.S. Zamvil, K. Akassoglou, Blood coagulation protein fibrinogen promotes autoimmunity and demyelination via chemokine release and antigen presentation, Nature Communications 6(1) (2015) 8164.

[18] M. Bessa-Goncalves, A.M. Silva, J.P. Bras, H. Helmholz, B.J.C. Luthringer-Feyerabend, R. Willumeit-Romer, M.A. Barbosa, S.G. Santos, Fibrinogen and magnesium combination biomaterials modulate macrophage phenotype, NF-kB signaling and crosstalk with mesenchymal stem/stromal cells, Acta Biomater 114 (2020) 471-484.

[19] J.W. Lee, H.S. Han, K.J. Han, J. Park, H. Jeon, M.R. Ok, H.K. Seok, J.P. Ahn, K.E. Lee, D.H. Lee, S.J. Yang, S.Y. Cho, P.R. Cha, H. Kwon, T.H. Nam, J.H. Han, H.J. Rho, K.S. Lee, Y.C. Kim, D. Mantovani, Long-term clinical study and multiscale analysis of in vivo biodegradation mechanism of Mg alloy, Proc Natl Acad Sci U S A 113(3) (2016) 716-21.

[20] H. Windhagen, K. Radtke, A. Weizbauer, J. Diekmann, Y. Noll, U. Kreimeyer, R. Schavan, C. Stukenborg-Colsman, H. Waizy, Biodegradable magnesium-based screw clinically equivalent to titanium screw in hallux valgus surgery: short term results of the first prospective, randomized, controlled clinical pilot study, Biomed Eng Online 12 (2013) 62.

[21] D. Zhao, S. Huang, F. Lu, B. Wang, L. Yang, L. Qin, K. Yang, Y. Li, W. Li, W. Wang, S. Tian, X. Zhang, W. Gao, Z. Wang, Y. Zhang, X. Xie, J. Wang, J. Li, Vascularized bone grafting fixed by biodegradable magnesium screw for treating osteonecrosis of the femoral head, Biomaterials 81 (2016) 84-92.

[22] M.D. Costantino, A. Schuster, H. Helmholz, A. Meyer-Rachner, R. Willumeit-Romer, B.J.C. Luthringer-Feyerabend, Inflammatory response to magnesium-based biodegradable implant materials, Acta Biomater 101 (2020) 598-608.

[23] B.J. Luthringer, F. Feyerabend, R. Willumeit-Romer, Magnesium-based implants: a mini-review, Magnes Res 27(4) (2014) 142-54.

[24] M. Razavi, Y. Huang, Assessment of magnesium-based biomaterials: from bench to clinic, Biomater Sci 7(6) (2019) 2241-2263.

[25] L.Y. Li, L.Y. Cui, R.C. Zeng, S.Q. Li, X.B. Chen, Y. Zheng, M.B. Kannan, Advances in functionalized polymer coatings on biodegradable magnesium alloys - A review, Acta Biomater 79 (2018) 23-36.

[26] J.J. El-Jawhari, E. Jones, P.V. Giannoudis, The roles of immune cells in bone healing; what we know, do not know and future perspectives, Injury 47(11) (2016) 2399-2406.

[27] Z. Julier, A.J. Park, P.S. Briquez, M.M. Martino, Promoting tissue regeneration by modulating the immune system, Acta Biomater 53 (2017) 13-28.

[28] N. Mokarram, R.V. Bellamkonda, A perspective on immunomodulation and tissue repair, Ann Biomed Eng 42(2) (2014) 338-51.

[29] R. Sridharan, A.R. Cameron, D.J. Kelly, C.J. Kearney, F.J. O'Brien, Biomaterial based modulation of macrophage polarization: a review and suggested design principles, Materials Today 18(6) (2015) 313-325.

[30] J. Li, X. Jiang, H. Li, M. Gelinsky, Z. Gu, Tailoring Materials for Modulation of Macrophage Fate, Advanced Materials 33(12) (2021) 2004172.

[31] D.B. Kuhns, D.A. Priel, J.I. Gallin, Induction of human monocyte interleukin (IL)-8 by fibrinogen through the toll-like receptor pathway, Inflammation 30(5) (2007) 178-88.

[32] J. Sugimoto, A.M. Romani, A.M. Valentin-Torres, A.A. Luciano, C.M. Ramirez Kitchen, N. Funderburg, S. Mesiano, H.B. Bernstein, Magnesium decreases inflammatory cytokine production: a novel innate immunomodulatory mechanism, J Immunol 188(12) (2012) 6338-46.

[33] T. Hu, H. Xu, C. Wang, H. Qin, Z. An, Magnesium enhances the chondrogenic differentiation of mesenchymal stem cells by inhibiting activated macrophage-induced inflammation, Sci Rep 8(1) (2018) 3406.

[34] L. Yang, L. Xiao, W. Gao, X. Huang, F. Wei, Q. Zhang, Y. Xiao, Macrophages at Low-Inflammatory Status Improved Osteogenesis via Autophagy Regulation, Tissue Eng Part A (2021).

[35] J.M. Sadowska, F. Wei, J. Guo, J. Guillem-Marti, Z. Lin, M.P. Ginebra, Y. Xiao, The effect of biomimetic calcium deficient hydroxyapatite and sintered beta-tricalcium phosphate on osteoimmune reaction and osteogenesis, Acta Biomater 96 (2019) 605-618.

[36] Z. Chen, C. Wu, W. Gu, T. Klein, R. Crawford, Y. Xiao, Osteogenic differentiation of bone marrow MSCs by beta-tricalcium phosphate stimulating macrophages via BMP2 signalling pathway, Biomaterials 35(5) (2014) 1507-18.

[37] E. Bosch-Rue, L. Diez-Tercero, B. Giordano-Kelhoffer, L.M. Delgado, B.M. Bosch, M. Hoyos-Nogues, M.A. Mateos-Timoneda, P.A. Tran, F.J. Gil, R.A. Perez, Biological Roles and Delivery Strategies for Ions to Promote Osteogenic Induction, Front Cell Dev Biol 8 (2020) 614545.

[38] X. Chen, M. Wang, F. Chen, J. Wang, X. Li, J. Liang, Y. Fan, Y. Xiao, X. Zhang, Correlations between macrophage polarization and osteoinduction of porous calcium phosphate ceramics, Acta Biomater 103 (2020) 318-332.

[39] B.N. Brown, R. Londono, S. Tottey, L. Zhang, K.A. Kukla, M.T. Wolf, K.A. Daly, J.E. Reing, S.F. Badylak, Macrophage phenotype as a predictor of constructive remodeling following the implantation of biologically derived surgical mesh materials, Acta Biomater 8(3) (2012) 978-87.

[40] K.E. Martin, A.J. Garcia, Macrophage phenotypes in tissue repair and the foreign body response: Implications for biomaterial-based regenerative medicine strategies, Acta Biomater (2021).

[41] E. Dondossola, B.M. Holzapfel, S. Alexander, S. Filippini, D.W. Hutmacher, P. Friedl, Examination of the foreign body response to biomaterials by nonlinear intravital microscopy, Nat Biomed Eng 1 (2016).

[42] M.T. Wolf, C.L. Dearth, C.A. Ranallo, S.T. LoPresti, L.E. Carey, K.A. Daly, B.N. Brown, S.F. Badylak, Macrophage polarization in response to ECM coated polypropylene mesh, Biomaterials 35(25) (2014) 6838-49.

[43] S.F. Badylak, J.E. Valentin, A.K. Ravindra, G.P. McCabe, A.M. Stewart-Akers, Macrophage phenotype as a determinant of biologic scaffold remodeling, Tissue Eng Part A 14(11) (2008) 1835-42.

[44] C.E. Witherel, D. Abebayehu, T.H. Barker, K.L. Spiller, Macrophage and Fibroblast Interactions in Biomaterial-Mediated Fibrosis, Adv Healthc Mater 8(4) (2019) e1801451.

[45] J.A. Palmer, K.M. Abberton, G.M. Mitchell, W.A. Morrison, Macrophage phenotype in response to implanted synthetic scaffolds: an immunohistochemical study in the rat, Cells Tissues Organs 199(2-3) (2014) 169-83.

[46] K. Sadtler, B.W. Allen, K. Estrellas, F. Housseau, D.M. Pardoll, J.H. Elisseeff, The Scaffold Immune Microenvironment: Biomaterial-Mediated Immune Polarization in Traumatic and Nontraumatic Applications<sup/>, Tissue Eng Part A 23(19-20) (2017) 1044-1053.

[47] K. Sadtler, M.T. Wolf, S. Ganguly, C.A. Moad, L. Chung, S. Majumdar, F. Housseau, D.M. Pardoll, J.H. Elisseeff, Divergent immune responses to synthetic and biological scaffolds, Biomaterials 192 (2019) 405-415.

[48] G. Curtale, M. Rubino, M. Locati, MicroRNAs as Molecular Switches in Macrophage Activation, Front Immunol 10 (2019) 799.

[49] X.Q. Wu, Y. Dai, Y. Yang, C. Huang, X.M. Meng, B.M. Wu, J. Li, Emerging role of microRNAs in regulating macrophage activation and polarization in immune response and inflammation, Immunology 148(3) (2016) 237-48.

[50] Z. Zhong, S. Mc Cafferty, F. Combes, H. Huysmans, J. De Temmerman, A. Gitsels, D. Vanrompay, J. Portela Catani, N.N. Sanders, mRNA therapeutics deliver a hopeful message, Nano Today 23 (2018) 16-39.

[51] C.M. Curtin, G.M. Cunniffe, F.G. Lyons, K. Bessho, G.R. Dickson, G.P. Duffy, F.J. O'Brien, Innovative collagen nano-hydroxyapatite scaffolds offer a highly efficient non-viral gene delivery platform for stem cell-mediated bone formation, Adv Mater 24(6) (2012) 749-54.

[52] J.P. Bras, A.M. Silva, G.A. Calin, M.A. Barbosa, S.G. Santos, M.I. Almeida, miR-195 inhibits macrophages pro-inflammatory profile and impacts the crosstalk with smooth muscle cells, PLoS One 12(11) (2017) e0188530.

[53] M.I. Almeida, A.M. Silva, D.M. Vasconcelos, C.R. Almeida, H. Caires, M.T. Pinto, G.A. Calin, S.G. Santos, M.A. Barbosa, miR-195 in human primary mesenchymal stromal/stem

cells regulates proliferation, osteogenesis and paracrine effect on angiogenesis, Oncotarget 7(1) (2016) 7-22.

[54] G.M. Cunniffe, F.J. O'Brien, S. Partap, T.J. Levingstone, K.T. Stanton, G.R. Dickson, The synthesis and characterization of nanophase hydroxyapatite using a novel dispersant-aided precipitation method, J Biomed Mater Res A 95(4) (2010) 1142-9.

[55] N.G. Schott, N.E. Friend, J.P. Stegemann, Coupling Osteogenesis and Vasculogenesis in Engineered Orthopedic Tissues, Tissue Eng Part B Rev 27(3) (2021) 199-214.

[56] W. Chen, X. Liu, Q. Chen, C. Bao, L. Zhao, Z. Zhu, H.H.K. Xu, Angiogenic and osteogenic regeneration in rats via calcium phosphate scaffold and endothelial cell co-culture with human bone marrow mesenchymal stem cells (MSCs), human umbilical cord MSCs, human induced pluripotent stem cell-derived MSCs and human embryonic stem cell-derived MSCs, J Tissue Eng Regen Med 12(1) (2018) 191-203.

[57] L. Xu, R. Willumeit-Romer, B.J.C. Luthringer-Feyerabend, Effect of magnesium-degradation products and hypoxia on the angiogenesis of human umbilical vein endothelial cells, Acta Biomater 98 (2019) 269-283.

[58] J. Ma, N. Zhao, D. Zhu, Biphasic responses of human vascular smooth muscle cells to magnesium ion, J Biomed Mater Res A 104(2) (2016) 347-56.

SUPPLEMENTARY RESULTS

ORIGINAL RESEARCH WORK

Biomaterial-based non-viral transfection of primary monocytes

Biomaterial-based non-viral transfection of primary monocytes

Bessa-Gonçalves M[a,b], González-Vázquez A[c,d], Sadowska J[c], O'Brien FJ[c,d,e], Santos SG[a,b]

[a]*i3S – Instituto de Investigação e Inovação em Saúde, and INEB - Instituto de Engenharia Biomédica, Universidade do Porto, Rua Alfredo Allen 208, 4200-135 Porto, Portugal;*

[b]*Instituto Ciências Biomédicas Abel Salazar da Universidade do Porto, Rua de Jorge Viterbo Ferreira 228, 4050-313 Porto, Portugal.*

[c]*Tissue Engineering Research Group, Department of Anatomy & Regenerative Medicine, Royal College of Surgeons in Ireland (RCSI), Ireland, Dublin 2 D02 YN77, Ireland*

[d]*Trinity Centre for Biomedical Engineering, Trinity Biomedical Sciences Institute, Trinity College Dublin (TCD), Dublin 2 D02 PN40, Ireland*

[e]*Advanced Materials Bio-Engineering Research (AMBER) Centre, Trinity College Dublin, Dublin 2, Ireland*

1. INTRODUCTION

With an increasingly elderly population, the demand for joint and bone repair surgeries has risen exponentially. To overcome the constraints of autologous and heterologous bone grafts, alternative therapies have been intensively investigated to promote bone repair, including biomaterial scaffolds, alone or combined with therapeutic molecules [1, 2].

The emerging field of molecular therapeutics offers potential in the development of next generation tissue engineering strategies [3].The delivery of genes of interest to the injured site is a strategy starting to be explored to improve bone healing. Non-coding RNAs, and particularly microRNAs (miRNAs), have been regarded as valuable regulators for bone repair therapies, due to their pleiotropic action that allows to simultaneously influence different aspects of the bone repair/regeneration process [4-6]. Yet, the development of a non-toxic and effective delivery system, that can transfect primary cells directly is challenging. Despite the high efficiency attributed to viral gene delivery, major drawbacks include cytotoxicity, immunogenicity and insertional mutagenesis [7]. Comparatively, non-viral strategies were reported to be less cytotoxic and overall safer for the host than viral vectors, albeit at the compromise of a generally lower efficiency [8]. The concept of combining biomaterials with therapeutic genes is a recent and innovative strategy, designed to improve the transfection efficiency of cells at the place of injury. Scaffolds offer structural support for the deposition of new tissue while acting simultaneously as a delivery device [9].

We hypothesized that 3D non-viral transfection of miRNA would constitute an alternative route by which macrophage phenotype could be modulated. miRNAs are important regulators of macrophage activation and polarization [10, 11]. Yet, optimization of gene-delivery strategies to monocytes/macrophages for an effective manipulation is a major challenge, because these are resistant to transfection [2, 12]. While viral delivery and electroporation are widely used approaches to transfect immune cells, they are associated with biosafety issues and cytotoxicity, as discussed above. Thus, with the collaboration of Prof. Fergal O'Brien's laboratory, we proceeded to test monocyte transfection using biomaterial-based delivery systems. The set of results presented below enlightens the potential of this system to be further explored as an alternative or complementary route to modulate inflammation and macrophage phenotype.

2. METHODS

2.1. Production of Nanohydroxyapatite (nHA) – siGLO/siRNA MMP9 and siGLO-activated scaffold systems.

nHA particles were synthesized following an *in situ* precipitation protocol established by Cunniffe et al. [13]. Briefly, a Darvan 821A dispersant reagent (RT Vanderbilt, CO, USA)-containing phosphate solution was added to an equal volume of calcium chloride solution and filtered through a 0.2 µm filter [13]. nHA particles (150 µl) were left empty or loaded with siGLO (Dharmacon – Horizon Discovery, CO, USA) or fluorescently tagged siRNA MMP9 prepared at a final concentration of 20 nM, as described in [14].

Fg scaffolds were prepared by diluting, in PBS, a Fg stock solution at 80 mg/mL (Grifols S.A., Barcelona, Spain) to a final concentration of 60 mg/mL. Fg$MgSO_4$ scaffolds were prepared by mixing a Fg stock solution at 80 mg/mL with 200 mM $MgSO_4$ concentrate stock solution, prepared in PBS, to have final concentrations of 60 mg/mL Fg and 10 mM of $MgSO_4$. Solutions were casted into 48-well plates (800 µL/well), frozen overnight at -20 ºC and freeze-dried for 72 h, at -80 ºC [15]. Scaffolds were cut into cylindrical discs (10 mm diameter x 2 mm height) and chemically crosslinked o.n. with N-(3-Dimethylaminopropyl)-N′-ethylcarbodiimide hydrochloride (EDC, E1769, Sigma-Aldrich Co., St Louis, MO, USA), as previously reported [15]. Then, scaffolds were disinfected, neutralized and soak-loaded on both sides with a 150 µl total volume of nHA-siGLO complexes (75 µl each side at a 20 nM concentration), following protocols adapted from [14].

2.2. Monocytes isolation and culture & siGLO/siRNA MMP9-nHA particles delivery

Primary human peripheral blood monocytes were isolated from surplus buffy coats (BC), from healthy blood donors, by negative selection using RosetteSep™ Human Monocyte Enrichment Cocktail (StemCell Technologies, Vancouver, Canada), as previously described [15]. Briefly, BC were centrifuged at RT for 20 min at 1200 g (Eppendorf Centrifuge 5810R, VWR International LLC, Radnor, PA, USA), without active acceleration or brake, for blood components separation. PBMC were collected and incubated with RosetteSep™ Human Monocyte Enrichment Cocktail at RT for 20 min under gentle mixing. The mixture was diluted 1:1 with PBS supplemented with 2% heat inactivated FBS (Biowest, Riverside, MO, USA) before being layered over Histopaque-1077 (Sigma-Aldrich Co., St Louis, MO, USA) and centrifuged as previously. The enriched monocyte layer was collected and washed three times with PBS by centrifugation at 17 min, 700 rpm, RT (Eppendorf

Centrifuge 5810R, VWR International LLC, Radnor, PA, USA), to ensure platelet removal. The pellet was resuspended in complete media RPMI 1640 media with L-glutamine (Corning, Manassas, VA, USA) supplemented with 10% heat-inactivated FBS (Biowest, Riverside, MO, USA), 100 U mL^{-1} penicillin and 100 µg/mL^{-1} streptomycin (P/S, both from Invitrogen, Carlsbad, CA, USA), in the presence of 50 ng/mL of recombinant human macrophage colony-stimulating factor (rh M-CSF, ImmunoTools, Friesoythe, Germany). Cells were used at seeding densities of 2 x 10^6 cells per well (6 well plates) for monolayer cultured monocytes. nHA particles/siGLO or nHA particles/siRNA MMP9 fluorescently tagged complexes were added to 2D cultured monocytes, 48h after their seeding on glass coverslips. Culture medium was changed 24h after particle incubation. Monocytes internalization and transfection efficiency was assessed, by confocal microscopy, 72h after particles delivery, by counting the cells were siGLO (20 nM) or siRNA MMP9 (20 nM) was inside the cell and co-localized with nuclei, respectively. Lastly, conditioned media from the following conditions was collected for MMP9 activity evaluation: (1) control - monocytes not exposed to nHA particles; (2) monocytes incubated with empty nHA particles; and (3) monocytes incubated with nHA particles carrying siRNA MMP9.

For 3D experiments, monocytes were seeded dropwise at 2 x 10^6 cells per siGLO-activated Fg and siGLO-activated 10 mM $FgMgSO_4$ scaffold system. Monocytes/macrophages internalization and transfection efficiency was assessed, by confocal microscopy, 48 hours (48h) and 7 days (7d) after particles delivery, by counting the cells were siGLO (20 nM) was inside the cell and co-localized with nuclei. At the indicated time points, samples were fixed in 4% PFA permeabilized with 0.1 % Triton- X100, blocked in 1% bovine serum albumin (BSA) in phosphate buffered saline (PBS) and afterwards incubated for 1h with Alexa Fluor™ 488 Phalloidin (16:1000, A12379, ThermoFisher Scientific, Waltham, MA, USA) and DAPI (1:1000, 62248, ThermoFisher Scientific, Waltham, MA, USA), and rinsed in PBS. Fluorescence emitted at 547 nm (red) from internalized and transfected siGLO was studied using a confocal microscope, 48h and 7d after particles loading. Staining with phalloidin and counterstaining with DAPI was performed to better discriminate between internalization (siGLO fluorescence inside the cell) and transfection (siGLO fluorescence co-localized with nuclei). Images were acquired with a confocal microscope (Leica TCS SP5) and analysed using Image J 2.0 software.

2.3. Gelatin Zymography

MMP9 activity was evaluated by gelatin zymography, as described in [16]. Briefly, conditioned media from (1), (2) and (3) was collected and centrifuged at 1200 rpm, 10 min, 4ºC to remove cell debris. Protein content was then quantified using DC-Protein Assay (Bio-Rad Laboratories, Irvine, CA, USA) and 30 µg of protein, per condition, and resolved in zymography gels, as described in [16]. Clear proteolytic activity bands were seen against the Coomassie-stained, gelatin blue background.

2.4. Statistical analysis

Statistical analysis was performed using GraphPad Prism software (San Diego, CA, USA, version 9). Data were tested for normality using Shapiro-Wilk normality test. To compare data from multiple groups Kruskal-Wallis tests followed by Dunn's multiple comparisons test were performed for non-parametric data, while ANOVA followed by Sidak's multiple comparisons test were used for parametric data. Data are represented as arithmetic mean ± standard deviation (SD) from at least three independent experiments. Statistical significance was considered for *$p<0.05$; **$p<0.01$; ***$p<0.001$;

3. RESULTS

3.1. Monocytes were efficiently transfected with siGLO and siRNA MMP9

Monocytes are resistant to transfection, often resulting in low transfection efficiencies and high cell death. Thus, we started by transfecting monocytes with the siGLO oligonucleotides to easily monitor transfection efficiency. Results show that siGLO combined with nHA particles (Fig. 1A) was successfully delivered to monocytes in 2D cultures, on glass slides (Fig. 1B). Internalization (siGLO fluorescence inside the cell) and transfection efficiencies (siGLO fluorescence co-localized with nuclei) were assessed 48h after particles delivery (Fig. 1C). Quantification across different donors showed a percentage of about 69,2 ± 9,7 and 53,3 ± 3,7 of internalization and efficient transfection, respectively (n=3) (Fig. 1D).

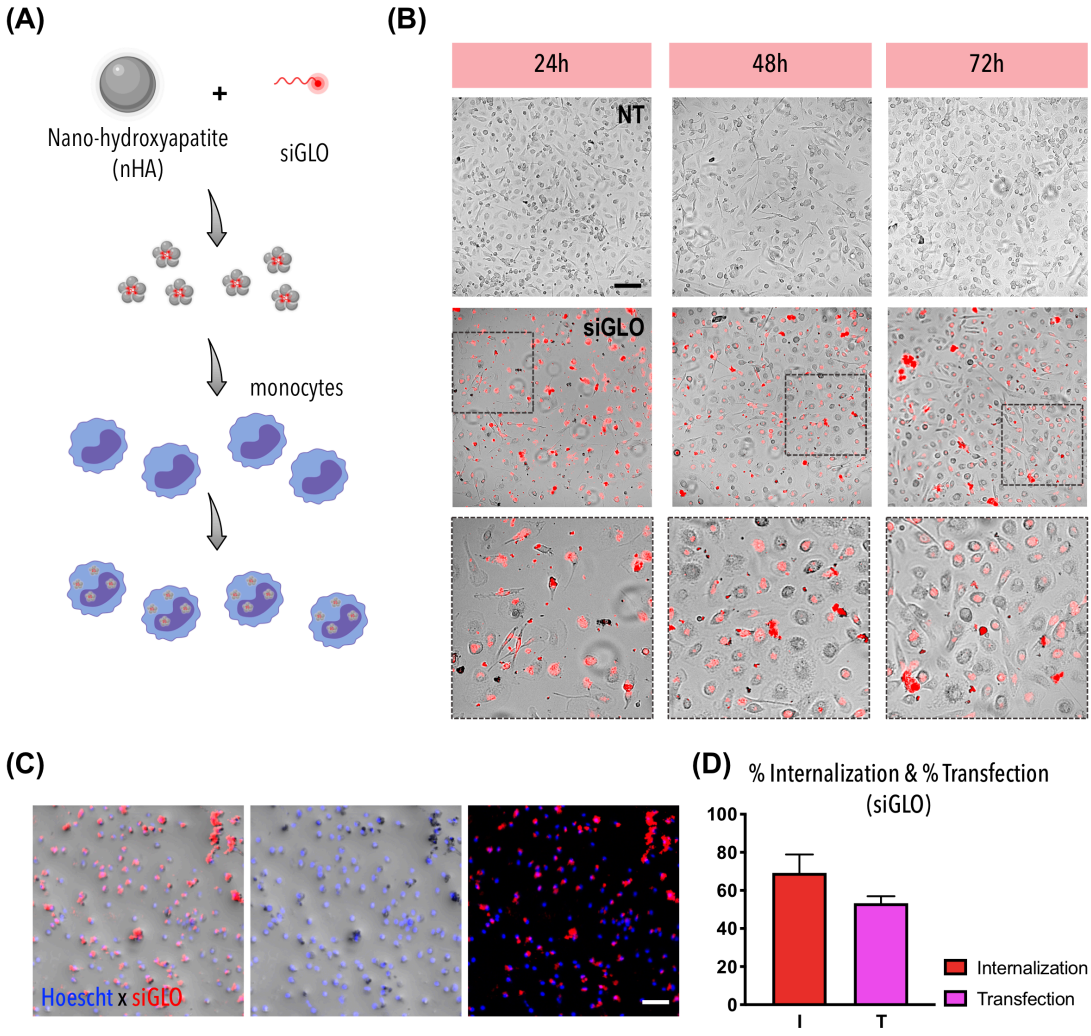


Fig. 1. siGLO expression in human monocytes cultured in monolayer. nHA particles were added to siGLO and delivered to 2D-cultured monocytes (3 days after isolation). **(A)** Diagram of experimental approach. **(B)** siGLO internalization was followed at 24h, 48h and 72h by ZOE Fluorescent Cell Imager. Images show cells in bright-field and siGLO in red. Scale bar = 100 µm. **(C)** Representative images of siGLO internalization and transfection, analysed by confocal microscopy showing cells in bright-field, nuclei in blue (Hoescht) and siGLO in red. Scale bar = 100 µm. **(D)** Quantification across different donors of siGLO internalization (I) and transfection (T) efficiency by counting the cells were siGLO was inside the cell and co-localized with nuclei, respectively.

A fluorescently tagged siRNA MMP9 combined with nHA particles was also successfully delivered to these cells (Fig. 2A). Internalization and transfection efficiencies were assessed 48h after particles delivering, and showed about 67,73 ± 6,3 % and 49,7 ± 4,6 %, respectively (Fig. 2B). To test the function of the siRNA for MMP9, we performed gelatin zymography and evaluated its enzymatic activity. Confirming that the siRNA for MMP9 was successfully transfected into monocytes, MMP9 activity was reduced when cells were incubated with nHA particles carrying siRNA MMP9, in comparison with negative control (no particles), or empty nHA particles (Fig. 2C).

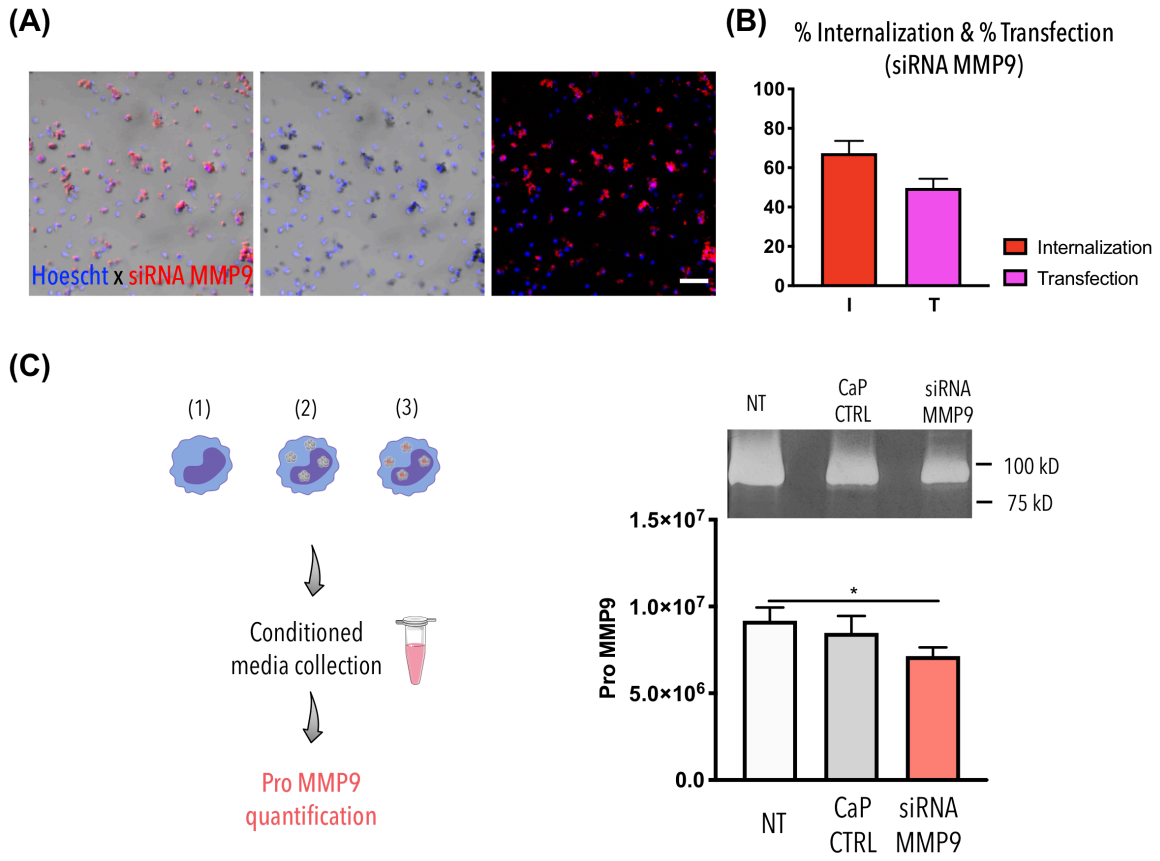


Fig. 2. siRNA MMP9 expression and assay of function in monolayer cultured human monocytes. nHA particles were added to fluorescently tagged siRNA MMP9 and delivered to 2D-cultured monocytes (3 days after isolation). **(A)** Representative images of siRNA MMP9 internalization and transfection, analysed by confocal microscopy showing cells in bright-field, nuclei in blue (Hoescht) and siGLO in red. **(B)** Quantification across different donors of siRNA MMP9 internalization (I) and transfection (T) efficiency by counting the cells were siRNA MMP9 was inside the cell and co-localized with nuclei, respectively. Scale bar = 100 μm. **(C)** Conditioned media from (1) Control - monocytes not exposed to nHA particles (NT); (2) monocytes incubated with empty nHA particles (CaP CTRL); and (3) monocytes incubated with nHA particles carrying siRNA MMP9, were collected, their protein content quantified and then MMP9 activity was evaluated by gelatin zymography . Data are mean ± SD, analyzed by Kruskal-Wallis test followed by Dunn's multiple comparison test (n=3). *p<0.05

3.2. siGLO-activated Fg and 10 mM $FgMgSO_4$ scaffolds are capable of transfecting monocytes/macrophages in 3D

Having successfully transfected primary macrophages in 2D cultures, we proceeded to produce gene-activated Fg scaffolds that could transfect monocytes directly in the scaffold. Fg and 10 mM $FgMgSO_4$ scaffolds were combined with nHA particles containing siGLO (Fig. 3A), and the percentage of internalization and transfection were assessed at 48h and 7 days of culture on the scaffolds. Cell nuclei and actin cytoskeleton labelling allowed the detection of siGLO in the cell cytoplasm, as well as in the proximity of, or superimposed to, the nucleus. From the microscopic analysis it was noted qualitatively that siGLO was co-

localized with the cell nuclei at the 48h timepoint, adopting a more cytoplasmic distribution at the 7d timepoint (Fig. 3B). When the numbers of cells internalizing siGLO were quantified across different donors, results showed similar internalization efficiencies in monocytes cultured both on Fg and on 10 mM $FgMgSO_4$ scaffolds at 48h, or 7 days after being seeded in siGLO-activated scaffolds. Interestingly, the internalization efficiency significantly increased in monocytes cultured on siGLO-activated 10 mM $FgMgSO_4$ scaffolds from 48h to 7 days (Fig. 3C). Regarding the quantification of the percentage of transfected cells (nuclear siGLO), results showed transfection efficiencies of about 35,8 ± 4,5 % and 37 ± 6,2 % on monocytes cultured in siGLO-activated Fg and 10 mM $FgMgSO_4$ scaffolds, respectively. It was also observed a significant decrease in the percentage of cells transfected at the 7 days timepoint, when compared with the 48h timepoint (8,7 ± 1,6 % and 20,36 ± 4,9 % for Fg and 10 mM $FgMgSO_4$, respectively). Curiously, at this late time point the percentage of cells transfected on 10 mM $FgMgSO_4$ was significantly higher to those transfected on Fg (Fig. 3D).

In summary, non-viral nHA particles synthesized following previously established protocols [13] were able to efficiently deliver siGLO and siRNA MMP9 in monolayered cultured monocytes; and siGLO on scaffolds where monocytes where subsequently seeded on.

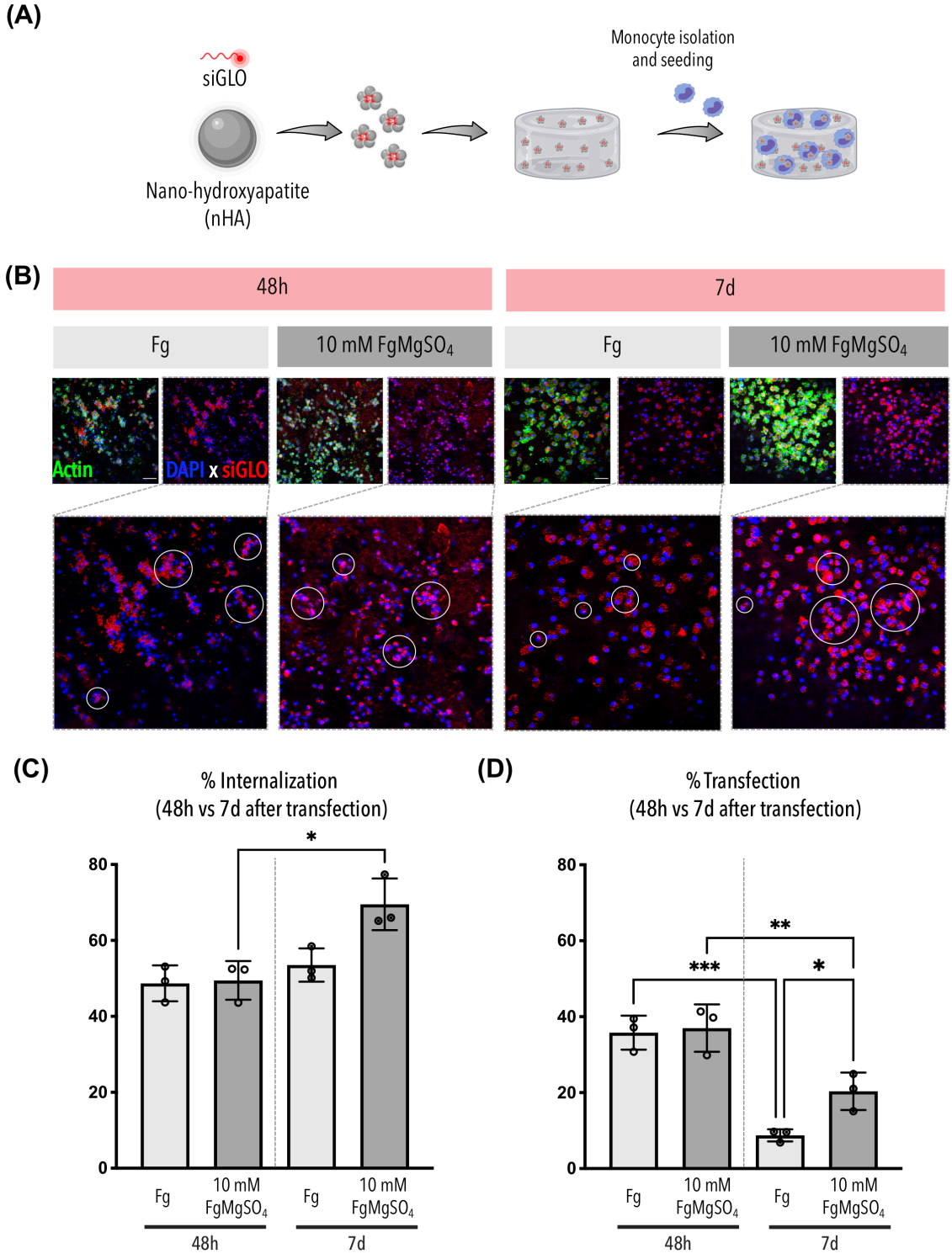


Fig.3. Monocytes transfection efficiency in gene-activated scaffolds. nHA particles with siGLO were incorporated into Fg and 10 mM $FgMgSO_4$ scaffolds, and monocytes were seeded **(A)**. After 48h and 7d scaffolds were fixed, actin (green) staining was performed, nuclei were stained with DAPI (blue) **(B)** and the percentage of siGLO (red) internalization **(C)** and transfection **(D)** was calculated by counting the cells where siGLO was localized in the cytoplasm and nucleus, respectively. Data are mean ± SD. One-way ANOVA followed by Sidak's multiple comparisons test were performed (n=3). *p<0.05; **p<0.01; ***p<0.001

4. DISCUSSION

The use of biomaterials for improving bone healing is being researched as new future therapies for bone repair/regeneration. Given the importance of inflammation modulation for osteoarticular health, strategies to improve tissue repair by modulating the associated immune response, namely macrophage phenotype, have been explored.

Thus, the main purpose of this work was to perform non-viral transfection of monocytes/macrophages using biomaterial-based delivery systems aiming, in the future, to develop a new approach able to modulate macrophage phenotype. In contrast to other cells, monocytes/macrophages are considered as hard-to-transfect cells particularly under *in vitro* conditions because these non-proliferating cells are programmed to recognize and neutralize foreign bodies [2, 12]. The protocol employed here, using CaP based gene delivery vectors (namely nHA particles that form complexes with the molecule of interest) has been validated for the transfection of MSCs [14, 17] but has not yet been validated for the transfection of primary monocytes/macrophages. For that reason, we started by performing non-viral transfection of monocytes under 2D conditions and assessing the internalization and transfection efficiencies, using siGLO as the transfection indicator. Results showed that we were able to successfully deliver both siGLO and a fluorescently tagged siRNA MMP9 combined with nHA particles to monocytes. To further corroborate the transfection efficiency results obtained, the function of the siRNA for MMP9 was tested by evaluating its enzymatic activity by gelatin zymography. Results confirmed that siRNA MMP9 was successfully transfected into monocytes, as MMP9 activity was significantly reduced in these cells when compared to the ones where no particles (NT) were delivered; or empty nHA particles. Using DharmaFECT3 transfection reagent from Dharmacon, Dong et al. [12] reported to obtain approximately 85% transfection efficiency in human macrophages. Similarly, Herb et al. [18] achieved about 85% transfection efficiency in human macrophages, using mRNA transcribed *in vitro* from DNA templates such as plasmids. In another study, Moradian et al. [2] investigated the dose-dependence of the transfection efficiency for monocytes and macrophages using the liposomal reagents Lipofectamine MessengerMax (LipoMM) and ScreenFect (ScrF) as well as the polymeric reagent Viromer RED (ViroR). Overall, monocytes and macrophages revealed increased transfection efficiency when increasing amounts of mRNA were applied to the cells. Higher transfection efficiencies were obtained with LipoMM comparing to ViroR and ScrF for both monocytes and macrophages (e.g. 80% 36% and 46% for macrophages). Also, this increase in the transfection efficiency was more pronounced in macrophages, in comparison with monocytes. In the current study, we were only able to achieve transfection

efficiencies rounding 53% and 50% for siGLO and siRNA MMP9, respectively. We speculate this great gap on transfection efficiency might be dependent not only on the employed carrier system but also on cell differentiation stage (monocytes versus macrophages) and their time in culture. Thus, it is conceivable that these variations on transfection efficiency are likely to occur and thus comparisons must be made very cautiously.

Next, we proceeded to produce gene-activated Fg and 10 mM $FgMgSO_4$ scaffolds that could transfect monocytes directly in the scaffold. In previous work from our team, we showed that the combination between Fg and Mg was able to modulate macrophage phenotype. Specifically, using FgMg extracts we've shown we were able to impair macrophage pro-inflammatory phenotype. In Chapter III of this PhD work, we developed this combination towards integrated 3D scaffolds, and showed that $FgMgSO_4$ scaffolds modulate macrophage phenotype towards M2 both *in vitro* and *in vivo*. Here we took that further by producing gene-activated scaffolds and comparing these Fg unmodified with modified FgMg scaffolds. The results demonstrated that monocytes/macrophages could be transfected by siGLO loaded nHA particles, demonstrating that these 3D scaffolds have the potential to act as GAMs (Gene-activated matrix). The observation of decreased transfection efficiencies in 3D, in comparison to results in 2D has been reported for MSCs [3, 19]. As for MSCs, we hypothesize this might be owed to the fact that 3D scaffold transfection relies on the migration of cells throughout the matrix. Therefore, the larger surface area in comparison to 2D, might explain the reduced exposure of cells to the transfection complexes [3]. Despite the similar internalization efficiencies obtained when monocytes were seeded on Fg or 10 mM $FgMgSO_4$ scaffolds, the same did not happen for the transfection efficiency values at the 7d timepoint. In fact, a decrease in the transfection efficiency over time was detected either in Fg or 10 mM $FgMgSO_4$. This may be explained by the cells' differentiation process, given that at the 48h timepoint cells are still monocytes whereas at 7d they were already fully differentiated into macrophages. In here, there was a higher capacity of 10 mM $FgMgSO_4$ scaffolds to sustain more transfected cells. Mg ions are reported to be necessary for successful gene electrotransference [20, 21]. However higher concentrations (above 10 mM) were shown to lead lower gene transfection [20, 21].

Further studies addressing functional transfection efficiencies will be valuable. Moreover, performing the seeding of macrophages previously differentiated in 2D would also provide crucial information on how the microenvironment affects the differentiation progress and its effect on the transfection efficiency, thus helping to understand the need to fine tune or not

the current employed protocol. Lastly, assessment of the effect that this procedure *per se* induces on macrophage polarization would also be relevant.

5. CONCLUSION

Taken together, these results suggest that non-viral transfection of monocytes/macrophages can be performed using biomaterial-based delivery systems. Overall, and to the best of our knowledge, this is the first report of successful application of a biomaterial-based non-viral transfection system for primary monocytes/macrophage transfection, and opens new avenues for *in vivo* transient transfection of monocytes/macrophages, thus modulating the inflammatory response to biomaterials.

REFERENCES

[1] G. Tang, Z. Liu, Y. Liu, J. Yu, X. Wang, Z. Tan, X. Ye, Recent Trends in the Development of Bone Regenerative Biomaterials, Front Cell Dev Biol 9 (2021) 665813.

[2] H. Moradian, T. Roch, A. Lendlein, M. Gossen, mRNA Transfection-Induced Activation of Primary Human Monocytes and Macrophages: Dependence on Carrier System and Nucleotide Modification, Sci Rep 10(1) (2020) 4181.

[3] I. Mencia Castano, C.M. Curtin, G.P. Duffy, F.J. O'Brien, Next generation bone tissue engineering: non-viral miR-133a inhibition using collagen-nanohydroxyapatite scaffolds rapidly enhances osteogenesis, Sci Rep 6 (2016) 27941.

[4] M. Hadjiargyrou, D.E. Komatsu, The Therapeutic Potential of MicroRNAs as Orthobiologics for Skeletal Fractures, J Bone Miner Res 34(5) (2019) 797-809.

[5] M.R. Iaquinta, C. Lanzillotti, C. Mazziotta, I. Bononi, F. Frontini, E. Mazzoni, L. Oton-Gonzalez, J.C. Rotondo, E. Torreggiani, M. Tognon, F. Martini, The role of microRNAs in the osteogenic and chondrogenic differentiation of mesenchymal stem cells and bone pathologies, Theranostics 11(13) (2021) 6573-6591.

[6] J. Freitas, S.G. Santos, R.M. Goncalves, J.H. Teixeira, M.A. Barbosa, M.I. Almeida, Genetically Engineered-MSC Therapies for Non-unions, Delayed Unions and Critical-size Bone Defects, Int J Mol Sci 20(14) (2019).

[7] D. Wang, P.W.L. Tai, G. Gao, Adeno-associated virus vector as a platform for gene therapy delivery, Nat Rev Drug Discov 18(5) (2019) 358-378.

[8] B. Gantenbein, S. Tang, J. Guerrero, N. Higuita-Castro, A.I. Salazar-Puerta, A.S. Croft, A. Gazdhar, D. Purmessur, Non-viral Gene Delivery Methods for Bone and Joints, Front Bioeng Biotechnol 8 (2020) 598466.

[9] E.G. Tierney, G.P. Duffy, S.A. Cryan, C.M. Curtin, F.J. O'Brien, Non-viral gene-activated matrices: next generation constructs for bone repair, Organogenesis 9(1) (2013) 22-8.

[10] G. Curtale, M. Rubino, M. Locati, MicroRNAs as Molecular Switches in Macrophage Activation, Front Immunol 10 (2019) 799.

[11] X.Q. Wu, Y. Dai, Y. Yang, C. Huang, X.M. Meng, B.M. Wu, J. Li, Emerging role of microRNAs in regulating macrophage activation and polarization in immune response and inflammation, Immunology 148(3) (2016) 237-48.

[12] S.X.M. Dong, R. Caballero, H. Ali, D.L.F. Roy, E. Cassol, A. Kumar, Transfection of hard-to-transfect primary human macrophages with Bax siRNA to reverse Resveratrol-induced apoptosis, RNA Biol 17(6) (2020) 755-764.

[13] G.M. Cunniffe, F.J. O'Brien, S. Partap, T.J. Levingstone, K.T. Stanton, G.R. Dickson, The synthesis and characterization of nanophase hydroxyapatite using a novel dispersant-aided precipitation method, J Biomed Mater Res A 95(4) (2010) 1142-9.

[14] I. Mencia Castano, C.M. Curtin, G. Shaw, J.M. Murphy, G.P. Duffy, F.J. O'Brien, A novel collagen-nanohydroxyapatite microRNA-activated scaffold for tissue engineering applications capable of efficient delivery of both miR-mimics and antagomiRs to human mesenchymal stem cells, J Control Release 200 (2015) 42-51.

[15] M. Bessa-Goncalves, A.M. Silva, J.P. Bras, H. Helmholz, B.J.C. Luthringer-Feyerabend, R. Willumeit-Romer, M.A. Barbosa, S.G. Santos, Fibrinogen and magnesium combination biomaterials modulate macrophage phenotype, NF-kB signaling and crosstalk with mesenchymal stem/stromal cells, Acta Biomater 114 (2020) 471-484.

[16] A.M. Silva, M.I. Oliveira, L. Sette, C.R. Almeida, M.J. Oliveira, M.A. Barbosa, S.G. Santos, Resveratrol as a natural anti-tumor necrosis factor-alpha molecule: implications to dendritic cells and their crosstalk with mesenchymal stromal cells, PLoS One 9(3) (2014) e91406.

[17] I. Mencia Castano, C.M. Curtin, G.P. Duffy, F.J. O'Brien, Harnessing an Inhibitory Role of miR-16 in Osteogenesis by Human Mesenchymal Stem Cells for Advanced Scaffold-Based Bone Tissue Engineering, Tissue Eng Part A 25(1-2) (2019) 24-33.

[18] M. Herb, A. Farid, A. Gluschko, M. Kronke, M. Schramm, Highly Efficient Transfection of Primary Macrophages with In Vitro Transcribed mRNA, J Vis Exp (153) (2019).

[19] P.D. Mariner, E. Johannesen, K.S. Anseth, Manipulation of miRNA activity accelerates osteogenic differentiation of hMSCs in engineered 3D scaffolds, J Tissue Eng Regen Med 6(4) (2012) 314-24.

[20] S. Haberl, D. Miklavcic, M. Pavlin, Effect of Mg ions on efficiency of gene electrotransfer and on cell electropermeabilization, Bioelectrochemistry 79(2) (2010) 265-71.

[21] J.J. Sherba, S. Hogquist, H. Lin, J.W. Shan, D.I. Shreiber, J.D. Zahn, The effects of electroporation buffer composition on cell viability and electro-transfection efficiency, Sci Rep 10(1) (2020) 3053.